

BENCHMARKING OF COMPUTER CODES  
FOR  
REPOSITORY DESIGN MODELS

PREPARED BY:

H. TAMMAGI, W.R. SWANSON, J.A. BOJE

ACRES INTERNATIONAL CORPORATION  
SUITE 1000 LIBERTY BUILDING  
424 MAIN STREET  
BUFFALO, NEW YORK 14202

UNDER CONTRACT TO:

TEKNEKRON TRANSPORTATION SYSTEMS, INC.  
2121 ALLSTON WAY  
BERKELEY, CALIFORNIA 94704

SEPTEMBER 1987

F I N A L D R A F T

8712140092 871015  
PDR WMRES EECCORS  
B-6985 PDR

88131214  
NM Projects: NM-10, 11, 16  
PDR w/encl  
(Return to NM, 623-SS)

NM Record File: B-6985  
LPDR w/encl

H

WM DOCKET CONTROL  
CENTER

'87 OCT 20 A11:20

WM Record File  
B6985

WM Project 10, 11, 16  
Docket No. \_\_\_\_\_

PDR   
XLPDR  (B, N, S)

Distribution:

T. Brooks \_\_\_\_\_

(Return to WM, 623-SS) \_\_\_\_\_

8712140681  
B-6985

Received w/Ltr Dated 10/15/87

4247

## ABSTRACT

This report presents results of benchmarking a number of computer codes against a series of problems. The problems include analytical problems with known solutions, hypothetical repository design problems, and problems simulating field experiments. Specific phenomena addressed are thermal conduction, convection, radiation, elastic stresses, plastic stresses, creep stresses, and thermal expansion. Code solutions are compared with each other and where applicable, with analytical results and field observations. Difficulties encountered during the running of the various codes are discussed and limitations of the codes addressed.

## TABLE OF CONTENTS

LIST OF FIGURES  
LIST OF TABLES

Page

1.0	INTRODUCTION	
1.1	Purpose of This Report	
1.2	Scope of This Report	
1.3	Previous Work	
2.0	SUMMARY OF FINDINGS	
2.1	Introduction	
2.2	Problem 2.6 - Transient Temperature Analysis of an Infinite Rectangular Bar with Anisotropic Conductivity	
2.3	Problem 2.8 - Transient Temperature Response to the Quench of an Infinite Slab with a Temperature-Dependent Convection Coefficient	
2.4	Problem 2.9 - Transient Temperature Response of a Slab Exposed to a Uniform Radiative Environment	
2.5	Problem 2.10 - Steady Radiation Analysis of an Infinite Rectangular Opening	
2.6	Problem 3.2a - Unlined Circular Tunnel (Long Cylindrical Hole) in an Infinite Elastic Medium With a Biaxial Stress Field	
2.7	Problem 3.2b - Circular Tunnel (Long Cylindrical Hole) in an Infinite Elastic-Plastic Medium Subjected to a Hydrostatic Stress Field	
2.8	Problem 3.3c - Viscoelastic Analysis of a Thick-Walled Cylinder Subjected to Internal Pressure	
2.9	Problem 3.5 - Plane Strain Compression of an Elastic-Plastic Material	
2.10	Problem 5.2B - Hypothetical Near Field Problem - Basalt	

## TABLE OF CONTENTS (Cont'd)

	<u>Page</u>
3.3.2 Problem 5.2 Hypothetical Near Field Problem	
3.3.3 Problem 5.3 Hypothetical Far Field Problem	
3.4 Field Validation Problems	
3.4.1 Problem 6.1 Project Salt Vault Thermomechanical Response Simulation Problem	
3.4.2 Problem 6.3 In Situ Heater Test - Basalt Waste Isolation Project	
4.0 BENCHMARKING OF ADINA	
4.1 Code Background and Capabilities	
4.2 Problem 3.2b - Circular Tunnel (Long Cylindrical Hole) in an Infinite Elastic-Plastic Medium Subjected to a Hydrostatic Stress Field	
4.3 Problem 3.3c - Viscoelastic Analysis of a Thick-Walled Cylinder Subjected to Internal Pressure	
4.4 Problem 3.5 - Plane Strain Compression of an Elastic-Plastic Material	
5.0 BENCHMARKING OF ADINAT	
5.1 Code Background and Capabilities	
5.2 Problem 2.6 - Transient Temperature Analysis of an Infinite Rectangular Bar with Anisotropic Conductivity	
5.3 Problem 2.8 - Transient Temperature Response to the Quench of an Infinite Slab with a Temperature-Dependent Convection Coefficient	
5.4 Problem 2.9 - Transient Temperature Response of a Slab Exposed to a Uniform Radiative Environment	
5.5 Problem 2.10 - Steady Radiation Analysis of an Infinite Rectangular Opening	
5.6 Problem 5.2B - Hypothetical Near Field Problem - Basalt	
5.7 Problem 6.1 - Project Salt Vault Thermomechanical Response Simulation Problem	

## TABLE OF CONTENTS (Cont'd)

	<u>Page</u>	
8.7	Problem 6.1 - Project Salt Vault - Thermomechanical Response Simulation Problem	
8.8	Problem 6.3 - In Situ Heater Test	
9.0	BENCHMARKING OF SALT4	
9.1	Code Background and Capabilities	
9.2	Problem 5.2S - Hypothetical Near-Field Problem - Salt	
10.0	BENCHMARKING OF COYOTE	
10.1	Code Background and Capabilities	
10.2	Problem 2.6 - Transient Temperature Analysis of an Infinite Rectangular Bar with Anisotropic Conductivity	
10.3	Problem 2.8 - Transient Temperature Response to the Quench of an Infinite Slab with a Temperature-Dependent Convection Coefficient	
10.4	Problem 2.9 - Transient Temperature Response of a Slab Exposed to a Uniform Radiative Environment	
10.5	Problem 2.10 - Steady Radiation Analysis of an Infinite Rectangular Opening	
10.6	Problem 5.2S - Hypothetical Near Field Problem - Salt	
10.7	Problem 6.3 - In Situ Heater Test Basalt Waste Isolation Project	

REFERENCES

APPENDIX

## LIST OF FIGURES (Cont'd)

<u>Figure</u>	<u>Title</u>	<u>Page</u>
10.3-1	COYOTE Problem 2.8 - Finite Element Mesh	
10.3-2	COYOTE Problem 2.8 - Program Subroutine Summary	
10.4-1	COYOTE Problem 2.9 - Finite Element Mesh	
10.4-2	COYOTE Problem 2.9 - Temperature History at Radiative Face	
10.4-3	COYOTE Problem 2.9 - Temperature History at Insulated Face	
10.6-1	COYOTE Problem 5.2 - Salt - Finite Element Mesh	
10.6-2	COYOTE Problem 5.2S - Program Subroutine Summary	
10.6-3	COYOTE Problem 5.2 - Salt - Temperature History 0-100 Years	
10.6-4	COYOTE Problem 5.2 - Salt - Temperature History 100-1,000 Years	
10.6-5	COYOTE Problem 5.2 - Salt - Temperature History 1,000-10,000 Years	
10.6-6	COYOTE Problem 5.2 - Salt - Temperature Contours	
10.6-7	COYOTE Problem 5.2 - Salt - Temperature Rise (100-1,000 Years) Along Pillar Centerline	
10.7-1	COYOTE Problem 6.3 - Finite Element Mesh	
10.7-2	COYOTE Problem 6.3 - Program Subroutine Summary	
10.7-3	COYOTE Problem 6.3 - Temperature History	
10.7-4	COYOTE Problem 6.3 - Radial Temperature Distribution on Day 260 at 4.5m Depth Below Repository Floor	
10.7-5	COYOTE Problem 6.3 - Vertical Temperature Profiles on Day 260	
10.7-6	COYOTE Problem 6.3 - Radial Temperature Distribution on Day 350 at 4.25m Depth Below Repository Floor	

## LIST OF FIGURES (Cont'd)

<u>Figure</u>	<u>Title</u>	<u>Page</u>
7.2-9	MATLOC Problem 3.2a - Run #2 - Minor Principal Stresses Along a Line 30 Degrees from Horizontal	
7.3-1	MATLOC Problem 6.3 - Finite Element Mesh	
7.3-2	MATLOC Problem 6.3 - Vertical Displacement History for Point E04	
7.3-3	MATLOC Problem 6.3 - Vertical Displacement History for Point E02	
7.3-4	MATLOC Problem 6.3 - Horizontal Displacement History for Point E02	
8.2-1	VISCOT Problem 3.2b - Finite Element Mesh	
8.2-2	VISCOT Problem 3.2b - Circumferential Stress Along A Line 30 Degrees From Horizontal	
8.2-3	VISCOT Problem 3.2b - Radial Stress Along a Line 30 Degrees from Horizontal	
8.2-4	VISCOT Problem 3.2b - Longitudinal Stress along a Line 30 Degrees from Horizontal	
8.3-1	VISCOT Problem 3.3c - Finite Element Mesh	
8.3-2	VISCOT Problem 3.3c - Circumferential Stress Along A Line 30 Degrees from Horizontal	
8.3-3	VISCOT Problem 3.3c - Radial Stress along a Line 30 Degrees from Horizontal	
8.3-4	VISCOT Problem 3.3c - Longitudinal Stress Along a Line 30 Degrees from Horizontal	
8.4-1	VISCOT Problem 3.5 - Finite Element Mesh	
8.5-1	VISCOT Problem 5.2B - Finite Element Mesh	
8.5-2	VISCOT Problem 5.2B - Program to Redefine Nodal Temperatures	
8.5-3	VISCOT Problem 5.2B - Major Principal Stress	
8.5-4	VISCOT Problem 5.2B - Minor Principal Stress	
8.5-5	VISCOT Problem 5.2B - Horizontal Displacement	

LIST OF FIGURES (Cont'd)

<u>Figure</u>	<u>Title</u>	<u>Page</u>
6.3-1	DOT Problem 5.2 - Basalt and Salt - Finite Element Mesh	
6.3-2	DOT Problem 5.2 - Basalt - Temperature History 0 to 100 Years	
6.3-3	DOT Problem 5.2 - Basalt - Temperature History 100-1,000 Years	
6.3-4	DOT Problem 5.2 - Basalt - Temperature History 1,000-10,000 Years	
6.3-5	DOT Problem 5.2 - Basalt - Temperature Contours	
6.3-6	DOT Problem 5.2 - Basalt - Temperature Rise Along Pillar Centerline (100-1,000 Years)	
6.4-1	DOT Problem 5.2 - Salt - Temperature History 0-100 Years	
6.4-2	DOT Problem 5.2 - Salt - Temperature History 100-1,000 Years	
6.4-3	DOT Problem 5.2 - Salt - Temperature History 1,000-10,000 Years	
6.4-4	DOT Problem 5.2 - Salt - Temperature Contours	
6.4-5	DOT Problem 5.2 - Salt - Temperature Rise Along Pillar Centerline (100-1,000 Years)	
6.5-1	DOT Problem 6.1P - Finite Element Mesh	
6.5-2	DOT Problem 6.1A - Finite Element Mesh	
6.5-3	DOT Problem 6.1P - Room 3 - Temperature History at Various Offsets at Mid-Heater Depth	
6.5-4	DOT Problem 6.1P - Room 3 - Horizontal Temperature Profiles Day 690	
6.5-5	DOT Problem 6.1P - Temperature Contours Below Room 3	
6.5-6	Project Salt Vault Field Values - Room 4 Temperature History at Various Offsets at Mid-Heater Depth	

LIST OF FIGURES (Cont'd)

<u>Figure</u>	<u>Title</u>	<u>Page</u>
3.4.1-1	Plan of Project Salt Vault Experimental Area (From Ratigan and Callahan, 1978)	
3.4.1-2	Project Salt Vault Field Test - Location of Sections A-A and B-B	
3.4.1-3	Project Salt Vault - Field Test as Used in Models - Problem 6.1	
4.2-1	ADINA Problem 3.2b - Finite Element Mesh	
4.2-2	ADINA Problem 3.2b Circumferential Stress Along a Line 30 Degrees Above Horizontal	
4.2-3	ADINA Problem 3.2b Radial Stress Along a Line 30 Degrees Above Horizontal	
4.2-4	ADINA Problem 3.2b Longitudinal Stress Along a Line 30 Degrees Above Horizontal	
4.3-1	ADINA Problem 3.3c - Finite Element Mesh	
4.3-2	ADINA Problem 3.3c Circumferential Stress Along a Line 30 Degrees Above Horizontal	
4.3-3	ADINA Problem 3.3c Radial Stress Along a Line 30 Degrees Above Horizontal	
4.3-4	ADINA Problem 3.3c Longitudinal Stress Along a Line 30 Degrees Above Horizontal	
4.4-1	ADINA Problem 3.5 - Finite Element Mesh	
5.2-1	ADINAT Problem 2.6 - Finite Element Mesh	
5.2-2	ADINAT Problem 2.6 Y-Axis Temperature Profiles at Time = 400,000 sec	
5.2-3	ADINAT Problem 2.6 Z-Axis Temperature Profiles at Time - 400,000 sec	

LIST OF FIGURES (Cont'd)

<u>Figure</u>	<u>Title</u>	<u>Page</u>
2.11-2	Problem 5.2S - Comparison of Codes DOT & COYOTE Percentage Difference Between Code Temperatures - 100 to 1000 Years	
2.11-3	Problem 5.2S - Comparison of Codes DOT & COYOTE Percentage Difference Between Code Temperatures - 1000 to 10,000 Years	
2.13-1	Problem 6.1 - Project Salt Vault Comparison of Codes ADINAT & DOT Average Temperature History at Various Depths	
2.13-2	Problem 6.1 - Project Salt Vault Comparison of Codes ADINAT & DOT Average Temperature History at Various Offsets	
2.13-3	Problem 6.1 - Project Salt Vault Comparison of Codes ADINAT & DOT Horizontal Temperature Profiles at Day 690	
2.14-1	Problem 6.3 - BWIP - Comparison of Codes DOT & COYOTE Radial Temperatures on Day 260	
2.14-2	Problem 6.3 - BWIP - Comparison of Codes DOT & COYOTE Temperature History at Mid Heater Offset 0.4M	
2.14-3	Problem 6.3 - BWIP - Comparison of Codes DOT & COYOTE Vertical Temperature Profiles on Day 260	
2.14-4	Problem 6.3 - BWIP - Comparison of Codes VISCOT & MATLOC Vertical Displacement at E02	
2.14-5	Problem 6.3 - BWIP - Comparison of Codes VISCOT & MATLOC Vertical Displacement at E04	
2.14-6	Problem 6.3 - BWIP - Comparison of Codes VISCOT & MATLOC Horizontal Displacement at E03	

## LIST OF TABLES

<u>Table</u>	<u>Title</u>	<u>Page</u>
3.1.2-1	Solution to Benchmark Problem 2.8 (From Kreith, 1958)	
3.1.4-1	Analytical Solution to Benchmark Problem 2.10	
3.4.1-1	Time History of Project Salt Vault (Bradshaw and McClain, 1971)	
5.1-1	ADINAT Capabilities Tested or Utilized	
5.2-1	Time Steps Used with ADINAT for Problem 2.6	
5.2-2	Solution Comparison for ADINAT Problem 2.6	
5.3-1	Benchmark Problem 2.8 Solution Comparison	
5.4-1	Time Steps Used with ADINAT in Benchmark Problem 2.9	
5.6-1	Conductivity and Specific Heat for ADINAT Problem 5.2 - Basalt	
5.6-2	Convection Coefficients for ADINAT Problem 5.2 - Basalt	
5.6-3	Externally Supplied Heat Flux for ADINAT Problem 5.2 - Basalt	
5.6-4	Effective Nodal Areas for Heat Flux Function for ADINAT Problem 5.2 - Basalt	
5.7-1	Time History of Project Salt Vault	
5.7-2	Conductivity for ADINAT Problems 6.1P and 6.1A	
5.7-3	Externally Supplied Heat Flux Functions for ADINAT Problems 6.1P and 6.1A	
5.7-4	Effective Area Factors for ADINAT Problems 6.1P and 6.1A	
6.1	DOT Capabilities Tested or Utilized	
6.2-1	Conductivity and Specific Heat for DOT - Problem 2.6	
6.2-2	Comparison of Solutions for DOT - Problem 2.6	

LIST OF TABLES (Cont'd)

<u>Table</u>	<u>Title</u>	<u>Page</u>
10.3-1	Solution Comparison for COYOTE Problem 2.8	
10.4-1	Time Steps Used by COYOTE Problem 2.9	
10.6-1	Time Step Data Used by COYOTE Problem 5.2S	
10.7-1	Time History of BWIP Heater Test #2 for COYOTE Problem 6.3	
10.7-2	Internal Heat Generation Function for COYOTE Problem 6.3	
10.7-3	Time Step Data Used for COYOTE Problem 6.3	

## 1.0 INTRODUCTION

## 1.0 INTRODUCTION

### 1.1 Purpose of This Report

The effective management of high-level radioactive wastes is essential to protect public health and safety. The Department of Energy (DOE), through responsibilities inherited from the Energy Research and Development Administration (ERDA) and the Atomic Energy Commission (AEC), is responsible for the safe disposal of these wastes. The Nuclear Regulatory Commission (NRC), through authority granted it by the Energy Regulation Act of 1974 that created the NRC, is responsible for the regulation of high-level waste management.

The Environmental Protection Agency (EPA) has the authority and responsibility for setting generally applicable standards for radiation in the environment. The NRC is responsible for implementing these standards in its licensing actions and assuring that public health and safety are protected. Although only a draft EPA standard for disposal of high-level radioactive wastes (HLW) exists, the NRC has proposed technical criteria for regulating geologic disposal of HLW. These proposed technical criteria have been developed to be compatible with the draft EPA Environmental Standard. The 10 CFR 60 performance objectives and criteria address the functional elements of geologic disposal of HLW and the analyses required to give confidence that these functional elements will perform as intended.

In discharging its responsibility, the NRC must review DOE performance assessments and independently evaluate the performance of the repository(ies) that DOE seeks to have NRC license. Because of the complexity and multiplicity of these performance assessments, computerized simulation modeling is used. Computer simulation models provide a framework incorporating the most important processes that will be active in a repository, thereby permitting assessment of repository behavior. The time frames associated with high-level waste management, ranging from decades to thousands of years, also necessitate the use of models.

To meet this demand, the NRC is evaluating and using models and computer codes for supporting these regulations and for performing reviews of proposed nuclear waste management systems. The DOE is also independently developing models and computer codes to assess repository sites and designs. As part of model and code development, a procedure for independent evaluation of the reliability of these models and codes is required. Codes must be evaluated to determine the limitations of theories and the reliability of supporting empirical relationships and laboratory tests used for evaluation of long-term repository performance.

### 1.2 Scope of This Report

This report is part of a series of reports dealing with the evaluation of computer models used for repository performance assessment. The models used for repository performance assessment have been divided into

NUREG/CR-3586 - "Parameters and Variables Appearing in Repository Design Models", December 1983.

NUREG/CR-3636 - "Benchmark Problems for Repository Design Models", February 1984.

This report summarizes the benchmarking of selected repository design codes.

Among the processes which must be considered in repository design are: (1) heat transfer; (2) geomechanical stresses and displacements; (3) ground water flow, for both saturated and unsaturated conditions in both porous and fractured media; (4) solute transport; (5) geochemistry; and (6) ventilation of the repository during construction and the initial operating phase. The emphasis of this report is on heat transfer and geomechanical and thermomechanical stresses. Ground water flow, solute transport and geochemistry have been considered with the repository siting parameters (Mercer et al., 1982) and therefore were not considered in this study. Ventilation is considered a secondary process and, as such, was not considered individually with the benchmark problems. Ventilation was included in this study only as a boundary condition in hypothetical design models.

Heat transfer analysis is required to ensure that the temperature rise in the initial period of repository performance can be controlled to allow retrieval of wastes within 50 years, if required. For the longer term performance of the repository systems, limitations on maximum temperatures will be required to limit degradation or physical or chemical changes to the medium, waste package canister, or engineered barriers.

Heat transfer phenomena considered include conduction through isotropic and anisotropic materials subjected to convection and radiation boundary conditions. Thermal analysis may include either steady state or transient conditions and may be either linear or nonlinear. Nonlinear codes are used to model materials with temperature-dependent properties, such as specific heat or thermal conductivity, and heat flow with nonlinear boundary conditions. Results of thermal analyses in the form of temperature distributions are used as input to stress analysis codes.

Geomechanical analyses are required to determine the redistribution of stresses around a repository, the deformations associated with these stresses and the overall stability of the openings. Stresses computed from the geomechanical analyses may be due to the initial stresses, excavation geometry, thermal loads, blast loads and/or earthquake loads. Both static and dynamic analyses must be considered for linear as well as nonlinear material behavior to assess stability during the construction and operational phases, both prior to repository sealing and during long-term storage of wastes.

Ground water analyses are used to determine the potential for transport of radionuclides to the accessible environment and thus assess the ultimate performance of the repository. Although ground water flow around a repository is most accurately modeled by the interactive consideration of heat transfer, stress, and flow effects, such a model would require a

section, the background and capabilities of the code considered are described, followed by a discussion of each benchmark problem modeled with the code. The following standard format has been developed for the discussion of the solution of a benchmark problem with a particular code:

- Problem Statement
- Input Data
- Run Problem
- Results

The problem statement is a brief description of the benchmark problem, included to familiarize the reader with the objectives of the model. Detailed problem descriptions are included in Section 2.

The input data section describes the physical and material properties used in modeling the problem with the specific code. In most cases, the input data were derived from the Benchmark Problems Report. Time-step data and various solution schemes considered, as well as necessary modifications to the input data, are discussed in the "run problem" section. The results are presented with discussions of code restrictions and difficulties encountered in running the problem.

### 1.3 Previous Work

The most extensive testing of the codes benchmarked was done during the development of the individual codes. Documentation available with most codes generally contains a minimum of two or three, and up to as many as 100, problems which have been solved by the code and checked against analytical solutions. These verification problems almost always show excellent agreement with theoretical problems simply because these are the type of problems used during development of the code. In addition, the developers will likely be more familiar with code capabilities than any of the future users and can thus set up a problem consistent with the solution method.

Although most of the routines in a code have been tested by the developer before its release, the codes should be tested by an independent user on independently developed problems, as in this study. Previous studies which have had this as an objective include the following:

- Sandia National Laboratories developed two benchmark problems for testing repository design codes. One problem deals with a repository in salt, and was run using nine structural codes including ANSALT, DAPROK, JAC, two implementations of MARC, REM, SANCHO, SPECTROM, and STEALTH (Morgan et al., 1981);
- The Office of Nuclear Waste Isolation (ONWI), compared the results of SPECTROM, a finite element code, and STEALTH, a finite difference code, for identical viscoelastic repository design problems (Wagner, 1982);
- As part of the SCEPTER project, ONWI has presented and coded several analytical problems which include infinite series in their solutions (INTERA, 1983); and

## 2.0 SUMMARY OF FINDINGS

## 2.0 SUMMARY OF FINDINGS

### 2.1 Introduction

This section compares the results of the codes benchmarked on a problem-by-problem basis. If analytical or field results exist for the problem, they have been added to the comparison. Each comparison consists of a brief problem statement outlining the type of problem and the limiting factors. A more descriptive summary of the problem is in Section 3. The second part of the comparison describes the model used for each code and any code-related problems that may have arisen while the code was executing. The concluding paragraphs compare the results of the individual codes to each other and to any analytical or field results.

Unless only one code was used for a problem, each section includes a set of graphs showing the comparison of the different codes. If only one code was applicable to the problem, the section for that code is indicated.

as field validation or hypothetical design models, a reduction in error comparable to that observed in this problem would be associated with a much larger increase in computational costs.

# PROBLEM 2.6 — COMPARISON OF CODES

Y - AXIS TEMPERATURES AT 400,000 sec.

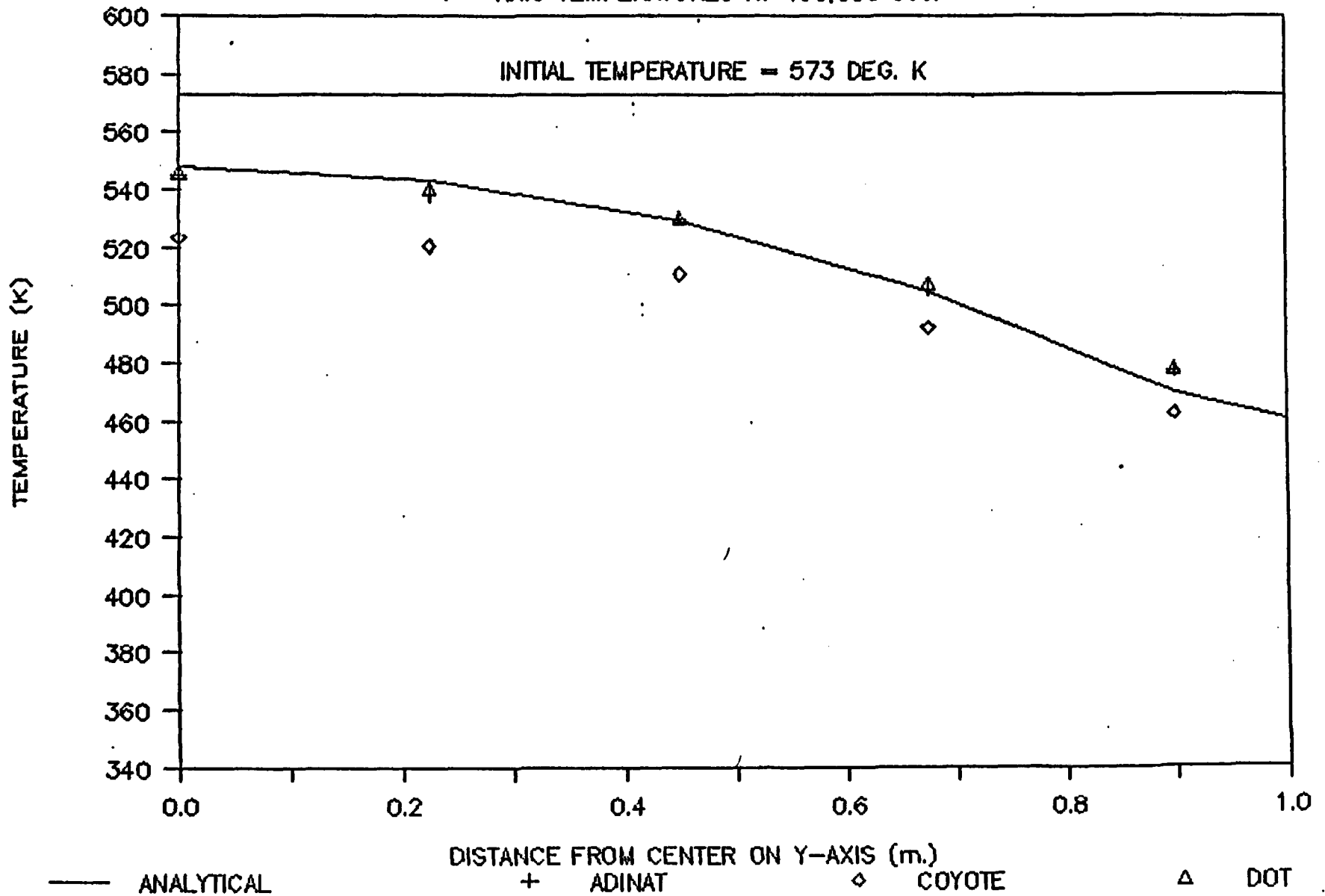


Figure 2.2-2 Problem 2.6 - Comparison of Codes ADINAT, COYOTE & DOT  
Y-Axis Temperatures at 400,000 sec

# PROBLEM 2.6 - COMPARISON OF CODES

Y - AXIS TEMP. ERRORS AT t=400,000 sec.

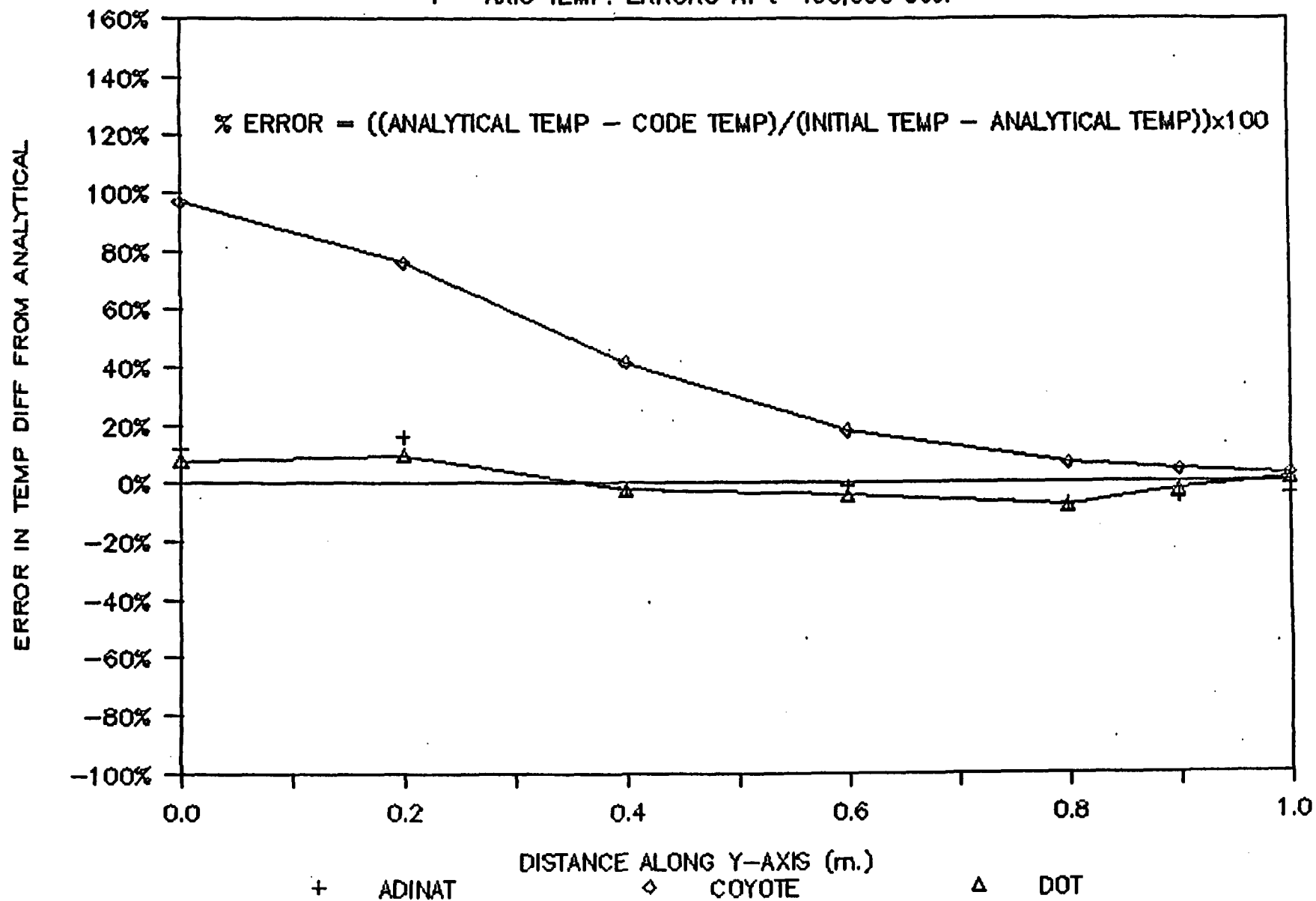


Figure 2.2-4 Problem 2.6 - Comparison of Codes ADINAT, COYOTE & DOT  
Y-Axis Temperature Errors At T=400,000 secs

# PROBLEM 2.8 — COMPARISON OF CODES

TEMPERATURE HISTORY AT QUENCH SURFACE

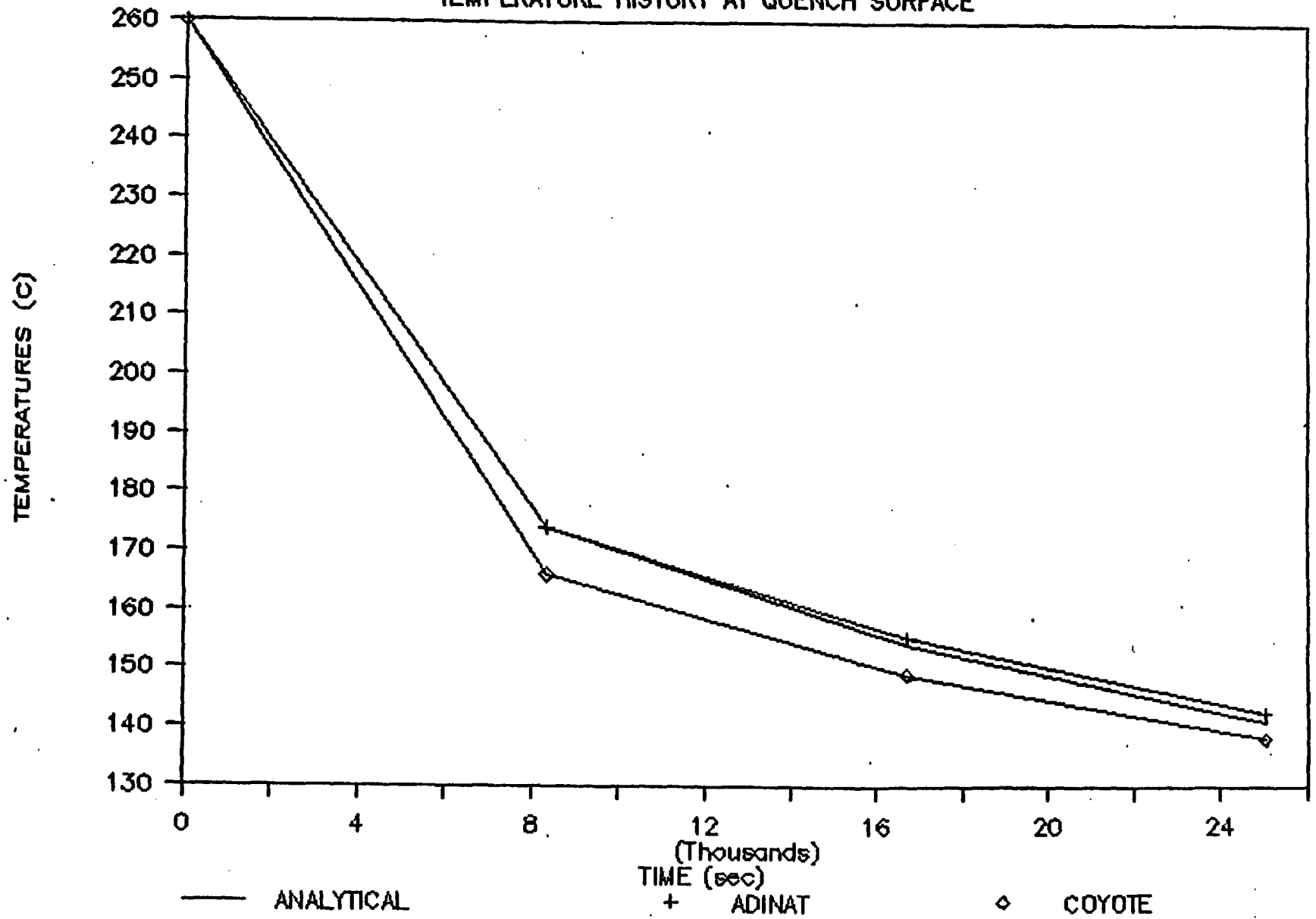


Figure 2.3-1 Problem 2.8 - Comparison of Codes ADINAT and COYOTE Temperature History at Quench Surface

## 2.4 Problem 2.9 - Transient Temperature Response of a Slab Exposed to a Uniform Radiative Environment

Problem Statement - This problem is concerned with the transient thermal analysis of an infinite slab, 0.25 m thick. The slab is initially at 546°K, one face is insulated, and the other is exposed to a radiative environmental temperature of 273°K at time zero. The temperature histories of both sides of the slab are to be determined.

Problem Comparison - Both ADINAT and COYOTE were evaluated with this problem. To model this problem, two different sets of elements were used. COYOTE was executed first, with a single row of two-dimensional conduction elements. When ADINAT was run, the same model caused excessive numerical noise and distorted the results. The problem was therefore modeled using 5 rows of 8-noded, two-dimensional conduction elements.

Except for the problem with the model for ADINAT, there was no code-related difficulties encountered while running Problem 2.9.

Figures 2.4-1 and 2.4-2 compare the temperature histories calculated by ADINAT and COYOTE to the analytical solution of the radiative and insulated faces, respectively. The results from the codes compare favorably with the analytical solutions.

# PROBLEM 2.9 — COMPARISON OF CODES

TEMPERATURE HISTORY AT INSULATED FACE

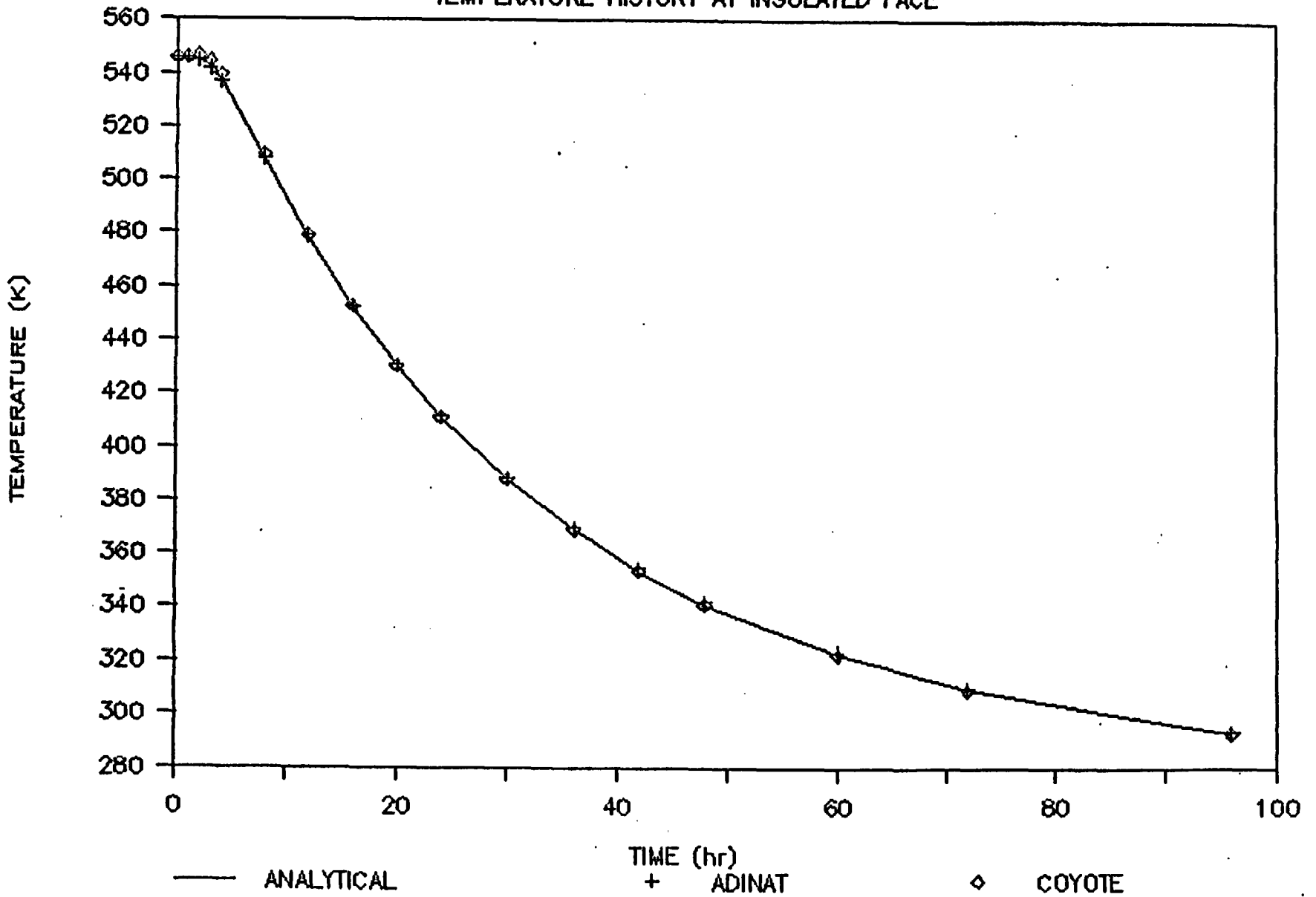


Figure 2.4-2 Problem 2.9 - Comparison of Codes ADINAT & COYOTE  
Temperature History at Insulated Face

**2.6 Problem 3.2a - Unlined Circular Tunnel  
(Long Cylindrical Hole) in an Infinite Elastic  
Medium With a Biaxial Stress Field**

Problem Statement - This problem concerns the stress distribution around a long circular tunnel, with a radius of 5 m, through an infinite elastic medium subjected to a biaxial stress field. Horizontal and vertical symmetry conditions allow reduction of the model to one quadrant of the circle, so long as displacements across the symmetry lines are prohibited. The outer model boundaries must be at a sufficient distance from the opening such that the principal stresses correspond to the biaxial loading directions.

Problem Comparison - Only one code, MATLOC, was used to model this problem. Refer to Section 7.2 for discussion and results.

# PROBLEM 3.2B - COMPARISON OF CODES

CIRCUMFERENTIAL STRESS IN MPa

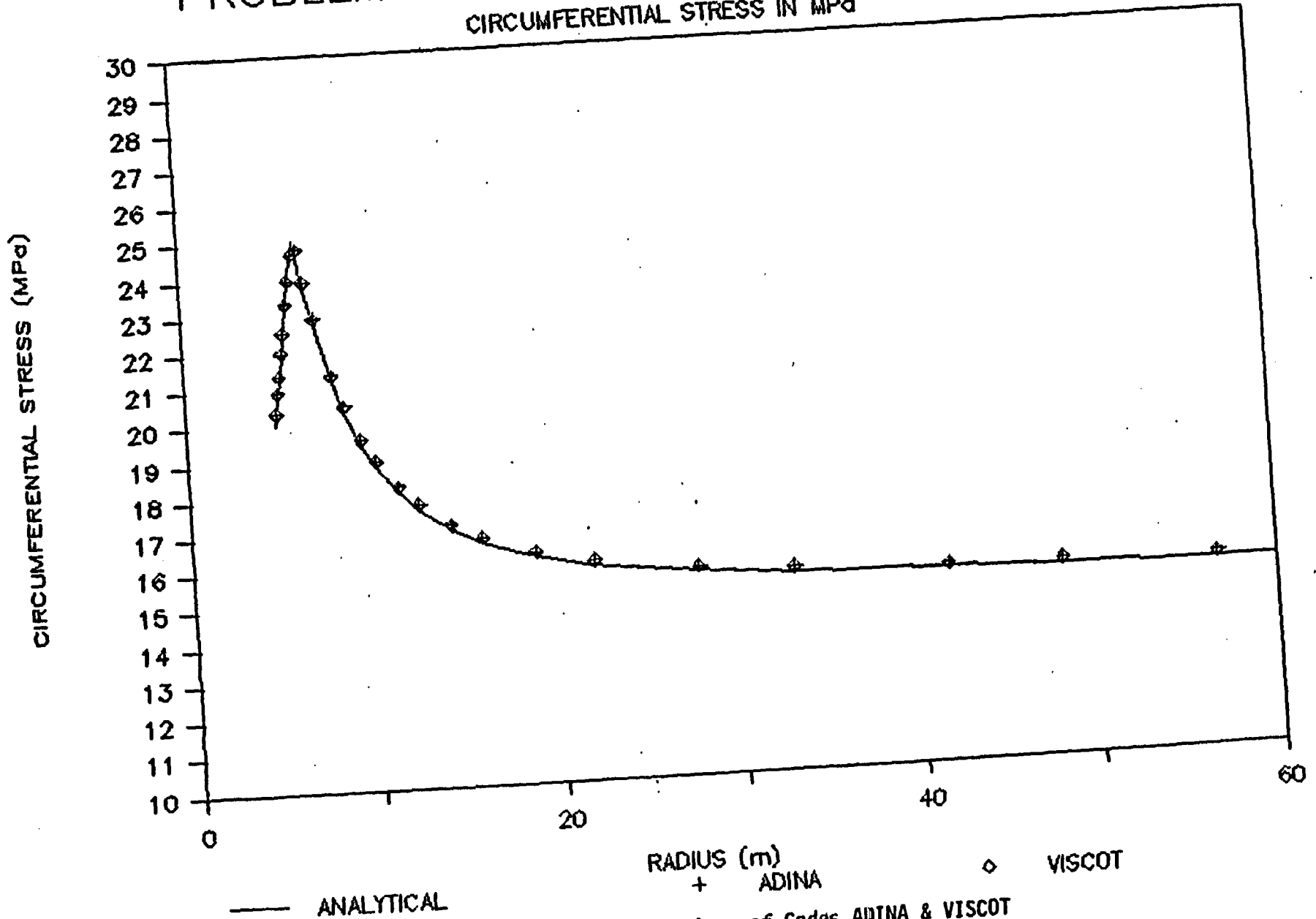


Figure 2.7-1 Problem 3.2B - Comparison of Codes ADINA & VISCOT  
Circumferential Stress

# PROBLEM 3.2B — COMPARISON OF CODES

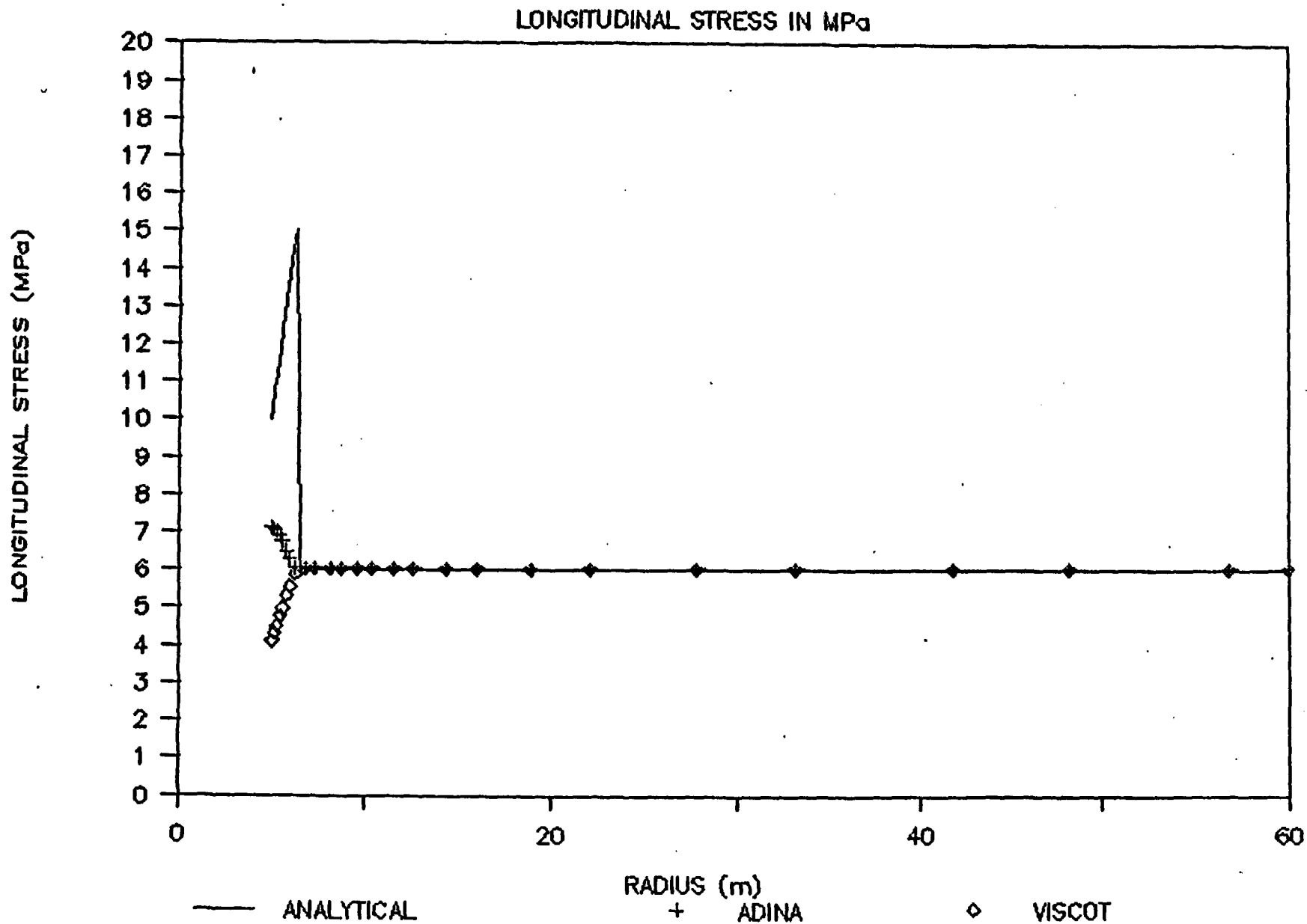


Figure 2.7-3 Problem 3.2B - Comparison of Codes ADINA & VISCOT  
Longitudinal Stress

# PROBLEM 3.3C – COMPARISON OF CODES

CIRCUMFERENTIAL STRESS IN MPa

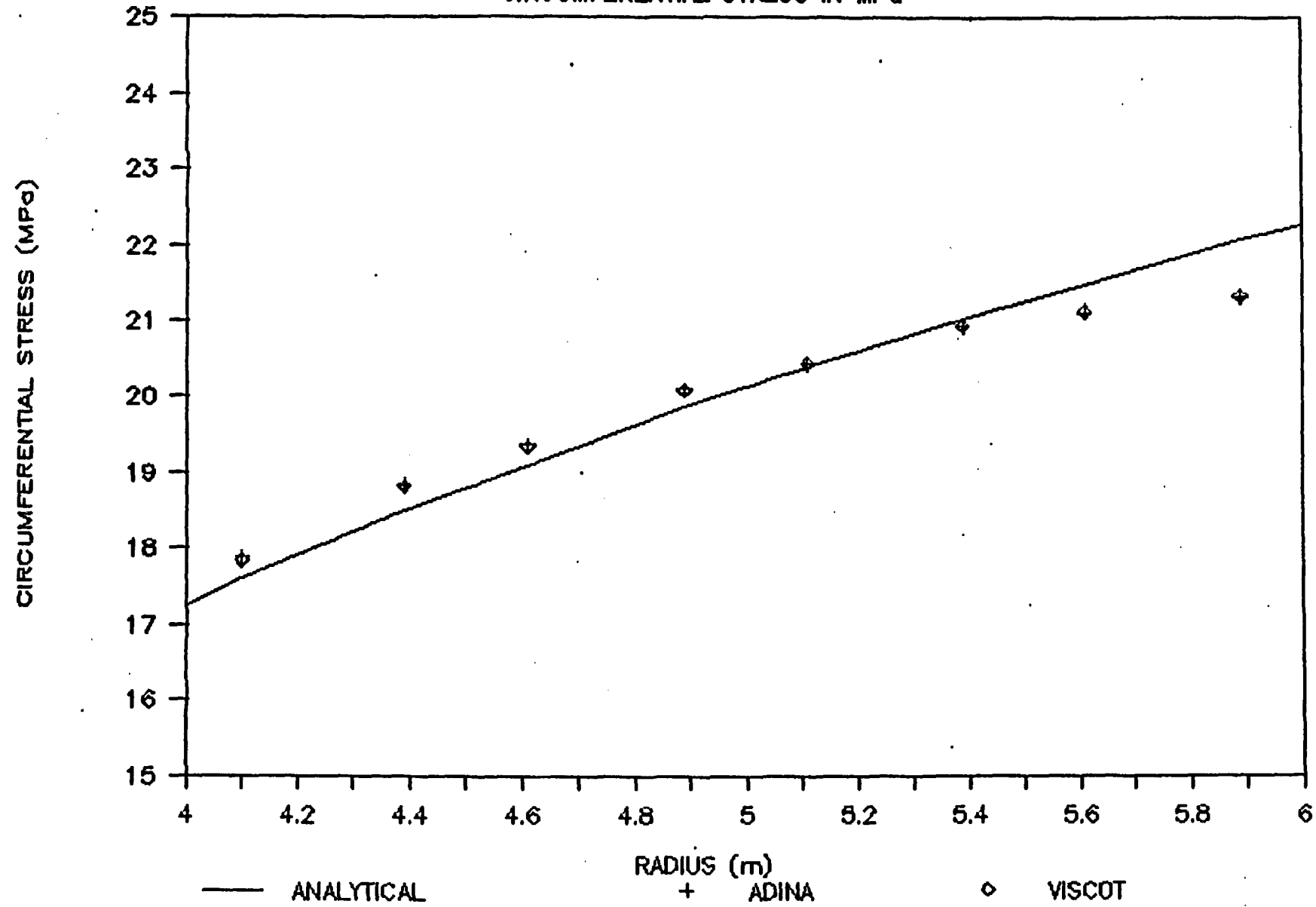


Figure 2.8-1 Problem 3.3C - Comparison of Codes ADINA & VISCOT Circumferential Stress

# PROBLEM 3.3C – COMPARISON OF CODES

LONGITUDINAL STRESS IN MPa

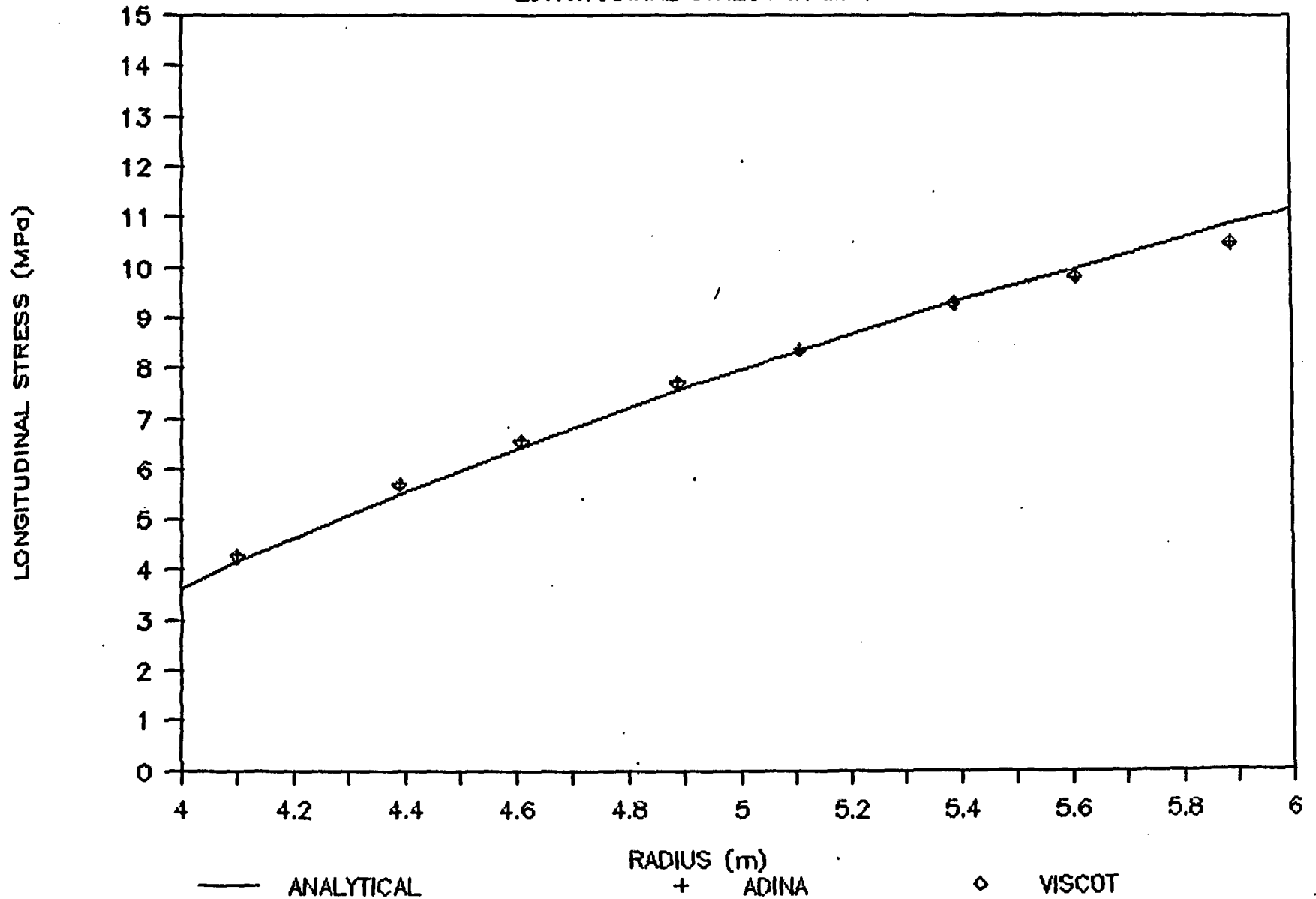


Figure 2.8-3 Problem 3.3C - Comparison of Codes ADINA & VISCOT  
Longitudinal Stress

## 2.10 Problem 5.2b - Hypothetical Near Field Problem - Basalt

Problem Statement - This problem consists of a transient thermal simulation of the near field (single room region) of a hypothetical repository located in basalt. Waste canisters, which are emplaced vertically below the room floor at regular intervals along the centerline, have been replaced for this analysis by an equivalent heat generating trench. This problem exercises general transient heat transfer with mechanisms of conduction, heat storage, radiation, and free and forced (ventilation) convection. The room is ventilated for the first 50 years, after which the room is sealed, and natural convection and radiation occur. This problem, and the accompanying very near field and far field problems of the same repository, are summarized in greater detail in Section 3.3.

Problem Comparison - Four codes were determined to be applicable to this problem, ADINAT, DOT, MATLOC, and VISCOT. All four codes used approximately the same model, a two-dimensional section through the repository. The model extended from the ground surface to a depth of -3500 m, and consisted of 8-noded isoparametric planar elements and 2-noded convection elements. Most of the elements were located between depths of -479 m and -510 m. The elements outside this region were "filler" elements with vertical dimensions approximately 1.5 to 2.0 times the vertical dimension of the preceding element.

This mesh had to be modified to accommodate VISCOT. In the other codes, triangular elements are defined by specifying the same node more than once. To get VISCOT to execute, nodes which overlapped in the standard mesh were replaced by a pair of very close nodes.

No code-related difficulties were encountered while running Problem 5.2b with DOT, MATLOC or VISCOT. It was not possible to successfully execute the problem with ADINAT. The reasons for this are discussed in Section 5.6. The solutions for DOT, MATLOC and VISCOT are all expressed in different forms, either graphed or drawn as contour lines making a direct comparison of the results obtained by the three codes impossible.

# PROBLEM 5.2S - COMPARISON OF CODES

PERCENT DIFF IN TEMP - YRS 0 TO 100

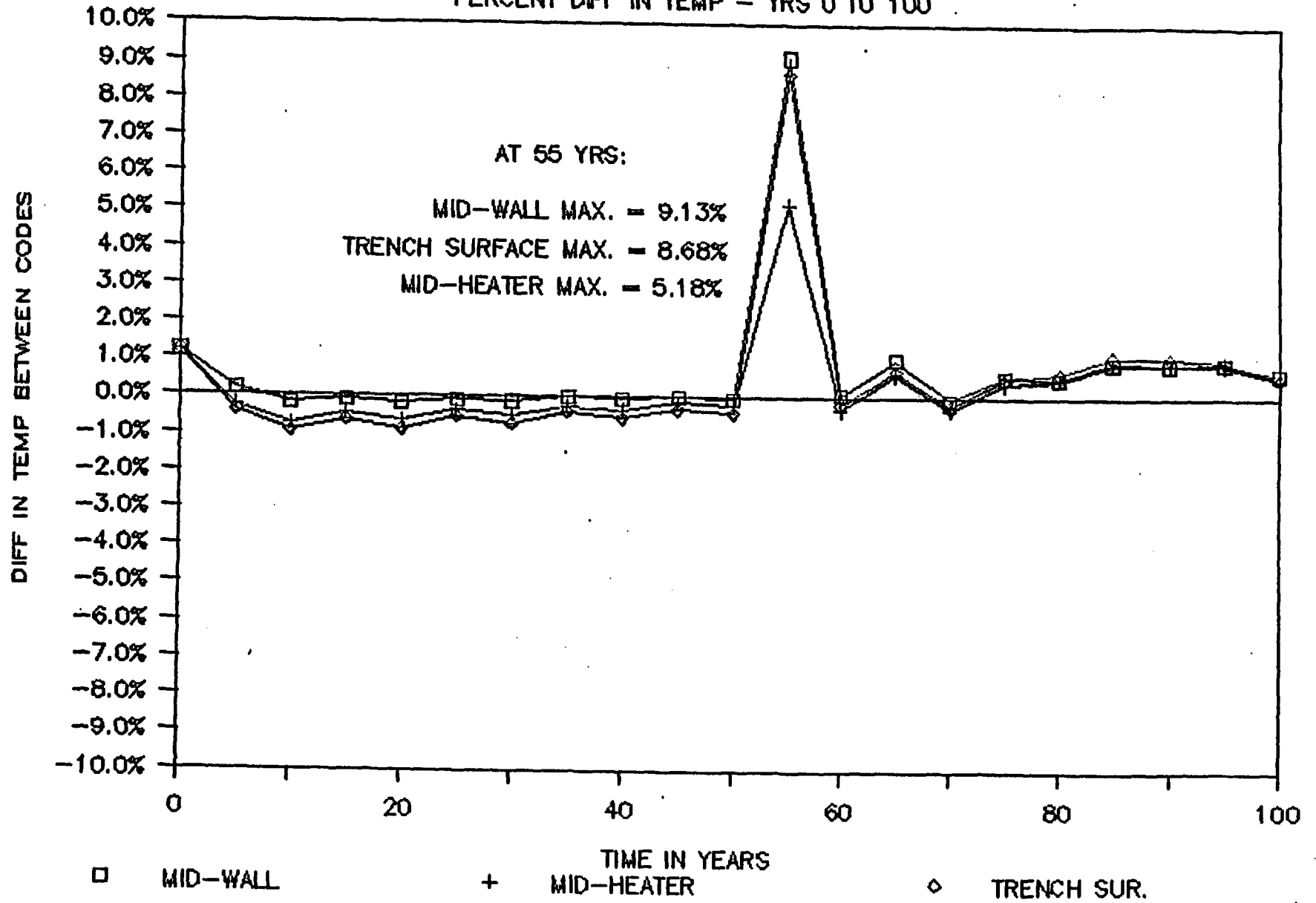


Figure 2.11-1 Problem 5.2S - Comparison of Codes DOT & COYOTE  
 Percentage Difference Between Code Temperatures - 0 to 100 Years

# PROBLEM 5.2S - COMPARISON OF CODES

PERCENT DIFF IN TEMP - YRS 1000 - UP

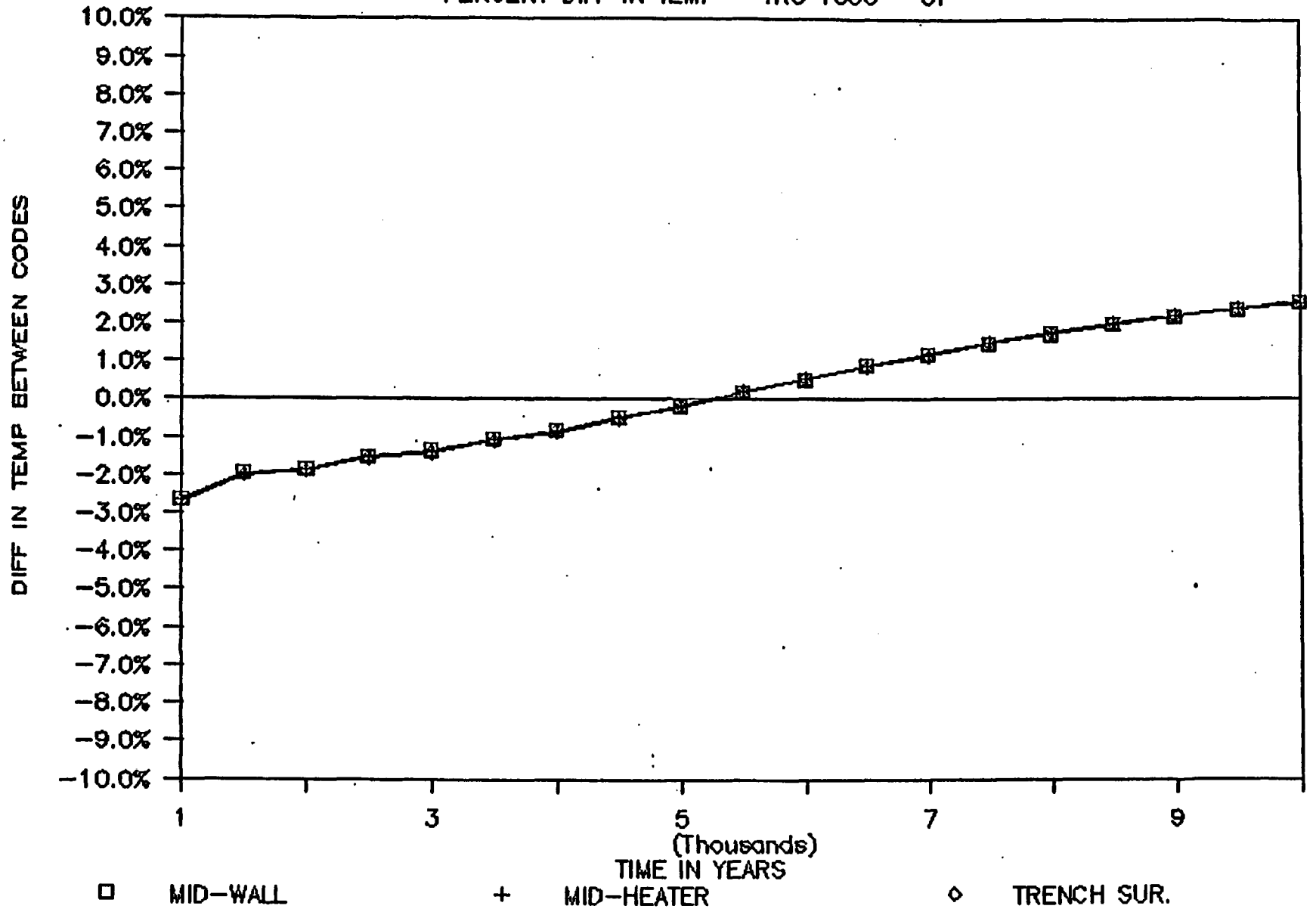


Figure 2.11-3 Problem 5.2S - Comparison of Codes DOT & COYOTE  
Percentage Difference Between Code Temperatures - 1000 to 10,000 Years

## 2.13 Problem 6.1 - Project Salt Vault Thermomechanical Response Simulation Problem

Problem Statement - Problem 6.1 concerns the analysis of two full-scale heater experiments performed simultaneously in adjacent rooms during Project Salt Vault (PSV). Heater experiments were conducted in four parallel rooms in PSV. A line of symmetry between Room 2 and Room 3 reduces the model to two rooms. The heater experiment in Room 3 consisted of a row of heaters parallel to the axis of the room, whereas the experiment in Room 4 involved a circular array of heaters.

Due to the differing geometric configurations of the heaters, the problem has been divided into two separate analyses. Problem 6.1P is a two-dimensional planar analysis of Room 3 and Problem 6.1A is a two-dimensional axisymmetric analysis of Room 4. The boundary between the two problems is located within the pillar between Rooms 3 and 4, one meter from the edge of Room 3. This location coincides with the lowest field-measured temperatures, and was chosen as a boundary to minimize the effect of the adjacent room.

Problem Comparison - No code-related difficulties were encountered while running Problem 6.1 with ADINAT, DOT or VISCOT. VISCOT was only used to execute Problem 6.1A, due to code limitations. The format of the VISCOT solution was not the same as the other two codes. See Section 8.7 for comparison of the field data.

The ADINAT and DOT solutions to Problem 6.1A were very similar. Figures 2.13-1 and 2.13-2 compare the average temperature histories from the benchmarked codes to the field results. Figure 2.13-1 compares the solutions at two depths below the room floor. Figure 2.13-2 compares the temperature histories at various offsets from the room center at mid-heater depth. The temperature histories from ADINAT and DOT are higher than the field data. The maximum temperatures in the axisymmetric model occurred on the last day of the experiment, Day 570.

Figure 2.13-3 compares the horizontal temperature profiles in Room 3 for Problem 6.1P. The temperature profiles are compared at floor surface, mid-heater height and 5.02 m below the floor surface on Day 690. The solution from DOT is higher than ADINAT.

# PROBLEM 6.1 (PSV) - COMPARISON OF CODES

TEMPERATURE HISTORY AT VARIOUS OFFSETS

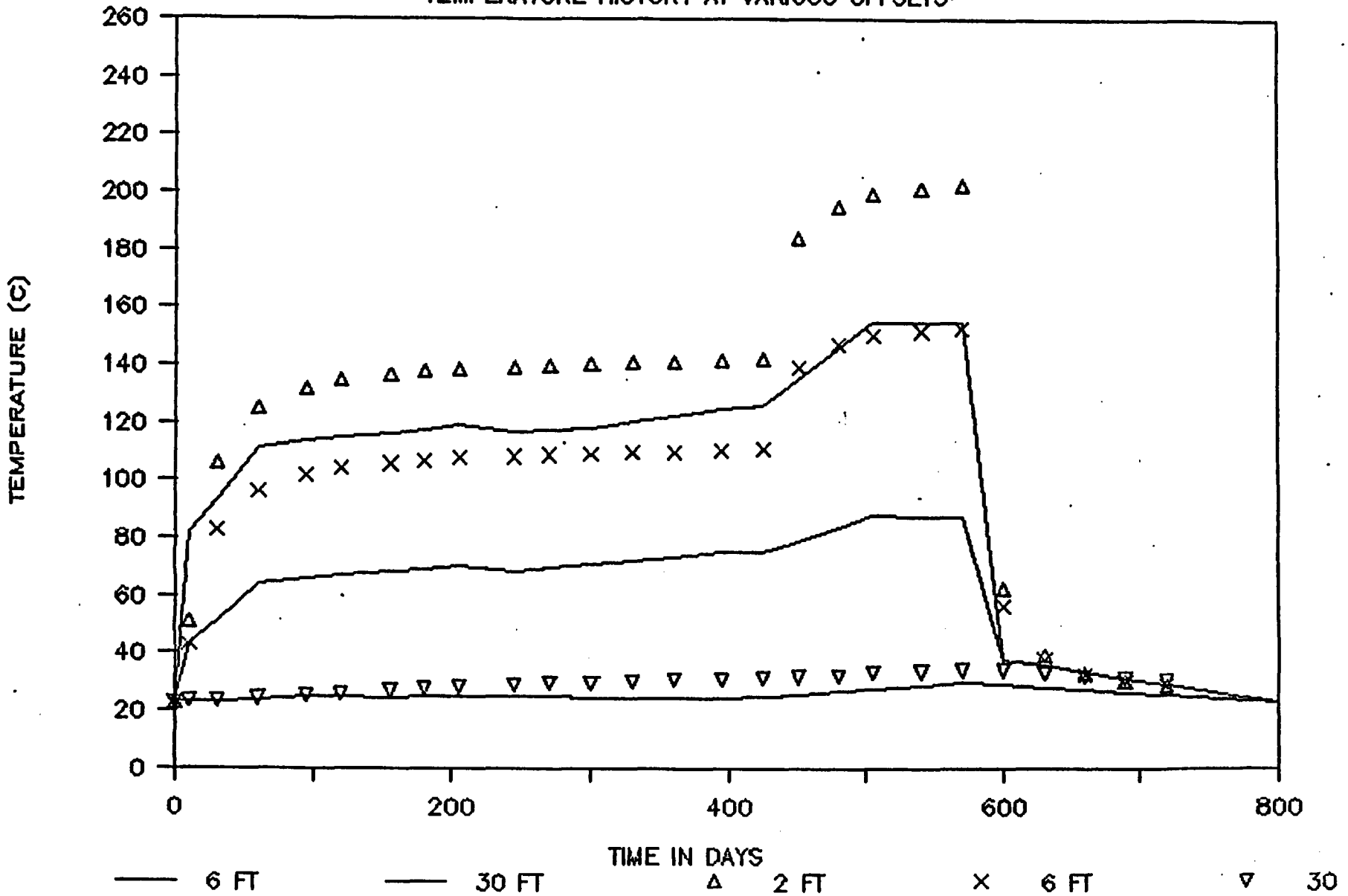


Figure 2.13-2 Problem 6.1 - Project Salt Vault Comparison Codes - ADINAT & DOT Average Temperature History at Various Offsets

## 2.14 Problem 6.3 - In Situ Heater Test - Basalt Waste Isolation Project (BWIP)

Problem Statement - This problem concerns the transient thermal simulation of basalt due to full-scale Heater Test 2, undertaken in 1980 at the Basalt Waste Isolation Project (BWIP), Hanford site near Richland, Washington. A single heater, vertically emplaced below the floor of a repository-type opening was operated for 527 days. During this time, the power level was incrementally increased to a maximum of 5 kW, as the thermal and mechanical response of the host rock was monitored. Laboratory-determined material properties of basalt accompany a detailed description of the problem in the Benchmark Problems Report. This description is summarized in Section 3.4.2.

Problem Comparison - ADINAT, DOT, MATLOC, VISCOT and COYOTE were applicable to Problem 6.3. Except for COYOTE, the problem was modelled using two-dimensional, 8-noded axisymmetric solid elements. The heater itself was modelled as a heat generating "solid" material with specific heat, density, and conductivity values for air. COYOTE used a finite element mesh comprised of 3, 4, 6, and 8-noded axisymmetric elements. The heater was modelled with the material properties of basalt. The axisymmetric model, which models a single heater in a circular repository, is not truly valid above the floor level. However, in the region below the floor level, where the temperatures will be compared to field measurements, the model is representative of actual conditions. Inclusion of the room and rock above the floor level provides a better representation of boundary conditions than if they had been excluded. Model boundaries are set at a distance where, based on the field data, adiabatic boundary conditions can be assumed.

No code-related difficulties were encountered while running Problem 6.3. Since this problem is a two-step problem, the initial results are temperature histories and profiles. There are two sets of comparisons used to determine displacements at chosen locations. The combination of codes used was: ADINAT/ADINA, DOT/MATLOC, DOT/VISCOT, and COYOTE. Due to problems in the codes, ADINAT/ADINA and COYOTE were never completed though a thermal run was completed for COYOTE.

Figures 2.14-1 through 2.14-3 compare the thermal runs of DOT and COYOTE to the measured field results. The solutions from the two codes are the same, and in general, compare well with the field results. Figures 2.14-4 through 2.14-6 compare the geostatic runs of MATLOC and VISCOT to the measured field results.

Field measured vertical displacements were specified at two depths, offset 1.24m from the heater centerline. These measurement points, E04 and E02, are 1m above and 1m below the heater, respectively. In both cases, the VISCOT results compare more favorably to the field results. Figure 2.14-6 compares the horizontal displacements at a point (E03),

# PROBLEM 6.3 BWIP - COMPARISON OF CODES

RADIAL TEMPERATURES ON DAY 260

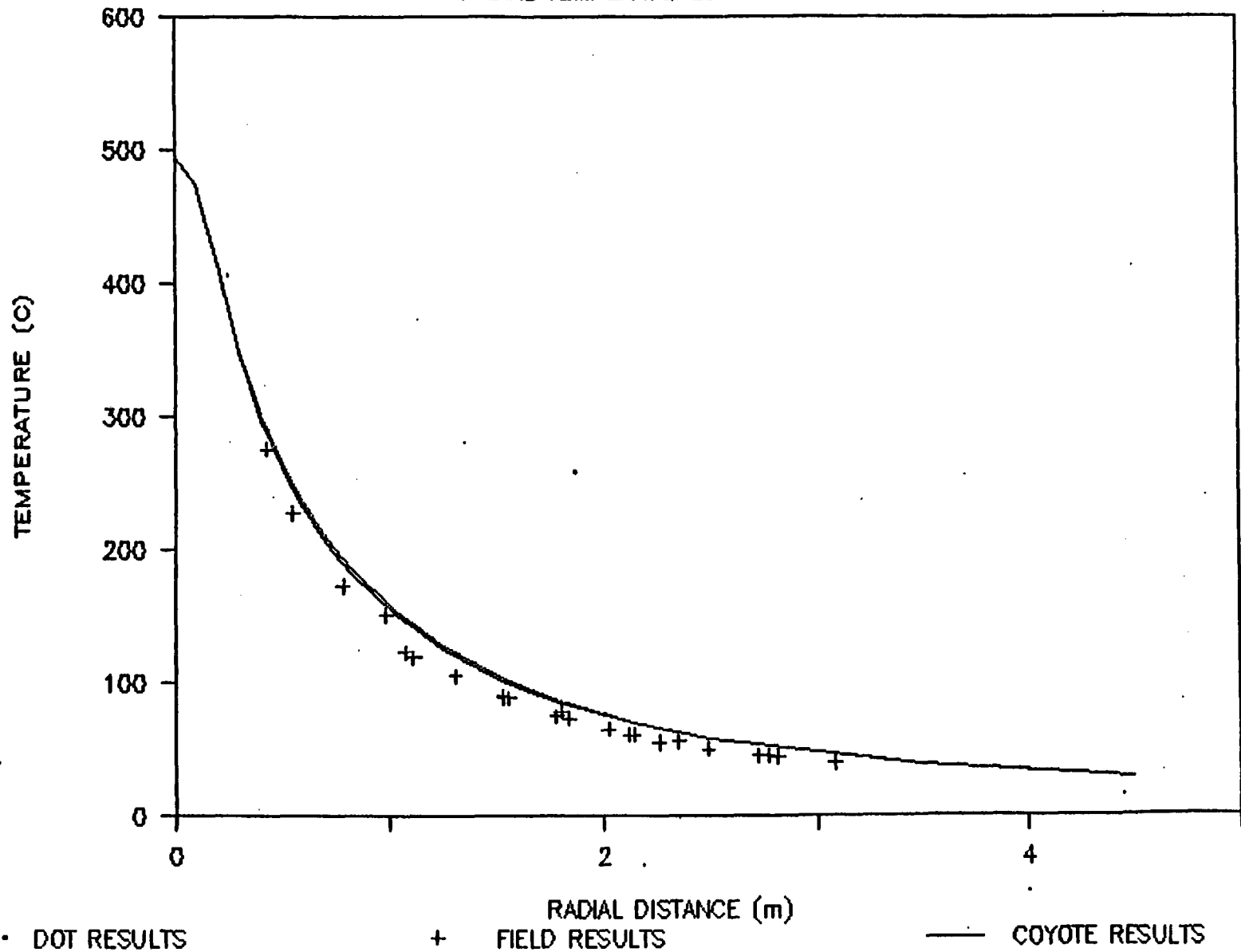
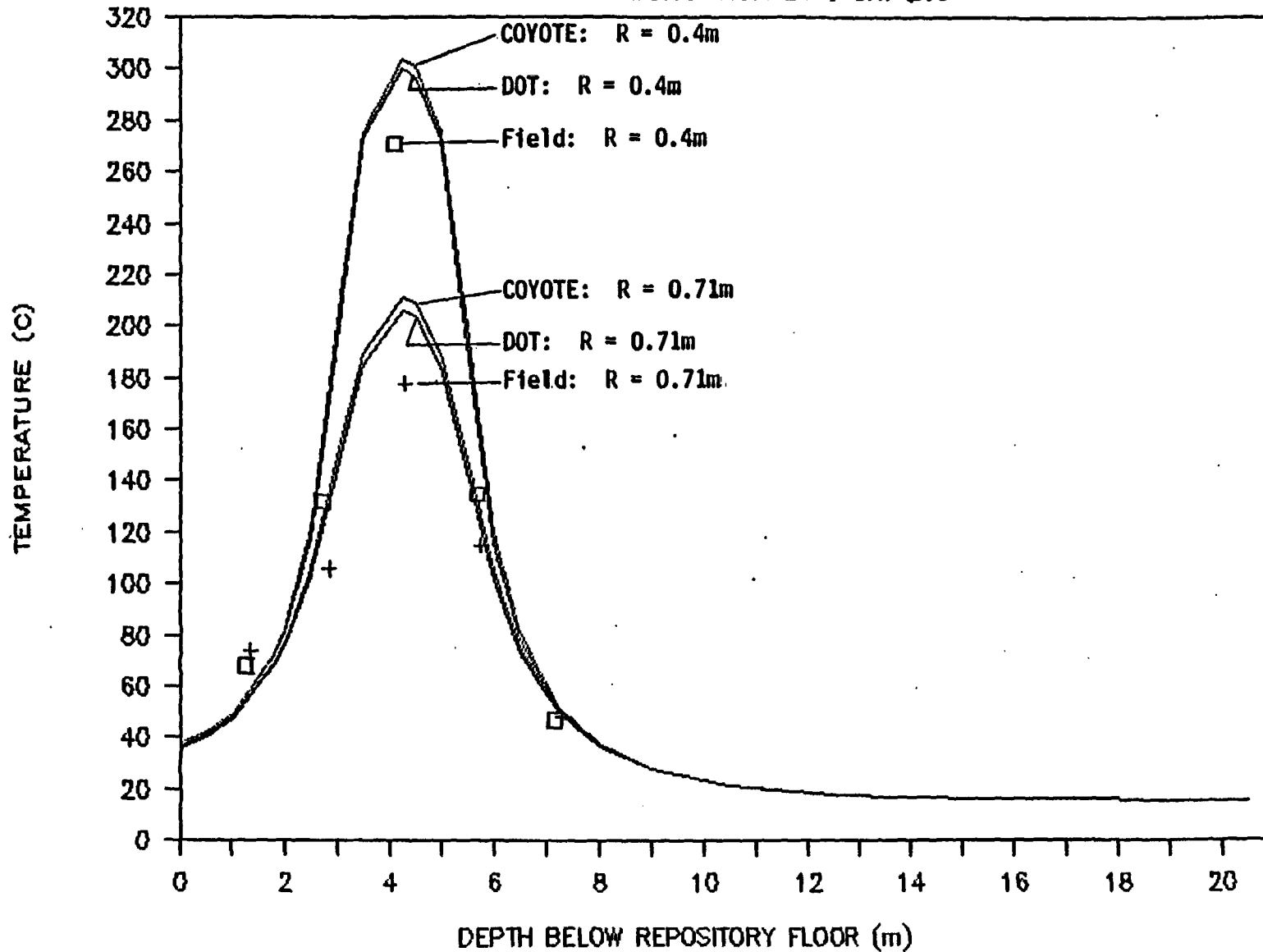


Figure 2.14-1 Problem 6.3 - BWIP - Comparison of Codes DOT & COYOTE  
Radial Temperatures on Day 260

# PROBLEM 6.3 BWIP - COMPARISON OF CODES

VERTICAL TEMPERATURE PROFILES @ DAY 260



1  
Figure 2.14-3 Problem 6.3 - BWIP - Comparison of Codes DOT & COYOTE  
Vertical Temperature Profiles on Day 260

# PROBLEM 6.3 BWIP - COMPARISON OF CODES

VERTICAL DISPLACEMENT (E04)

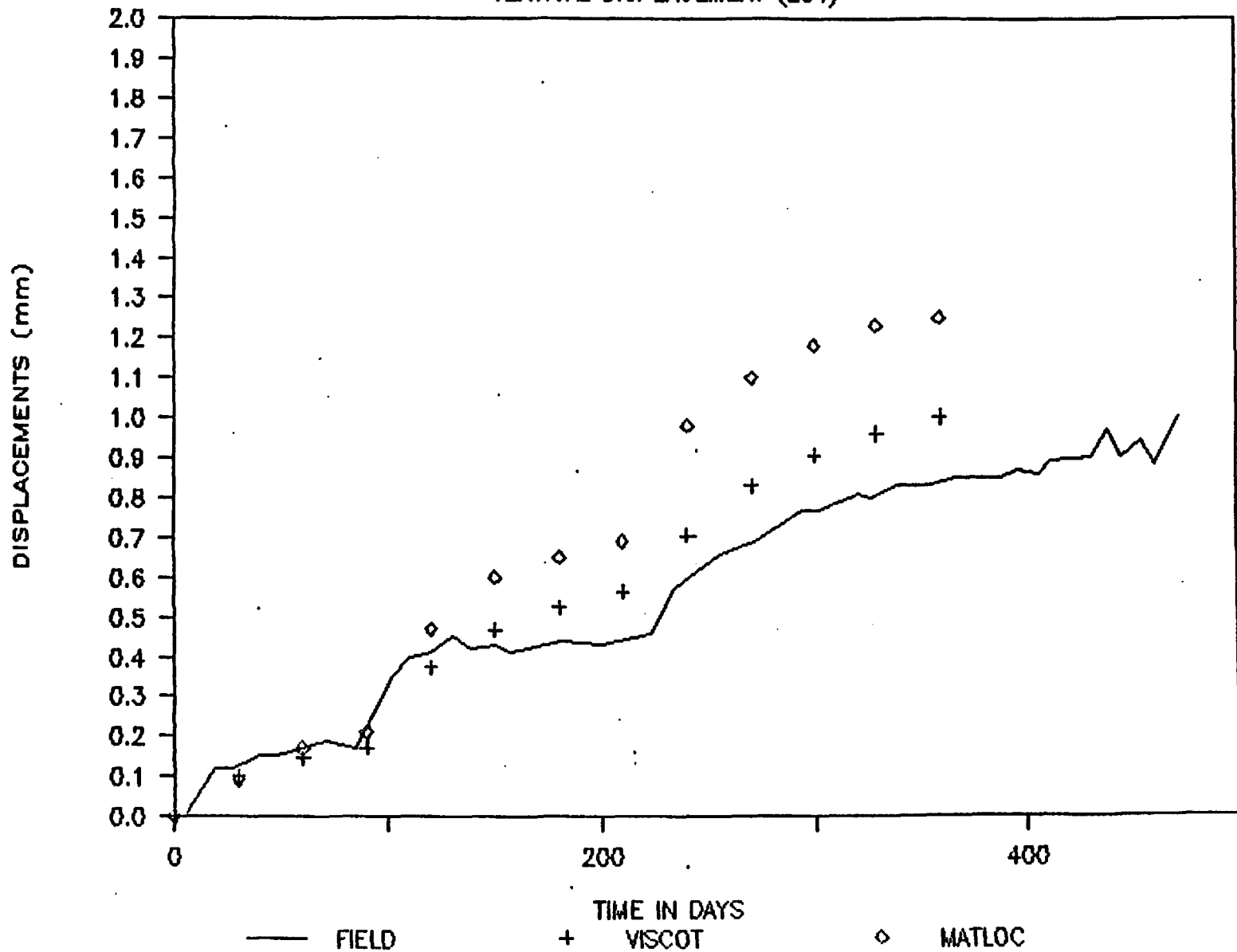


Figure 2.14-5 Problem 6.3 - BWIP - Comparison of Codes VISCOT & MATLOC  
Vertical Displacement at E04

### 3.0 PROBLEM DEFINITIONS

### 3.0 PROBLEM DEFINITIONS

This section contains summary descriptions of the analytical, hypothetical, and field validation problems used to benchmark the computer codes for nuclear repository design. The problem descriptions presented in this section are summaries of the problem descriptions originally presented in the Benchmark Problems Report, NUREG/CR-3636, dated February, 1984.

The description of each problem in the Benchmark Problems Report, in general, consists of the following:

- Problem statement
- Objectives
- Analytical solution, semi-analytical solution, or physical description
- Assumptions
- Input specifications
- Output specifications

The problem statement describes the problem and presents the processes and conditions being considered. The objectives section explains what features of the code the problem will test. If an analytical or semi-analytical solution is available, as in thermal and geomechanical problems, the solution is described.

The physical systems modeled in hypothetical and field validation problems are described in detail. Assumptions made in the development of the model, such as boundary locations, are explicitly defined.

The input specifications are actually restatements of the physical description in terms that are directly applicable to the model. They include values for all necessary physical parameters and loading conditions.

Output specifications define the spatial and temporal requirements for the comparison of analytical, field and code-predicted results. These results are best presented in graphical form. Anticipated problems or other information that may be useful in setting up or running the models is included as special comments.

Grid sizes and time steps have not been specified for the problems. This will permit the use of different values for different codes, so as to optimize the use of each code.

In general, problem descriptions contained herein consist of the problem statement, objectives and assumptions made in the development of the model, where applicable. For a full description of the supporting theory (for analytical problems) and field data (for field validation problems), as well as material properties, boundary and loading conditions, the reader is referenced to the Benchmark Problems Report, to be read in conjunction with the modified pages presented in Appendix A to this report.

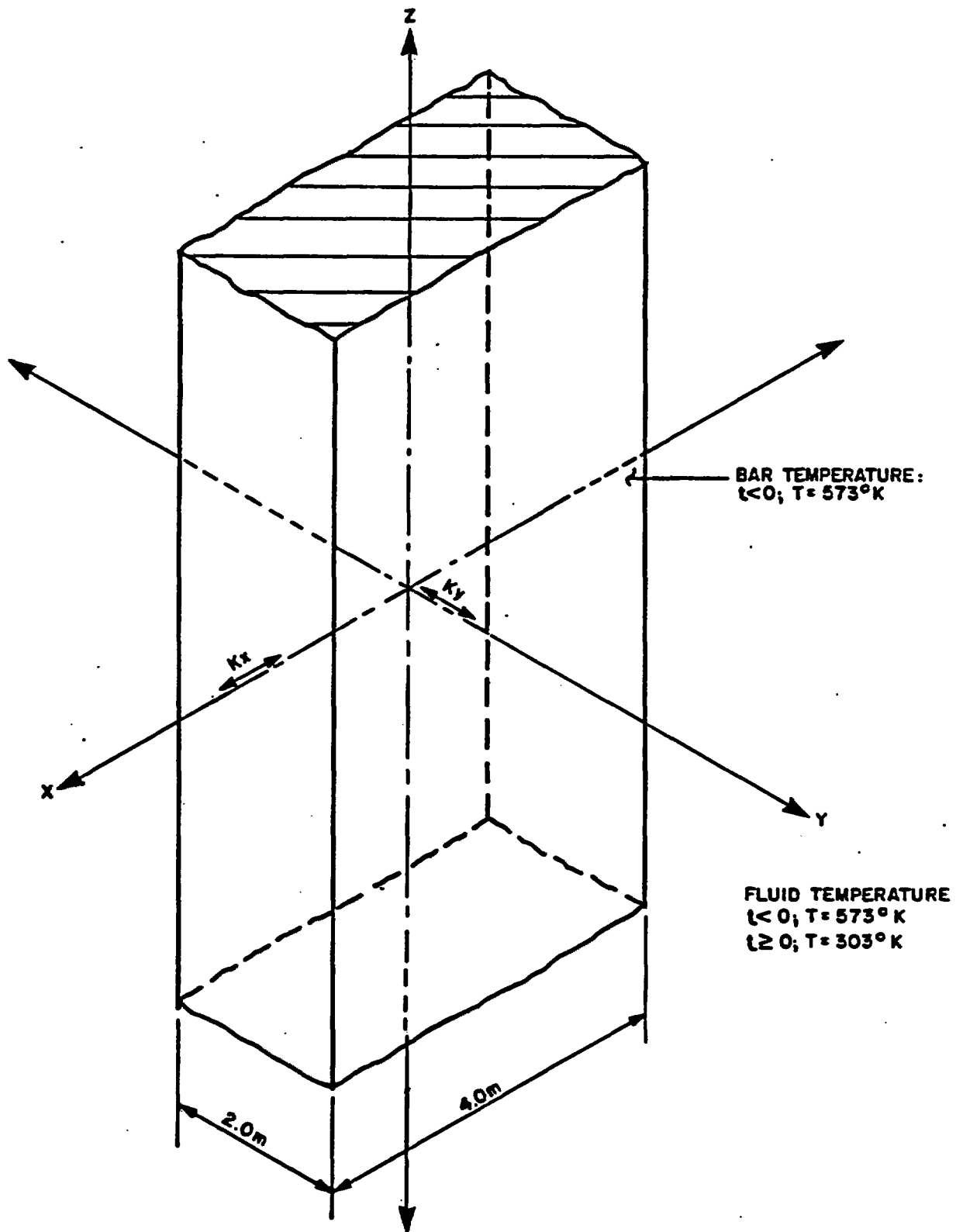


Figure 3.1.1-1 Rectangular Bar with Anisotropic Conductivity - Problem 2.6

# PROBLEM 2.6 – ANALYTICAL SOLUTION

Y-AXIS TEMPERATURES AT VARIOUS TIMES

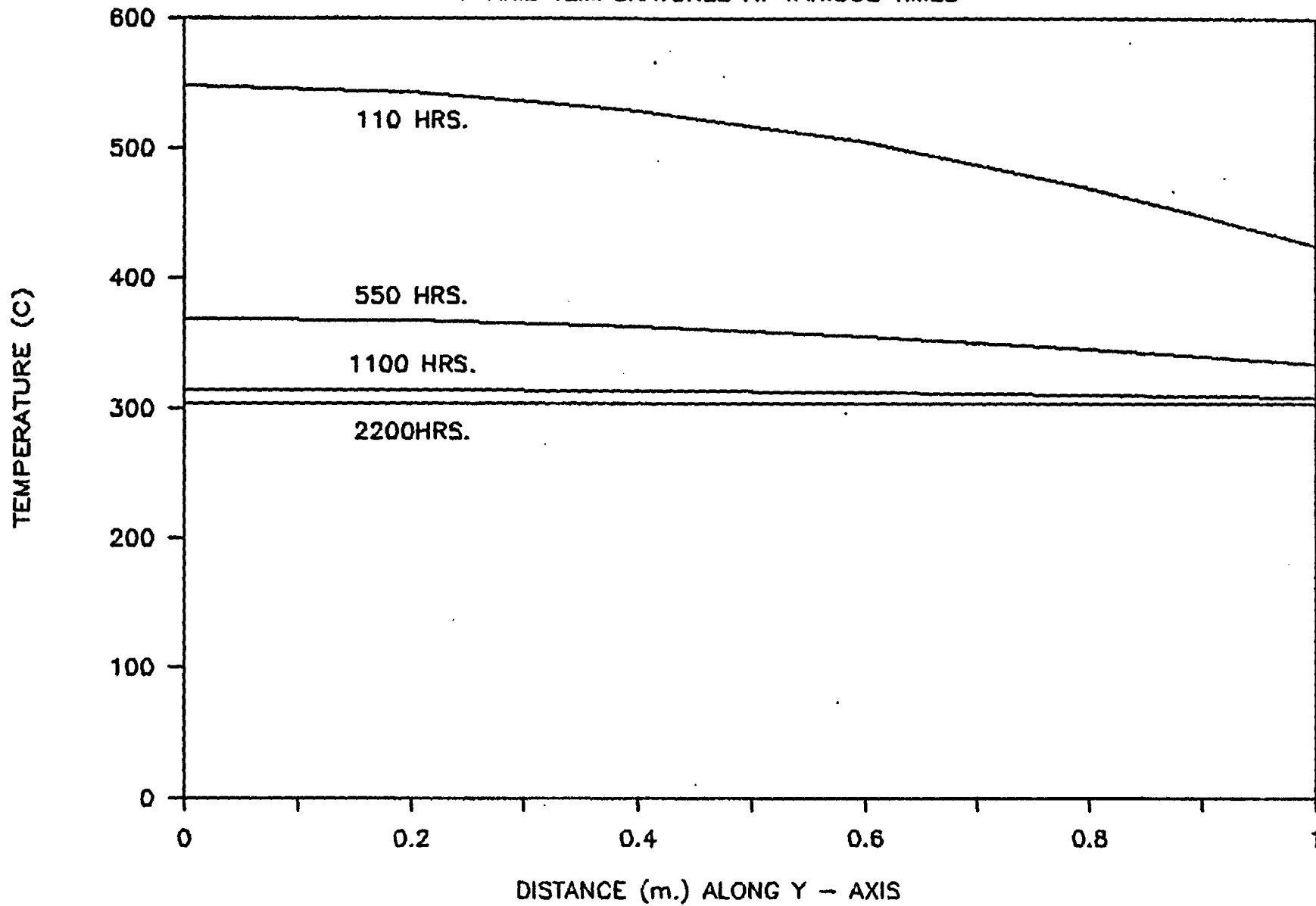


Figure 3.1.1-3 Problem 2.6 Analytical Solution  
Y-Axis Temperature Profiles

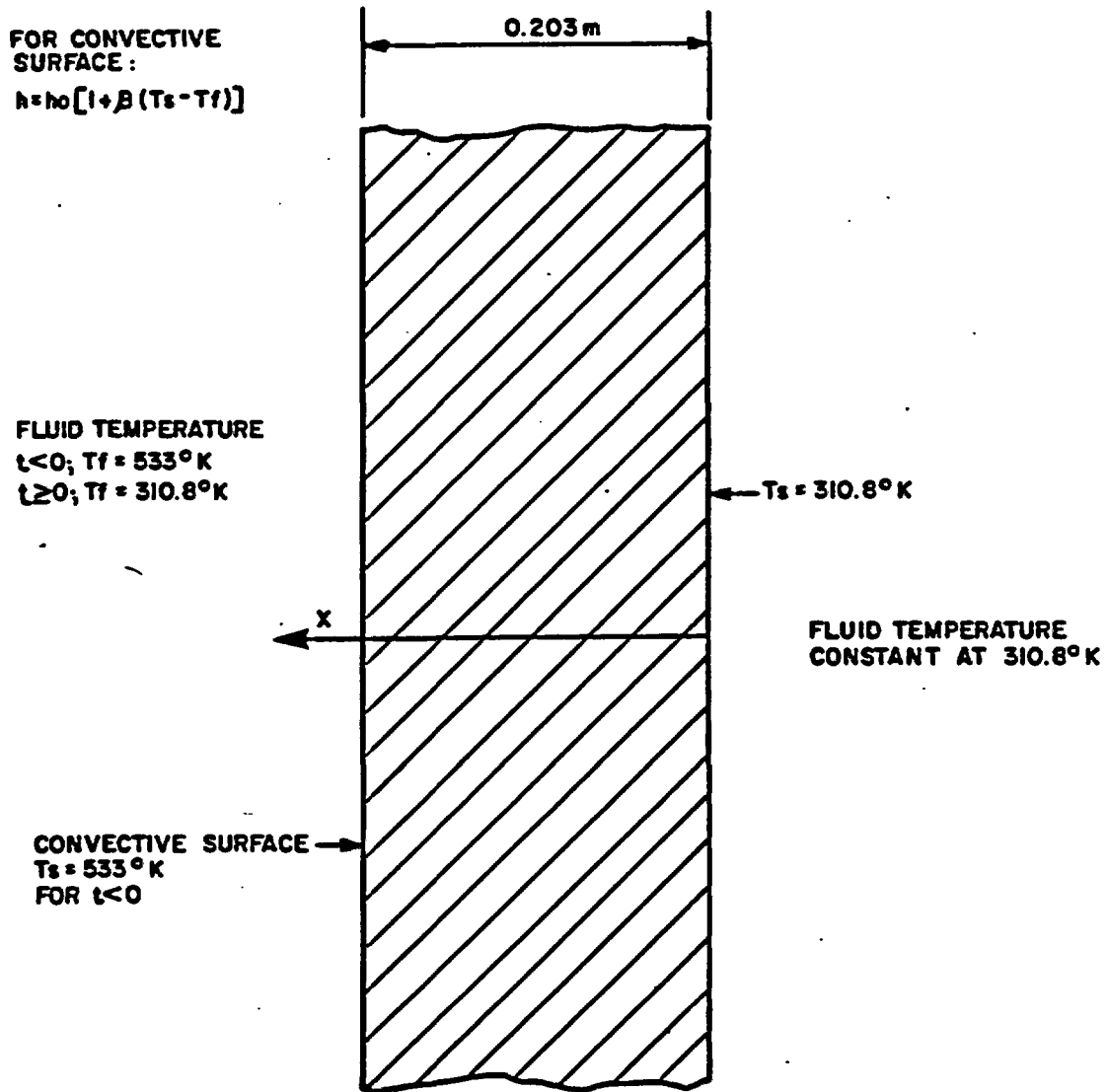


Figure 3.1.2-1 Transient Response to the Quench of an Infinite Slab with a Temperature-Dependent Convection Coefficient - Problem 2.8

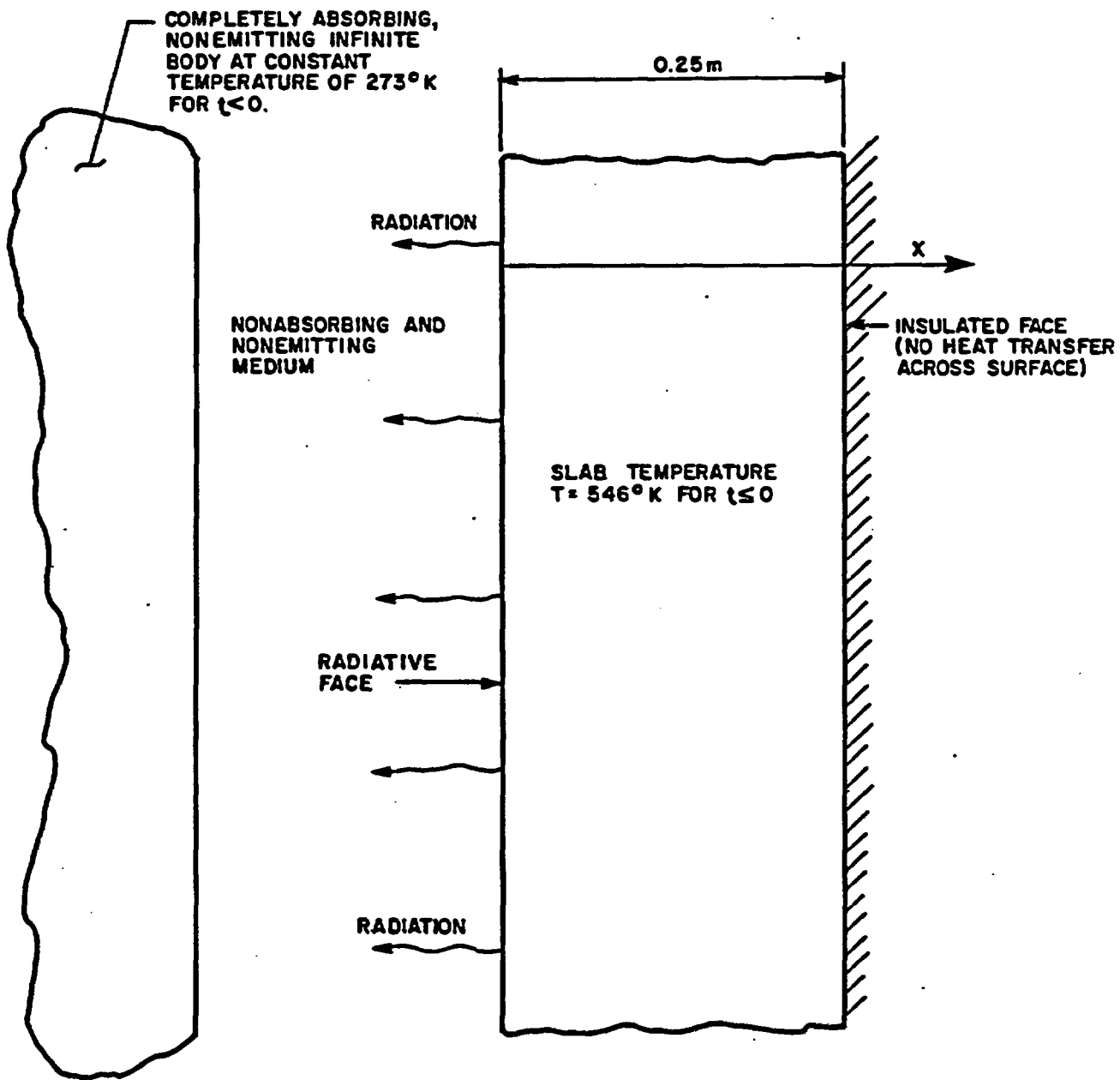


Figure 3.1.3-1 Radiation from a Slab - Problem 2.9

**Assumptions** - The assumptions made in solving the governing heat transfer equations include:

- Material properties are constant;
- The transmitting medium is nonabsorbing and nonemitting;
- Radiation is the only applicable boundary condition on the noninsulated surface; and
- The radiative environment is uniform and of constant temperature.

**3.1.4 Problem 2.10 Steady Radiation Analysis of an Infinite Rectangular Opening (Rohsenow and Hartnett, 1973, pp. 15-32)**

**Problem Statement** - This problem deals with the steady radiation analysis of an infinite length rectangular opening, of shape similar to a duct, 8 m wide by 10 m high. The floor, walls, and roof of the opening are maintained at different temperatures as shown in Figure 3.1.4-1. The medium within the opening is nonabsorbing and nonemitting. The net heat loss from each surface due to steady-state radiation is to be calculated.

**Objective** - The purpose of this problem is to investigate a code's ability to model radiant surface-to-surface heat transfer.

**Solution** - The analytical solution was obtained by solving a set of simultaneous equations for the surface radiosities, then substituting the obtained values into the governing radiation heat transfer equation for each surface. The radiosity and heat transfer equations are given in the Benchmark Problems Report. Table 3.1.4-1 summarizes the analytical solution results by listing the radiosity and net heat loss per unit area for each surface.

**Assumptions** - The assumptions made in solving the governing heat transfer equations include:

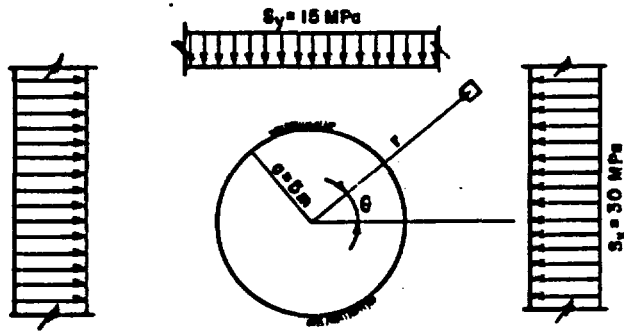
- Material properties and temperatures are constant and uniform on each surface;
- The transmitting media is nonabsorbing and nonemitting; and
- Radiation is the only applicable boundary condition.

TABLE 3.1.4-1

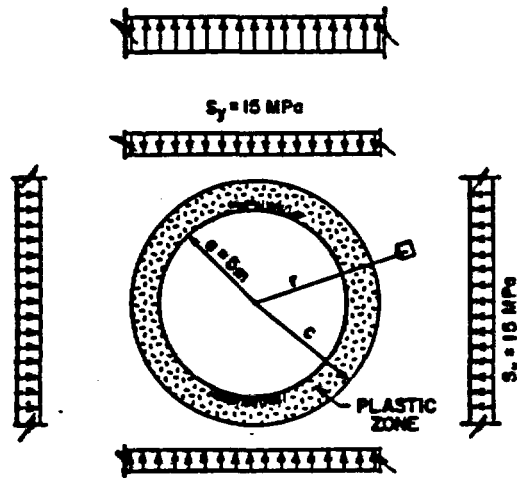
## ANALYTICAL SOLUTION TO BENCHMARK PROBLEM 2.10

<u>Surface</u>	<u>Temperature °K</u>	<u>Radiosity (W/m<sup>2</sup>)</u>	<u>Net Heat Loss (W/m<sup>2</sup>)</u>
Floor	473	2712.2	1213.5
Roof	343	911.2	-1217.9
Wall	423	1815.1	1.7
Wall	423	1815.1	1.7

(a) Elastic Medium



(b) Elastic-Plastic Medium



(c) Elastic Medium with Liner

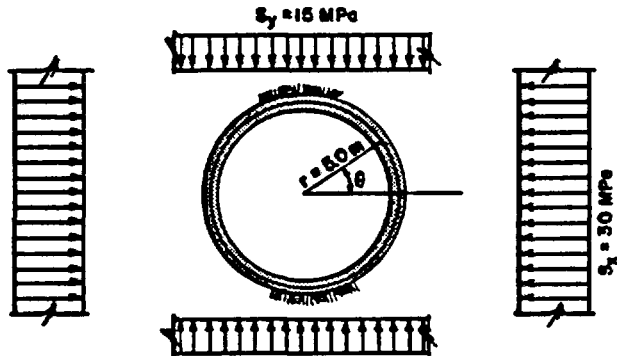


Figure 3.2.1-1 Circular Tunnel - Problem 3.2

# PROBLEM 3.2a – ANALYTICAL SOLUTION

## MAJOR AND MINOR PRINCIPAL STRESSES

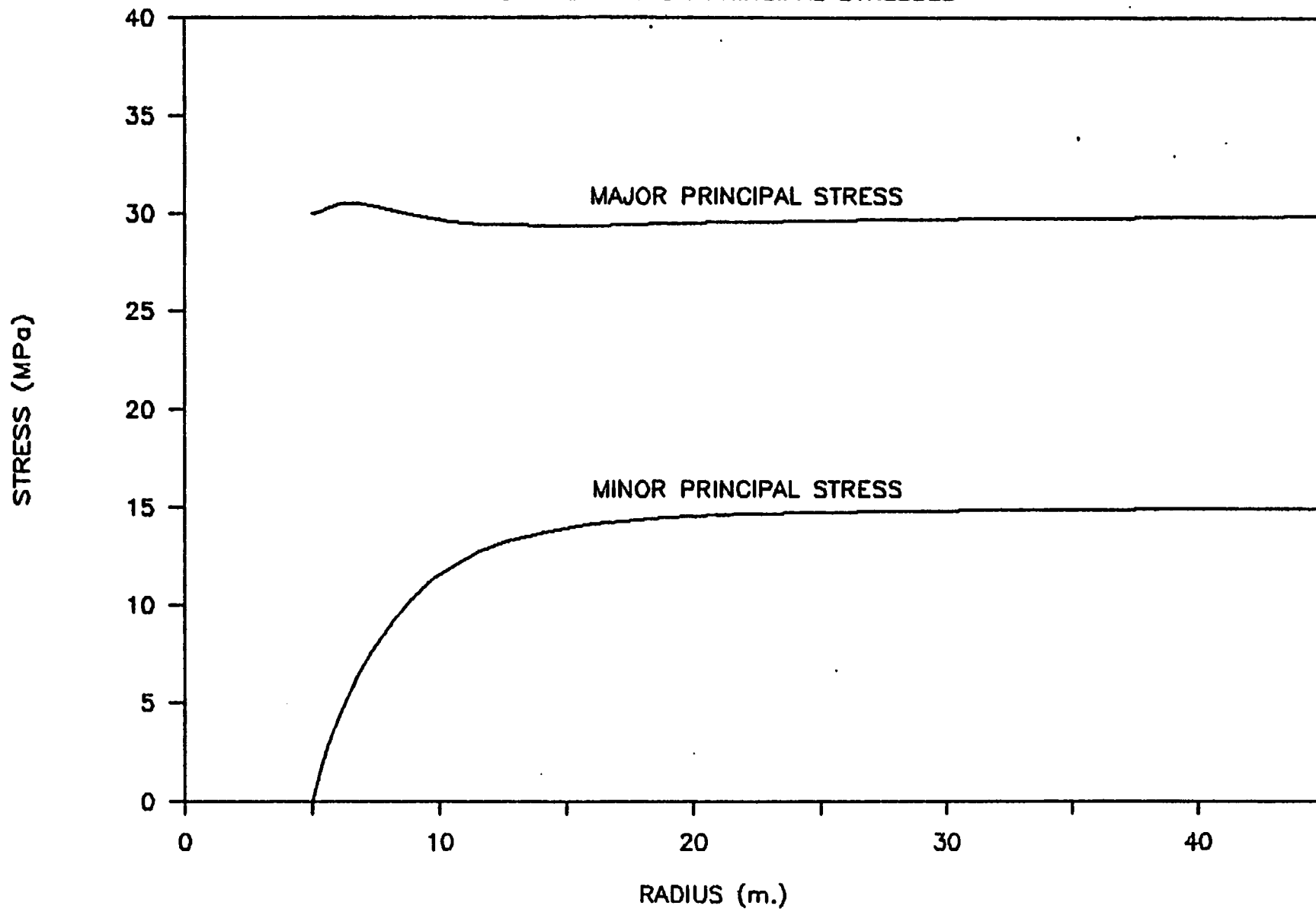


Figure 3.2.1-2 Problem 3.2a Analytical Solution  
Major and Minor Principal Stresses  
Along Radial Line 30° Above Horizontal

# PROBLEM 3.2b – ANALYTICAL SOLUTION

STRESSES AT VARIOUS RADII

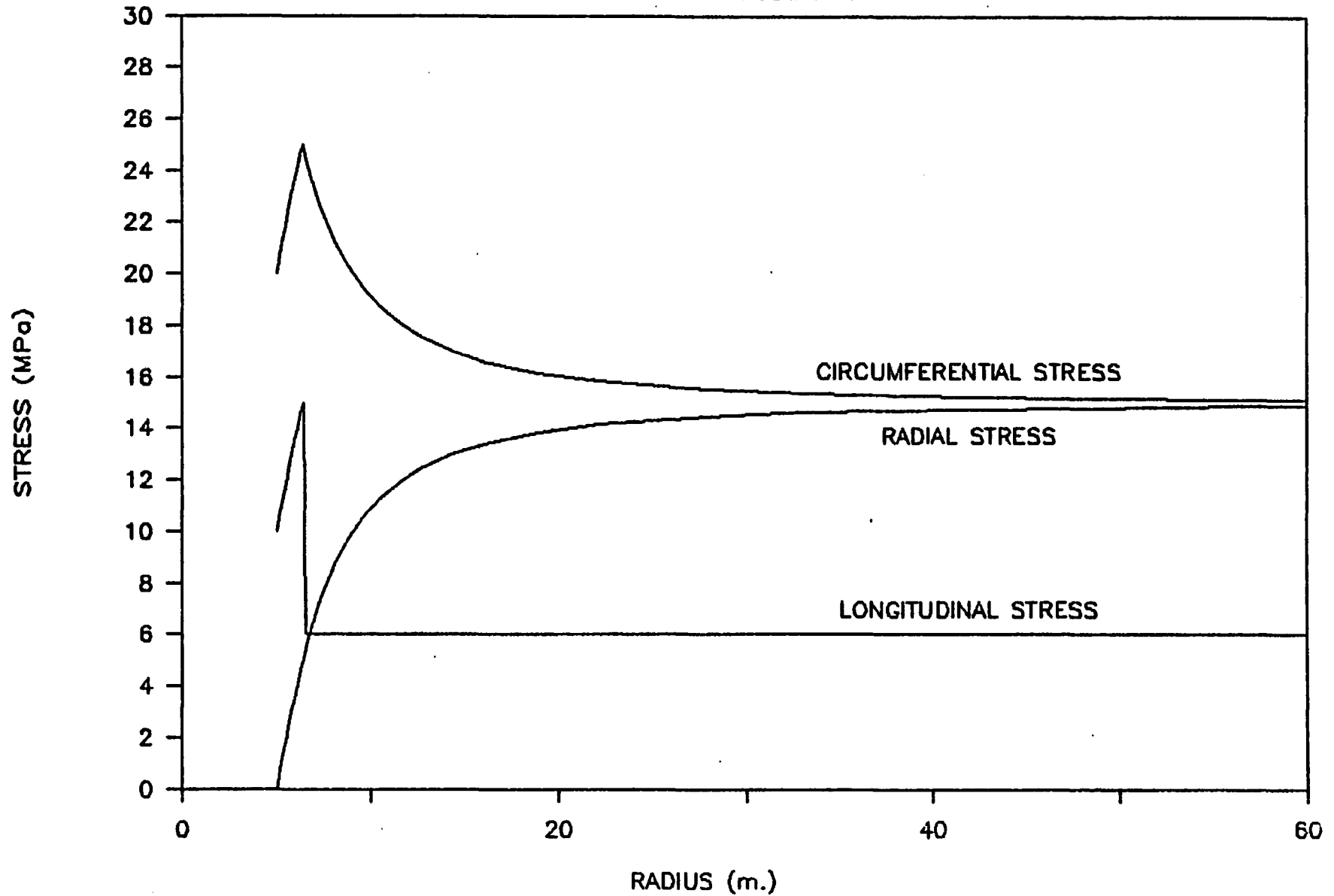
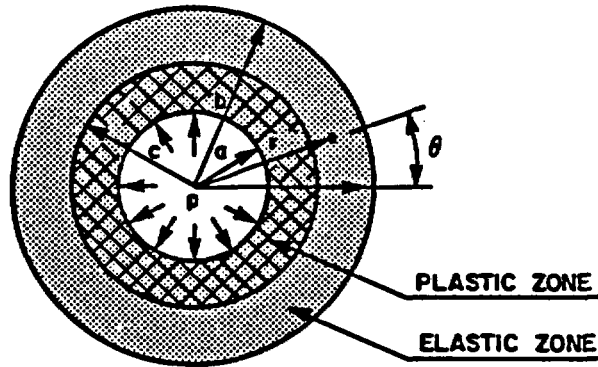
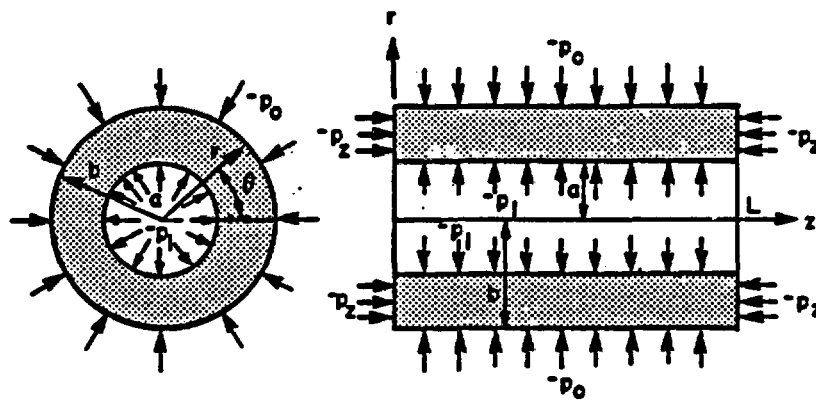


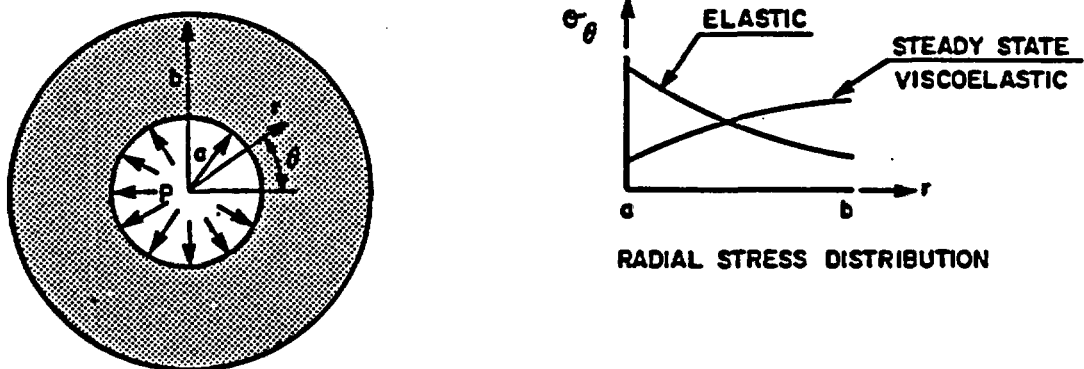
Figure 3.2.1-4 Problem 3.2b Analytical Solution  
Stresses Along Radial Line  $30^\circ$   
Above Horizontal



**(a) ELASTIC-PLASTIC ANALYSIS**



**(b) ELASTIC ANALYSIS**



**(c) VISCOELASTIC ANALYSIS**

Figure 3.2.2-1 Thick-walled Cylinder Subjected to Internal and/or External Pressure- Problem 3.3

Assumptions - Assumptions which are implicit in the theoretical solutions used for Part (c) of this problem include:

- The material is viscoelastic, homogeneous, and isotropic;
- The steady-state creep condition has been reached and thus stresses are constant with time;
- Temperature is constant with time and uniform throughout; and
- Strain rates are constant with time.

### 3.2.3 Problem 3.5 Plane Strain Compression of an Elastic-Plastic Material

Problem Statement - This problem concerns the plastic yielding and flow of a rectangular block loaded by a uniform pressure in the vertical orthogonal direction, constrained in the longitudinal orthogonal direction, and free to expand in the horizontal orthogonal direction. These boundary conditions allow the reduction of this problem to a plane strain model, as illustrated in Figure 3.2.3-1.

To minimize edge effects, the width (direction of free expansion) is much greater than the height (direction of loading) and the loading platens are assumed frictionless. The medium is isotropic and homogeneous. With these criteria, the principal stresses will always be aligned with the orthogonal directions of the rectangular block and will be constant throughout. Thus, the maximum principal stress will equal the applied vertical pressure.

As the vertical load increases, the block first behaves according to elastic stress-strain relationships. When the yield strength of the material is reached, as defined by one of two yield criteria, plastic flow is initiated. Post-yielding stress-strain relationships are defined by the Prandtl-Reuss flow rule.

This problem has been divided into two parts, defined by the following yield criteria:

- von Mises criterion; and
- Drucker-Prager criterion.

Objective - The objective of this problem is to test the von Mises and Drucker-Prager yield criteria subroutines and the plastic flow subroutines of selected repository design codes.

Solution - Within the elastic range, the stresses and strains can be determined from Hooke's law.

When the magnitude of the applied pressure reaches the yield value defined by one of the yield criteria, plastic flow initiates. The total strain then becomes the sum of the elastic strain and plastic strain components.

When the magnitude of the applied pressure reaches the yield value defined by one of the yield criteria, plastic flow initiates. The total strain then becomes the sum of the elastic strain and plastic strain components.

The von Mises theory predicts that ultimate failure will occur when the maximum principal stress reaches twice the value of the unconfined yield stress in pure shear. It predicts that from the point of initial yield, a condition that is dependent on the deviatoric (shear) stress state, the plastic stresses will increase according to a logarithmic function until ultimate failure occurs.

The Drucker-Prager criterion is a generalization of the von Mises theory, but it includes the effects of deviatoric as well as confining stresses. In contrast to the von Mises theory, which fits a logarithmic stress curve between initial yield and ultimate failure, the Drucker-Prager theory states that the material strength increases with the confining stress state. Thus, for this problem, the Drucker-Prager theory does not predict failure of the material.

Assumptions - Assumptions implicit in the analytical solutions to Parts (a) and (b) to this problem are:

- The bulk modulus is constant, even after plastic deformation;
- There is neither strain hardening nor softening; and
- The material is homogeneous and the stress state within the material is constant throughout.

qualitative differences in response. Compromises between local detail and generality (average response in a region) will become evident, and the adequacy of typical modeling approaches and scales can be evaluated.

Thermally, this problem exercises general transient heat transfer, with mechanisms of conduction, heat storage, radiation and free (natural) and forced (ventilation) convection. The analysis is applied to the canister as a bulk body, the rock, and the intervening solid materials and gases. Natural convection and radiation in the canister-sleeve gap, and ventilation in the room, are considered for the initial 50 years after emplacement. After room-sealing at 50 years, the ventilation is replaced by natural convection and radiation heat transfer between room surfaces.

In the stress analysis, the simulations will evaluate elastic, elasto-plastic and viscoelastic behavior of the rock around the placement hole. The phenomena under consideration will depend on the medium assumed. Non-rock materials are not modeled in the stress analysis.

Physical Description - The single level repository, of unspecified extent, is located at a depth of 500 m (canister mid-height) in the host rock. A geothermal heat flux is present, specified by a temperature rise of 20°C per kilometer of depth below the surface, which is at a temperature of 15°C. The in situ stress state is isotropic ( $K_0 = 1.0$ ) with the vertical stress equal to the weight of the overburden.

The waste is ten-year old pressurized water reactor (PWR) spent fuel. The decay heat from PWR spent fuel as a function of time was given in the Benchmark Problems Report. Waste canisters contain one intact fuel assembly and are stored in vertical emplacement holes in the floors of an array of parallel rooms. Each emplacement hole contains one canister. The rooms are spaced on 15 m centers and the canister spacing in the rooms is 3 m on center.

The canister emplacement hole is lined with a mild steel sleeve and capped by a concrete shield plug. The stainless steel canister hangs by a steel shield block located inside the top of the sleeve. There is backfill in the sleeve-emplacment hole annulus and air between the canister and the sleeve. Details and dimensions of the rooms, pillars and canister emplacement are shown on Figure 3.3.1-1.

Thermal and mechanical properties for the alternative candidate host rock formations of salt, basalt and granite, as well as for the back-fill, steel and canister were published in the Benchmark Problems Report, together with convection coefficients, radiation, creep law, and failure criteria parameters.

Assumptions - The primary modeling of this problem should be done in three dimensions. Using room and pillar centerlines as symmetry planes in the longitudinal direction, and canister and mid-canister centerlines as symmetry planes in the transverse direction, the region for modeling reduces to 3500 m deep from ground surface by 7.5 m wide by 1.5 m thick as shown on Figure 3.3.1-1. One-quarter of a canister is contained in the modeled region. Boundaries are defined at distances of 100 m above and below the cavern for stress analysis.

The thermal boundary conditions are adiabatic (insulated) on the vertical symmetry planes, with fixed temperatures at the top and bottom, defined by the natural geothermal conditions. The room interior is ventilated for 50 years after emplacement of the waste, then sealed but not backfilled. For simplicity, initial thermal conditions at the start of simulation are defined by the geothermal conditions, including the waste and other material in the emplacement hole.

The stress boundary conditions are normal restraint on symmetry boundaries and on the bottom of the model, and a free boundary on the top of the model.

Other major assumptions for the analysis are:

- The analysis is done for the central canister of an infinite array, all waste being emplaced at the same time in order for symmetry conditions to be strictly valid;
- The heat generated in the canister is uniformly distributed throughout the volume of the canister. The only thermal mechanisms active within the canister itself are conduction and heat storage, also assumed to be homogeneous over the volume and based on estimated average properties; and
- Codes without radiation and natural convection capability will use an 'equivalent' solid conductivity in an assumed fill material. Adjustment of material parameters will be necessary to achieve the desired result.

### 3.3.2 Problem 5.2 Hypothetical Near Field Problem

Problem Statement - This problem consists of transient thermal simulation of the near field (single-room region) of a hypothetical repository, followed by static stress analysis at two specified times. This and the accompanying very near field (canister region) and far field (repository region) problems form a set of problems at different scales of modeling for the same hypothetical repository configuration.

Objectives - The general objectives of this hypothetical problem are similar to those presented in Section 3.3.1. Specifically, this problem tests two-dimensional plane thermal and plane strain geometry and symmetry conditions of selected computer codes as applied to a repository-scale model.

Thermally, this problem exercises general transient heat transfer, with mechanisms of conduction, heat storage, radiation, and free (natural) and forced (ventilation) convection. The analysis is applied to the emplacement hole (in which the canister and other hole contents are modeled with the inter-canister rock as an emplacement trench in two dimensions), the remainder of the surrounding rock, and the room above. The room is ventilated for the initial 50 years after emplacement. After room sealing at 50 years, the ventilation is replaced by natural convection and radiation heat transfer between room surfaces.

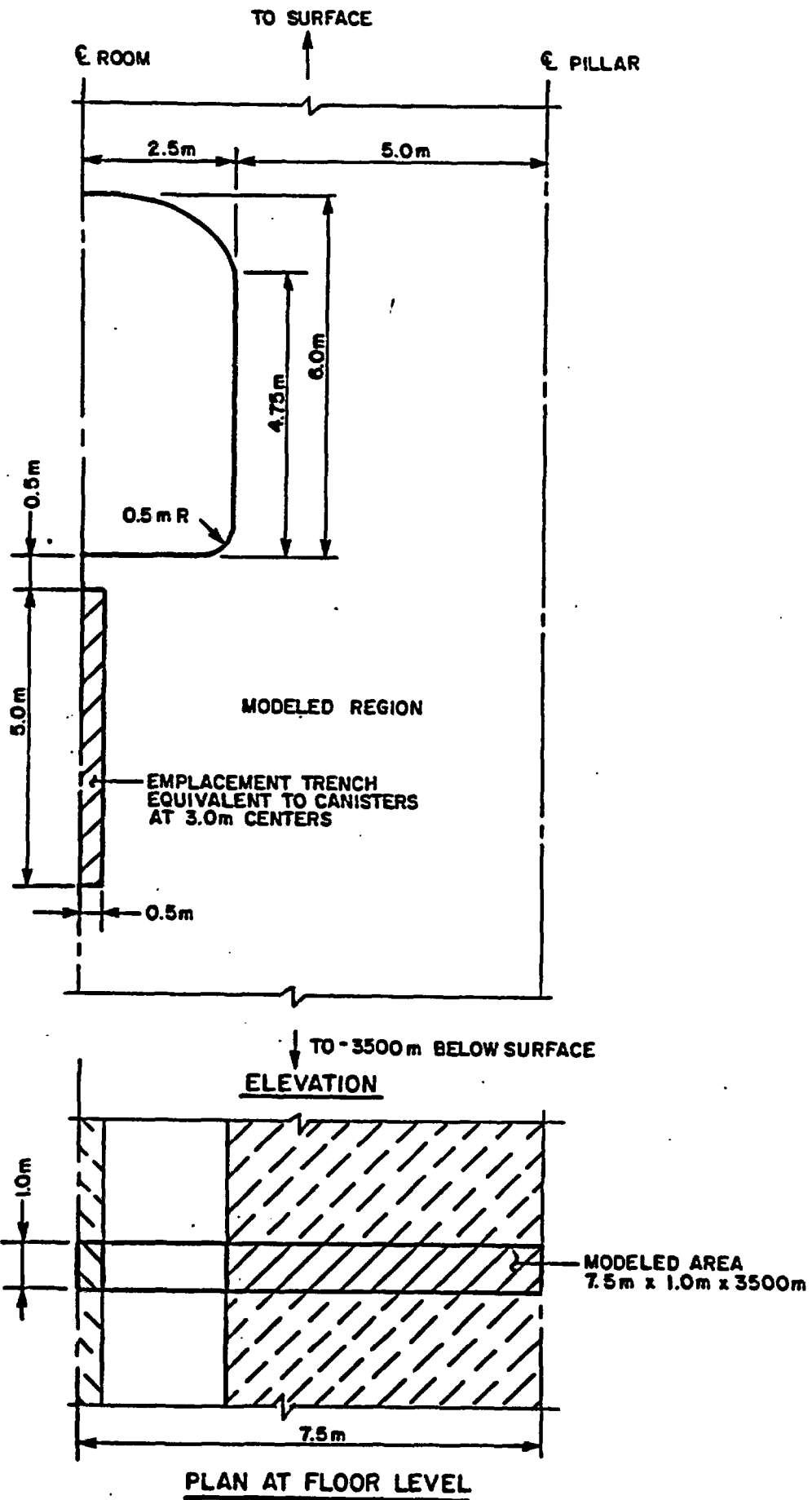
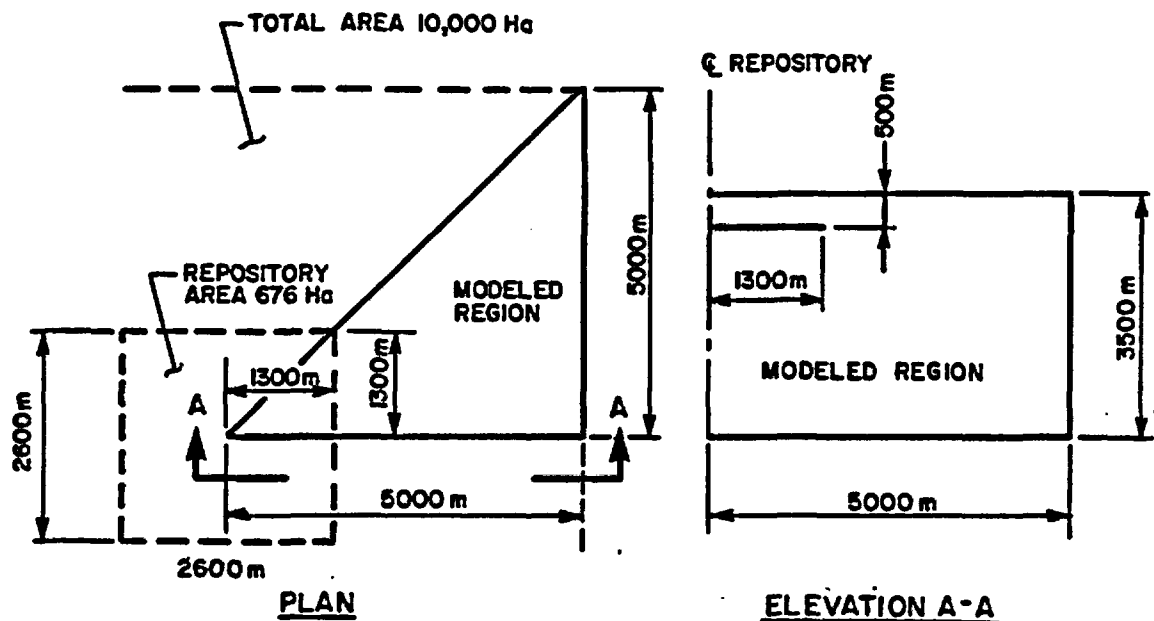
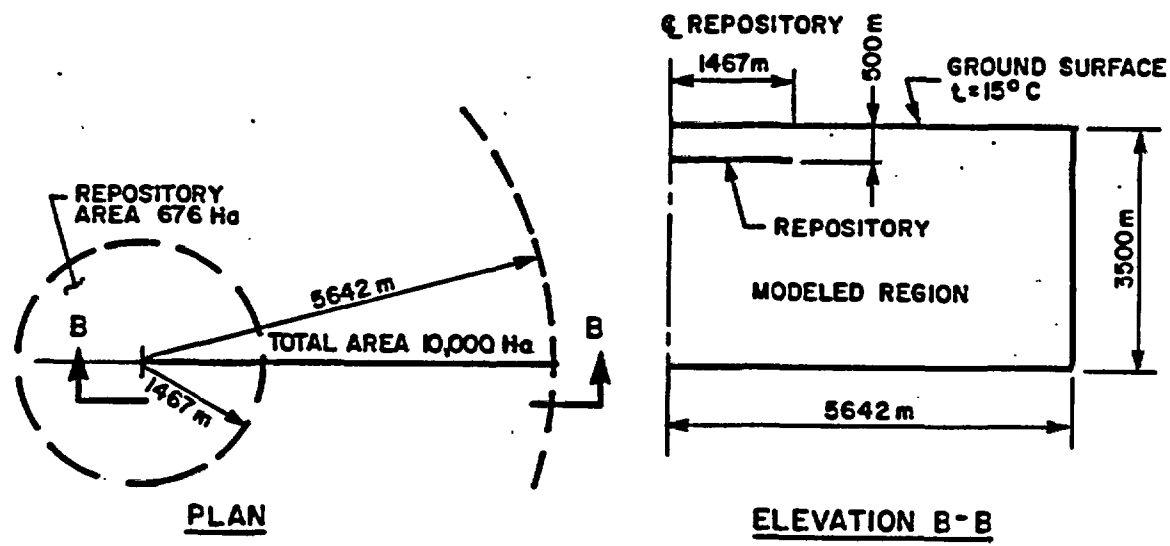


Figure 3.3.2-1 Near Field (Room) Model - Problem 5.2



3-D MODEL



AXISYMMETRIC MODEL

Figure 3.3.3-1 Far Field (Repository) Models - Problem 5.3

### 3.4 FIELD VALIDATION PROBLEMS

Unlike the previous problems discussed in this report, field validation problems test not only the performance of the repository design codes but also the validity of the mathematical models on which the codes are based. This is accomplished by comparing the results of relatively large scale field tests, involving many cubic meters of rock, with predictions made by numerical analysis codes.

Ideally these problems should be the ultimate test of a code's applicability for repository design; however, this is not always the case. Precise correlation with field results cannot be expected, but this does not necessarily indicate that a code is invalid for repository design. Factors which may contribute to poor agreement between measured and predicted results include:

- Variations in values of parameters and variables used as input (conductivity, elastic constants, in situ stresses, etc.) to the models. Input parameters are generally measured in a laboratory and the values may, and generally do, differ from the average values for a large volume. These inaccuracies may be overcome somewhat by adjusting the parameter values to force the model to predict the same results as the field experiment. In this way, the field experiment becomes an indirect measurement of the basic rock mass parameters.
- Inaccuracy in measuring results of the field test. Temperatures of the rock can generally be measured quite accurately. However, measurements of stress changes involve mechanical measurements of minute strains and conversion of strains to stresses using elastic constants. Both of these steps are possible sources for relatively large errors.
- Geological materials do not have completely uniform properties and therefore cannot be precisely modeled as isotropic or, in some cases, orthotropic materials.
- Difficulty in modeling boundary conditions. The boundaries occurring in the field are generally much more complex than those which can be modeled by a computer code.

The above factors, which undoubtedly lead to inaccuracies associated with modeling field tests, are equally applicable to the thermo-mechanical response of rock surrounding a repository. Similarly, good correlation of the code results with measured data from one site does not guarantee that a code can be applied successfully to the analysis of another site. These problems will give an indication of the magnitude of inaccuracies associated with repository design analyses. In actual repository design, rather than using a single analysis with a fixed set of parameters, a number of analyses will be performed with a range of input parameters. These will "bracket" the geologic response that might be expected from repository loading.

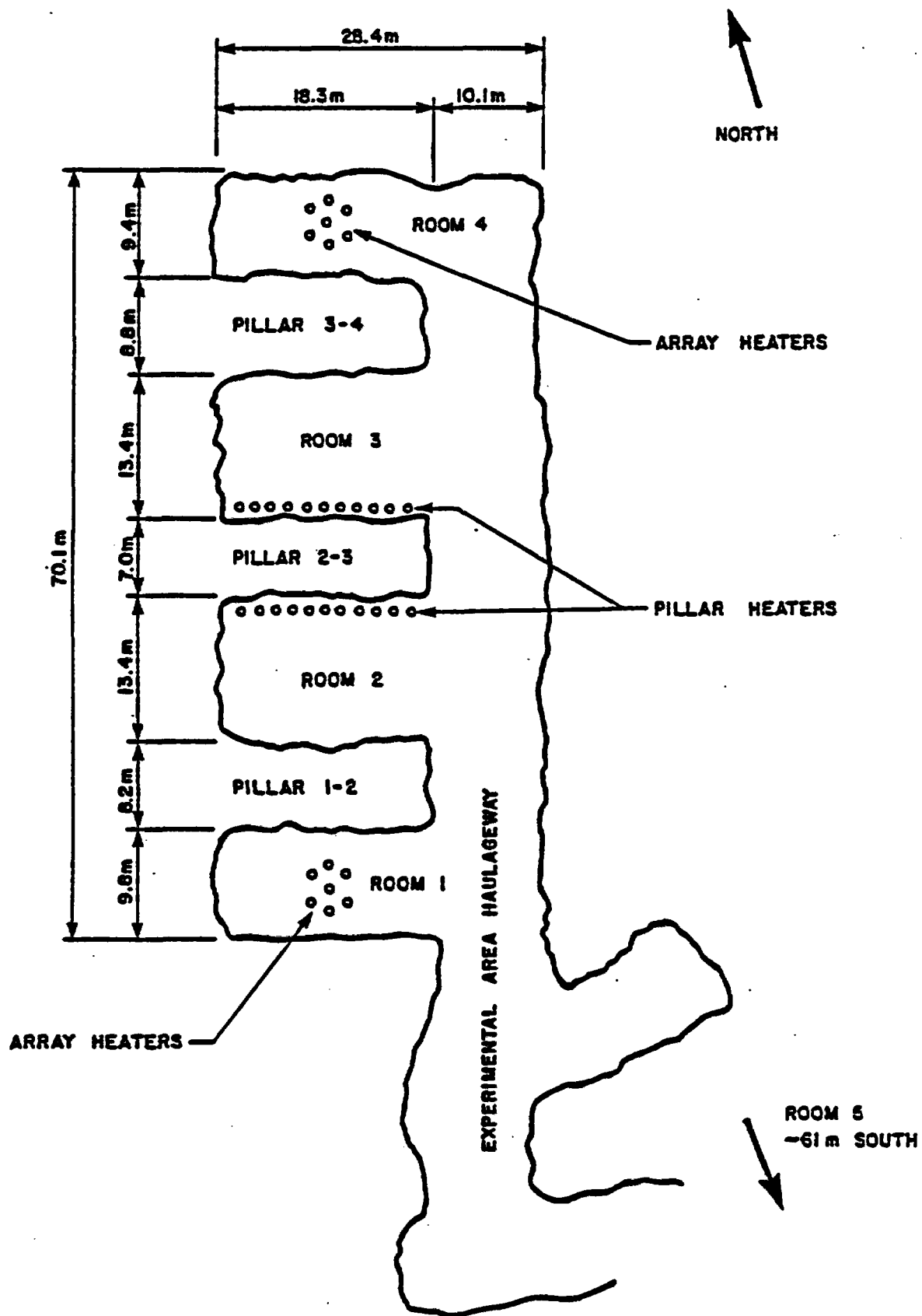


Figure 3.4.1-1 Plan of Project Salt Vault Experimental Area (From Ratigan and Callahan, 1978)

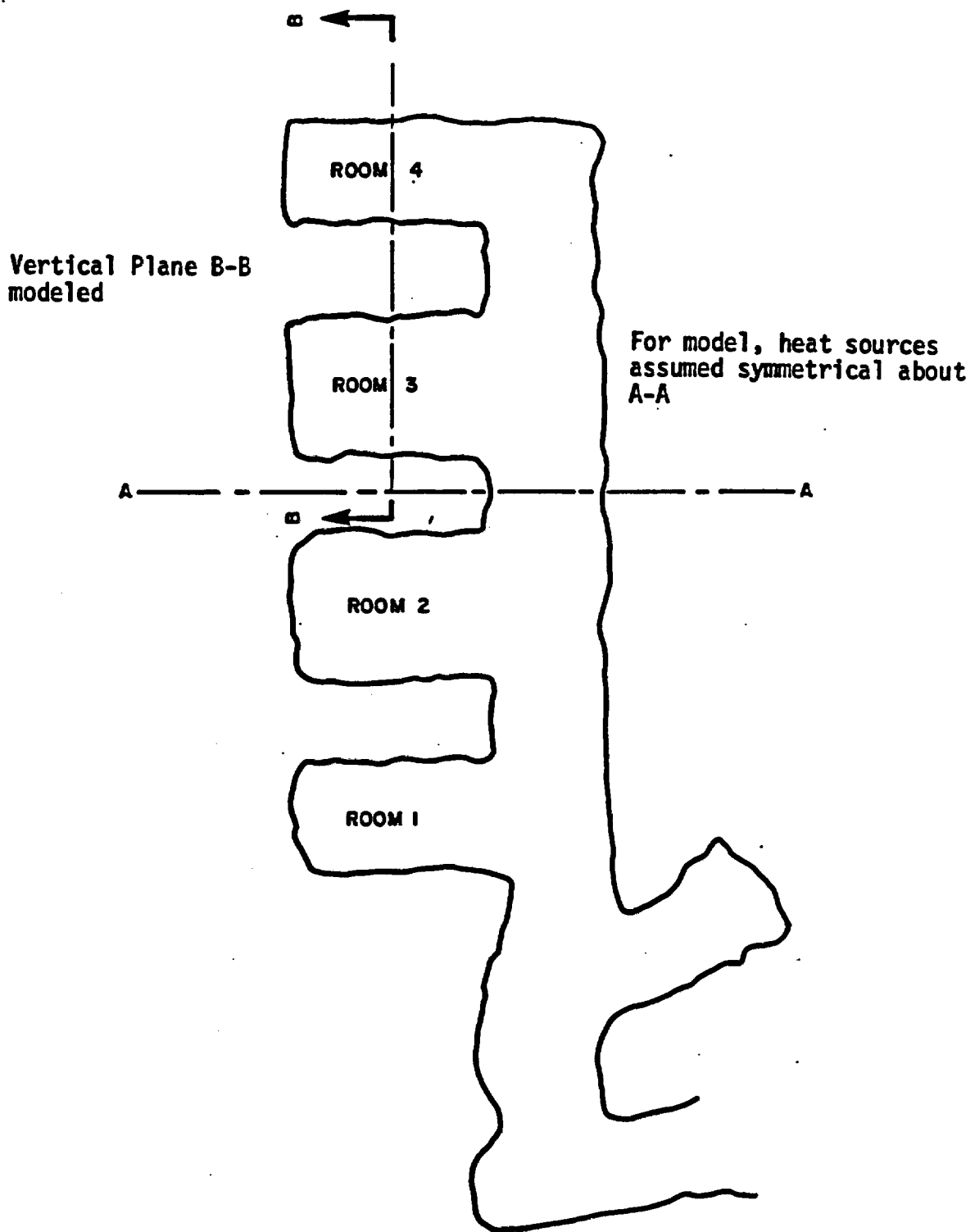


Figure 3.4.1-2 Project Salt Vault  
Field Test - Location of  
Sections A-A and B-B

Thermal boundary conditions include adiabatic boundaries on both sides and isothermal boundaries at 23°C on the top and bottom. The rooms are maintained at an ambient temperature of 23°C. The entire system is initially at 23°C.

The mechanical boundary conditions include horizontally rigid (but vertically free) boundaries for the left and right sides and a vertically rigid (but horizontally free) boundary on the bottom. The top boundary is a constant stress,  $\sigma_t$  of 6.392 MPa, which represents an overburden of 281 m with an average density of 2318 kg/m<sup>3</sup>. The left and right boundaries attempt to simulate an infinite medium.

### **3.4.2 Problem 6.3 In Situ Heater Test - Basalt Waste Isolation Project**

#### **Problem Statement**

Two full-scale heater tests were undertaken at the Basalt Waste Isolation Project (BWIP) site between July 1980 and October 1982. The purpose of these tests was to provide a better understanding of the behavior of a rockmass under thermal loadings similar to that which would occur in a waste repository. The heater tests were located in the Near Surface Test Facility (NSTF) constructed in the Pomona Member basalt on the Hanford site. The test facilities consist of three access tunnels and two test tunnels located in Gable Mountain at a depth of approximately 50 m.

Heater Test 1 used a main electrical heater operated at a power level increasing in steps to 2.0 kW after 226 days and eight peripheral heaters with power levels increased in three steps to 1.0 kW after 226 days. Test 2 consisted of a single heater with power levels increased to 5.0 kW after 226 days. An inspection of the heater hole for Test 2 after 671 days showed minimal damage. After the inspection, the heater was reinstalled and the test was continued at power levels of up to 9.0 kW.

Both heater tests were located in the floor of Test Area I at a spacing along the tunnel axis of 21.3 m (70 ft). Instrumentation was installed in vertical holes surrounding the heaters and in horizontal holes drilled from an extensometer room located 12.2 m north, approximately 6.5 m below Test Area I. With the exception of mechanical-type measurements, the instrumentation readings during the test were made and recorded using a computer located in the portal area of the NSTF.

This problem concerns the thermal and mechanical response of basalt due to a repository-type loading from Heater Test 2. Results predicted by the various codes were compared to selected field measurements.

The problem is a three-dimensional problem but will be approximated by an axisymmetric model. A transient analysis is to be performed for the first 500 days of the test with temperatures, displacements and stresses calculated at specified time steps.

## 4.0 BENCHMARKING OF ADINA

## 4.0 BENCHMARKING OF ADINA

### 4.1 Code Background and Capabilities

ADINA, an acronym for Automatic Dynamic Incremental Nonlinear Analysis, is a finite element code for the static and dynamic stress and displacement analysis of solids, structures and fluid-structure systems. The program can be employed to perform linear and nonlinear analysis of one-, two-, and three-dimensional models. Two-dimensional elements may be either planar or axisymmetric.

The ADINA code was developed and is leased and supported by K.J. Bathe and his associates at ADINA Engineering, Inc., Watertown, Mass. Version 1981-NL10 of ADINA was obtained from ADINA Engineering, and installed on the BNL computer system with a slight modification. The variable MTOT, which specifies the total memory space requirements to run a problem with ADINA, was reduced from 25,000 to 20,000 in order to compile the program.

ADINA is an out-of-core solver, which means that the equilibrium equations are processed in blocks, so that very large systems can be considered. Finite elements are grouped into blocks by the user, according to their type and whether they are linear or nonlinear. In the solution, low-speed storage is used to store all information pertaining to each block of finite elements, which, in the case of nonlinear elements, is updated during the time integration. The amount of low-speed storage required governs the size of the finite element system that can be considered. Thus, the reduction of MTOT will have a limiting effect on the size of finite element group that can be used by ADINA at BNL.

In this benchmarking study, the ADINA code was used to solve nonlinear, two- and three-dimensional thermomechanical and geostatic stress problems. In two-dimensional problems, both planar and axisymmetric elements have been tested. A thermal stress analysis of repository models with ADINA, is accomplished in two stages. First, the initial geostatic stress state in the rock mass due to the room excavation is computed and the results are stored on a tape file. It is usually assumed that the geostatic stress state is reached under elastic conditions. In the second stage of the analysis, the geostatic stresses are used as initial conditions, and temperature data from a previous heat transfer analysis with ADINAT are used as thermal loads. If time-dependent loading conditions or material properties exist, a transient analysis which corresponds to the ADINAT temperature data must be made.

The ADINA code provides the user with ten material models for two- and three-dimensional solid elements. These include isotropic, orthotropic linear elastic and thermo-elastic models, concrete, elastic-plastic models with isotropic or kinematic strain hardening, using the von Mises or Drucker-Prager yield criterion, and thermo-elastic-plastic creep models. In addition, provisions are made for user-supplied models, and a plane-stress model is given for two-dimensional elements.

**4.2 Problem 3.2b - Circular Tunnel (Long Cylindrical Hole)  
in an Infinite Elastic-Plastic Medium  
Subjected to a Hydrostatic Stress Field**

**Problem Statement** - This problem concerns the stress analysis around a long circular opening with a radius of 5 m in an elastic-plastic medium with a hydrostatic stress field. The objective of this problem is to test the code's ability to compute plastic stresses and deformations using the Tresca yielding criterion. The material is assumed to be elastic-perfectly plastic, and will yield when the difference between the maximum and minimum principal stresses reaches twice the shear yield stress (Tresca criterion).

**Input Data** - A two-dimensional, planar model of the tunnel cross-section and surrounding rock mass was used to analyze this problem. Horizontal and vertical symmetry conditions permitted the reduction of the model to one quadrant, with circumferential displacements restrained along the symmetry boundaries. A circular outer boundary was defined at 12 radii (60 m) from the tunnel centerline. This distance was considered sufficient to minimize changes in the boundary stress state. The finite element mesh used for this problem is shown in Figure 4.2-1. The von Mises yield criterion was selected, and parameters related to the viscoplastic material model were defined. Since the model considers a plane strain analysis, the element thickness was set to zero. The input data to ADINA for Problem 3.2b were taken from the Benchmark Problems Report and included:

● **Material Properties**

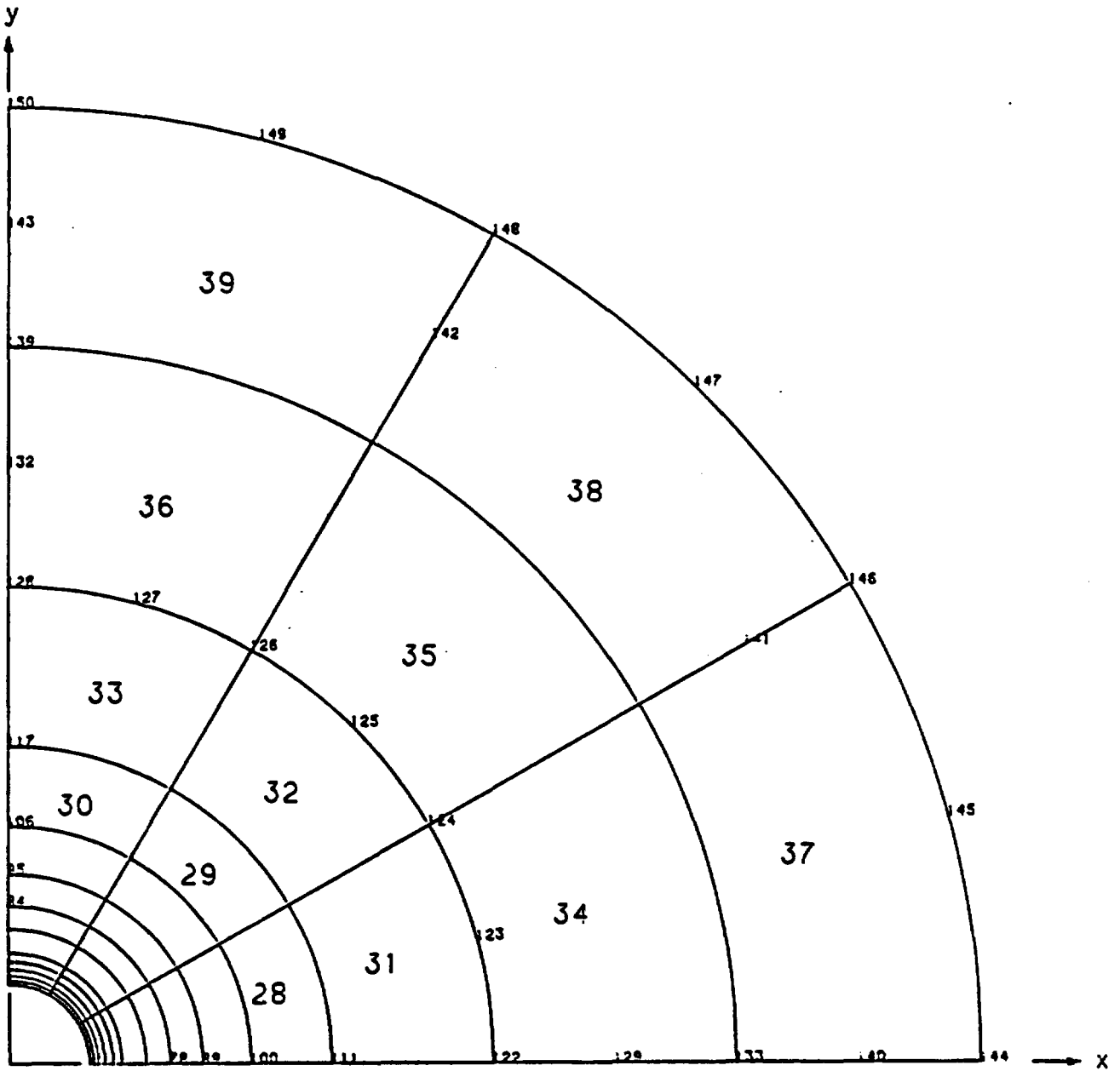
- |                                  |                        |
|----------------------------------|------------------------|
| - Modulus of Elasticity          | $E = 6000 \text{ MPa}$ |
| - Poisson's Ratio                | $\nu = 0.2$            |
| - Yield Stress in Simple Tension | $K = 20 \text{ MPa}$   |
| - Strain Hardening Modulus       | $E_T = 0.0$            |

● **In Situ Stresses**

- |                     |                        |
|---------------------|------------------------|
| - Horizontal Stress | $S_x = 15 \text{ MPa}$ |
| - Vertical Stress   | $S_y = 15 \text{ MPa}$ |

**Run Problem** - Although this is a static problem, an arbitrary time step of 0.01 sec. was defined to accomplish a nonlinear analysis in ADINA. A total of ten "time steps" were used to allow the program to reach steady state conditions. No code-related difficulties were encountered while running Problem 3.2b with ADINA.

**Results** - Comparisons of the ADINA results to the analytical solution are made at points along a radial line inclined  $30^\circ$  above the horizontal. The analytical solution predicts that the interface between plastic and elastic stress states occurs at a radial distance of 6.42 m. Figure 4.2-2, which compares the ADINA calculations of the circumferential (tangential) stresses to the analytical solution, indicates that ADINA calculated the plastic/elastic interface slightly closer to the center of the tunnel than the analytical solution. ADINA predicts radial stress continuity across this interface, as demonstrated in Figure 4.2-3, which shows the code-predicted and analytical radial stresses.



+-----+ 4.0 m in X  
 +-----+ 4.0 m in Y

Figure 4.2-1 ADINA Problem 3.2b  
Finite Element Mesh

# ADINA - PROBLEM 3.2b

## RADIAL STRESS

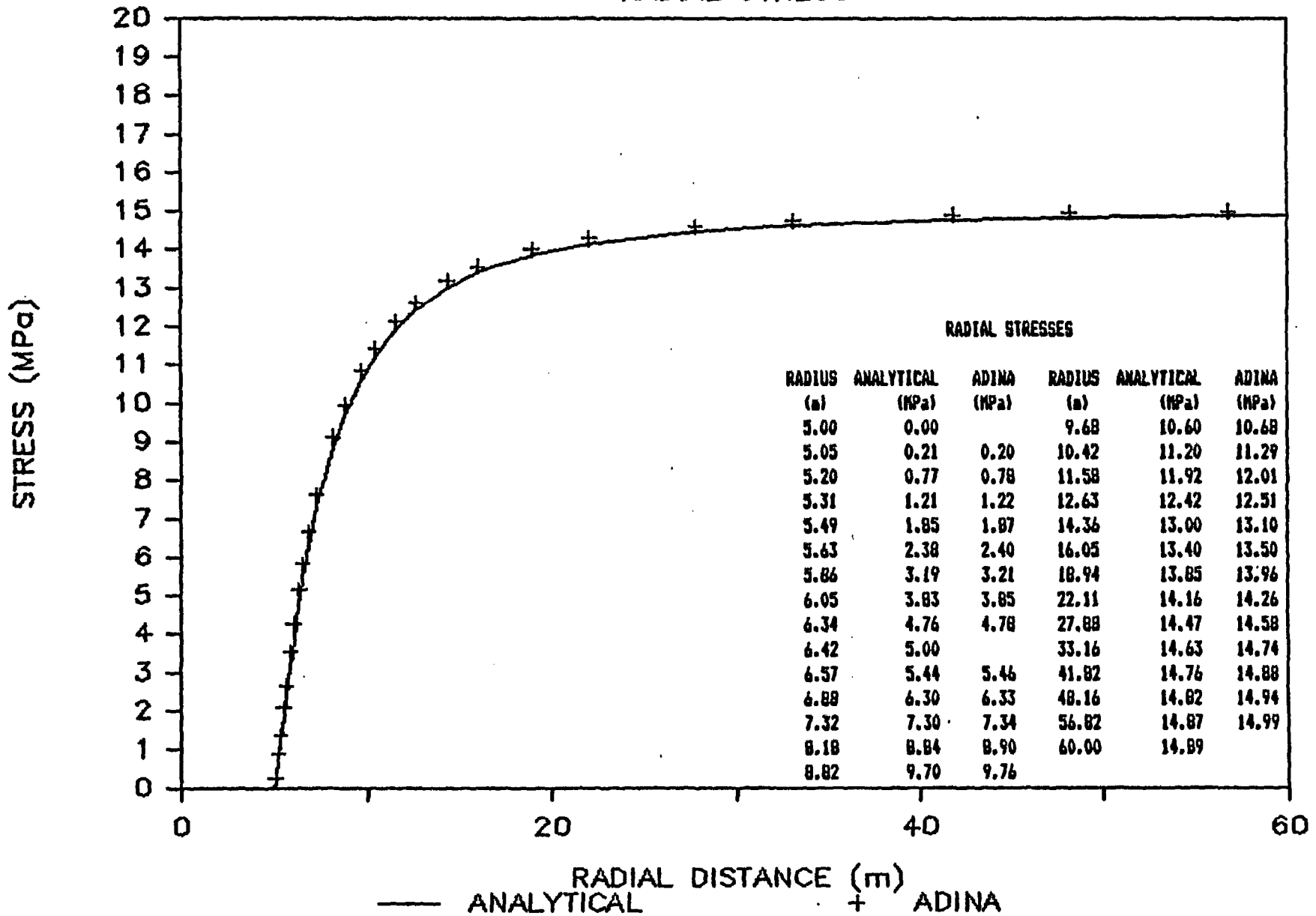


Figure 4.2-3 ADINA Problem 3.2b  
 Radial Stress Along a  
 Line 30 Degrees Above Horizontal

### 4.3 Problem 3.3c - Viscoelastic Analysis of a Thick-Walled Cylinder Subjected to Internal Pressure

**Problem Statement** - This problem concerns the stress analysis of an infinite length thick-walled cylinder, subjected to an internal pressure of 10 MPa. The cylinder has an inner radius of 4 m, an outer radius of 6 m, and is comprised of a homogeneous, isotropic, creep sensitive, material at a uniform constant temperature. The objective of this problem is to test the code's capability to calculate creep stresses and deformations against a known analytical solution. In the analytical solution, it is assumed that the steady-state creep condition has been reached: thus stresses and strain rates are constant with time.

**Input Data** - Symmetry conditions allow the reduction of this problem to one-quarter of the cylinder cross section. The two-dimensional, planar finite element mesh shown in Figure 4.3-1 was used to model this problem with ADINA. To accommodate the symmetry conditions, circumferential displacements were restrained along the horizontal and vertical symmetry boundaries. Since this model considers a plane strain analysis, the element thickness was set to zero.

A power-law creep function, dependent upon time, temperature, and stress, was defined for this problem. ADINA provides a power-law creep function, but considers stress and time only. Since this problem uses a constant temperature of 300°K, this limitation did not present a major difficulty. The coefficient which multiplies the entire function was modified from the value given in the Benchmark Problems Report to account for the temperature and exponent. Input data to ADINA for Problem 3.3c were taken from the Benchmark Problems Report and included:

#### ● Material Properties

- Modulus of Elasticity  $E = 5000 \text{ MPa}$
- Poisson's Ratio  $\nu = 0.4999$
- Power Law Creep Function  $\epsilon = A\sigma^m t^n T^p$

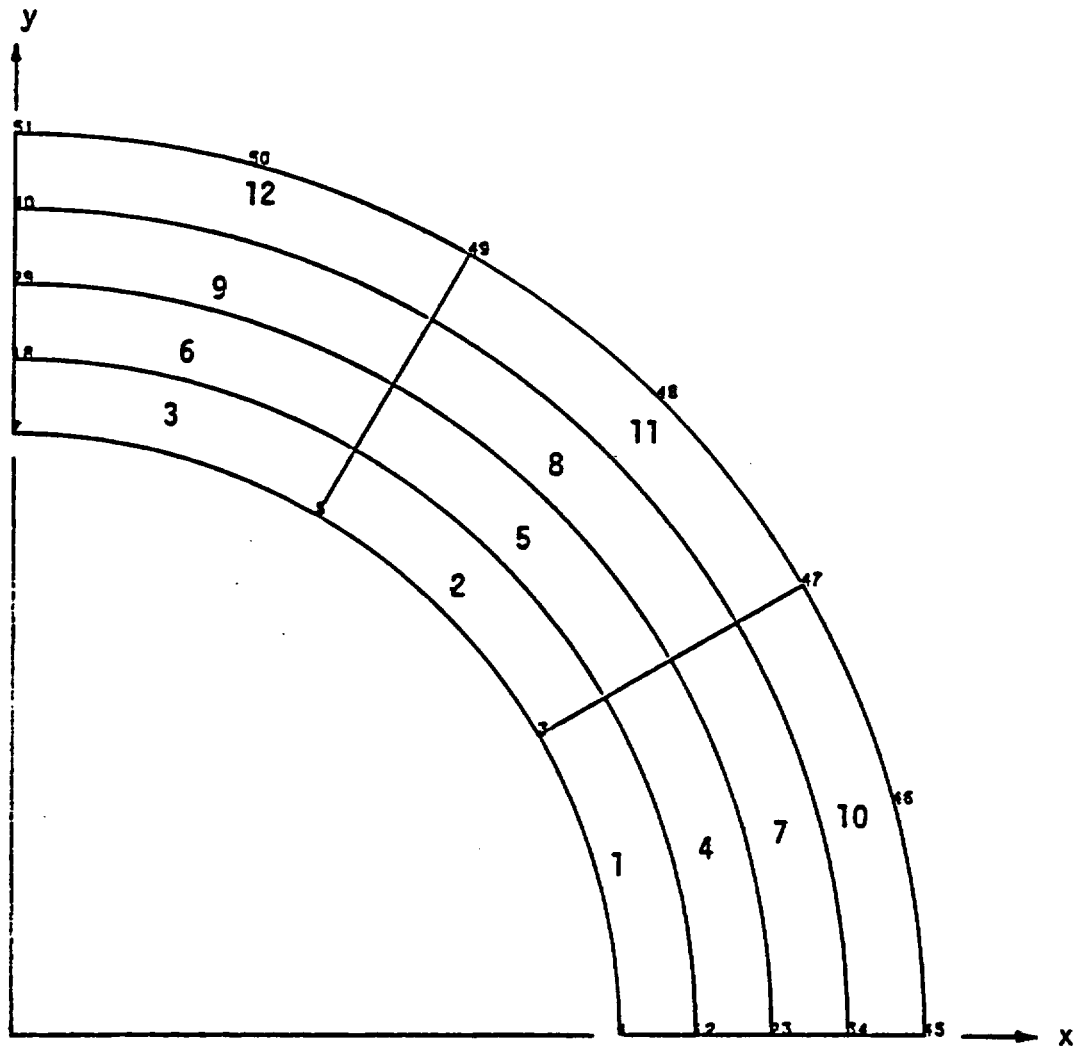
where:

- Coefficient  $A = 2.0 \times 10^{-21}$
- Temperature Exponent  $p = 2.0$
- Stress Exponent  $m = 4.0$
- Time Exponent  $n = 1.0$

#### ● Loading

- Internal Pressure  $P = 10 \text{ MPa}$
- Constant Temperature  $T = 300^\circ\text{K}$

**Run Problem** - This problem was run with ADINA using a time step of 1,600,000 sec. An initial run, which used a Poisson's ratio of 0.50 (perfectly plastic material), resulted in fatal execution errors. A successful analysis was made by using a Poisson's ratio of 0.4999, to eliminate division by zero. No other code-related difficulties were encountered in running this problem with ADINA.



⇄ 0.5 m in X  
 ⇄ 0.5 m in Y

Figure 4.3-1 ADINA Problem 3.3c  
Finite Element Mesh

# ADINA — PROBLEM 3.3c

## RADIAL STRESS

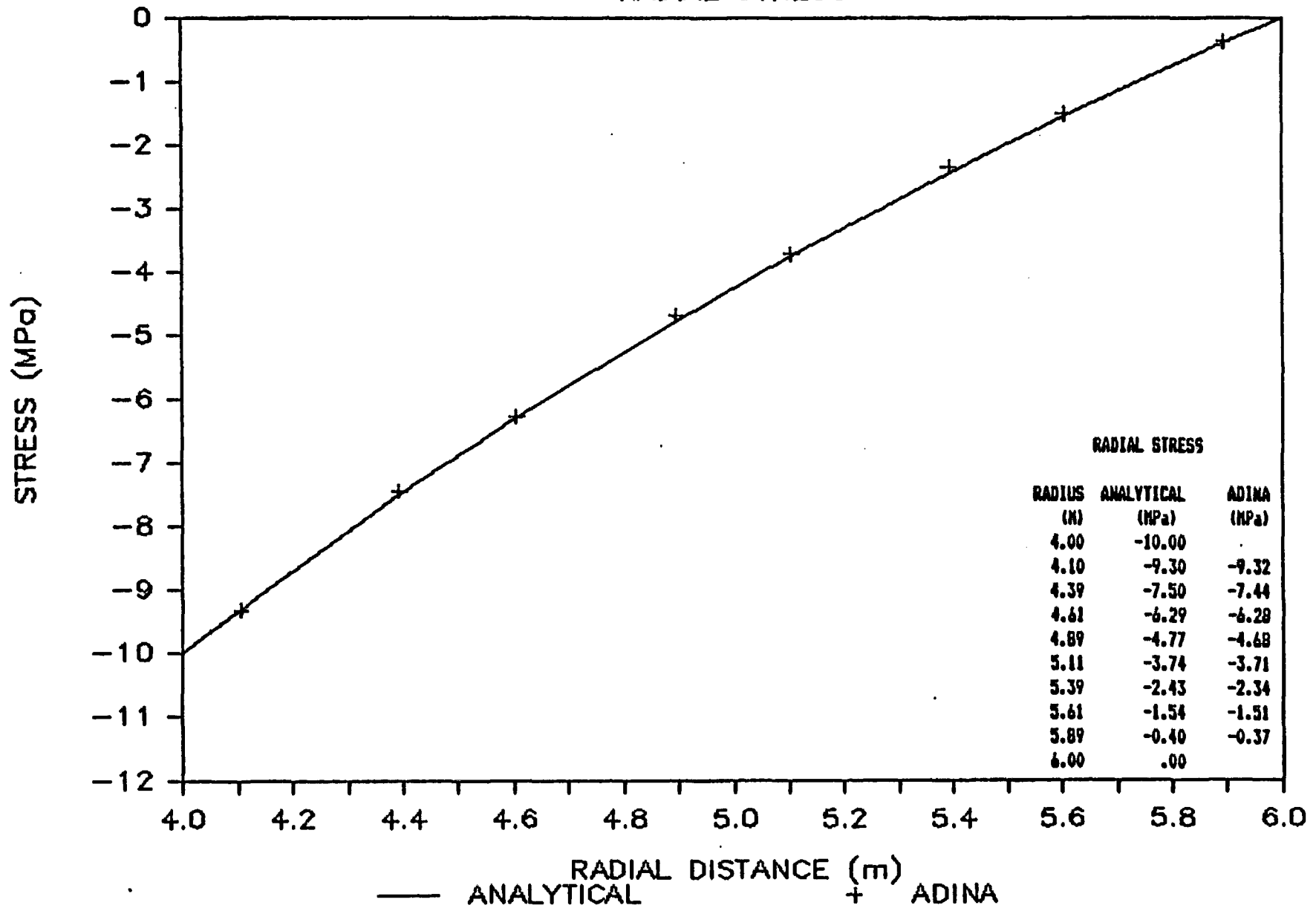


Figure 4.3-3 ADINA Problem 3.3c  
Radial Stress Along a  
Line 30 Degrees Above Horizontal

#### 4.4 Problem 3.5 - Plane Strain Compression of an Elastic-Plastic Material

Problem Statement - This problem concerns the yielding and plastic flow of a rectangular block, 15 m wide by 5 m high, loaded with a uniform pressure in the vertical orthogonal direction, constrained in the longitudinal orthogonal direction, and free to expand laterally. These boundary conditions allow this problem to be modeled with two-dimensional plane strain elements. Two elastic-plastic analyses are to be made using each of the von Mises and Drucker-Prager yield criteria. In the von Mises analysis, an initial vertical pressure of 300 MPa will be increased incrementally until ultimate failure is reached. The Drucker-Prager theory does not predict ultimate failure; thus, the loading will be increased well into the plastic flow range.

Input Data - Symmetry about the vertical centerline allows the reduction of this two-dimensional model to one-half the block width (7.5 m) by the full height (5 m). The finite element mesh used to solve this problem with ADINA is shown in Figure 4.4-1. Symmetry and boundary conditions are preserved by restricting horizontal displacements along the original vertical centerline and vertical displacement along the frictionless bottom surface. Since the problem is a plane strain analysis, an element thickness of zero was used. The input data to ADINA for Problem 3.5 were taken from the Benchmark Problems Report and include:

- Material Properties
  - Modulus of Elasticity  $E = 45,000 \text{ MPa}$
  - Poisson's Ratio  $\nu = 0.20$
- von Mises Failure Criterion Parameter  $K_M = 190 \text{ MPa}$   
(Yield Stress in Pure Shear)
- Drucker-Prager Yield Criterion Parameters  $K_{DP} = 36$   
 $\alpha = 0.35$

Run Problem - This problem has not been successfully run with ADINA.

## 5.0 BENCHMARKING OF ADINAT

## 5.0 BENCHMARKING OF ADINAT

### 5.1 Code Background and Capabilities

ADINAT, an acronym for Automatic Dynamic Incremental Non-linear Analysis of Temperatures, is a finite element code for one-, two-, and three-dimensional heat transfer analysis. Two-dimensional problems may be either planar or axisymmetric.

The code was developed and is leased and supported by K. J. Bathe and his associates at ADINA Engineering, Inc., Watertown, Mass. Version 1981-NL9 of ADINAT was obtained from ADINA Engineering, and installed on the BNL computer system.

ADINAT may be used as a thermal pre-processor to the structural analysis code ADINA, allowing thermomechanical analyses. The 1981 version of the structural analysis code ADINA, was obtained from ADINA Engineering and installed on the BNL computer system with a slight modification. The variable MTOT, which specifies the total memory space requirements to run a problem with ADINA, was reduced from 25,000 to 20,000. A similar variable in ADINAT, also called MTOT, was reduced to the same value. Due to its complexity, the ADINA code requires more storage space than ADINAT. Consequently, some large thermomechanical models which run successfully with ADINAT may exceed the limitations of ADINA at BNL.

Conduction is the principal mechanism of heat transfer considered in ADINAT. In addition, convection, radiation, or specified temperature boundary conditions and volumetric heat generation are used. Heat storage may be due to both specific and latent heat. Temperatures defined for all boundary conditions may be time-dependent, and all material properties, including heat transfer coefficients, may be temperature-dependent. Specifically, boundary conditions in ADINAT may include:

- Constant or time-dependent temperature and heat flux functions.
- Convection from a node, line, or surface with a constant or temperature-dependent convection coefficient to a constant or time-dependent environmental temperature.
- Radiation to/from a node, line, or surface from/to a constant or time-dependent source/sink temperature.

ADINAT has a restart option which saves problem solution information on tape files for further problem processing.

A total of seven benchmark problems were used to test ADINAT. These included:

1. Problem 2.6 - Transient Temperature Analysis of an Infinite Rectangular Bar with Anisotropic Conductivity;

TABLE 5.1-1

## ADINAT CAPABILITIES TESTED OR UTILIZED

	Problem						
	<u>2.6</u>	<u>2.8</u>	<u>2.9</u>	<u>2.10</u>	<u>5.2</u>	<u>6.1</u>	<u>6.2</u>
<b>Problem Type</b>							
- One-Dimensional							
- Two-Dimensional - Planar	T	T	T		U	U	
- Two-Dimensional - Axisymmetric						U	U
- Three-Dimensional							
<b>Equation Solution</b>	T	T	T		U	U	U
<b>Phase Changes</b>							
<b>Conductivity</b>							
- Isotropic		T	T		U		
- Anisotropic	T						
- Temperature Dependent						U	U
<b>Specific Heat</b>							
- Constant	T	T	T			U	
- Temperature Dependent							U
<b>Concentrated Heat Sources</b>							
- Constant							
- Time Dependent						U	U
<b>Distributed Heat Fluxes</b>							
- Constant							
- Time Dependent							
<b>Specified Nodal Point Temperatures</b>							
- Constant						U	U
- Time Dependent							

## 5.2 Problem 2.6 - Transient Temperature Analysis of an Infinite Rectangular Bar with Anisotropic Conductivity

**Problem Statement** - This problem concerns the thermal response of a rectangular bar, 4.0 m wide (y) by 2.0 m deep (z) of infinite length, initially at 573°K throughout, exposed on all four sides at time zero to a large mass of fluid at 303°K. The thermal conductivity of the bar is anisotropic with its principal directions coincident with the y and z axes. The principal mechanisms of heat transfer include convection from the surface to a fluid at constant temperature, and conduction within the bar. Symmetry conditions along the y and z axes reduce the modeled area to one quarter of the bar cross section.

**Input Data** - One-quarter of the bar cross-section was modeled using two-dimensional, planar, 8-noded conduction elements. The finite element mesh utilized for this problem is shown in Figure 5.2-1. Surface convection was applied directly as a boundary condition to the conduction elements.

Input data to ADINAT for this problem were taken from the Benchmark Problems Report and included:

### ● Material Properties

- Conductivity in y-direction  $k_y = 2.0 \text{ W}/(\text{m}^\circ\text{K})$
- Conductivity in z-direction  $k_z = 1.0 \text{ W}/(\text{m}^\circ\text{K})$
- Heat Capacity  $c = 2.001 \times 10^6 \text{ J}/(\text{m}^3 \cdot ^\circ\text{K})$
- Thermal diffusivity in y- and z-directions  $y = 9.9950 \times 10^{-7} \text{ (W.m}^2\text{)}/\text{J}$   
 $z = 4.9975 \times 10^{-7} \text{ (W.m}^2\text{)}/\text{J}$

### ● Initial Conditions/Boundary Conditions

- Initial Bar Temperature  $T_i = 573^\circ\text{K}$
- Environmental Fluid Temperature  $T_o = 303^\circ\text{K}$
- Convection Heat Transfer Coefficient  $h = 2.0 \text{ W}/(\text{m}^2 \cdot ^\circ\text{K})$

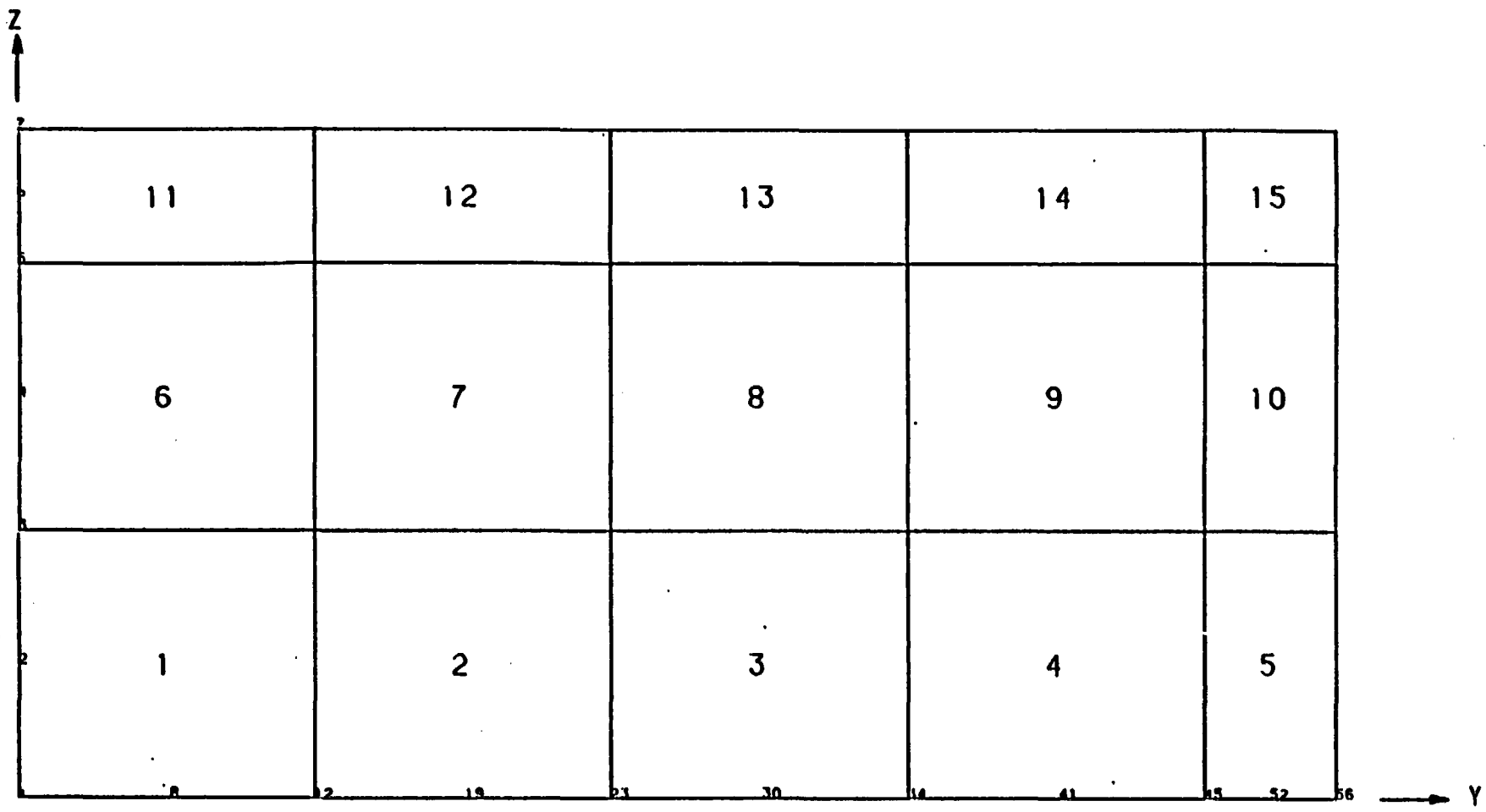
**Run Problem** - This problem was solved in two separate analyses with different time step schemes to determine the relative accuracy of the solution. In the first run, an initial time step of 100,000 sec. was estimated using a procedure developed by Nickell and Levi, and outlined by Gartling in the COYOTE User Manual. Other time steps throughout the remainder of the solution range were selected accordingly. In the second run, time steps were one-tenth the size of those used in the first run. Table 5.2-1 summarizes the time steps used by ADINAT in Runs 1 and 2 of Problem 2.6.

No code-related difficulties were encountered while running Problem 2.6 with ADINAT.

**Results** - Temperatures predicted by ADINAT from Runs 1 and 2 are compared to the analytical solutions at a time of 400,000 sec (110 hours). This time was chosen for comparison in the analysis of the DOT results

TABLE 5.2-1  
TIME STEPS USED WITH ADINAT FOR PROBLEM 2.6

<u>Time Range</u> <u>(x10<sup>-6</sup> sec)</u>	<u>RUN 1</u>		<u>RUN 2</u>	
	<u>Time Step</u> <u>(sec)</u>	<u>No. of Time Steps</u>	<u>Time Step Size</u> <u>(sec)</u>	<u>No. of Time Steps</u>
0-2	100,000	20	10,000	200
2-4	200,000	10	20,000	100
4-8	400,000	10	40,000	100



+-----+ .j m in Y  
 +-----+ .j m in Z

Figure 5.2-1 ADINAT Problem 2.6  
Finite Element Mesh

# ADINAT - PROBLEM 2.6

Z-AXIS TEMPERATURES (at t=400,000 s)

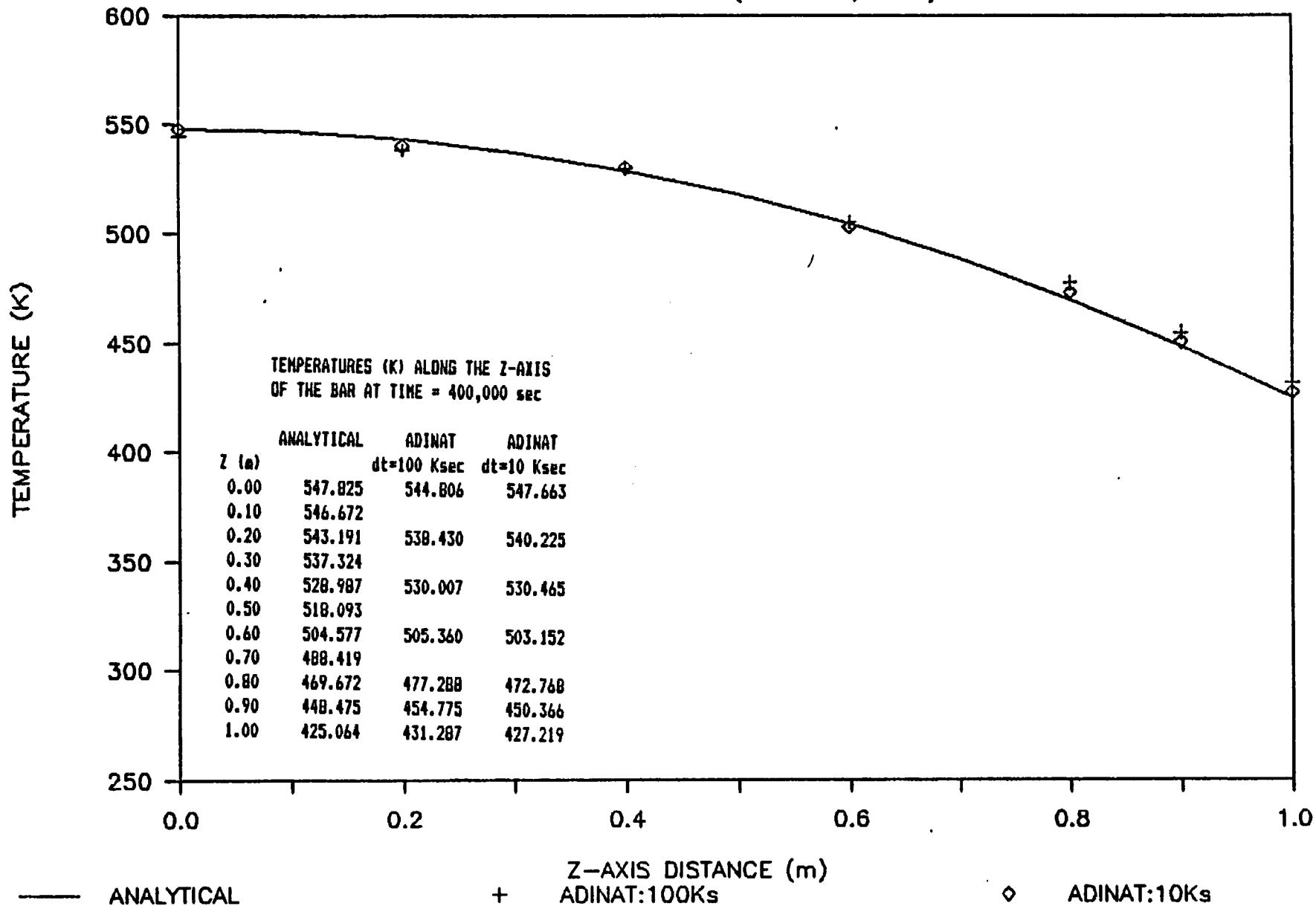


Figure 5.2-3 ADINAT Problem 2.6  
Z-Axis Temperature Profiles  
at Time = 400,000 sec

TABLE 5.3-1

BENCHMARK PROBLEM 2.8  
SOLUTION COMPARISON

<u>Time (sec)</u>	<u>Temperature (°C) of Quenched Surface</u>		<u>% Error</u>
	<u>Analytical Solution</u>	<u>ADINAT Solution</u>	
0	260	260	0
8,350	174	174.1	0.12
16,700	154	155.2	1.32
25,050	141	142.3	1.09

#### 5.4 Problem 2.9 - Transient Temperature Response of a Slab Exposed to a Uniform Radiative Environment

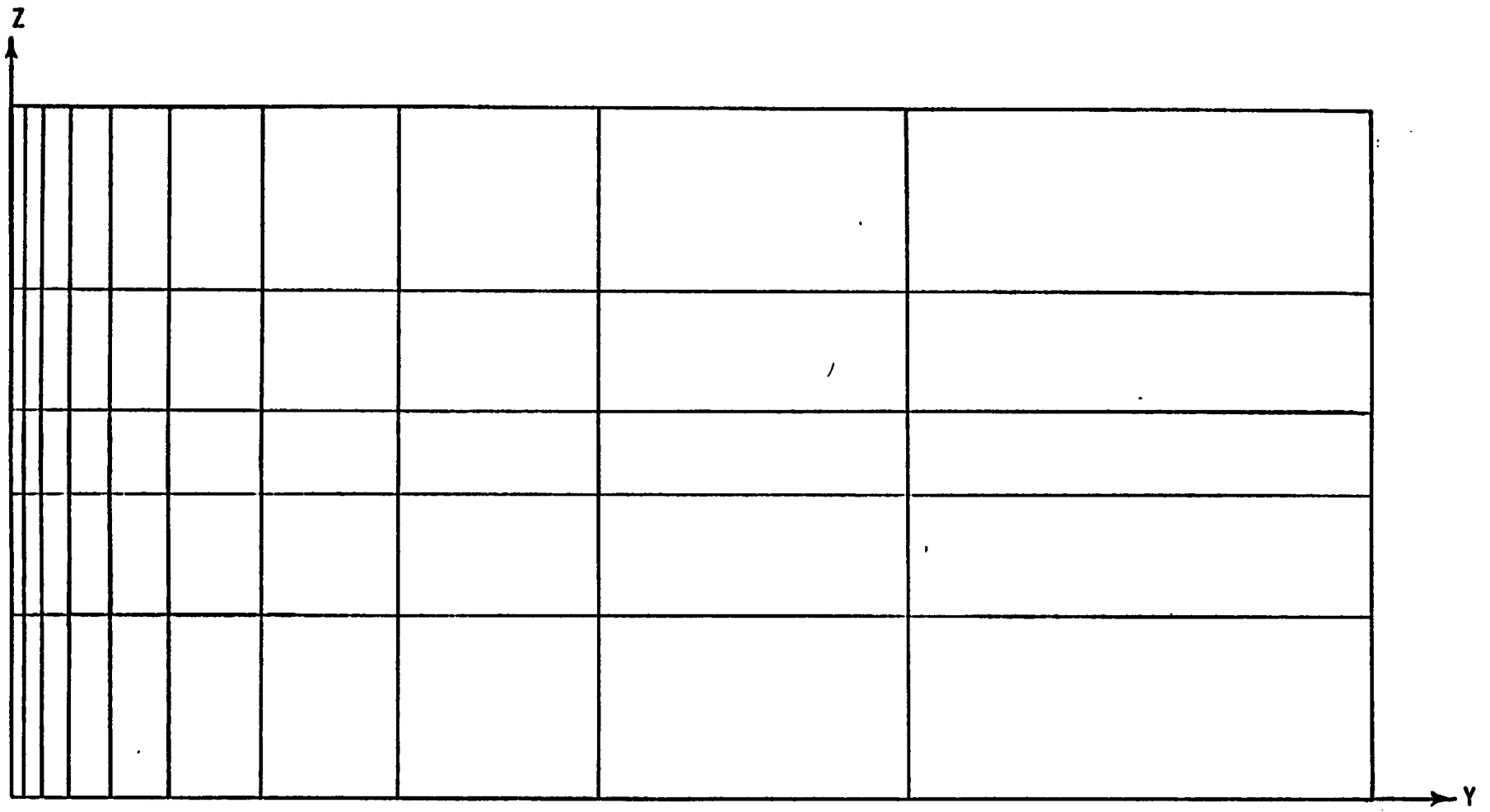
Problem Statement - This problem is concerned with the transient thermal analysis of an infinite slab, 0.25 m thick. The slab is initially at 546°K, one face is insulated, and the other is exposed to a radiative environmental temperature of 273°K at time zero. The temperature histories of both sides of the slab are to be determined.

Input Data - A preliminary run, using a single row of elements, resulted in a very slight temperature gradient in the z-direction, due to numerical noise. This problem was therefore modeled using 5 rows of 8-noded, two-dimensional conduction elements, as shown in Figure 5.4-1. The following input data, taken from the Benchmark Problems Report, were used to run this problem with ADINAT:

- Material Properties
  - Thermal Conductivity  $k = 1.15 \text{ W/(m}\cdot\text{°K)}$
  - Heat Capacity  $c = 2.124 \times 10^6 \text{ J/(m}^3\cdot\text{°K)}$
- Initial Conditions
  - Radiative Environmental Temperature  $T_2 = 273^\circ\text{K}$
  - Initial Slab Temperature  $T_0 = 546^\circ\text{K}$

Run Problem - The time step estimation outlined by Gartling in the COYOTE user manual indicated that the initial time step should be 3 seconds. A review of the analytical solution (see Figure 3.1.3-2) indicated that a steep temperature gradient exists on the radiative face for the initial 10 hours. The use of a 3 second time step would require 1200 integrations during this period. Computational effort of this degree seemed extreme, thus the problem was run using the time steps listed in Table 5.4-1. No code-related difficulties were encountered while running Problem 2.9 with ADINAT.

Results - Figures 5.4-2 and 5.4-3 compare the temperature histories calculated by ADINAT to the analytical solution of the radiative and insulated faces, respectively. The ADINAT results using the selected time steps compare favorably with the analytical solutions. Further refinement of the time steps may be made if desired, although it is not considered necessary for the purpose of benchmarking the ADINAT code.



+—+ 0.1 m in Y  
+—+ 0.2 m in Z

Figure 5.4-1 ADINAT Problem 2.9  
Finite Element Mesh

# ADINAT PROBLEM 2.9

TEMPERATURE HISTORY AT INSULATED FACE

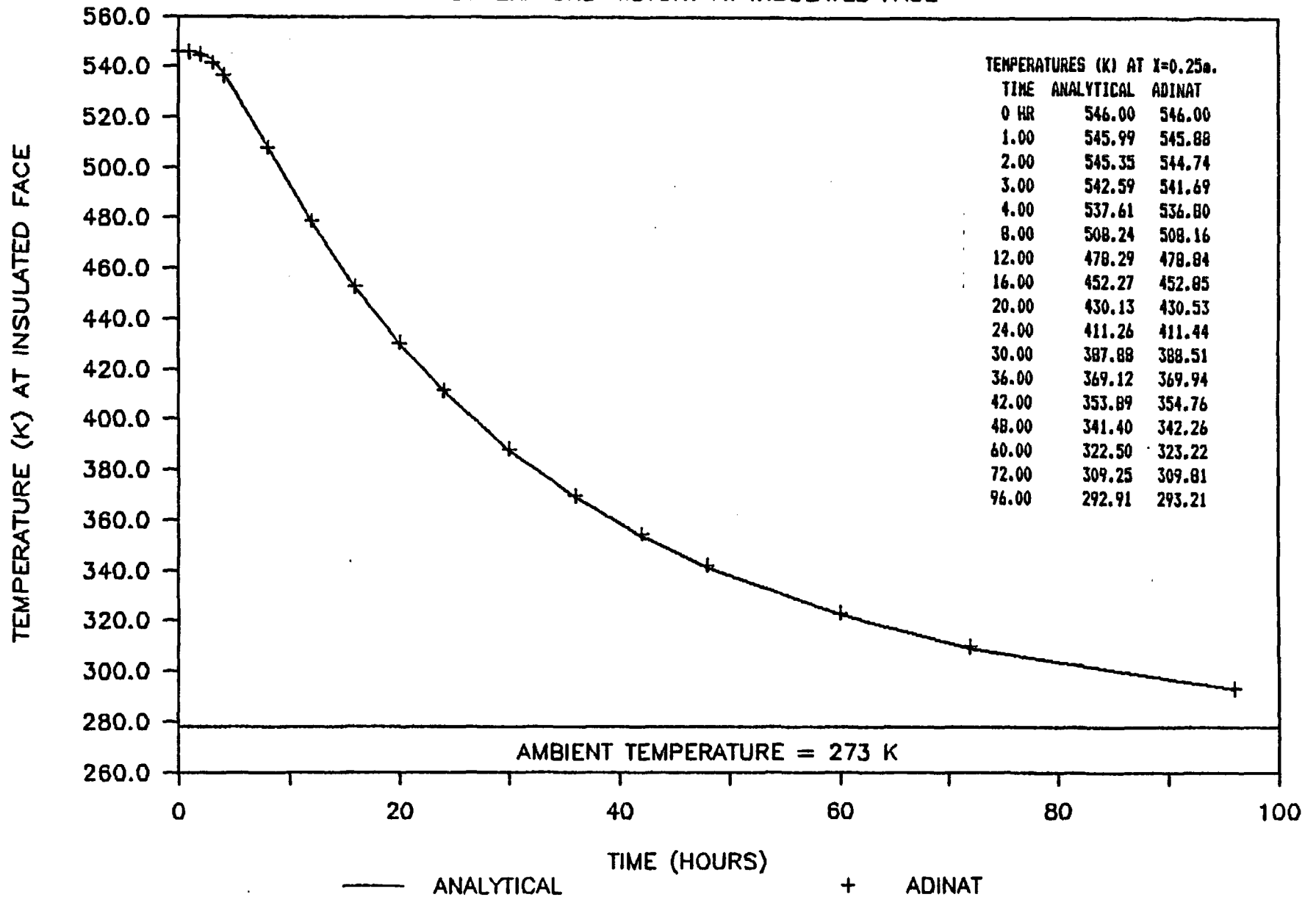


Figure 5.4-3 ADINAT Problem 2.9  
Temperature History at  
Insulated Face

## 5.6 Problem 5.2B - Hypothetical Near Field Problem - Basalt

**Problem Statement** - This problem consists of the two-dimensional transient thermal simulation of the very near field (single room region) of a hypothetical repository. Waste canisters, emplaced vertically below the room floor at regular intervals along the centerline, have been replaced by an equivalent heat generating trench for this analysis. This problem exercises general transient heat transfer with mechanisms of conduction, heat storage, and free and forced (ventilation) convection. Ventilation is maintained for the first 50 years, after which the room is sealed and natural convection and radiation occurs. This problem, and the accompanying far field problem of the same repository, are summarized in greater detail in Section 3.3

The output from the thermal analysis of this problem with ADINAT will be used as input to ADINA for a thermomechanical analysis. In these analyses the material properties of basalt will be used.

**Input Data** - The heat flux function in ADINAT used to define heat input from the canisters in this model applied the heat at nodes. Therefore, the heat flow given in Table 5.6-3 was multiplied by the effective nodal areas listed in Table 5.6-4. Input data to ADINAT for Problem 5.1 were taken from the Benchmark Problems Report and included:

- Thermal Properties of All Materials Modeled
  - Conductivity Table 5.6-1
  - Heat Capacity Table 5.6-1
- Initial Conditions/Boundary Condition
  - Initial Temperatures
    - between  $Z = -479\text{m}$  and  $Z = -510\text{m}$   $T_0 = 25^\circ\text{C}$
    - all other depths  $T_0 = (15 - 0.02Z)^\circ\text{C}$
  - Environmental Room Temperature  $T_e = 15^\circ\text{C}$
  - Convection Coefficients Table 5.6-2
  - Constant Temperature at  $Z = 0$   $T = 15^\circ\text{C}$
  - Constant Temperature at  $Z = -3500\text{m}$   $T(3500) = 85^\circ\text{C}$
  - Externally Supplied Heat Flux Table 5.6-3

**Run Problem** - ADINAT permits the definition of convection coefficients as constants, functions of element surface temperature, or functions of the temperature difference between the element surface and the environment. In Benchmark Problem 2.6 (Section 5.2), the constant temperature coefficient was tested. In Problem 2.8 (Section 5.3), the temperature-dependent convection coefficient was tested. This problem was attempted using the temperature difference dependent convection coefficient listed in Table 5.6-2, but no successful runs were made. Several modifications were made to the input set, including reduction of the time step, redefinition of convective surfaces using two or three nodes, and using a single temperature difference dependent convection coefficient for all surfaces. In all attempts, the program terminated while in a convection-calculating subroutine and issued the fatal error message "overflow condition". The model was run successfully with no convection elements, as a check of the remaining input, but the results were not meaningful since no comparison could be made with other codes.

TABLE 5.6-1

CONDUCTIVITY AND SPECIFIC HEAT FOR ADINAT  
 PROBLEM 5.2 - BASALT

Temperature (°C) T	Conductivity (W/m°C)			Specific Heat (J/kg°C) C
	$k_x$	$k_y$	$k_{xy}$	
-100	1.1	1.1	0	835
*10,000	1.1	1.1	0	835

\*Values were defined at 10,000°C to prevent temperatures from going out of range.

TABLE 5.6-3  
 EXTERNALLY SUPPLIED HEAT FLUX FOR ADINAT  
 PROBLEM 5.2 - BASALT

<u>Time (years)</u>	<u>Time (sec)</u>	<u>Heat Flux (W/m<sup>2</sup>)</u>
0	0	20.000
10	3.156 x 10 <sup>8</sup>	15.068
20	6.312 x 10 <sup>8</sup>	11.352
30	9.468 x 10 <sup>8</sup>	8.552
40	1.264 x 10 <sup>9</sup>	6.443
50	1.578 x 10 <sup>9</sup>	4.854
60	1.894 x 10 <sup>9</sup>	3.657
70	2.209 x 10 <sup>9</sup>	2.755
100	3.156 x 10 <sup>9</sup>	1.178
150	4.734 x 10 <sup>9</sup>	0.286
200	6.312 x 10 <sup>9</sup>	0.069
300	9.468 x 10 <sup>9</sup>	0.004
350	1.105 x 10 <sup>10</sup>	0.001
500	1.578 x 10 <sup>10</sup>	0.0
11000	3.472 x 10 <sup>11</sup>	0.0

## 5.7 Problem 6.1 - Project Salt Vault Thermomechanical Response Simulation Problem

**Problem Statement** - Problem 6.1 concerns the analysis of two full-scale heater experiments performed simultaneously in adjacent rooms during Project Salt Vault (PSV). Heater experiments were conducted in four parallel rooms in PSV. A line of symmetry between Room 2 and Room 3 reduces the model to two rooms. The heater experiment in Room 3 consisted of a row of heaters parallel to the axis of the room, whereas the experiment in Room 4 involved a circular array of heaters.

Due to the different geometric configurations of the heaters, the problem has been divided into two separate analyses. Problem 6.1P is a two-dimensional planar analysis of Room 3, and Problem 6.1A is a two-dimensional axisymmetric analysis of Room 4. The boundary between the two problems is located within the pillar between Rooms 3 and 4, one meter from the edge of Room 3. This location coincides with the lowest field-measured temperatures, and was chosen as a boundary to minimize the effect of the adjacent room.

The events of the heater experiments in Rooms 3 and 4, as they pertain to the solution of Problems 6.1P and 6.1A with ADINAT, are shown in Table 5.7-1. The temperature distributions determined by ADINAT for this problem will be compared to other thermal analysis code solutions and used as input to the ADINA code for a thermomechanical analysis.

**Input Data** - The finite element meshes for the planar and axisymmetric problems are shown in Figures 5.7-1 and 5.7-2, respectively. The upper and lower boundaries of both models were located at positions which, from the given field data, could be assumed adiabatic. Other input data were obtained from the Benchmark Problems Report, and included:

- **Material Properties**

- Conductivity  $c = 2.002 \times 10^6 \text{ J}/(\text{m}^3\text{C})$
- Heat Capacity Table 5.7-2

- **Initial Conditions/Boundary Conditions**

- Initial Temperature  $T_0 = 23^\circ\text{C}$
  - Environmental Temperature in Rooms  $T_e = 23^\circ\text{C}$
  - Convection Coefficient  $h = 5.886 \text{ W}/\text{m}^2\text{C}$
  - Externally Supplied Heat Flux Table 5.7-3
- Functions

The externally supplied heat flux function was multiplied by the effective area factors listed in Table 5.7-4 to give the appropriate nodal heat fluxes.

**Run Problem** - A time step of 15 days was chosen for both models since it agrees well with the time history shown in Table 5.7-1. The analysis for Problem 6.1P (Room 3) started on Day 360 and continued until 30 days beyond the conclusion of the experiment (Day 720). The solution of Problem 6.1A (Room 4) was begun on Day 0, and concluded 15 days after the array heaters were turned off. The temperature data for both

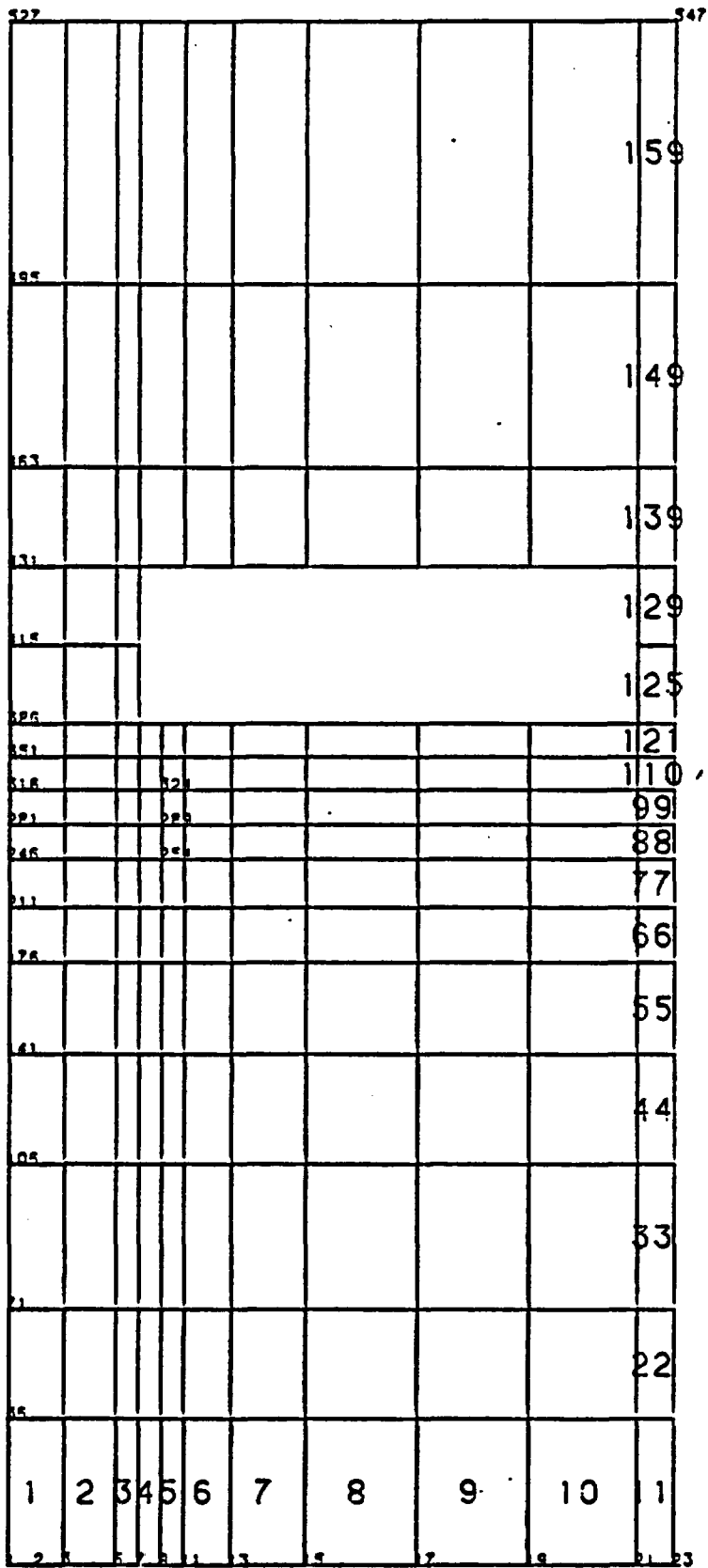
**TABLE 5.7-1**  
**TIME HISTORY OF PROJECT SALT VAULT**

<u>Time (Days)</u>		<u>Event</u>
<u>Standard</u>	<u>Model</u>	
806	0	Room 4 (6.1A) heaters turned on at 1.53 kW/heater.
1170	360	Room 3 (6.1P) heaters turned on at 1.50 kW/heater.
1240	435	Room 4 (6.1A) heaters boosted to 2.14 kW/heater.
1382	570	Room 4 (6.1A) heaters turned off.
1499	690	Room 3 (6.1P) heaters turned off.

TABLE 5.7-3

EXTERNALLY SUPPLIED HEAT FLUX FUNCTIONS FOR ADINAT  
PROBLEMS 6.1P AND 6.1A

Planar Analysis		Axisymmetric Analysis	
Time (sec)	Heat Flux (W)	Time (sec)	Heat Flux (w/rad/heater)
0.0	0.0	0.0	243.5
$3.144 \times 10^7$	0.0	$3.749 \times 10^7$	243.5
$3.145 \times 10^7$	1353.0	$3.750 \times 10^7$	340.6
$6.070 \times 10^7$	1353.0	$4.976 \times 10^7$	340.6
$6.071 \times 10^7$	0.0	$4.977 \times 10^7$	0.0
$1.0 \times 10^8$	0.0		



+-----+ 2 m in y  
 +-----+ 2 m in z

Figure 5.7-1 ADINAT Problem 6.1P  
Finite Element Mesh

# ADINAT - PROBLEM 6.1P - ROOM 3

## TEMPERATURE HISTORY AT VARIOUS OFFSETS

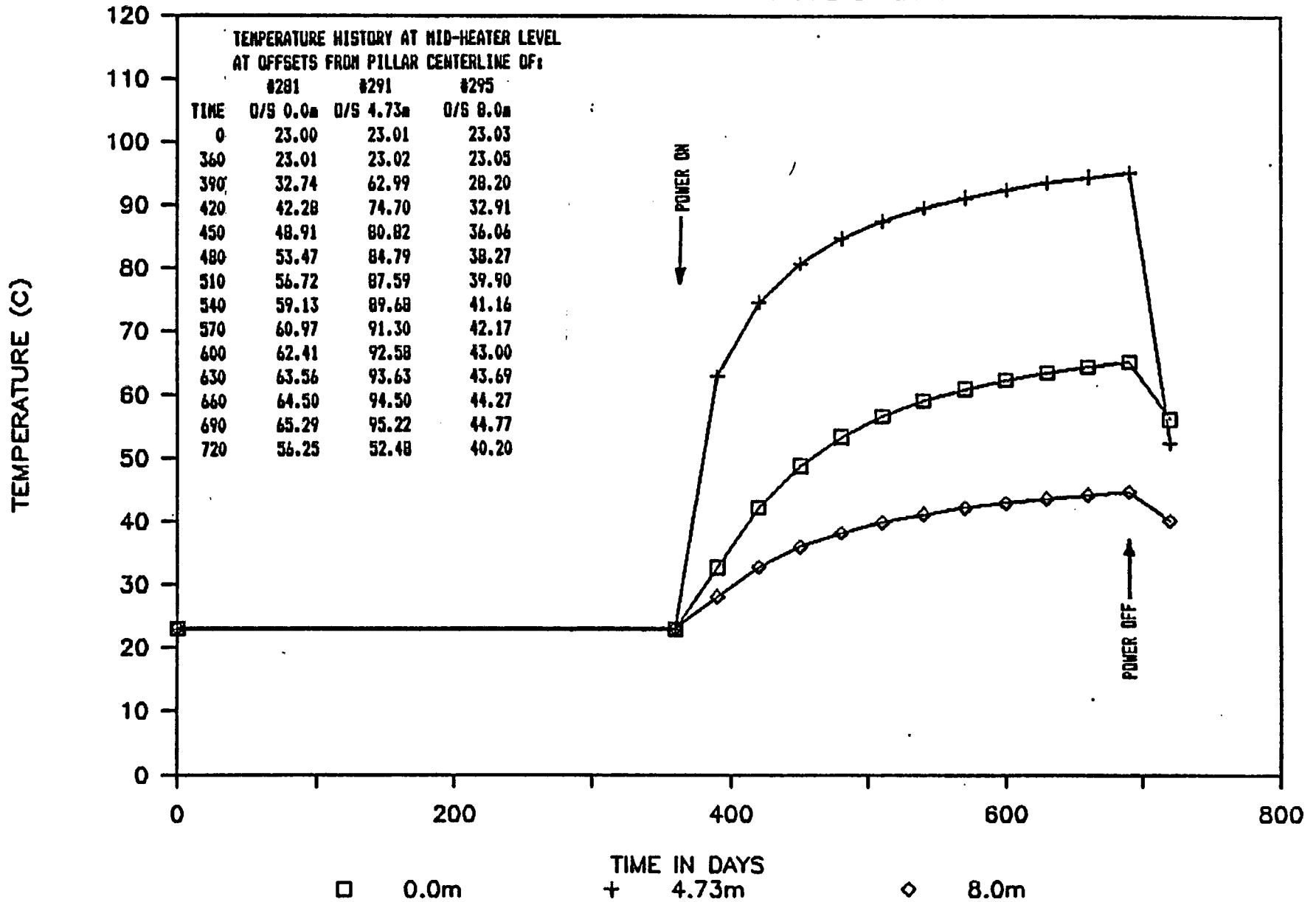


Figure 5.7-3 ADINAT Problem 6.1P - Room 3  
Temperature History at Various Offsets  
Depth = 2.8 m

# PROBLEM 6.1A – ROOM 4 – FIELD VALUES

TEMPERATURE HISTORY AT VARIOUS OFFSETS

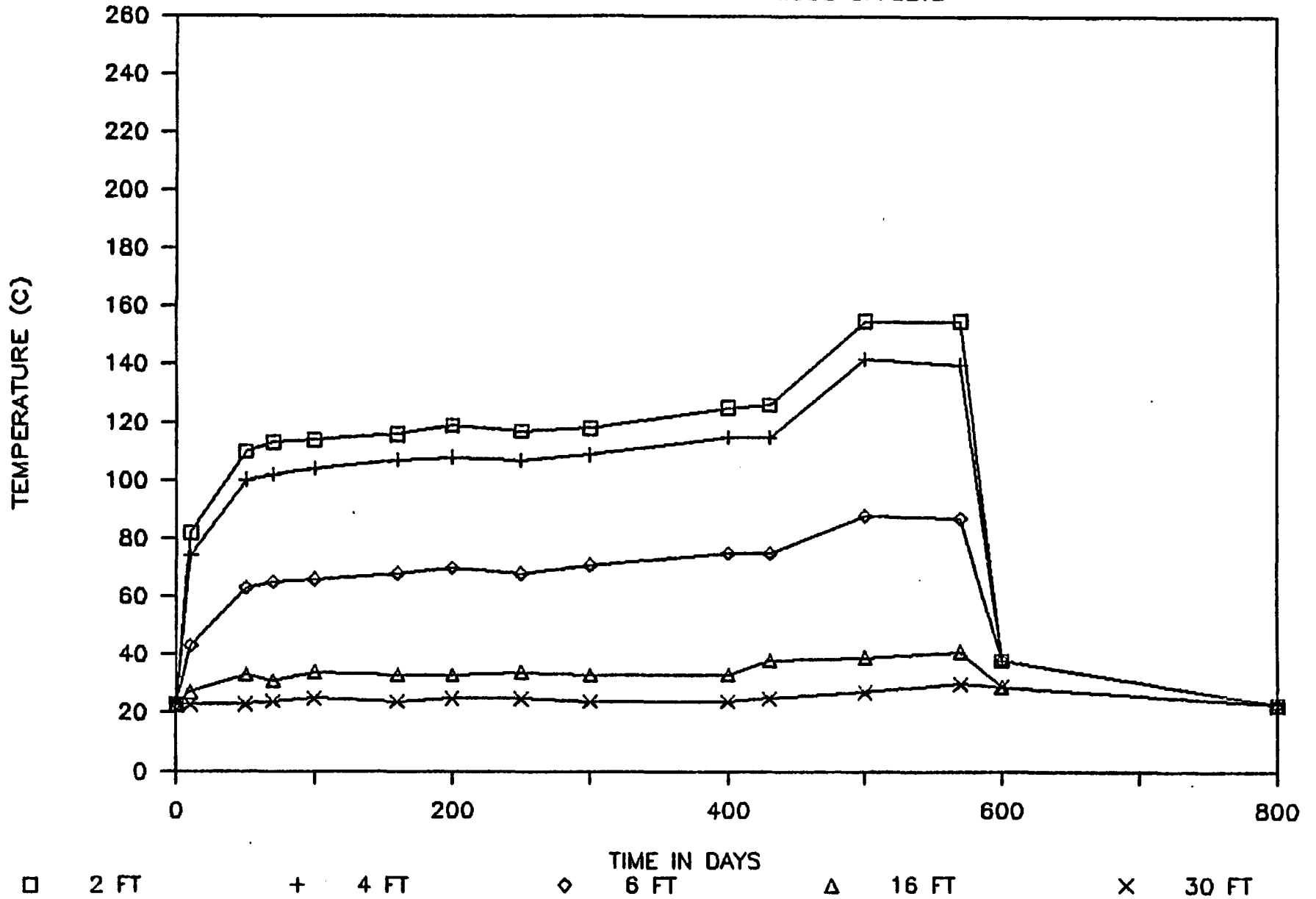


Figure 5.7-5 · Project Salt Vault Field Values  
Temperature History at Various Offsets  
at Mid-Heater Depth

# PROBLEM 6.1A - ROOM 4 - FIELD VALUES

## TEMPERATURE HISTORIES AT VARIOUS DEPTHS

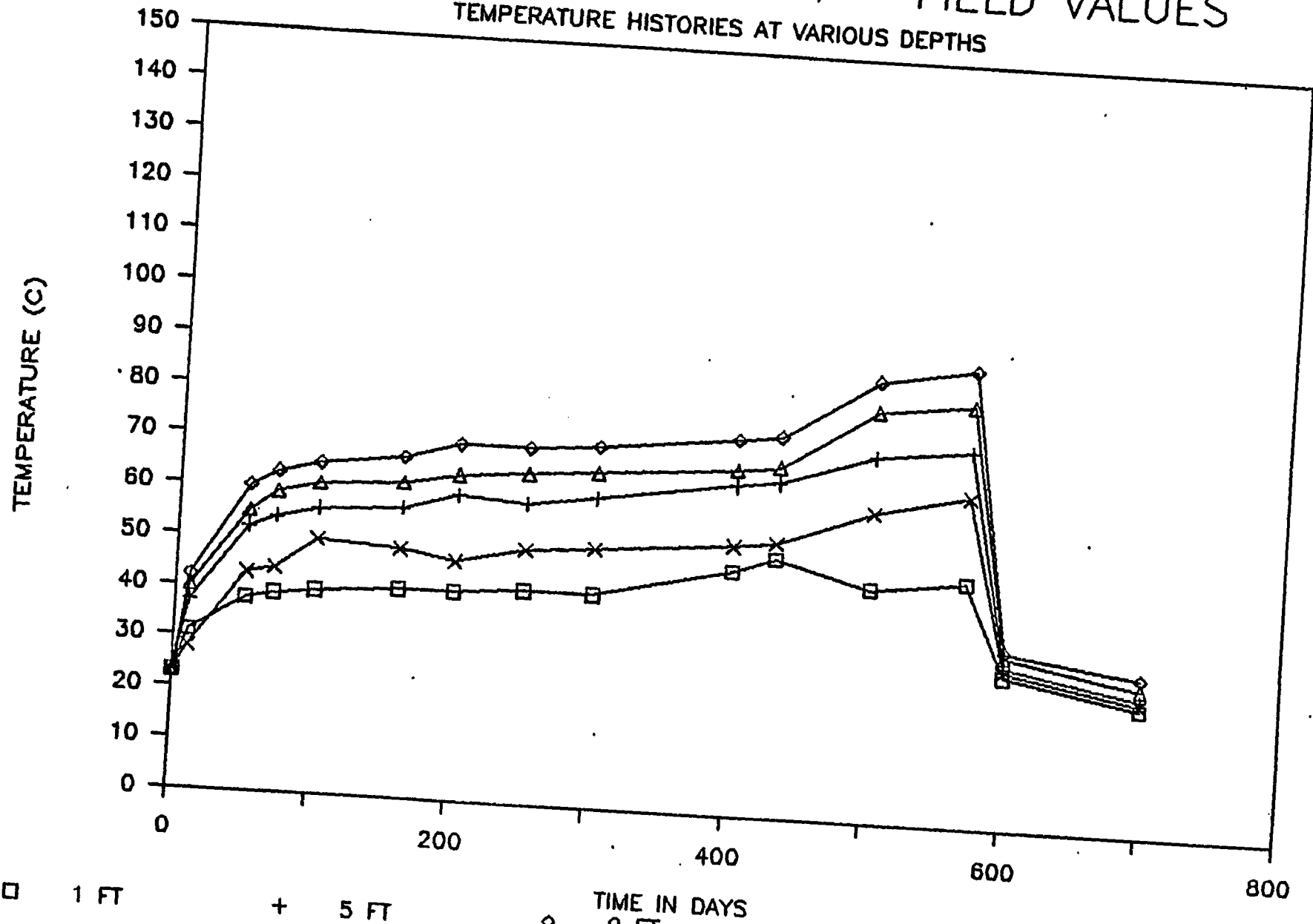


Figure 5.7-7 Project Salt Vault Field Values  
 Temperature History at Various Depths  
 Offset = 2.4 m from Pillar Centerline

## 6.0 BENCHMARKING OF DOT

## 6.0 BENCHMARKING OF DOT

### 6.1 Code Background and Capabilities

DOT, an acronym of Determination Of Temperature, is a two-dimensional finite element heat conduction computer program developed by R.M. Polivka and E.L. Wilson<sup>(12)</sup> at the University of California - Berkeley. The program and documentation<sup>(7)</sup> were obtained from the Office of Nuclear Waste Isolation (ONWI). DOT is one of the codes documented as part of the SPECTER technology package. The QA identification number for this version is 420--05C-02.

The DOT program can be used for the solution of both linear and non-linear two-dimensional planar and axisymmetric heat transfer problems. The code incorporates anisotropic conductivity. Temperature-dependent thermal properties, including conductivity and specific heat, may be input directly. The code performs a piecewise linear interpolation from the input of these functions. Boundary conditions with DOT may include:

- Time-dependent temperature and heat flux functions;
- Convection with time-dependent environmental temperature and a temperature-dependent convection coefficient; and
- External radiation (i.e., radiation to or from a time-dependent temperature sink or source).

The DOT program contains cooling pipe elements which may be used to create a heat sink at a node. Although these are useful for mass concrete problems, DOT provides convection and radiation boundary conditions, so cooling pipe elements will probably be of little use for repository design problems.

The SPECTER version of DOT incorporates a subroutine which automatically stores nodal temperatures in a format compatible for input to the MATLOC, VISCOT, and UTAH2 geomechanical analysis code. The code can also prepare a tape file which is used in restarting the DOT analysis. Restarting DOT, however, involves editing the restart tape and using the final temperatures as initial temperatures for the new run. Thus, from a computational point of view, a restart of DOT is actually a new analysis, with initial conditions equal to the final temperatures from a previous analysis.

A total of five benchmark problems were run using DOT. These included:

1. Problem 2.6 - Transient Temperature Analysis of an Infinite Rectangular Bar with Anisotropic Conductivity;
2. Problem 5.2B - Hypothetical Near Field Problem - Basalt;
3. Problem 5.2S - Hypothetical Near Field Problem - Salt;

**TABLE 6.1**  
**DOT CAPABILITIES TESTED OR UTILIZED**

<u>Capability Within DOT</u>	<u>Benchmark Problem</u>				
	<u>2.6</u>	<u>5.2B</u>	<u>5.2S</u>	<u>6.1</u>	<u>6.3</u>
Problem Type					
- Planar	T	U	U	U	
- Axisymmetric				U	U
Equation Solution	T	U	U	U	U
Conductivity					
- Linear	T				
- Nonlinear					
- Anisotropic	T				
Convection					
- Linear	T	U	U	U	U
- Temperature Dependent Coefficient					
- Time-Dependent Environmental Temperature					
Radiation					
- External Source/Sink					
Cooling Pipes					

T = Tested by comparison with Analytical Solution.

U = Utilized and results of analysis compared with other code results.

The problem was originally run using 20 time steps of 400,000 sec. An estimation of the maximum time step size was made, using a procedure originally developed by Nickell and Levi and outlined by Gartling<sup>(7)</sup> in the COYOTE user manual, and a second analysis was run using 80 time steps of 100,000 sec.

Results - According to the Benchmark Problems Report, output for this problem should consist of temperature profiles at various solution times. Figures 6.2-2 and 6.2-3 present temperature profiles at 110, 550 and 1100 hours along the x and y axes, respectively, for the 100,000 sec time step analysis (Run 2). Data at 2200 hours are tabulated but not plotted on these figures. A visual comparison of these figures reveals that the largest error in the DOT solution occurs at 110 hours. Thus, all further comparisons of computer results for this problem will be made at 110 hours only.

Since this was the only analytical benchmark problem run with DOT, a comparison of the solution accuracy using different time steps was made. Figures 6.2-4 and 6.2-5 present the temperature profiles along the x and y axes, respectively, for the 400,000 sec and 100,000 sec time step analyses. For both runs, the largest difference between the analytical and DOT solutions is along the x-axis.

As shown in the comparisons in Table 6.2-2, the reduction of the time step size increases the accuracy of the DOT solution. For the two analyses considered, the reduction of error far outweighs the increase in computational cost. However, this may not be the case for all models. Computer cost is affected by several factors including read/write functions, internal data generation, and numerical computations. Hence, for larger scale problems, such as field validation and hypothetical design models, a reduction in error comparable to the reduction observed in this problem will probably be associated with a greater increase in computer costs.

TABLE 6.2-2  
COMPARISON OF SOLUTIONS FOR DOT  
PROBLEM 2.6

<u>Analysis</u>	<u>Time Step Size (sec)</u>	<u>Maximum Temperature Difference (°K)</u>	<u>Maximum* Error (%)</u>	<u>Cost (CCUS)</u>
Run 1	400,000	21.45	4.60	1.624
Run 2	100,000	10.62	2.28	1.926

\* Error expressed as % of analytical result at  $x = 1.80$  of  $465.89^{\circ}\text{K}$   
(ref. Figure 6.2-4).

# DOT - PROBLEM 2.6

## X-AXIS TEMPERATURES AT VARIOUS TIMES

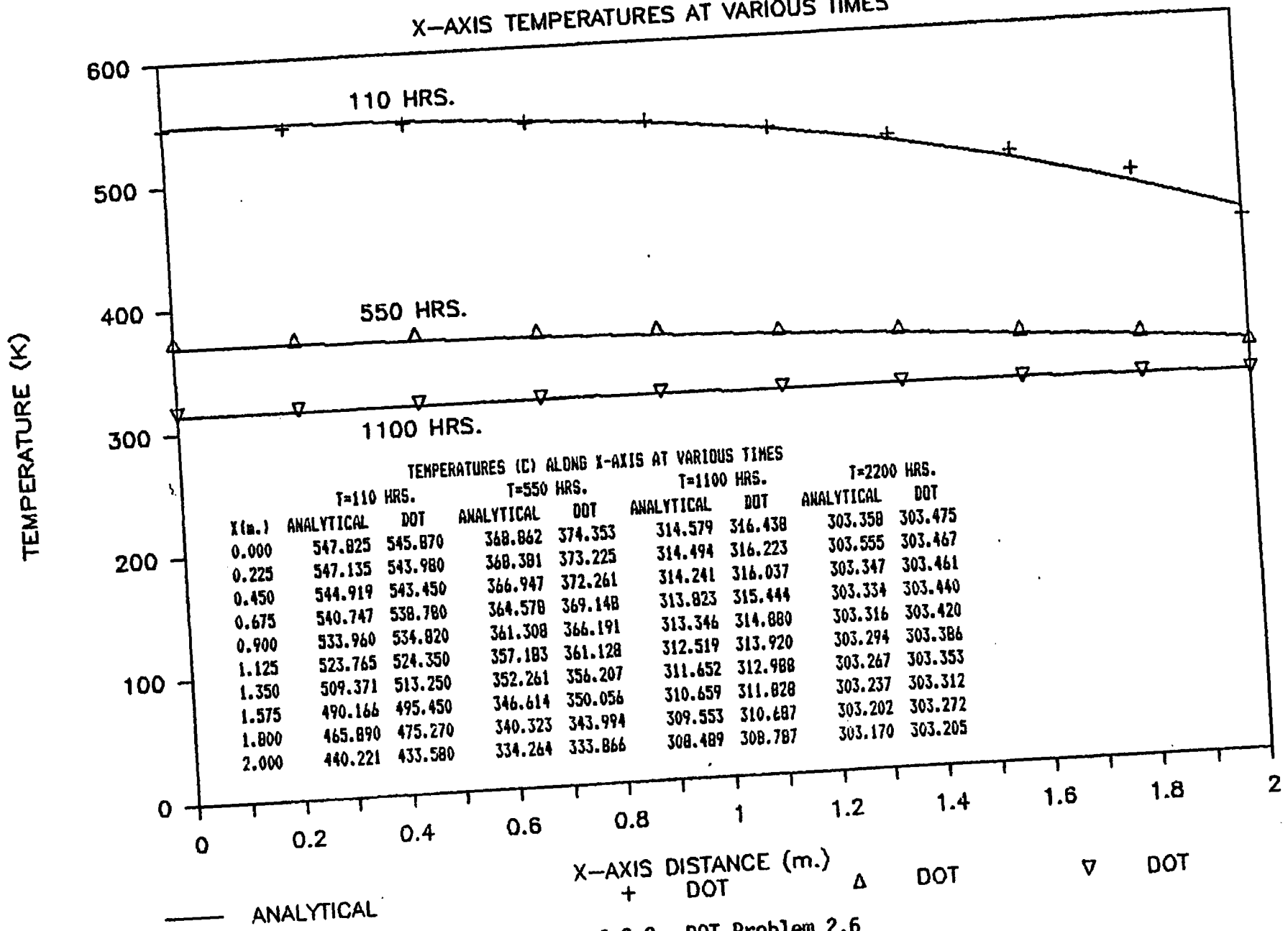


Figure 6.2-2 DOT Problem 2.6  
Temperature Profile Along X-Axis at Various Times

# DOT PROBLEM 2.6

X-AXIS TEMPERATURES AT 110 HR

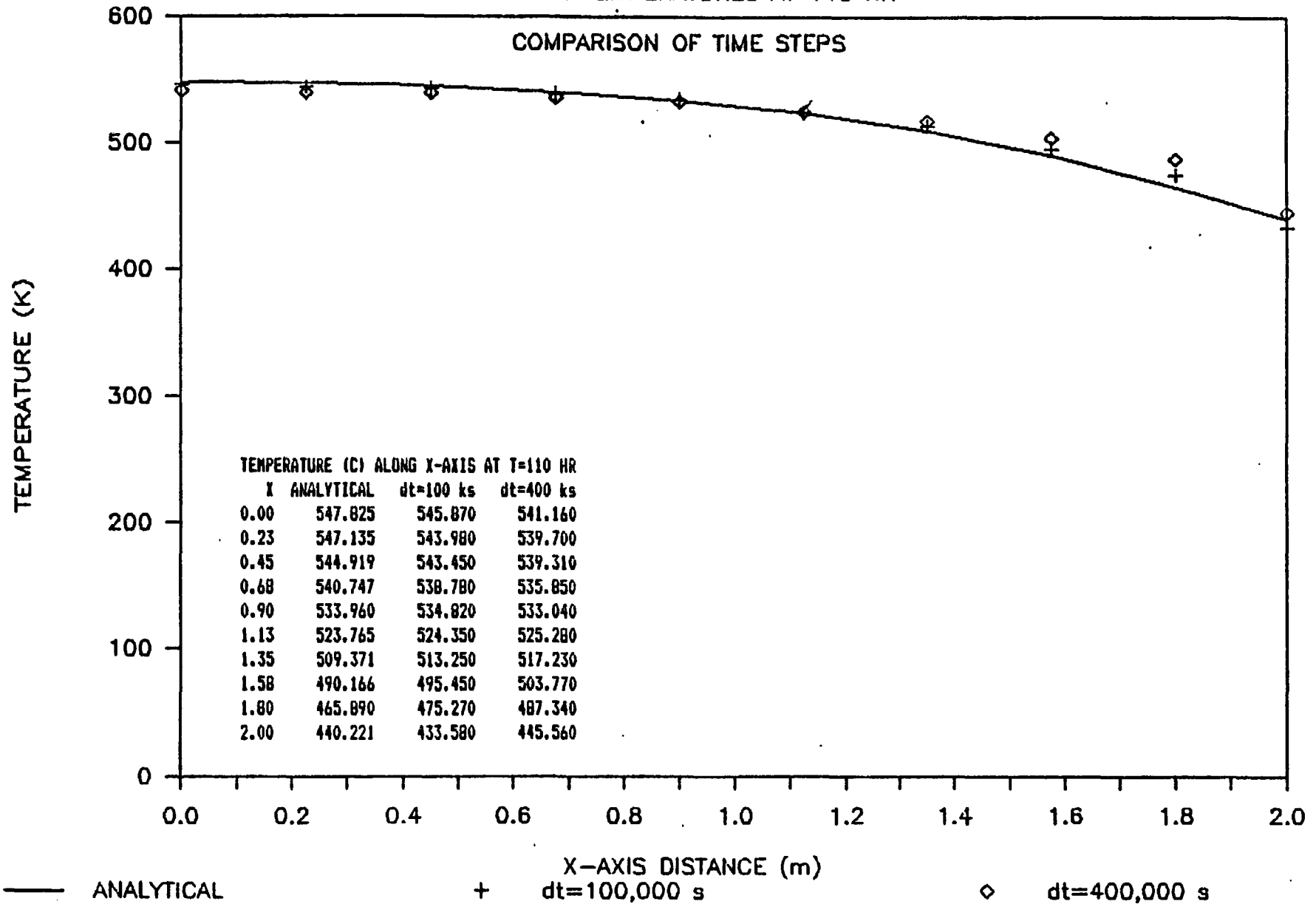


Figure 6.2-4 DOT Problem 2.6  
Temperature Profile Along X-Axis at 110 hrs  
Comparison of Time Steps

### 6.3 Problem 5.2B - Hypothetical Near Field Problem - Basalt

**Problem Statement** - This problem consists of a two-dimensional transient thermal simulation of the near field (single room region) of a hypothetical repository located in basalt. Waste canisters, emplaced vertically below the room floor at regular intervals along the centerline, have been replaced by an equivalent heat generating trench for this analysis. This problem exercises general transient heat transfer with mechanisms of conduction, heat storage, radiation, and free and forced (ventilation) convection. Ventilation is maintained for the first 50 years, after which the room is sealed, and natural convection and radiation occur. This problem is summarized in greater detail in Section 3.3.

**Input Data** - A two-dimensional section through a repository with an infinite number of rooms was modeled using 8-noded isoparametric planar elements and two-noded convection elements. Although the model extended from ground surface to a depth of -3500 m, most of the elements used in the model were located between depths of -479 m and -510 m. This region is shown in Figure 6.3-1. The remainder of the model consisted of "filler" elements with vertical dimensions of each element not exceeding 1.5 to 2.0 times the vertical dimension of the previous element. Although the aspect ratio of these "filler" elements appears extreme, numerically they model the boundary conditions imposed upon the repository very well.

Input data used to model problem 5.2B with DOT were taken from the Benchmark Problems Report and included:

● **Material Properties of Basalt**

- Density  $\rho = 2700 \text{ kg/m}^3$
- Conductivity Table 6.3-1
- Specific Heat Table 6.3-1

● **Initial Conditions/Boundary Conditions**

- Initial Temperatures
  - between  $Z = -479 \text{ m}$  and  $Z = -510 \text{ m}$   $T_0 = 25^\circ\text{C}$
  - all other depths  $T_0 = (15 - 0.02Z)^\circ\text{C}$
- Environmental Room Temperature  $T_e = 15^\circ\text{C}$
- Convection Coefficient  $h = 0.40 \text{ W/m}^2\text{C}$
- Constant Temperature at  $Z=0$   $T(\emptyset) = 15^\circ\text{C}$
- Constant Temperature at  $Z = -3500 \text{ m}$   $T(3500) = 85^\circ\text{C}$
- Externally Supplied Heat Flux Table 6.3-2

Since the heat flux function in DOT defines the heat input at each node along the canister surface, the heat flux function shown in Table 6.3-2 was multiplied by the equivalent area of the canister surface at each node. The effective areas of each node, to which the heat flux function was applied, are listed in Table 6.3-3.

Ideally, the heat transfer within the room after repository sealing should be modeled. The heat transfer mechanisms would include a combination of natural convection, radiation, and conduction through the air mass. The DOT model does not allow radiation or convection between

TABLE 6.3-1  
 CONDUCTIVITY AND SPECIFIC HEAT FOR DOT  
 PROBLEM 5.2 - BASALT

Temperature (°C) T	Conductivity (W/m°C)			Specific Heat (J/kg°C) C
	$k_x$	$k_y$	$k_{xy}$	
-100	1.1	1.1	0	835
*10,000	1.1	1.1	0	835

\*Values were defined at 10,000°C to prevent temperatures from going out of range.

TABLE 6.3-3

EFFECTIVE NODAL AREAS FOR HEAT FLUX FUNCTION FOR DOT  
PROBLEM 5.2 - BASALT

<u>Node</u>	<u>Effective Area Factor</u>
248	0.0833
265	0.3333
274	0.2500
291	0.6667
300	0.3333
317	0.6667
326	0.3333
343	0.6667
352	0.3333
369	0.6667
378	0.2500
395	0.3333
404	0.0833

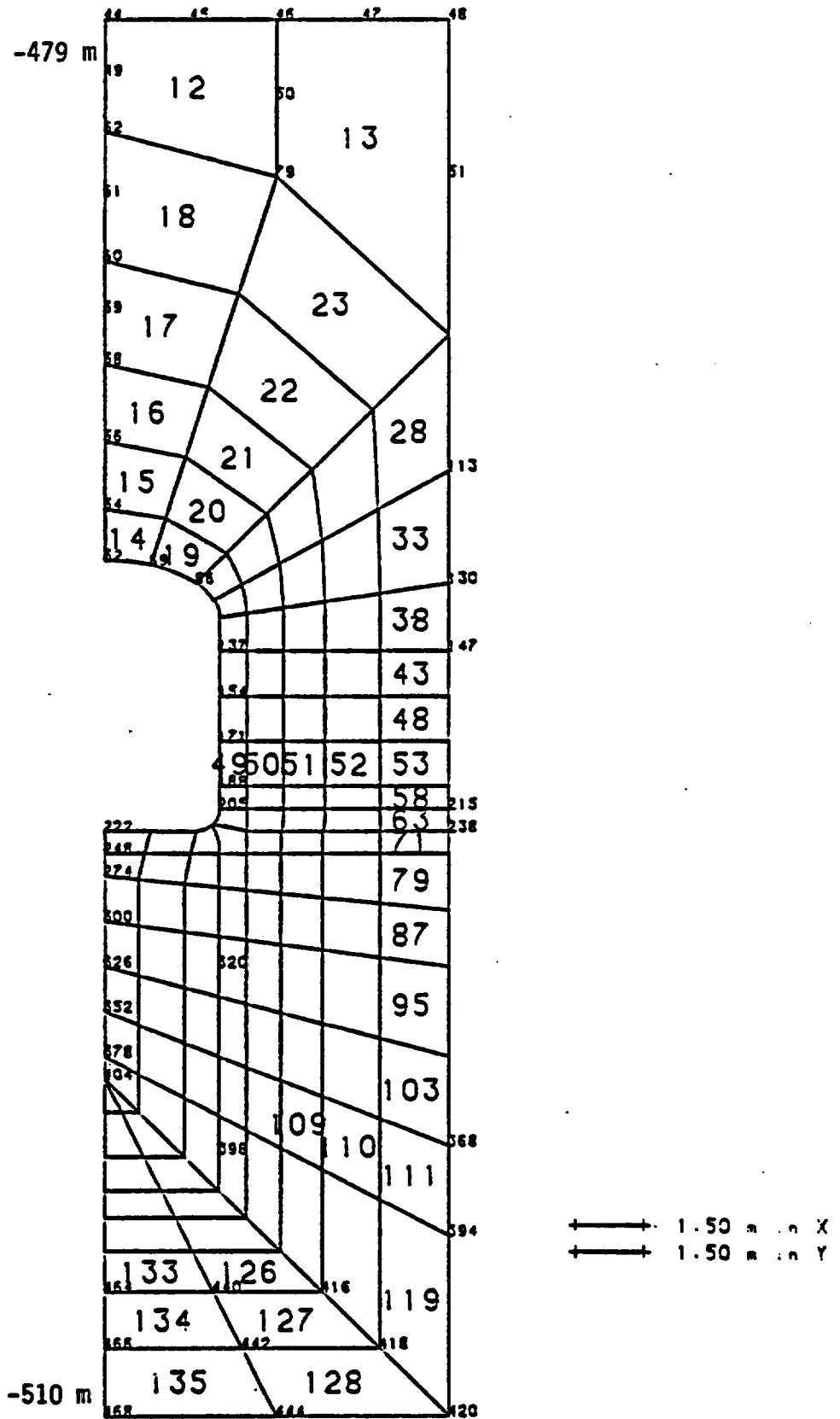


Figure 6.3-1 DOT Problem 5.2 - Basalt and Salt Finite Element Mesh

# DOT PROBLEM 5.2—BASALT

## TEMPERATURE HISTORY

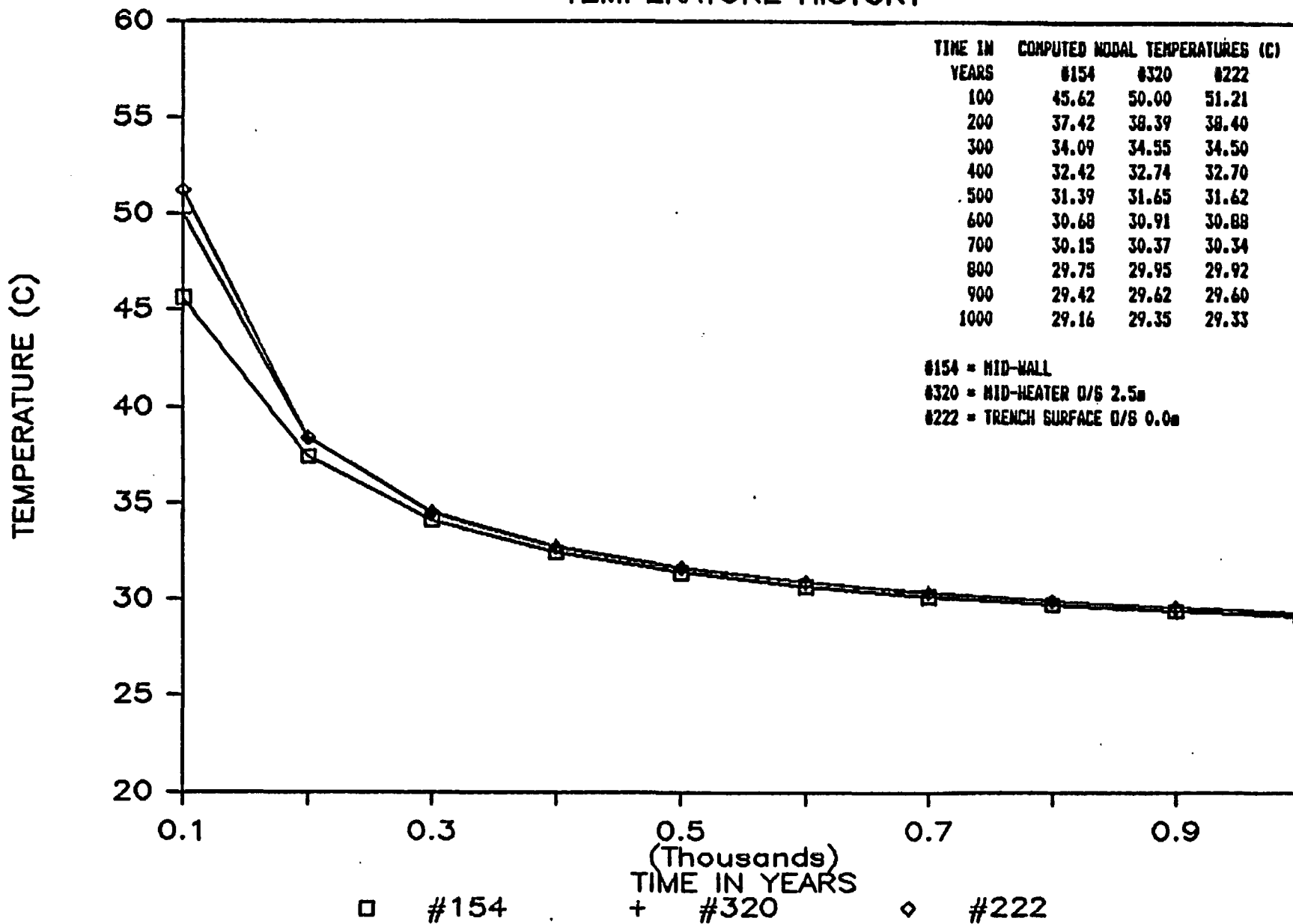
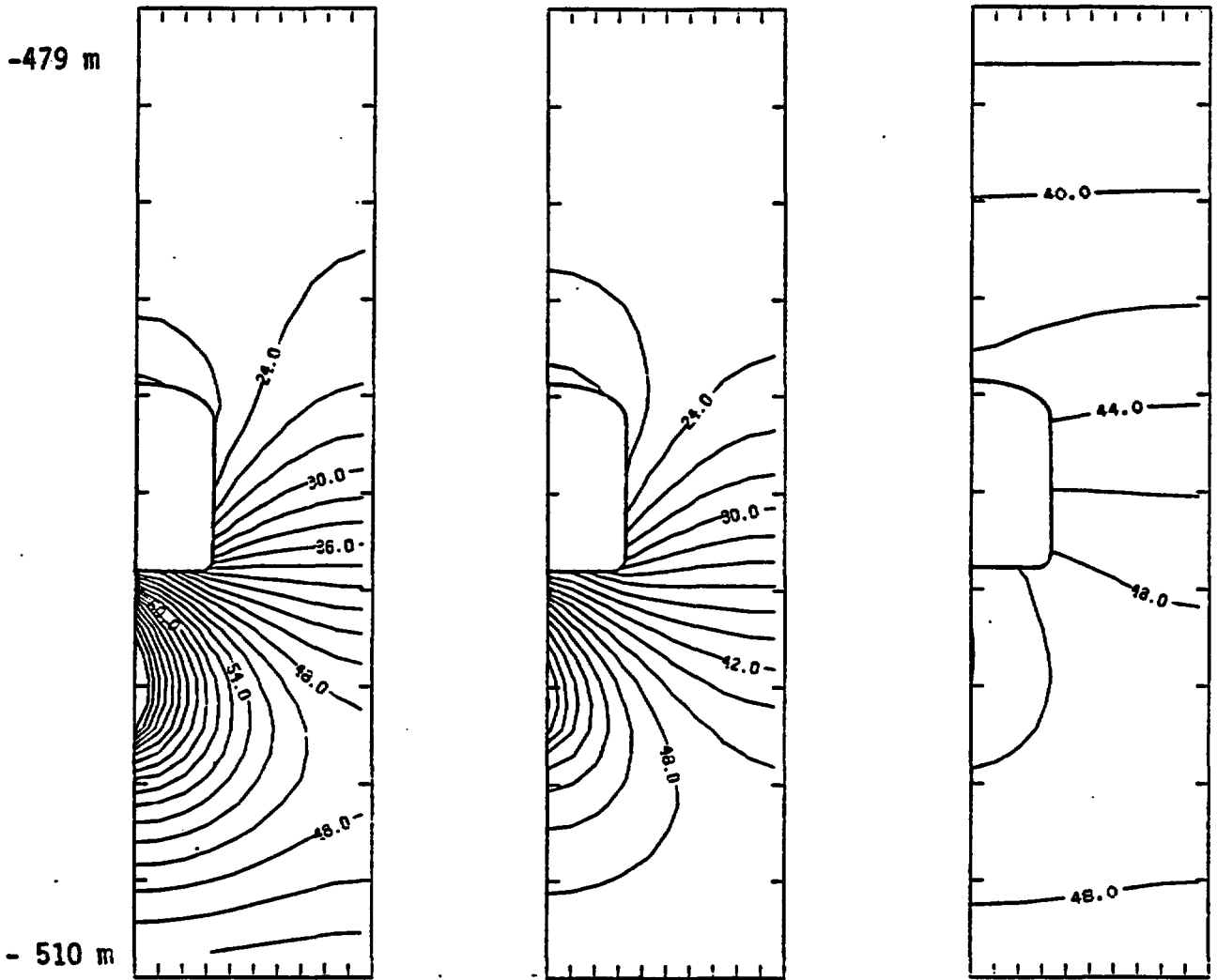


Figure 6.3-3 DOT Problem 5.2 - Basalt  
Temperature History 100-1,000 years



Time = 10 years

Time = 30 years

Time = 100 years

Temperature in °C

Contour Interval = 2°C

Initial Temperature = 25°C

Figure 6.3-5 DOT Problem 5.2-Basalt Temperature Contours

## 6.4 Problem 5.2S - Hypothetical Near Field Problem - Salt

Problem Statement - This problem is the same as Problem 5.2B, described in Section 6.3, except that the repository is located in salt.

Input Data - The geometry and finite element mesh used for this problem is the same as that used for Problem 5.2B (Figure 6.3-1). Input data specific to the salt problem were taken from the Benchmark Problems Report, and included:

- Material Properties of Salt

- Density  $\rho = 2150 \text{ kg/m}^3$
- Conductivity Table 6.4-1
- Specific Heat Table 6.4-1

- Initial Conditions/Boundary Conditions

Same as for DOT Problem 5.2B - see Section 6.3.

Run Problem - Problem 5.2S was run using the same four time ranges defined for Problem 5.2B in Section 6.3. For this problem, DOT was used to compute temperature distributions for input to the geomechanical codes MATLOC and VISCOT. Both of these codes require that elements be constructed using 4 or 8 nodes. As in Problem 5.2B, 4-noded triangular elements were accommodated in DOT and MATLOC by specifying the same node number more than once. VISCOT, however, does not allow a node to be used more than once in an element. The geometry of the mesh was altered slightly to accommodate the VISCOT requirement, as discussed in Section 8.5. No code related difficulties were encountered while running Problem 5.2S with DOT.

Results - Temperature histories from 0 to 10,000 years have been developed for three points in the model; 1) mid-height; 2) cavern floor at the room center; and 3) cavern wall within the rock mass at mid-height level, offset 2.5 m. The temperature histories have been divided into three parts and are shown in Figures 6.4-1 through 6.4-3.

Temperature contours within the modeled region between elevations -479 m and -510 m are shown at times of 10, 30 and 100 years in Figure 6.4-4. Vertical temperature profiles along the pillar centerline are shown in Figure 6.4-5 for times of 100, 300 and 1000 years.

# DOT PROBLEM 5.2-SALT

## TEMPERATURE HISTORY

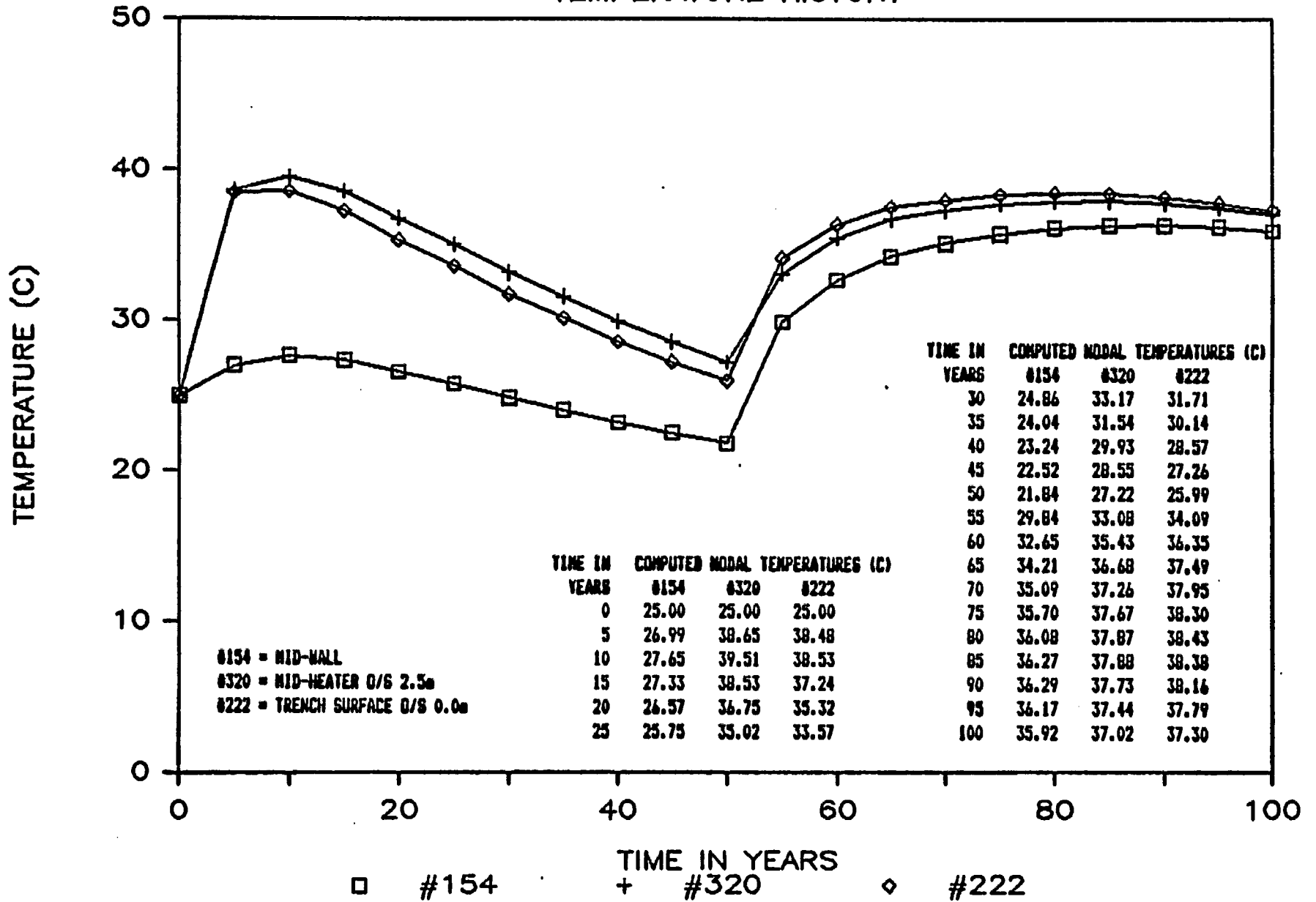


Figure 6.4-1 DOT Problem 5.2 - Salt  
Temperature History 0-100 Years

# DOT PROBLEM 5.2-SALT TEMPERATURE HISTORY

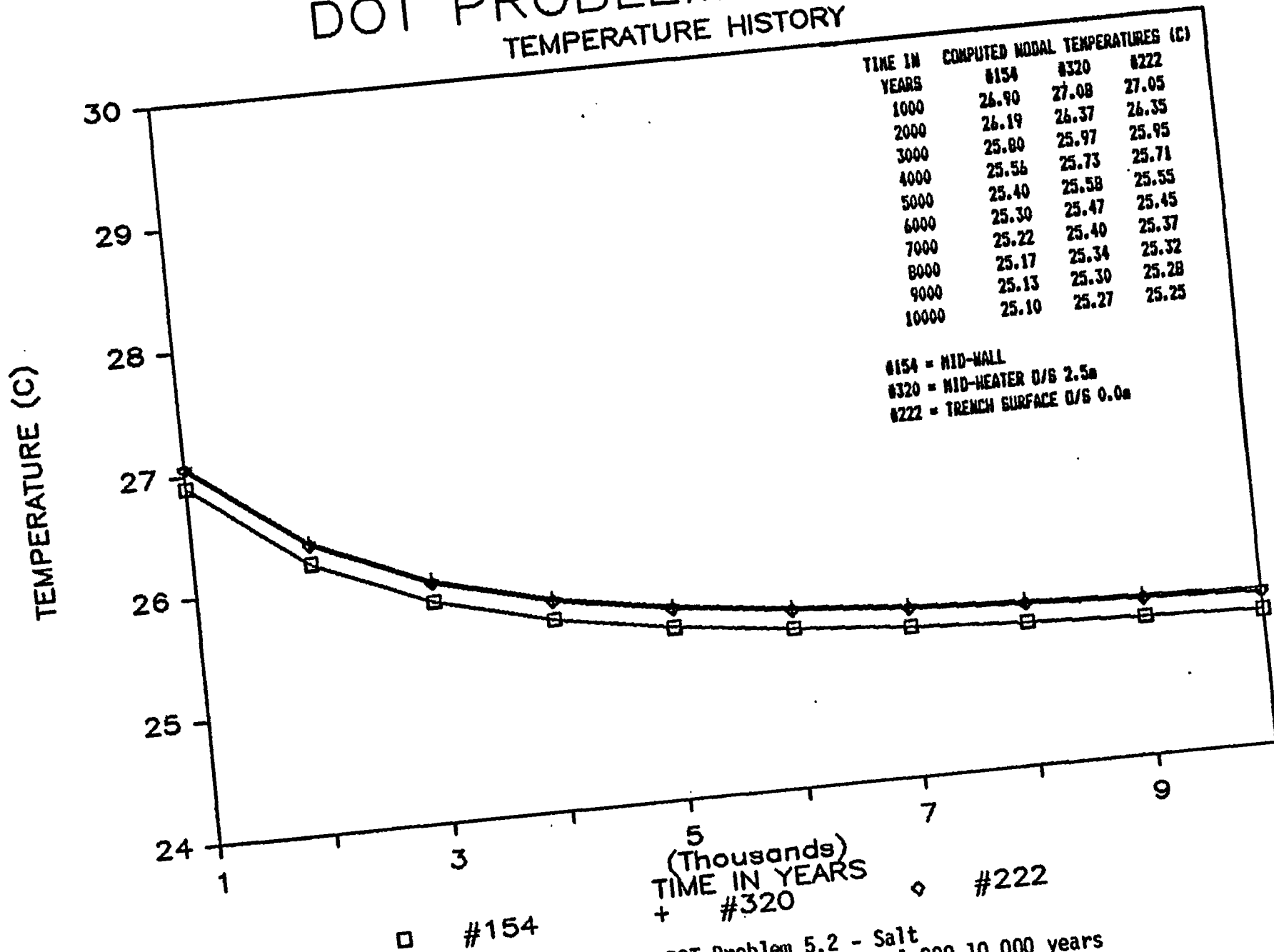


Figure 6.4-3 DOT Problem 5.2 - Salt Temperature History 1,000-10,000 years

# DOT PROBLEM 5.2-SALT

TEMPERATURE RISE vs. DEPTH

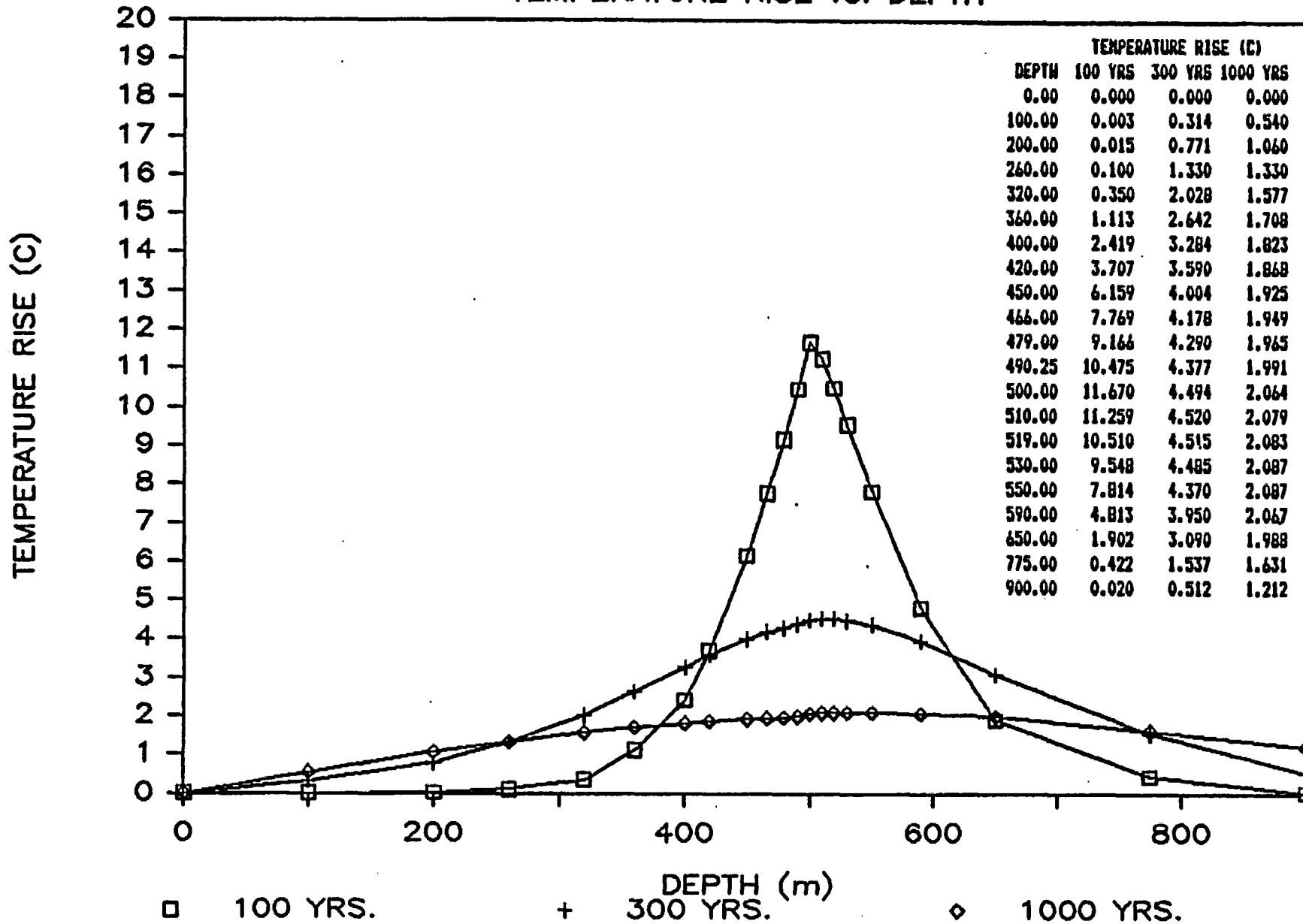


Figure 6.4-5 DOT Problem 5.2 - Salt Temperature Rise along Pillar Centerline (100-1,000 years)

A time step of 15 days was chosen for both models, since it agrees well with the time history shown in Table 6.5-1. The analysis for Problem 6.1P (Room 3) started on Day 360 and was continued 30 days beyond the conclusion of the experiment (Day 720). The solution of Problem 6.1A (Room 4) was begun on Day 0 and concluded 15 days after the array heaters were turned off. No code related difficulties were encountered while solving these problems with DOT.

Results - Temperature histories have been developed for three locations in the planar model (Room 3) as shown in Figure 6.5-3. The locations considered are along a line at mid-heater depth (2.75 m below the floor) at three distances from the pillar centerline. As seen in this figure, the maximum temperatures occur on Day 690, the last day of the experiment. Figure 6.5-4 presents profiles of temperatures across the model at the floor surface, mid-heater depth, and at 5.02 m below the floor surface on Day 690. Although the distance from the center of the heater to the floor surface and 5.02 m are nearly the same, the temperatures on the floor surface are much lower due to the effects of convection. A comparison of the temperatures predicted by DOT to field measurements below Room 3 is shown in Figure 6.5-5.

The results from the axisymmetric analysis (Room 4) are compared to the field measured values in Figures 6.5-6 through 6.5-9. The field measurements and DOT results of temperature histories at various offsets from the room center at mid-heater depth are shown in Figures 6.5-6 and 6.5-7, respectively. Figures 6.5-8 and 6.5-9 show the field and DOT temperatures at various depths below the room floor at an offset of 2.4 m. The maximum temperatures in the axisymmetric model occur on the last day of the experiment, Day 570.

The radial temperature profiles below Room 4 on Day 570, at the three depths used in the planar model, are shown in Figure 6.5-10. As in the planar model, the temperatures at the room floor are lower than temperatures 5.02 m below the floor due to the effects of convection into the room.

TABLE 6.5-2  
 CONDUCTIVITY AND SPECIFIC HEAT FOR DOT  
 PROBLEMS 6.1P AND 6.1A

Temperature (°C) T	Conductivity (W/m°C)			Specific Heat (J/kg°C) C
	$k_x$	$k_y$	$k_{xy}$	
0	6.109	6.109	0	930.97
25	5.524	5.524	0	930.97
50	5.020	5.020	0	930.97
75	4.590	4.590	0	930.97
100	4.227	4.227	0	930.97
150	3.666	3.666	0	930.97
200	3.277	3.277	0	930.97
250	2.997	2.997	0	930.97
300	2.763	2.763	0	930.97
500	1.051	1.051	0	930.97
*1000	1.000	1.000	0	930.97

\*Values were defined at 1000°C to prevent temperatures from going out of range.

TABLE 6.5-4

EFFECTIVE AREA FACTORS FOR DOT  
PROBLEMS 6.1P and 6.1A

<u>Planar Problem</u>		<u>Axisymmetric Problem</u>	
<u>Node</u>	<u>Effective Area Factor</u>	<u>Node</u>	<u>Effective Area Factor</u>
254	0.0833	183	0.0833
273	0.3333	200	0.3333
289	0.1667	209	0.1667
308	0.3333	226	0.3333
324	0.0833	235	0.0833
		187	0.50
		202	2.00
		213	1.00
		228	2.00
		239	0.50

Central

Heater

Nodes

Peripheral

Heater

Nodes

118							
110							
102	538						
93							
91							
88							
80							
72							
64							
56							
48							
40							
32							
24							
16							
1	2	3	4	5	6	7	8

+-----+ 2n in X
   
 +-----+ 2n in Y

Figure 6.5-2 DOT Problem 6.1A  
Finite Element Mesh

# DOT PROBLEM 6.1P - ROOM 3

## HORIZONTAL TEMPERATURE PROFILE @ DAY 690

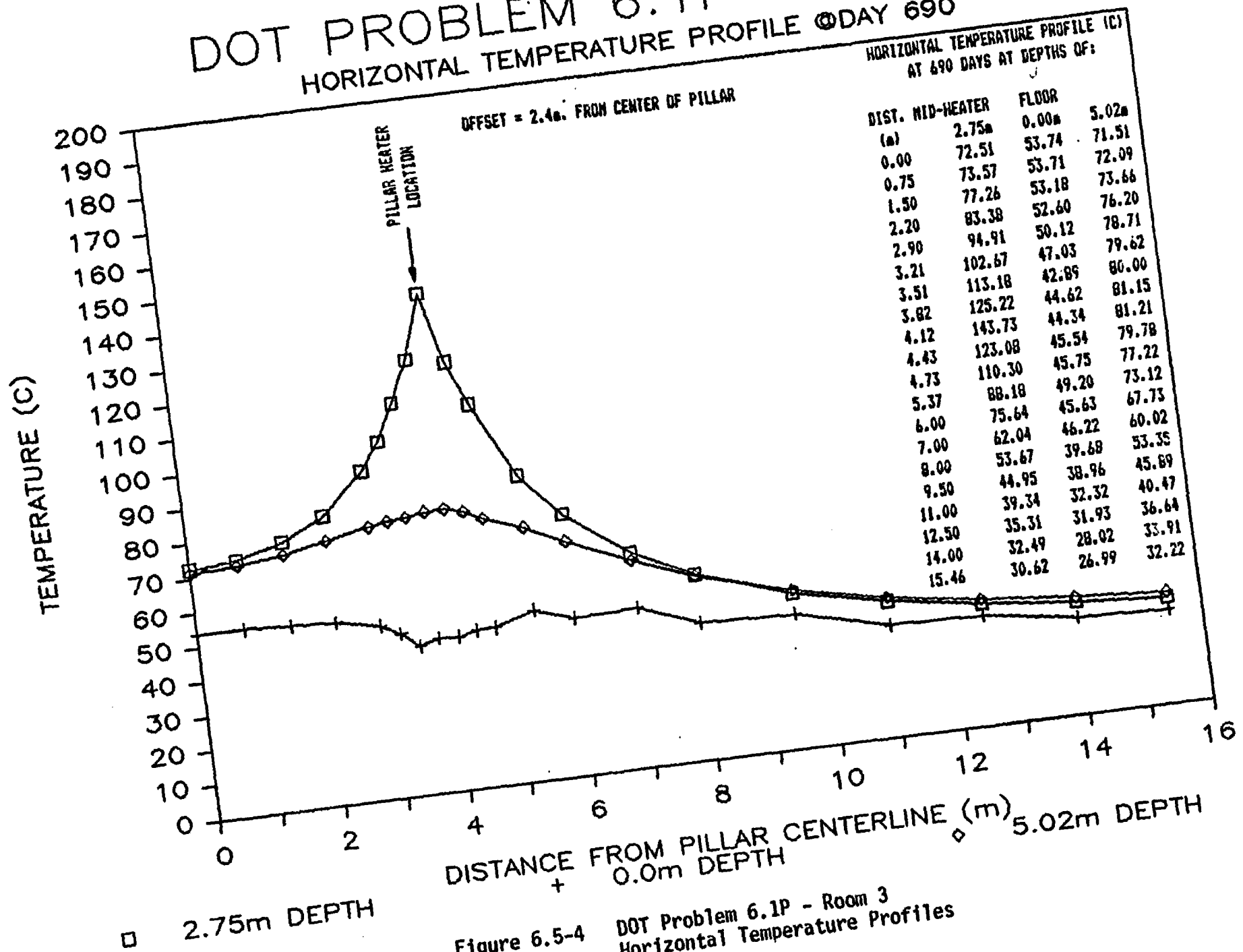


Figure 6.5-4 DOT Problem 6.1P - Room 3  
Horizontal Temperature Profiles  
Dry 690

# PROBLEM 6.1A - ROOM 4 - FIELD VALUES

## TEMPERATURE HISTORY AT VARIOUS OFFSETS

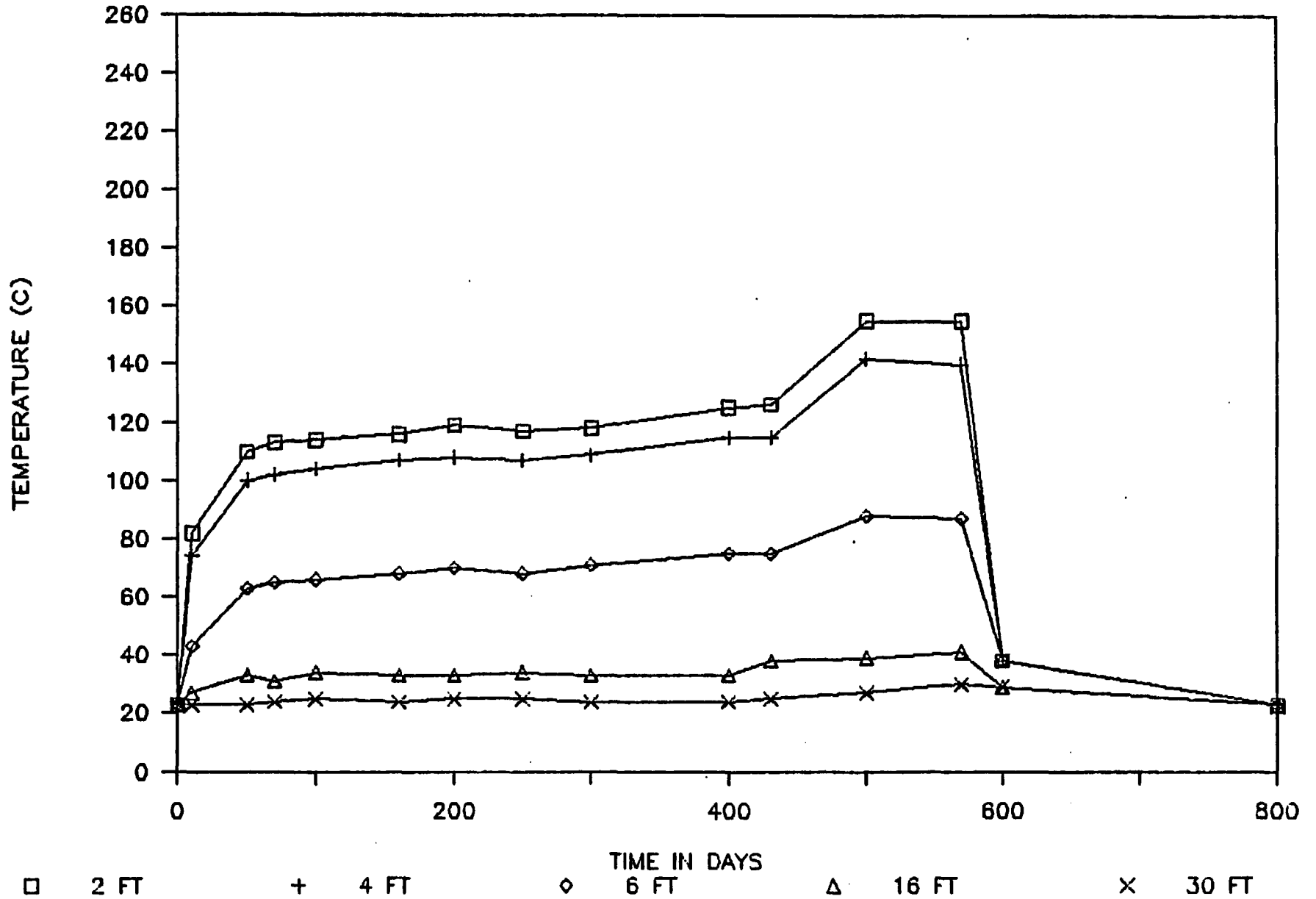


Figure 6.5-6 Project Salt Vault Field Values - Room 4  
Temperature History at Various Offsets at  
Mid-Heater Depth

# PROBLEM 6.1A - ROOM 4 - FIELD VALUES

## TEMPERATURE HISTORY AT VARIOUS DEPTHS

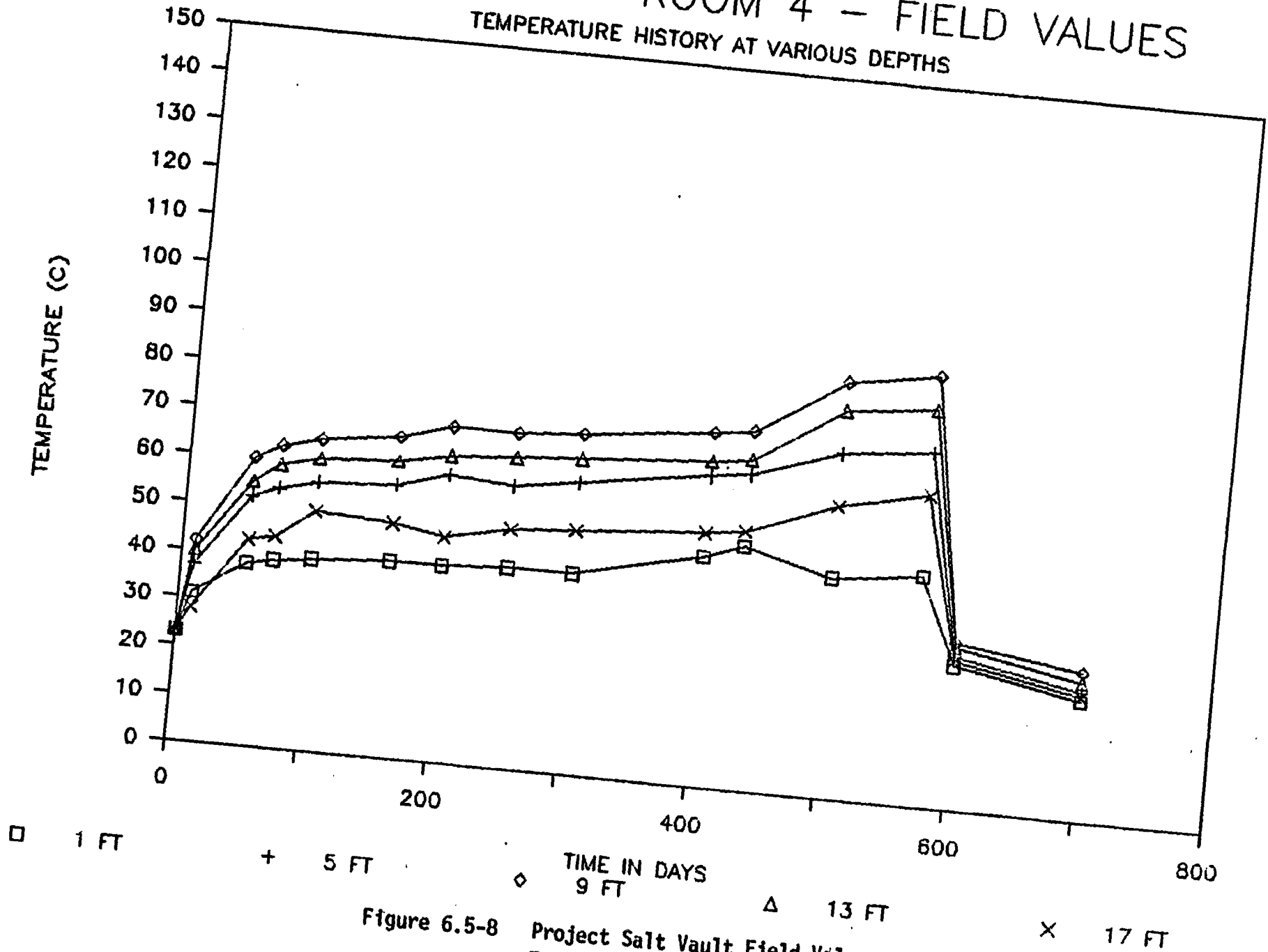


Figure 6.5-8 Project Salt Vault Field Values - Room 4  
 Temperature History at Various Depths  
 Offset = 2.4m.

# DOT PROBLEM 6.1A - ROOM 4

## RADIAL TEMPERATURE PROFILE - DAY 570

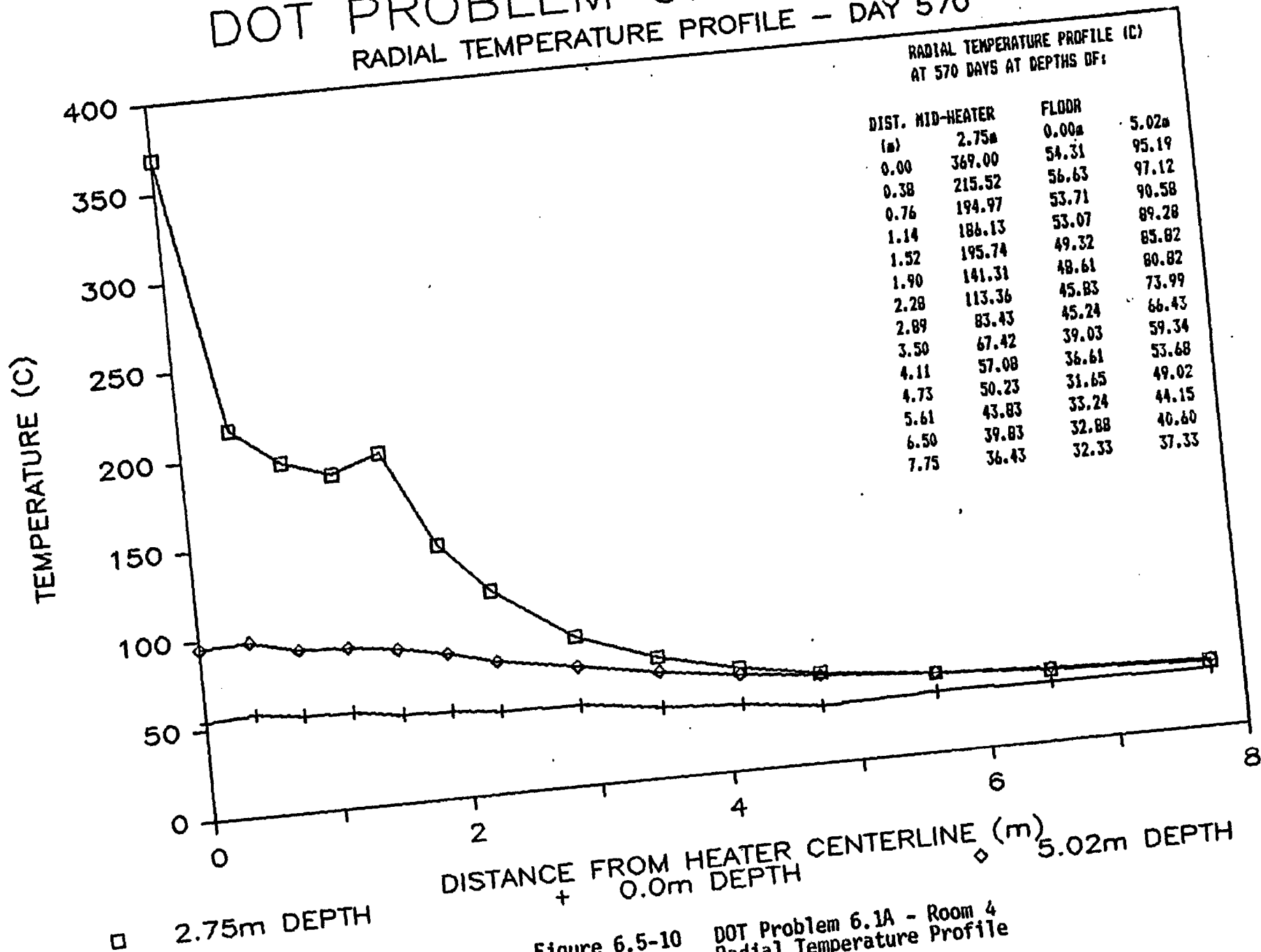


Figure 6.5-10 DOT Problem 6.1A - Room 4  
Radial Temperature Profile  
Day 570

Run Problems - A constant time step of 15 days was selected for compatibility with the internal heat generation function. To accommodate the time-dependent loading conditions, restarts were necessary. The temperature distribution computed by DOT was used for input to the geo-mechanical codes MATLOC and VISCOT. Finite element compatibility requirements for these codes, as discussed in Sections 6.3 and 6.4, were satisfied in the selection of the mesh. No code-related difficulties were encountered in running this problem.

Results - The temperature history for a point at mid-heater depth, offset 0.4 m from the heater centerline, is shown in Figure 6.6-2. Radial and vertical temperature distributions on Day 259 are shown in Figures 6.6-3 and 6.6-4, respectively. The radial temperature distribution at Day 350 (temperatures interpolated between time steps) is shown in Figure 6.6-5. For each of these figures, the temperatures computed with DOT agree well with field measurements.

TABLE 6.6-2  
 CONDUCTIVITY AND SPECIFIC HEAT OF AIR FOR DOT  
 PROBLEM 6.3

Temperature (°C) T	Conductivity (W/m°C)			Specific Heat (J/kg°C) C
	$k_x$	$k_y$	$k_{xy}$	
0	0.0244	0.0244	0.0	1004
60	0.0291	0.0291	0.0	1004
125	0.0335	0.0335	0.0	1013
250	0.0425	0.0425	0.0	1032
350	0.0490	0.0490	0.0	1054
427	0.0538	0.0538	0.0	1076
*10000	0.6473	0.6473	0.0	3982

\*Values were defined at 10,000°C to prevent temperatures from going out of range.

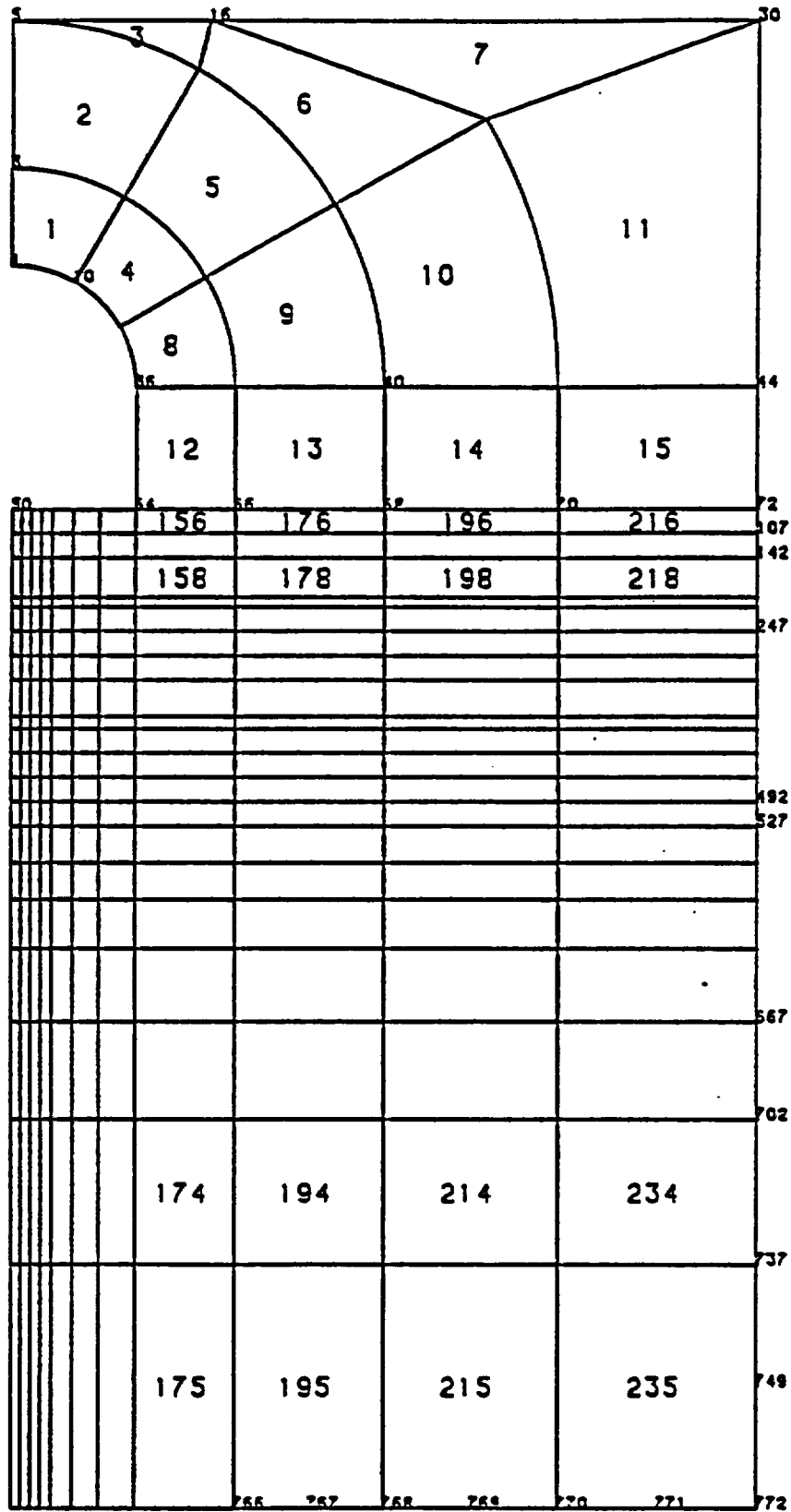


Figure 6.6-1 DOT Problem 6.3  
Finite Element Mesh

# DOT PROBLEM 6.3 — BWIP

## RADIAL TEMPERATURES ON DAY 260

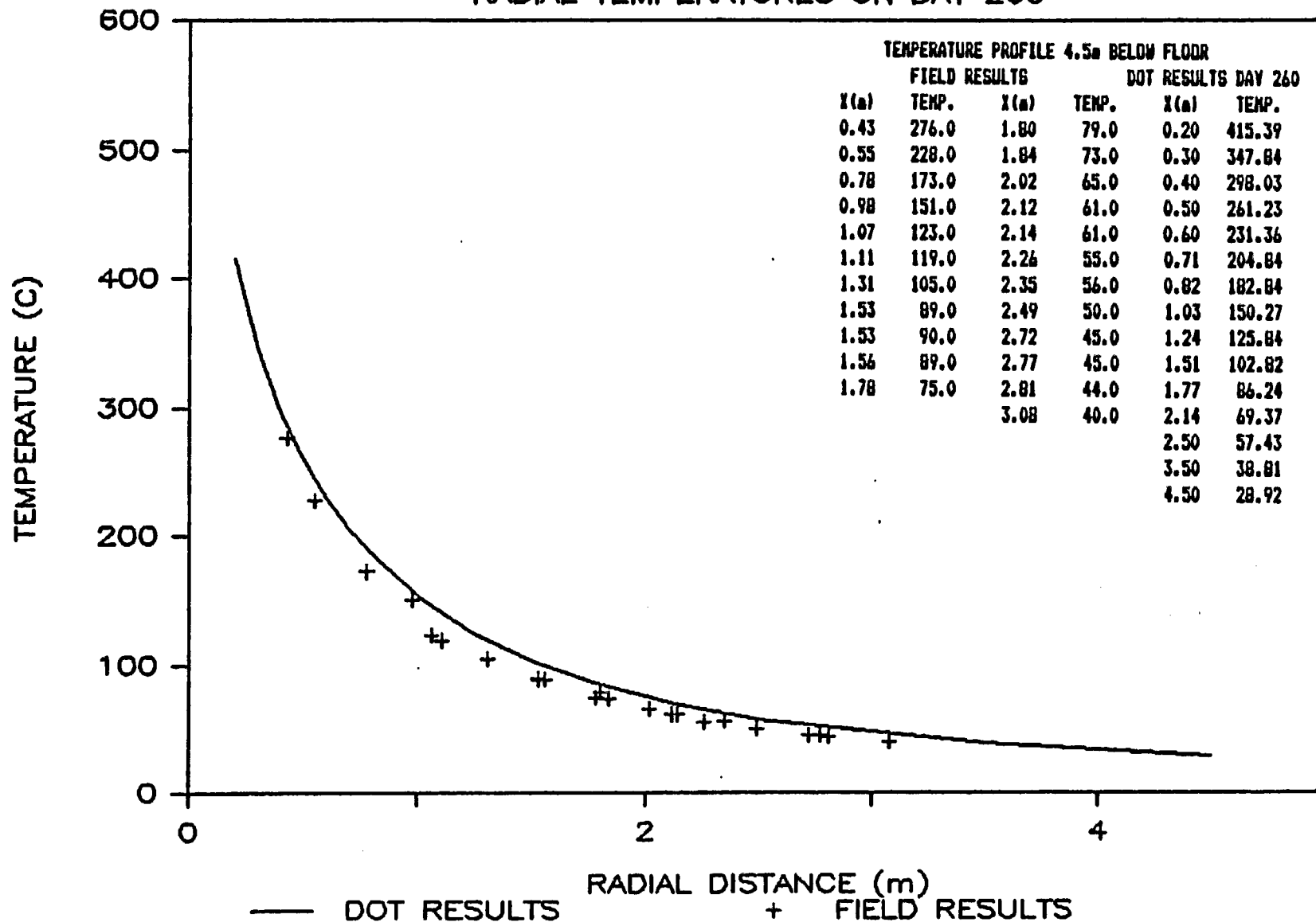


Figure 6.6-3 DOT Problem 6.3  
Radial Temperature Distribution  
on Day 260 at 4.5m Depth Below  
Repository Floor

# DOT PROBLEM 6.3 – BWIP

RADIAL TEMPERATURE PROFILE ON DAY 350

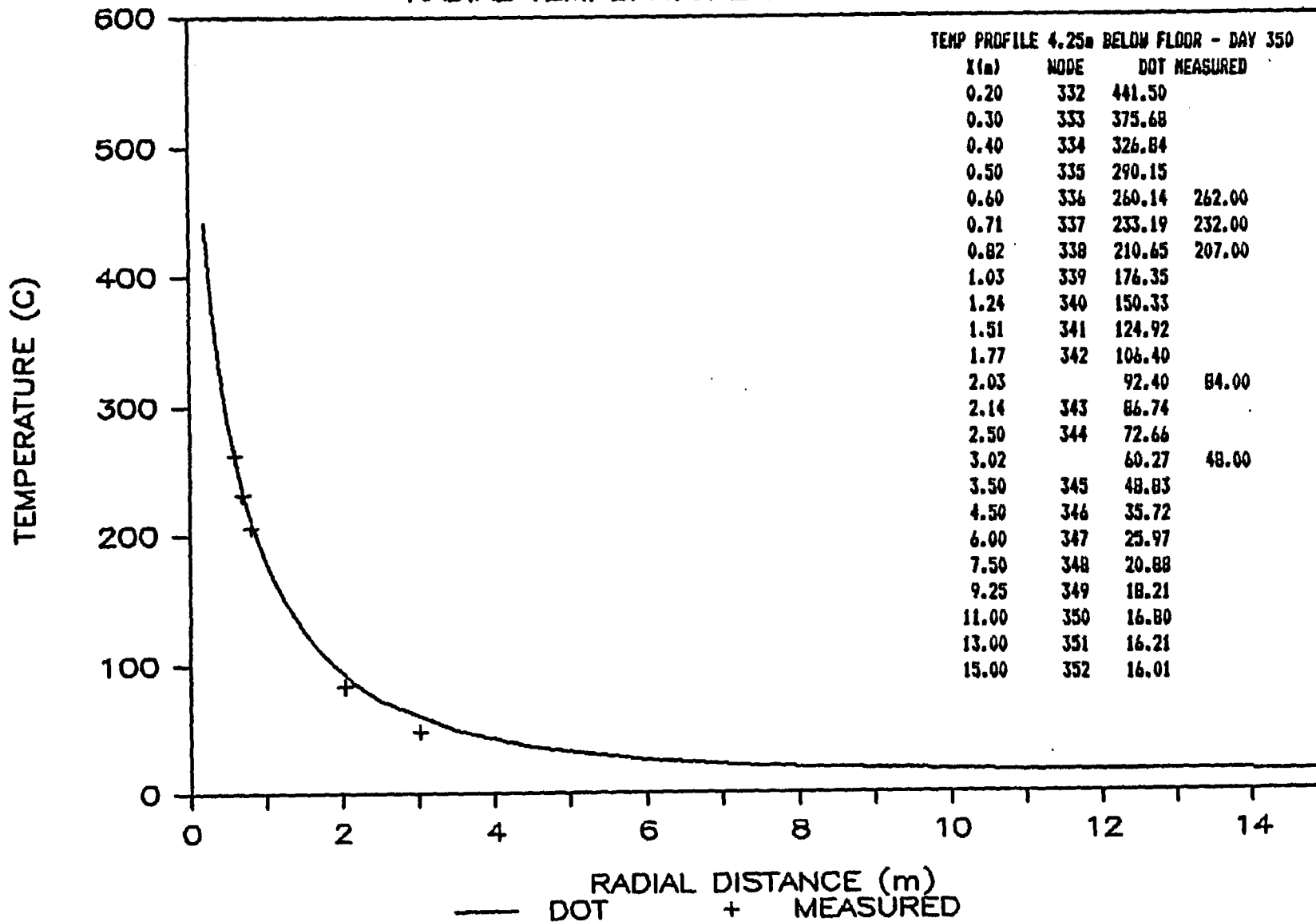


Figure 6.6-5 DOT Problem 6.3  
 Radial Temperature Distribution on Day 350 at 4.25m Depth Below Repository Floor

## 7.0 BENCHMARKING OF MATLOC

## 7.0 BENCHMARKING OF MATLOC

### 7.1 Code Background and Capabilities

MATLOC is a nonlinear two-dimensional finite element computer program developed to predict the induced deformations and stresses due to excavation processes and transient thermal conditions in fractured rock media. The original documentation for MATLOC, the thermal stress analysis module of the thermomechanical code DAMSWEL, was written at Dames and Moore by the code developers, P. Boonlualohr, et al. for the DOE. As part of the SCEPTER technology package, the earlier documentation of MATLOC was extensively restructured and enlarged to its present form by Graham Mustoe of INTERA Environmental Consultants, Inc. The program and documentation<sup>(8)</sup> were obtained from the Office of Nuclear Waste Isolation (ONWI). The QA identification number for this version is 420--12C-02.

The MATLOC program can be used to solve nonlinear two-dimensional planar and axisymmetric thermomechanical and/or geostatic stress problems. Thermomechanical stress analyses require the specification of nodal temperatures at the applicable loading increments. Nodal temperatures may be included directly in the MATLOC input file or may be read from a properly formatted tape file. In this study, transient thermal stress solutions with MATLOC used temperature data stored in tape files by the heat transfer code DOT<sup>(7)</sup>. Geostatic stress analyses with MATLOC require the inclusion of nodal loads and initial stresses. A preliminary analysis, in which nodal loads are included in the input data, is made to generate the initial stress data. These data may be stored on a tape file and used with temperature data in subsequent MATLOC analyses.

The MATLOC code is not capable of viscoelastic (creep) analysis, but does have the ability to account for fractures within the rock mass. The stress-dependent bilinear constitutive behavior within the code provides an equivalent continuum model of the fractured rockmass, but cannot simulate the deformation of individual fractures. The MATLOC code is not applicable to creep-sensitive materials such as salt, but is well suited for the analyses of fractured rocks, such as basalt.

While MATLOC allows for the choice of 4- or 8-noded elements, only 8-noded elements can be used if a direct coupling with the heat transfer code DOT is required. Finite element mesh boundary conditions are incorporated by specifying nodal fixities and displacements. Thermal and geostatic loads must be specified at the nodes. MATLOC provides a restart option which writes nodal displacements and Gauss point stress components to a tape file for input to further analyses.

The major limitations of the MATLOC code include:

- The present version of MATLOC does not have any formal error processing subroutines. Input data errors can cause major difficulties to inexperienced users.

**TABLE 7.1**  
**MATLOC CAPABILITIES TESTED OR UTILIZED**

	Problem		
	3.2a	5.2b	6.3
Problem Type			
- Planar	T	U	
- Axisymmetric			U
Equation Solution	T	U	U
Analysis			
- Geomechanical	T	U	U
- Thermomechanical		U	U
Bilinear Stress-Strain			U

**T = Tested by comparison with Analytical Solution.**

**U = Utilized and results of analysis compared with other code results.**

Results - The results of the analysis are tabulated and shown graphically in Figures 7.2-2 through 7.2-6. In general, the MATLOC solution seems to compare well with the analytical solution. The results used for comparison to the analytical solution were taken along a radial line inclined 30 degrees above the horizontal.

Figures 7.2-2 and 7.2-3 show the major and minor principal stresses, respectively, along the 30° radial line. While the principal stresses calculated by MATLOC compare well with the analytical solution for radial distances less than about 6.5 m, significant errors occur at radial distances greater than 6.5 m. This error is believed to be due to the coarseness of the finite element mesh used. The minor principal stresses calculated by MATLOC compare well with the analytical solution throughout the model. Figure 7.2-4 compares the MATLOC and analytical values of the angle between the principal stress and the 30° radial line. As with the other figures, the MATLOC results compare well with the analytical results.

Figures 7.2-5 and 7.2-6 show the displacements in the radial and circumferential directions of points along the 30° radial line. In both figures, the MATLOC calculated displacements are slightly greater than the analytical values. This results directly from the overestimation of principal stresses by MATLOC, as shown in previous figures. The calculation of larger stresses in an elastic material results in greater displacements. Both the radial and the circumferential displacements calculated by MATLOC follow the analytical curve well, but are in error by a nearly constant displacement of about 0.001 m. This error may be due to the coarseness of the finite element mesh at distances away from the tunnel, or to an accuracy tolerance built into the MATLOC program. A second analysis, using a finite element mesh with twice as many elements, was made in an attempt to reduce this error.

The finite element mesh used for Run 2 is shown in Figure 7.2-7. All other input data were the same as in the first run. The major and minor principal stresses along the 30° radial line for Run 2 are shown in Figures 7.2-8 and 7.2-9. A visual comparison of Figure 7.2-8 and Figure 7.2-4 reveals that reducing the size of the elements led to a reduction of the error by about 50%. This reduction of error was associated with a negligible rise in computation costs.

# MATLOC — PROBLEM 3.2a

## MAJOR PRINCIPAL STRESS

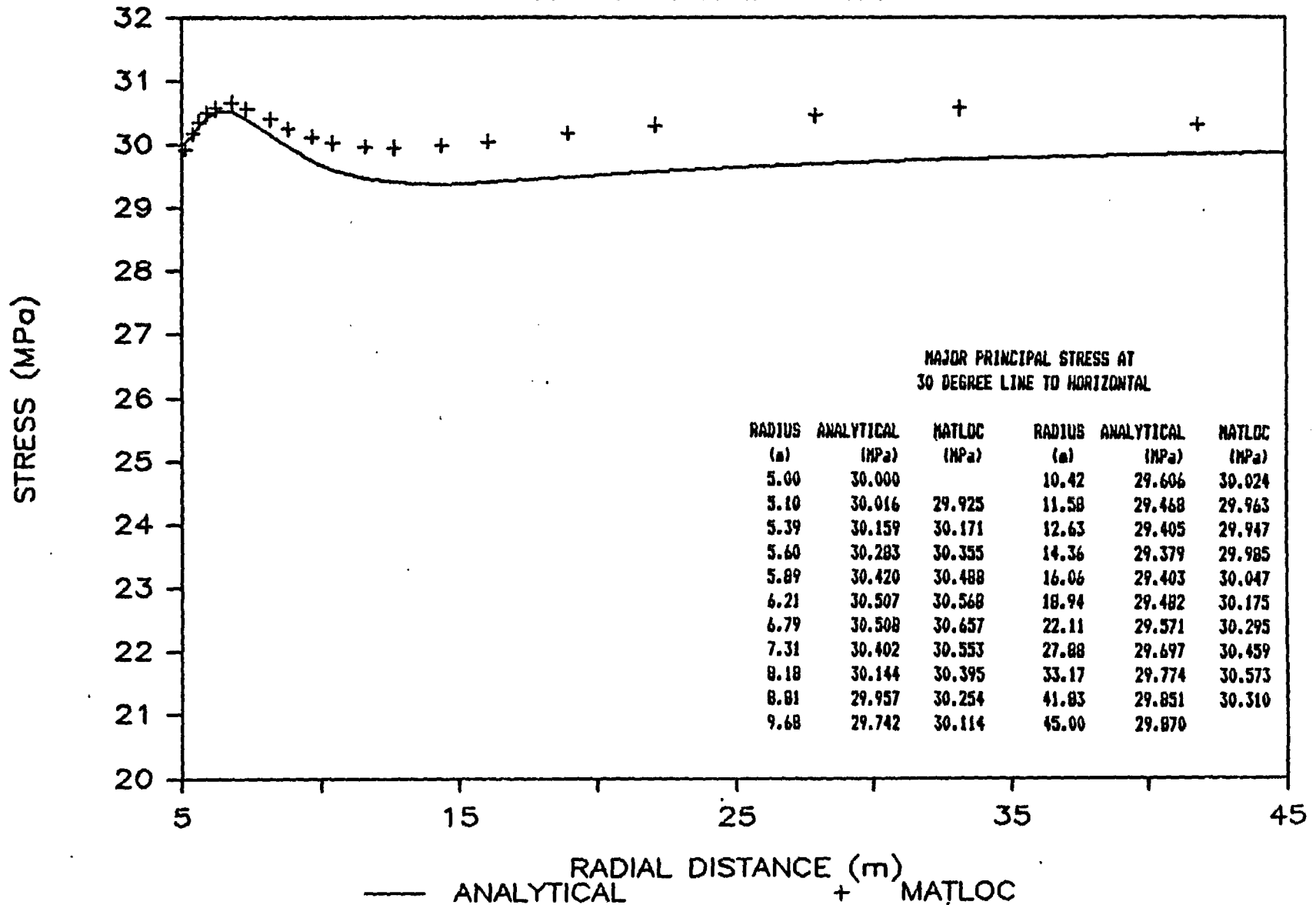


Figure 7.2-2 MATLOC Problem 3.2a  
Major Principal Stresses along a  
Line 30 Degrees from Horizontal

# MATLOC — PROBLEM 3.2a

## ANGLE TO PRINCIPAL STRESS

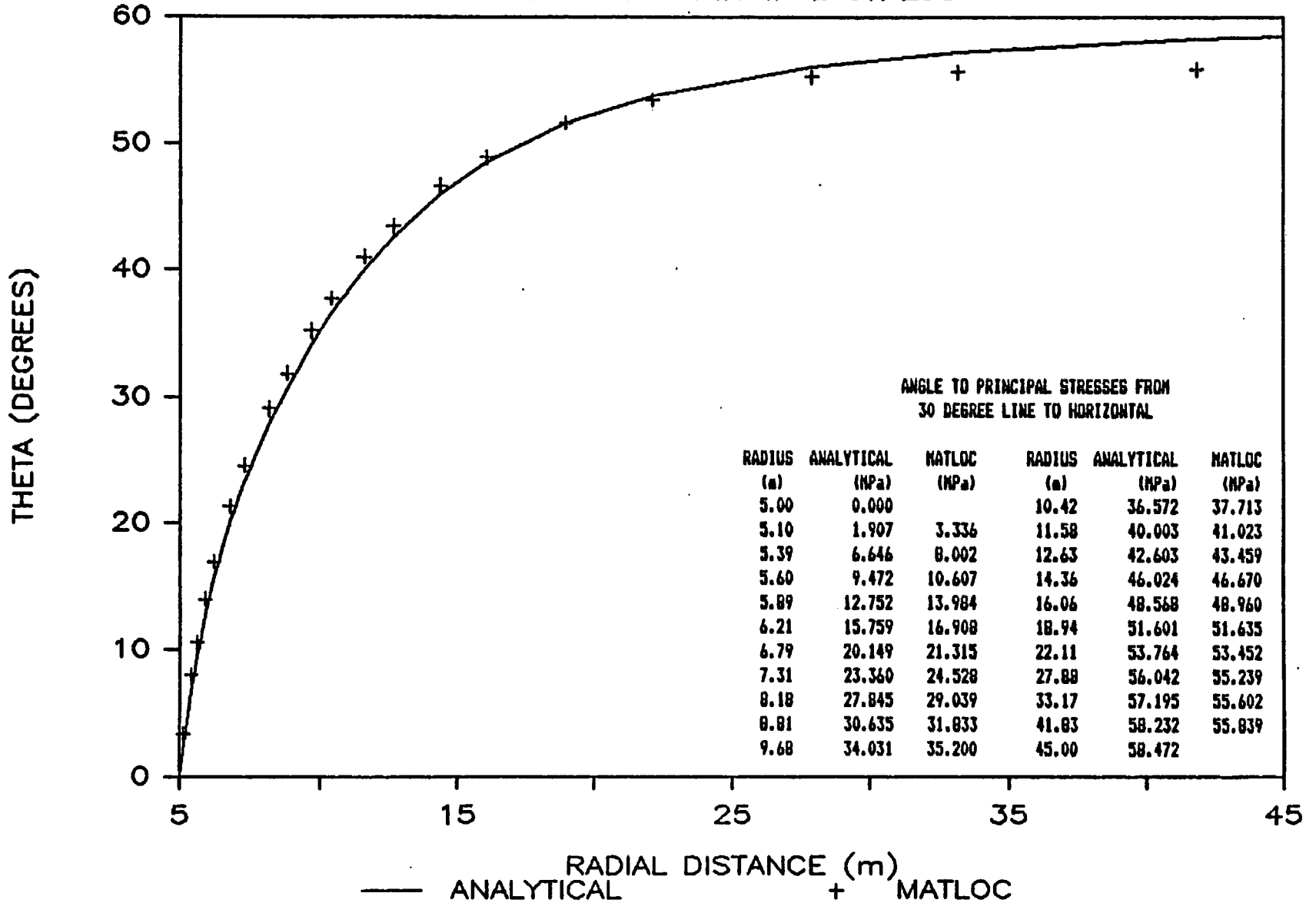


Figure 7.2-4 MATLOC Problem 3.2a  
Angle to Principal Stresses Measured  
to a Line 30 Degrees from Horizontal

# MATLOC PROBLEM 3.2a

## CIRCUMFERENTIAL DISPLACEMENTS

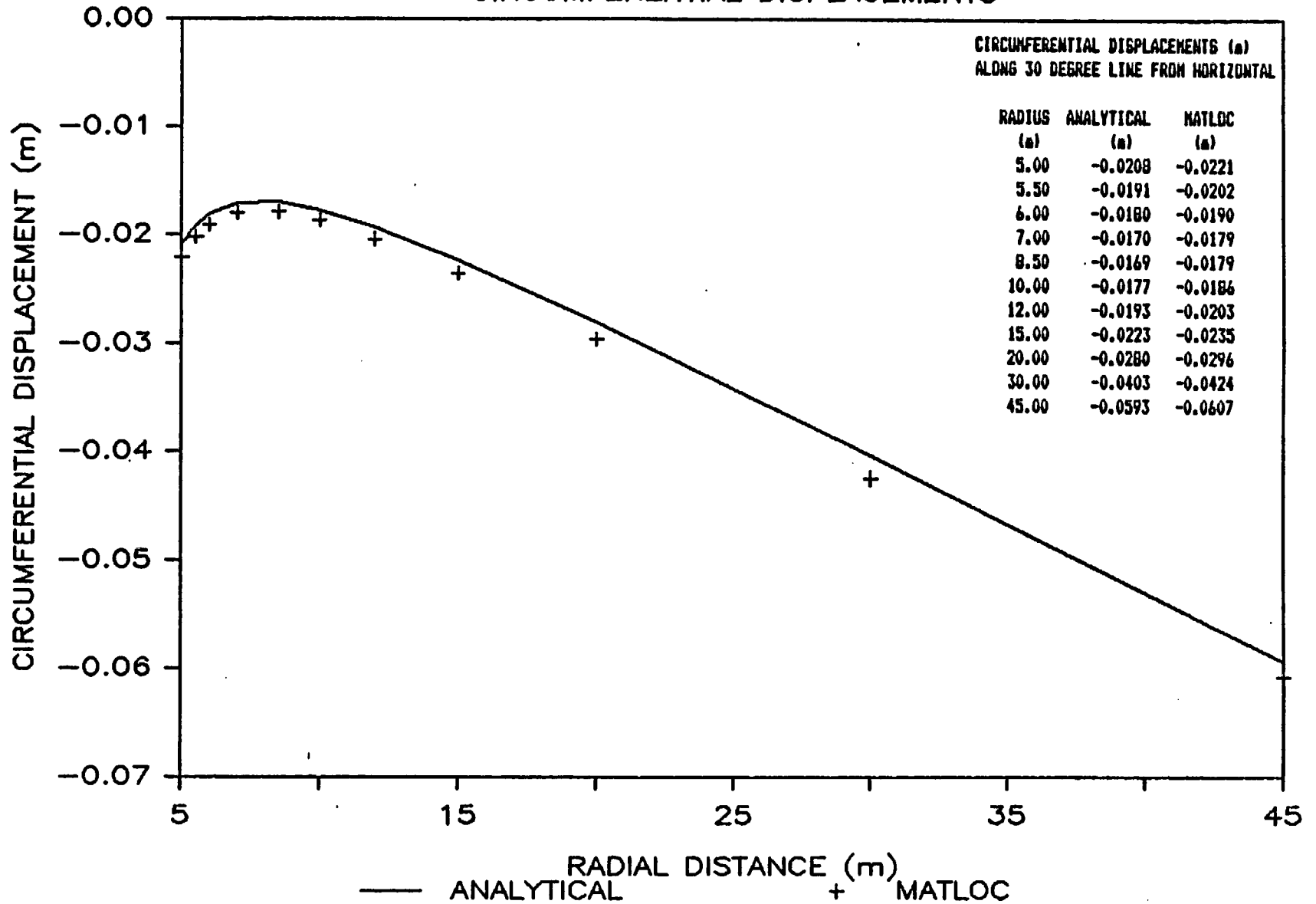


Figure 7.2-6 MATLOC Problem 3.2a  
Circumferential Displacements along a  
Line 30 Degrees from Horizontal

# MATLOC — PROBLEM 3.2a (RUN #2)

MAJOR PRINCIPAL STRESS

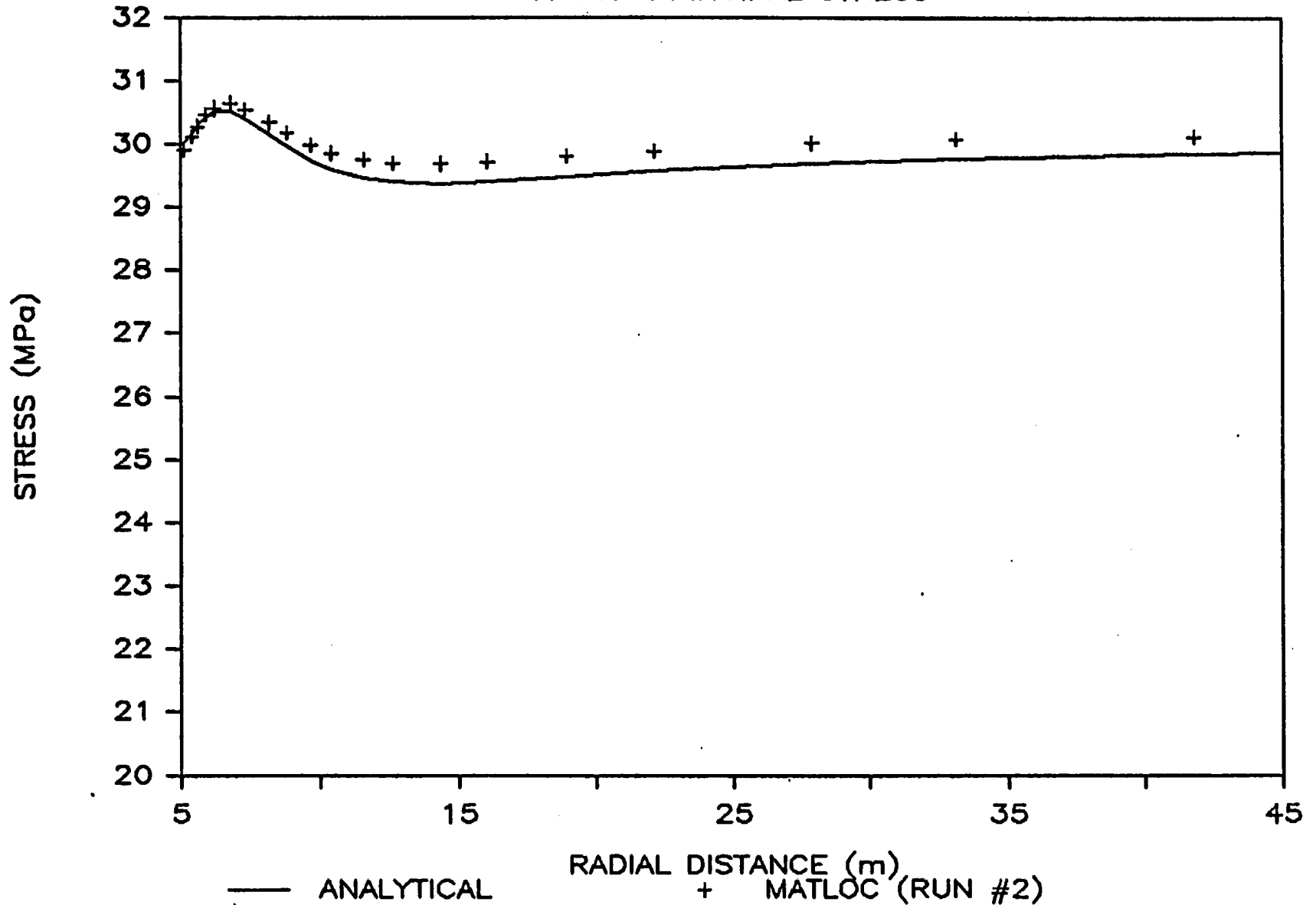


Figure 7.2-8 MATLOC Problem 3.2a - Run #2  
Major Principal Stresses Along a  
Line 30 Degrees from Horizontal

### 7.3 Problem 6.3 - In Situ Heater Test - Basalt Waste Isolation Project

Problem Statement - This problem concerns the transient thermal simulation of basalt due to full-scale Heater Test 2, undertaken in 1980 at the Basalt Waste Isolation Project (BWIP) Hanford site near Richland, Washington. A single heater, vertically emplaced below the floor of a repository-type opening, was operated for 527 days. During this time, the power level was incrementally increased to a maximum of 5 kW, as the thermal and mechanical response of the host rock was monitored. Laboratory-determined material properties of basalt accompany a detailed description of this problem in the Benchmark Problems Report. This description has been summarized in Section 3.4.2.

Input Data - This problem was modeled using two-dimensional, 8-noded axisymmetric elements. The heater was modeled as a heat generating "solid" material with thermal material properties for air. The geometry and the finite element mesh utilized is shown in Figure 7.3-1. The axisymmetric model is not truly valid above the floor level; but in the region where the nodal displacements are to be calculated, the model is representative of actual conditions. Boundaries were set at locations where, based on field data, adiabatic boundary conditions could be assumed.

MATLOC is capable of modeling stress-dependent, bilinear elastic materials. This feature was utilized in this problem because of the fractured state of the Pomona Basalt member. At stress levels below 300 Pa, the elastic constants are low, to allow for closing of the fractures. At stress levels above 3,000 Pa, the fractures are assumed to be closed, and the material stiffness is greater.

Input data to MATLOC for Problem 6.3 were obtained from the Benchmark Problems Report and included:

o Material Properties

- Density = 2,850 kg/m<sup>3</sup>
- Coefficient of thermal expansion =  $5.82 \times 10^{-6}/^{\circ}\text{C}$
- Stress dependent variables Table 7.4-1

o In Situ Stresses

- Vertical Stress  $S_y = 2.0 \text{ MPa}$
- Horizontal Stress  $S_x = 4.5 \text{ MPa}$

Run Problem - The analysis of this problem required two separate runs; a geostatic and a thermal run. The geostatic run was required to determine the initial stresses and displacements of the model prior to thermal loading. The geostatic load case included the effect of stress redistribution resulting from excavation of the repository opening. This stress redistribution was accomplished by applying a set of normal tensile loads, of the same magnitude as the in situ stresses prior to excavation, to the room surfaces and superimposing the in situ compressive stress state. Stress redistribution around the canister borehole was considered negligible compared to the room opening, and was not considered in this model.

TABLE 7.3-1

ELASTIC CONSTANTS AT VARIOUS STRESS LEVELS FOR MATLOC  
PROBLEM 6.3

<u>Elastic Constant</u>	<u>Stress &lt;3.0 MPa</u>	<u>Stress &gt;3.0 MPa</u>
$E_x$	6,000 MPa	30,000 MPa
$E_y$	8,000 MPa	40,000 MPa
$G_y$	2,000 MPa	10,000 MPa
$\nu_y$	0.02	0.30
$\nu_y$	0.03	0.26

# MATLOC - PROBLEM 6.3 BWIP

## VERTICAL DISPLACEMENT (E04)

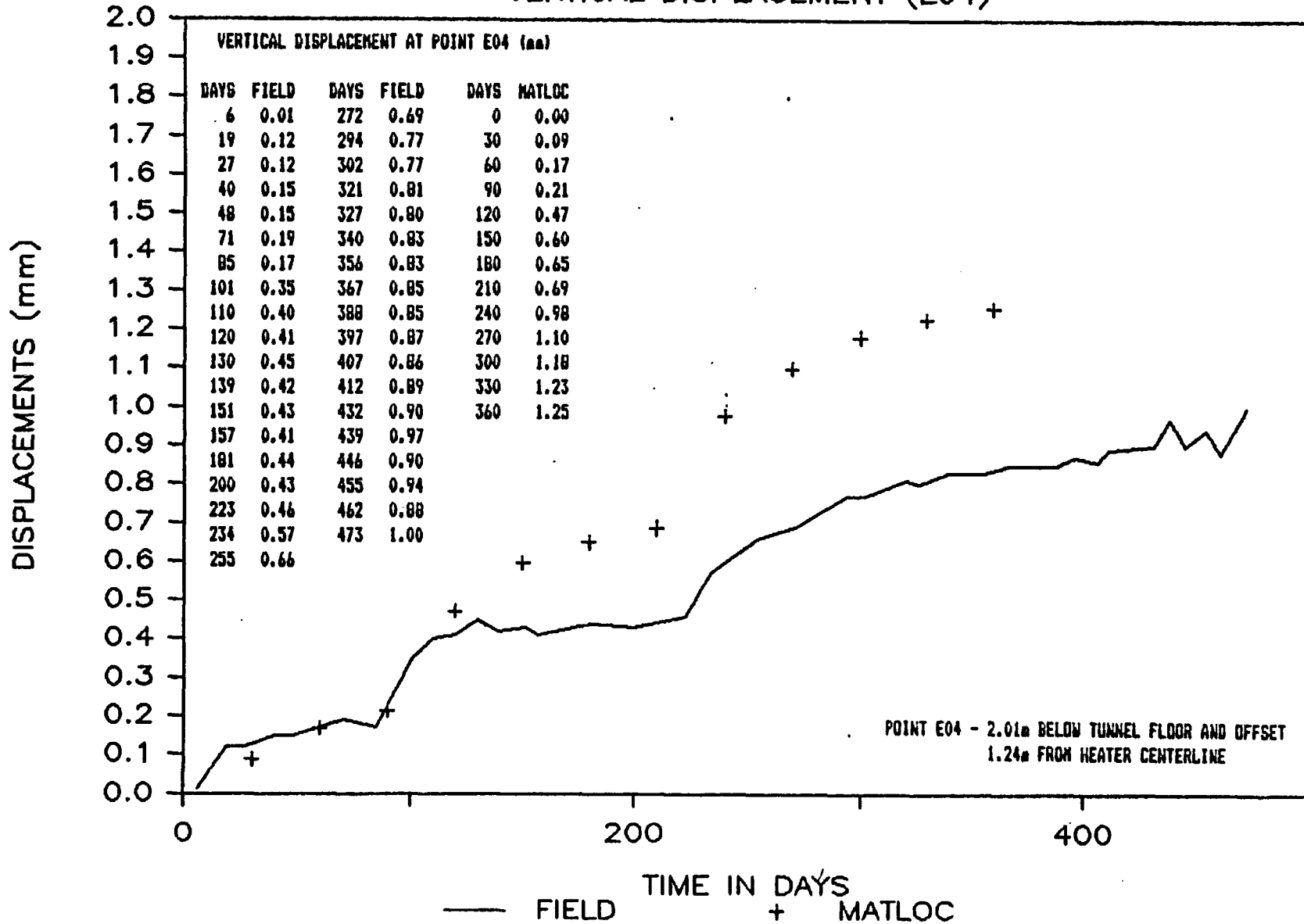


Figure 7.3-2 MATLOC Problem 6.3  
Vertical displacement History  
for Point E04

# MATLOC — PROBLEM 6.3 BWIP

## HORIZONTAL DISPLACEMENT (E03)

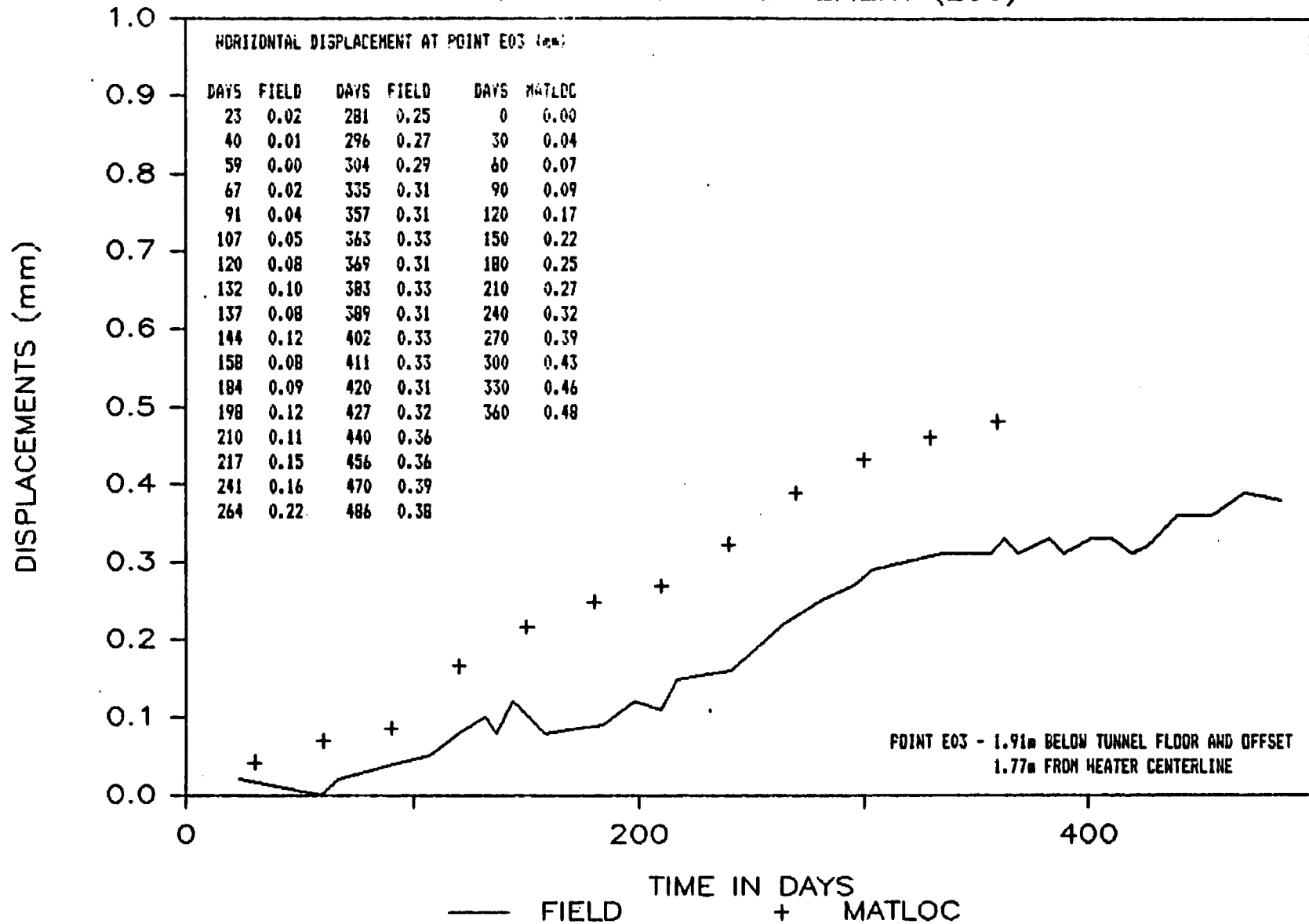


Figure 7.3-4 MATLOC Problem 6.3  
Horizontal Displacement History  
for Point E02

## 8.0 BENCHMARKING OF VISCOT

## 8.0 BENCHMARKING OF VISCOT

### 8.1 Code Background and Capabilities

VISCOT is a two-dimensional, non-linear, transient finite element computer program designed to determine the viscoplastic deformation of a rock mass due to mechanical and thermal loadings. The code was assembled by GeoTrans, Inc. and consists of adaptations of subrouting given in Owen and Hinton (1980). Additional modifications, made by INTERA Environmental Consultants, Inc. as part of the SCEPTER technology package, enhanced the viscoelastic capabilities of the code. The VISCOT program and documentation (INTERA, 1983; ENWL-437) were obtained from the Office of Nuclear Waste Isolation (ONWI). The QA identification number for this version is 420-11C-02.

The VISCOT code can be used to solve nonlinear, two-dimensional planar, and axisymmetric thermomechanical and/or geostatic stress problems. Thermal stress calculations with VISCOT, in which the rock mass is modeled as a nonlinear temperature and stress-dependent viscoelastic material, require a two-stage analysis. First, VISCOT is used to compute the initial geostatic stress state in the rock mass due to the room excavation and store the results on a tape file. It is usually assumed that the geostatic stress state is reached under elastic conditions. In the second stage of the analyses, the geostatic stresses are used as initial conditions, and temperature data from a previous heat transfer analysis with DOT (INTERA, 1983; ENWL-420) are used as thermal loads. If time-dependent material properties such as creep laws are used, a transient analysis which corresponds to the DOT temperature data, must be made.

The viscoplastic material model within VISCOT can be described by a Tresca, von Mises, Drucker-Prager, or Mohr-Coulomb yield criteria (with or without strain hardening) with an associated flow rule which can be a power or exponential law. The viscoelastic material model is a temperature- and stress-dependent law which was developed specifically for salt rock masses. These two material behavior models cannot be combined in one material type.

The main applications of the VISCOT code are room and canister scale analyses for evaluating room closure rates, stability, floor heave, and canister integrity in rock masses such as salt, basalt, granite, tuff, or shale. The inclusion of time-dependent material models make this code well suited for modeling salt. However, the thermal and mechanical material properties are assumed isotropic, which limit the code's applicability to fractured media such as basalt or shale, where bilinear material properties are often required.

The major limitations of the VISCOT code include:

- The code cannot model anisotropic or fractured media.
- Problems involving large deformation or geometrical nonlinearities (nonlinear strain versus displacement relationships) cannot be modeled.

## 8.2 Problem 3.2b Circular Tunnel (Long Cylindrical Hole) in an Infinite Elastic-Plastic Medium Subjected to a Hydrostatic Stress Field

**Problem Statement** - This problem concerns the stress analysis around a long circular opening with a radius of 5 m in an elastic-plastic medium with a hydrostatic stress field. The objective of this problem is to test the code's ability to compute plastic stresses and deformations using the Tresca yielding criterion. The material is assumed to be elastic-perfectly plastic, and will yield when the difference between the maximum and minimum stresses reaches twice the shear yield stress (Tresca criterion).

**Input Data** - A two-dimensional, planar model of the tunnel cross-section and surrounding rock mass was used to analyze this problem. Horizontal and vertical symmetry conditions permitted the reduction of the model to one quadrant, with circumferential displacements restrained along the symmetry boundaries. A circular outer boundary was defined at 12 radii (60 m) from the tunnel centerline. This distance was considered sufficient to minimize changes in the boundary stress state. The finite element mesh used for this problem is shown in Figure 8.2-1. The Tresca yield criterion was selected, and parameters related to the viscoplastic material model were defined. Since the model considers a plane strain analysis, the element thickness was set to zero. The input data to VISCOT for Problem 3.2b were taken from the Benchmark Problems Report and include:

- Material Properties
  - Modulus of Elasticity  $E = 6000 \text{ MPa}$
  - Poisson's Ratio  $\nu = 0.2$
  - Yield Stress in Pure Shear  $K = 10 \text{ MPa}$
  - Viscoplastic Flow Rate  $(F) = (F/Y_0)^N$

Where:

$F = \sigma - Y = 0$  for elastic stress state and at onset of yielding  
 $> 0$  for plastic stress state

$\sigma$  = effective stress

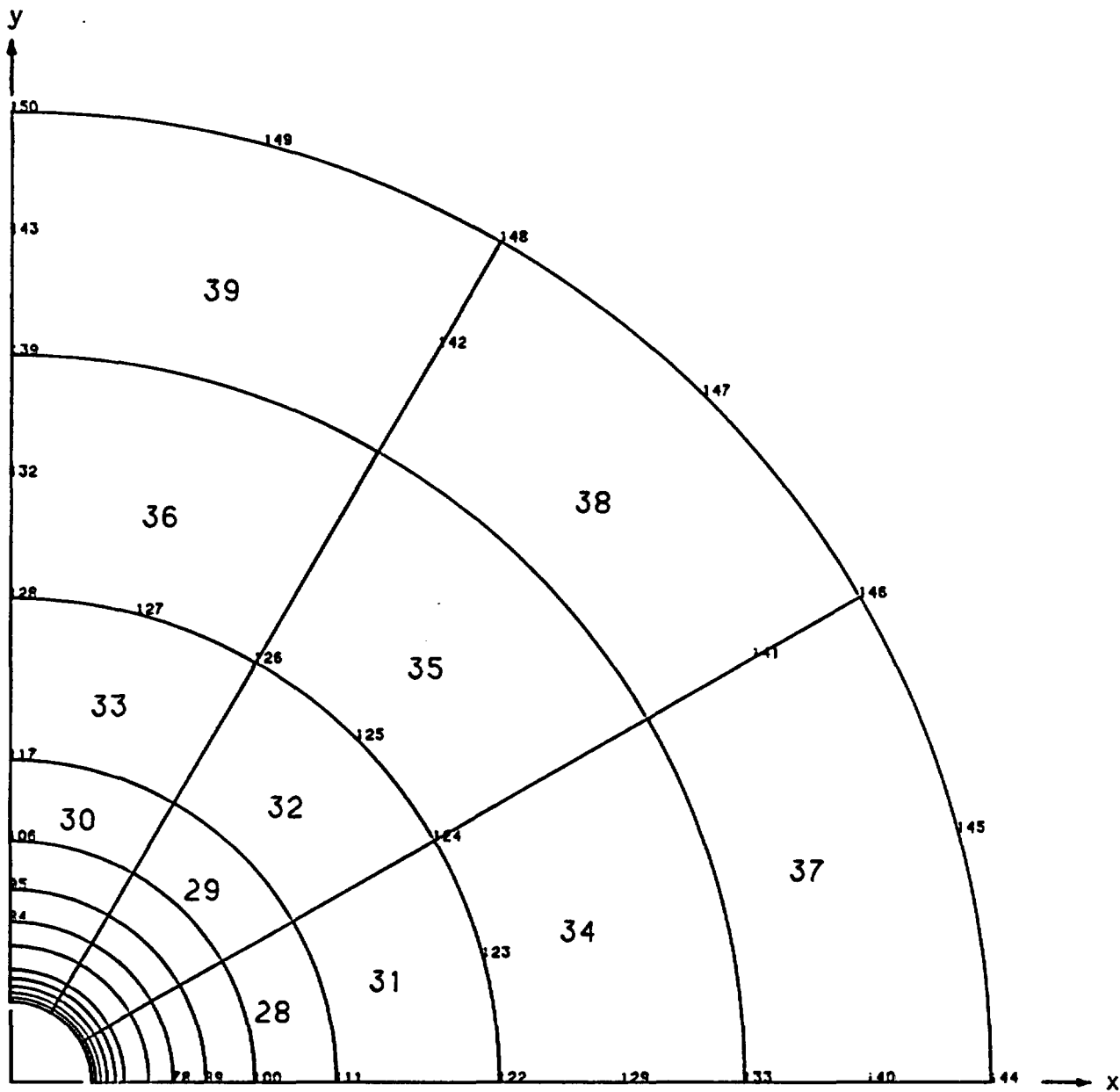
$Y$  = yield stress

$Y_0$  = initial yield stress - not differentiated  
from  $Y$  in VISCOT user manual

$N$  = exponent for power-law flow rule  $N = 1.0$

- In Situ Stresses
  - Horizontal Stress  $S_x = 15 \text{ MPa}$
  - Vertical Stress  $S_y = 15 \text{ MPa}$

**Run Problem** - Although this is a static problem, an arbitrary time step of 0.01 sec. was defined to facilitate incremental loading in VISCOT. The load factor was initially set at 0.5, and was increased in 10 increments of 0.05 each. No code-related difficulties were encountered while running Problem 3.2b with VISCOT.



+-----+ 4.0 m in X  
 +-----+ 4.0 m in Y

Figure 8.2-1 VISCOT Problem 3.2b  
Finite Element Mesh

# VISCOT - PROBLEM 3.2b

## RADIAL STRESS

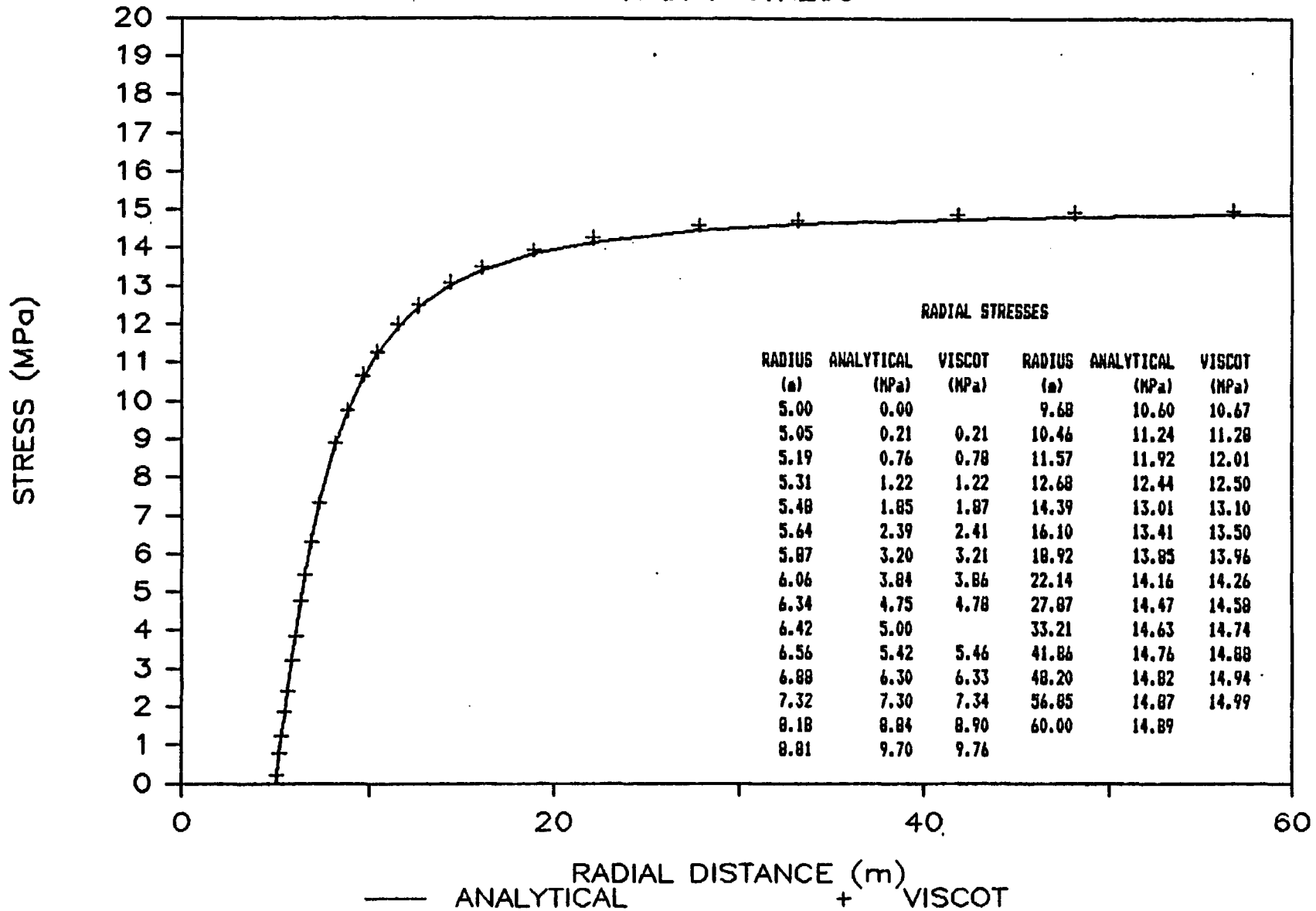


Figure 8.2-3 VISCOT Problem 3.2b  
 Radial Stress Along a  
 Line 30 Degrees from Horizontal

### 8.3 Problem 3.3c - Viscoelastic Analysis of a Thick-Walled Cylinder Subjected to Internal Pressure

**Problem Statement** - This problem concerns the stress analysis of an infinite length, thick-walled cylinder, subjected to an internal pressure of 10 MPa. The cylinder has an inner radius of 4 m, an outer radius of 6 m, and is comprised of a homogeneous, isotropic, creep sensitive material at a uniform constant temperature. The objective of this problem is to test the code's capability to calculate creep stresses and deformations against a known analytical solution. In the analytical solution, it is assumed that the steady-state creep condition has been reached, thus stresses and strain rates are constant with respect to time.

**Input Data** - Symmetry conditions allow the reduction of this problem to one-quarter of the cylinder cross section. The two-dimensional, planar finite element mesh shown in Figure 8.3-1 was used to model this problem with VISCOT. To accommodate the symmetry conditions, circumferential displacements were restrained along the horizontal and vertical symmetry boundaries. Since this model considers a plane strain analysis, the element thickness was set to zero. Input data to VISCOT for Problem 3.3c were taken from the Benchmark Problems Report and included:

● **Material Properties**

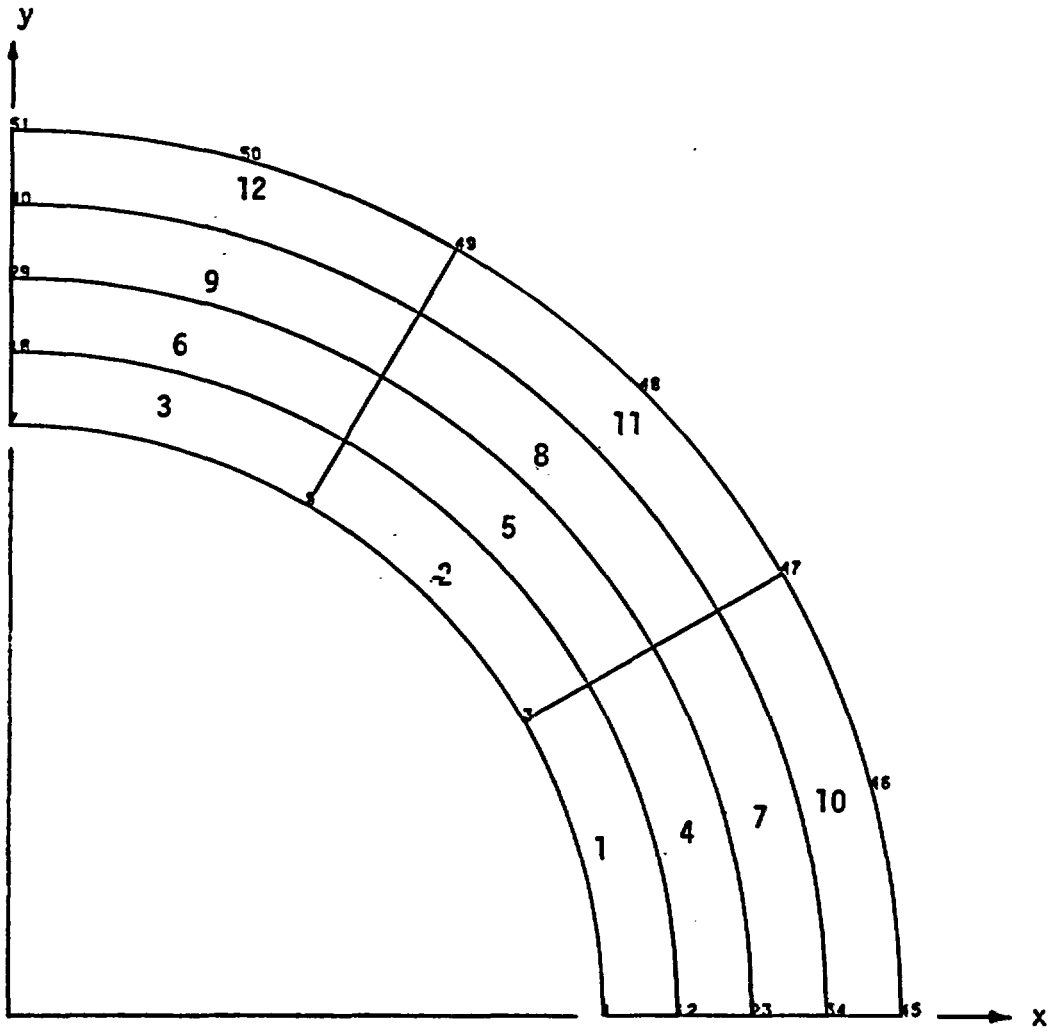
- Modulus of Elasticity  $E = 5000 \text{ MPa}$
- Poisson's Ratio  $\nu = 0.4999$
- Power Law Creep Function  $\epsilon = A \sigma^m t^n T^p$   
where:
  - Coefficient  $A = 2.0 \times 10^{-21}$
  - Stress Exponent  $m = 4.0$
  - Time Exponent  $n = 1.0$
  - Temperature Exponent  $p = 2.0$

● **Loading**

- Internal Pressure  $P = 10 \text{ MPa}$
- Constant Temperature  $T = 300^\circ\text{K}$

**Run Problem** - This problem was run with VISCOT using a time step of 1,600,700 sec. An initial run, which used a Poisson's ratio of 0.50 (perfectly plastic material), resulted in fatal execution errors. A successful analysis was made by using a Poisson's ratio of 0.4999, to eliminate division by zero. No other code-related difficulties were encountered in running this problem with VISCOT.

**Results** - Comparisons of the VISCOT results to the analytical solution are made at points along a radial line inclined  $30^\circ$  above the horizontal. Figures 8.3-2 through 8.3-4 compare the circumferential, radial, and longitudinal stresses from the steady state analytical solution to the values predicted by VISCOT at the point where steady-state conditions were indicated, 80,000,000 seconds.



+-----+ 0.5 m in X  
 +-----+ 0.5 m in Y

Figure 8.3-1 VISCOT Problem 3.3c  
Finite Element Mesh

# VISCOT - PROBLEM 3.3c

## RADIAL STRESS

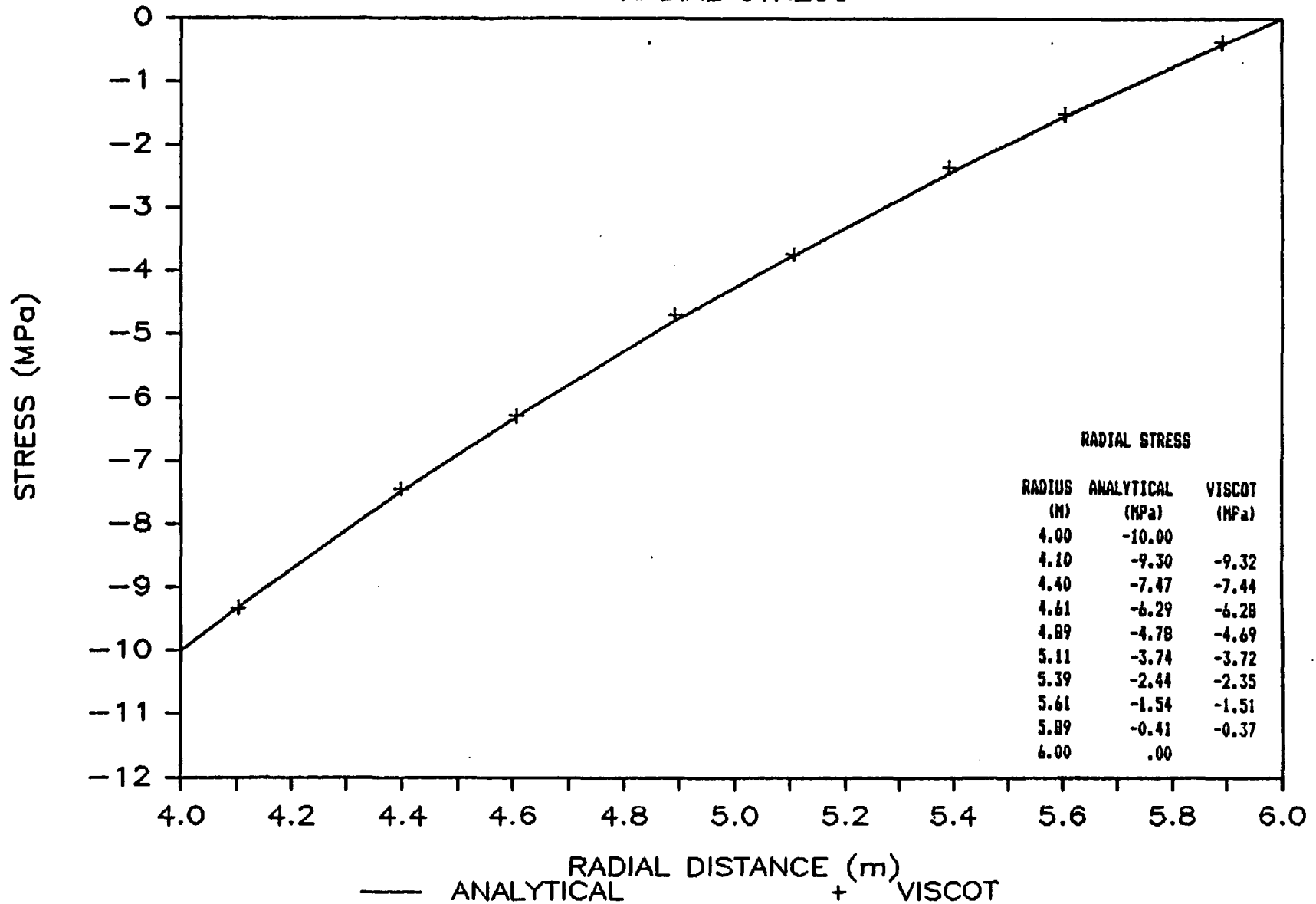


Figure 8.3-3 VISCOT Problem 3.3c  
 Radial Stress Along a  
 Line 30 Degrees from Horizontal

#### 8.4 Problem 3.5 - Plane Strain Compression of an Elastic-Plastic Material

Problem Statement - This problem concerns the yielding and plastic flow of a rectangular block, 15 m wide by 5 m high, loaded with a uniform pressure in the vertical orthogonal direction, constrained in the longitudinal orthogonal direction, and free to expand laterally. These boundary conditions allow this problem to be modeled with two-dimensional plane strain elements. An elastic-plastic analysis is to be made using both the von Mises and Drucker-Prager yield criteria. In the von Mises analysis, an initial vertical pressure of 300 MPa will be increased incrementally until ultimate failure is reached. The Drucker-Prager theory does not predict ultimate failure, thus the loading will be increased well into the plastic flow range.

Input Data - Symmetry about the vertical centerline allows the reduction of this two-dimensional model to one-half the block width (7.5 m) by the full height (5 m). The finite element mesh used to solve this problem with VISCOT is shown in Figure 8.4-1. Symmetry and boundary conditions are preserved by restricting horizontal displacements along the original vertical centerline and vertical displacement along the frictionless bottom surface. Since the problem is a plane strain analysis, an element thickness of zero was used. The input data to VISCOT for Problem 3.5 were taken from the Benchmark Problems Report and include:

- Material Properties
  - Modulus of Elasticity  $E = 45,000 \text{ MPa}$
  - Poisson's Ratio  $\nu = 0.20$
- von Mises Failure Criterion Parameter  $K_M = 190 \text{ MPa}$   
(Yield Stress in Pure Shear)
- Drucker-Prager Yield Criterion Parameters  $K_{(DP)} = 36$   
 $\alpha = 0.35$

Run Problem - This problem has not been successfully run with VISCOT.

## 8.5 Problem 5.2B - Hypothetical Near-Field Problem - Basalt

**Problem Statement** - This problem consists of the transient thermo-viscoelastic stress analysis of the near-field (single room region) of a hypothetical repository containing an infinite number of equally spaced infinite-length rooms. Symmetry assumptions permit the reduction of this problem to a two-dimensional planar model of one-half of a single room, and the surrounding rock. Equally-spaced canisters along the centerline of the room have been replaced by an equivalent heat generating trench. For structural analysis simplicity, this trench is assumed to be filled solid with the host rock material. The VISCOT code will use material properties defined for basalt, and the temperature data previously determined by DOT (see Section 6.3).

**Input Data** - The two-dimensional, 8-noded finite element mesh defined for the DOT analysis was slightly modified to accommodate requirements for VISCOT. Triangular elements are defined in the DOT mesh by specifying the same node number more than once. VISCOT, however, will produce fatal execution errors if a node is used more than once in an element. For the VISCOT mesh, nodes which overlapped in the DOT mesh were replaced by a pair of very close nodes. Thus, some nodes were added. The finite element mesh used for the VISCOT model is shown in Figure 8.5-1. Elements which appear as triangles in this figure are actually quadrilaterals. Compatibility between the temperatures stored on tape files by DOT, and the new finite element mesh defined for VISCOT, was accomplished by a FORTRAN program which redefined these node numbers and applied the temperatures of the previously overlapping nodes (single node number) to the pair of adjacent nodes. The FORTRAN program used for the redistribution of nodal temperatures is shown in Figure 8.5-2.

The material model for this problem used the Tresca yield criterion. Since this problem consists of a plane strain analysis, an element thickness of zero was used. Consequently, the density was also set to zero, and mass effects were not considered. A power-law creep function was selected; however, all coefficients and exponents to this model were set to zero, thereby eliminating creep considerations for basalt.

Input data to VISCOT for Problem 5.2B were taken from the Benchmark Problems Report and include:

- Material Properties of Basalt
  - Modulus of Elasticity  $E = 35,000 \text{ MPa}$
  - Poisson's Ratio  $\nu = 0.26$
  - Coefficient of Thermal Expansion  $= 6.5 \times 10^{-6} \text{ } ^\circ\text{C}^{-1}$
  
- Tresca Failure Criterion Parameters
  - Initial Uniaxial Yield Stress  $K = 140 \text{ MPa}$

**Run Problem** - The thermal stress analysis of this problem with VISCOT was made in two stages. The first stage consisted of a geostatic analysis to obtain the stress state within the rock mass due to the room excavation. For this run, normal tensile loads, equivalent to the

TABLE 8.5-1  
TIME RANGES USED FOR VISCOT  
PROBLEM 5.2b

<u>Run Number</u>	<u>Time Range (years)</u>	<u>Time Step Size (years)</u>	<u>Number of Time Steps</u>
1	0 - 50	5	10
2	50 - 100	5	10
3	100 - 1000	100	9
4	1000 - 10,000	1000	9

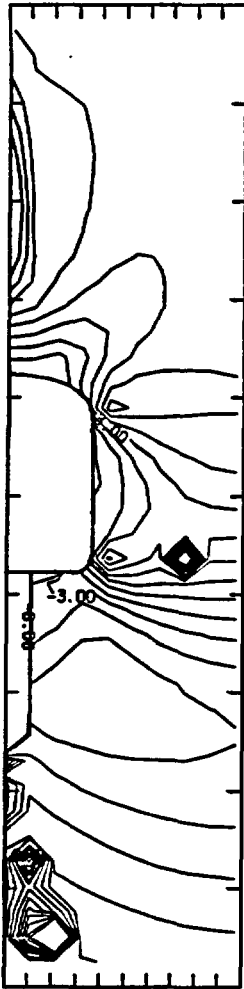
```
PROGRAM VIS2TEMP (INPUT,OUTPUT,TAPE17,TAPE18,TAPES=INPUT,  
1TAPE6=OUTPUT)
```

```
C  
C  
C  
C  
C  
C  
C
```

```
    DIMENSION TEMP(600)  
    READ(5,10) NNDPREV,NNDNOW,INCREM  
10  FORMAT (3I5)  
    WRITE(6,20) NNDPREV,NNDNOW,INCREM  
20  FORMAT (" PREVIOUS NO. OF NODES=",I5/" REVISED NO. OF NODES=",  
1I5/" NO. OF TEMPERATURE INCREMENTS =",I5)  
    READ(17) NDUM  
    WRITE(18) NDUM  
    DO 100 I=1,INCREM  
    READ(17) TIMEP  
    READ(17) (TEMP(J),J=1,NNDPREV)  
    TEMP(540)=TEMP(21)  
    TEMP(541)=TEMP(21)  
    TEMP(542)=TEMP(30)  
    TEMP(543)=TEMP(30)  
    TEMP(544)=TEMP(23)  
    TEMP(545)=TEMP(23)  
    TEMP(546)=TEMP(404)  
    TEMP(547)=TEMP(404)  
    TEMP(548)=TEMP(404)  
    TEMP(549)=TEMP(404)  
    TEMP(550)=TEMP(497)  
    TEMP(551)=TEMP(497)  
    TEMP(552)=TEMP(490)  
    TEMP(553)=TEMP(490)  
    TEMP(554)=TEMP(499)  
    TEMP(555)=TEMP(499)  
    WRITE(18) TIMEP  
    WRITE(18) (TEMP(K),K=1,NNDNOW)  
    WRITE(6,50) I,TIMEP,K,TEMP(K)  
50  FORMAT (" INCREMENT NO.=",I5,6X," TIME=",12E.4,6X," LAST NODE",  
1I5," IS AT TEMPERATURE",F10.3)  
100 CONTINUE  
    STOP  
    END
```

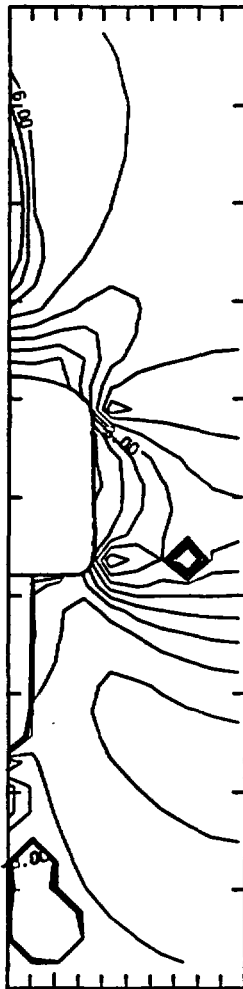
Figure 8.5-2 VISCOT Problem 5.2B  
Program to Redefine  
Nodal Temperatures

-479 m

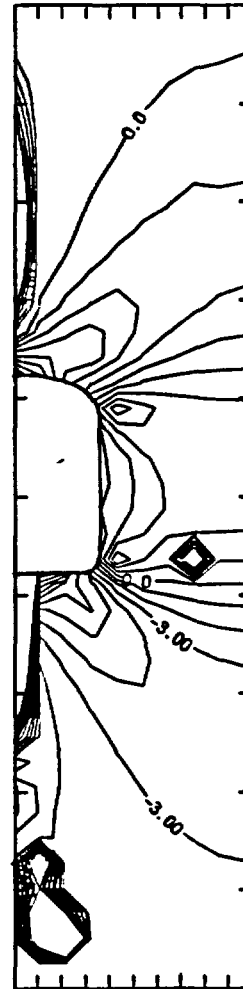


-510 m

Time = 10 years



Time = 30 years

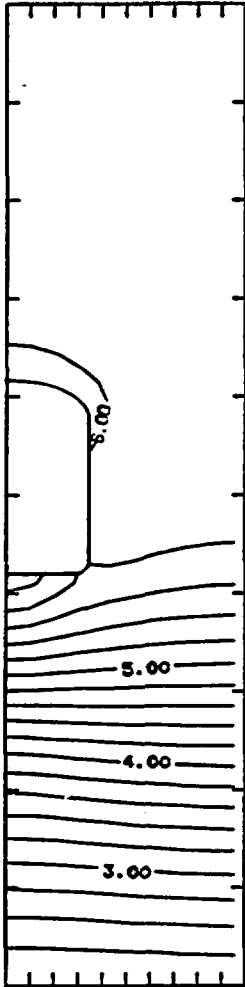


Time = 100 years

Stress in MPa  
Contour Interval = 1.0 MPa

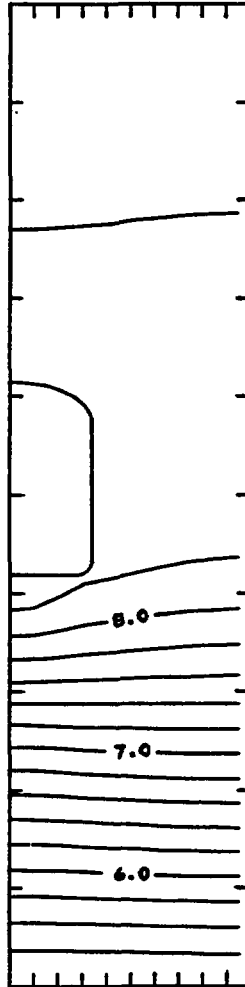
Figure 8.5-4 VISCOT Problem 5.2B  
Minor Principal Stress

=479 m

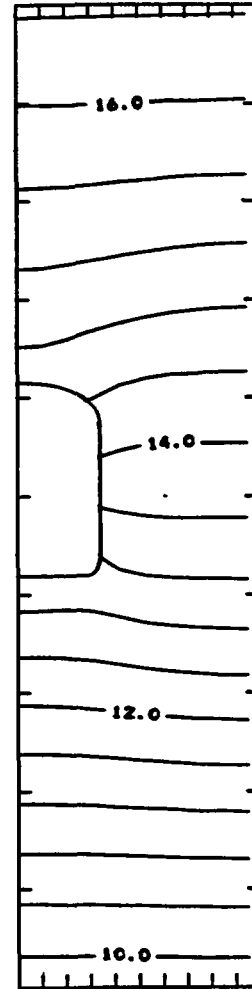


-510 m

Time = 10 years



Time = 30 years



Time = 100 years  
(Contour Interval = 0.4 m)

Displacement in mm  
Contour Interval = 0.2 mm except as noted

Figure 8.5-6 VISCOT Problem 5.2B  
Vertical Displacement

Problem 5.2B models one-half of a single room and pillar, therefore, gravity-induced vertical stresses cannot arch to the far-field rock. In reality, stresses in the pillar region should be reduced, as the gravity load above the room is redistributed to the far-field material. In the model, however, vertical stresses within the pillar are not reduced because the model does not allow the transference of vertical loads beyond the vertical model boundaries. Thus, excessive creep strains are predicted in the pillar region. The far-field material is not included in this model; therefore, arching effects must be approximated.

Arching action becomes important in "displacement-controlled" problems. Two displacement-controlled loads exist in Problem 5.2S; creep and thermal. Therefore, both creep and thermal stresses are affected by the model boundary conditions. The boundary conditions used in this model were based on symmetry, and are representative for a large number of rooms. For cases where few rooms exist, arching must be approximated by vertical fixity above and below the rooms. However, this would overestimate arching effects and limit the creep strains to unrealistically low values.

A second difficulty with Problem 5.2S is the creep law itself. The creep law used in VISCOT is linearly time-dependent and was developed from laboratory data received for only a few hundred days. When extrapolated to 10,000 years, the creep law will predict excessive strains due to the limited accuracy of the model in this time range. The error in the creep law is amplified by the overestimation of stresses by VISCOT, due to the geometric constraints of this near-field analysis. Consequently, the VISCOT code is not capable of accurately modeling Problem 5.2 - Salt, as defined in the Benchmark Problems Report.

Results - The axisymmetric model used for this problem considers a circular room with a radius equal to one-half the room width ( $r=4.7$  m). Field measurements of the room convergence were made at three points; at the north and south walls along the centerline across the width of the room (gages 162 and 159), and at the west wall on the centerline along the room length (gage 161). The distance from the center of the room to gage 161 is 9.15 m, which is nearly twice the modeled room opening. As a result of using an axisymmetric model, comparisons of the VISCOT solution to field measured convergence can only be made for gages 162 and 159 (offset 4.7 m from the room center).

Figure 8.7-2 shows the field measured vertical convergence at the three locations discussed above. The vertical convergences computed by VISCOT at various offsets from the center of the room are shown on Figure 8.7-3. A comparison of the VISCOT convergence at 4.7 m to the measurements at gages 159 and 162 indicate that VISCOT underestimates the convergence at the room wall. Field measurements of the floor uplift due to the heater experiment are shown in Figure 8.7-4. The data plotted indicate the total uplift that occurred from the time the heaters were turned on (Day 806) to Day 900, Day 1240 and Day 1382.

Floor uplift profiles for the same time gages, calculated by the VISCOT code, are shown in Figure 8.7-4. A comparison of these figures indicates that VISCOT overestimates the vertical displacement of the room floor. This is believed to stem from the creep law used for this problem.

# PROBLEM 6.1A – ROOM 4 – FIELD VALUES

VERTICAL CONVERGENCE AT VARIOUS OFFSETS

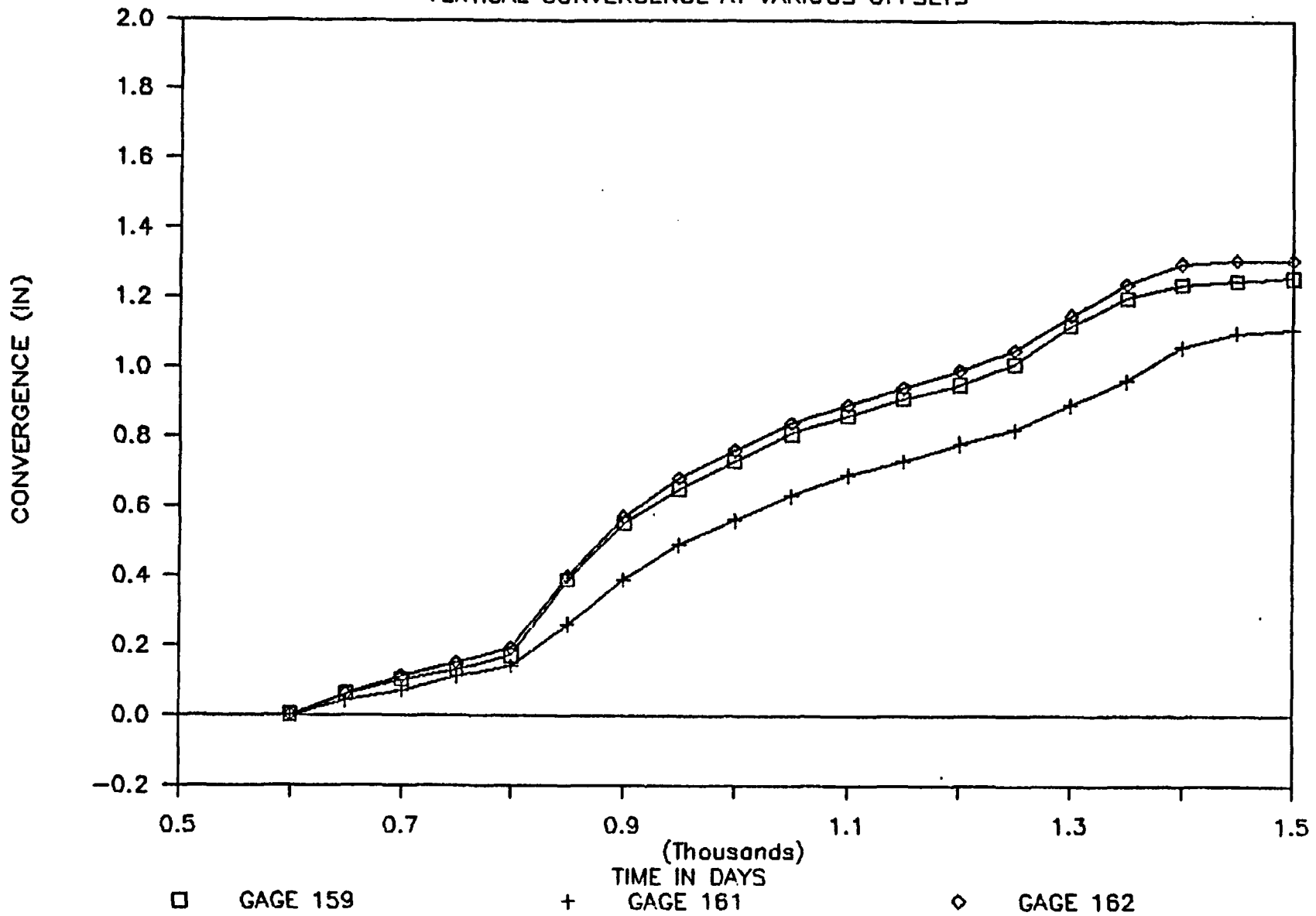


Figure 8.7-2 Project Salt Vault Field Values  
Vertical Convergence of Room 4

# PROBLEM 6.1A - FIELD VALUES

ROOM 4 - FLOOR UPLIFT AT VARIOUS TIMES

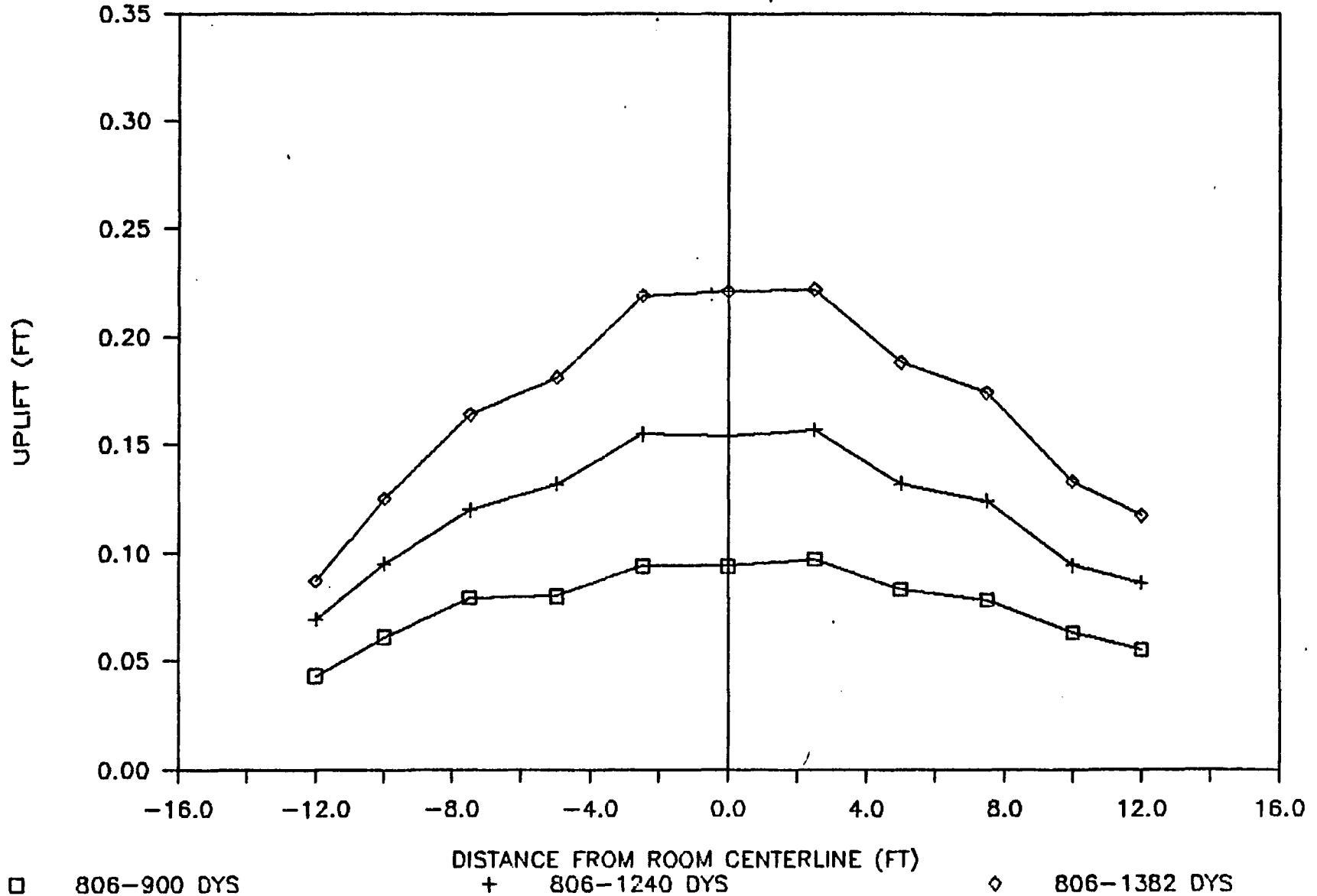


Figure 8.7-4 Project Salt Vault Field Values  
Floor Uplift in Room 4

## 8.8 Problem 6.3 - In Situ Heater Test

**Problem Statement** - This problem concerns the thermomechanical simulation of full-scale Heater Test 2 in the Pomona Member Basalt, undertaken by the Basalt Water Isolation Project (BWIP). Heater Test 2 consisted of a single heater, situated below the floor of a repository-scale tunnel, with an incremental power output. Field data, which specified measured displacements at various locations below the room floor, were given.

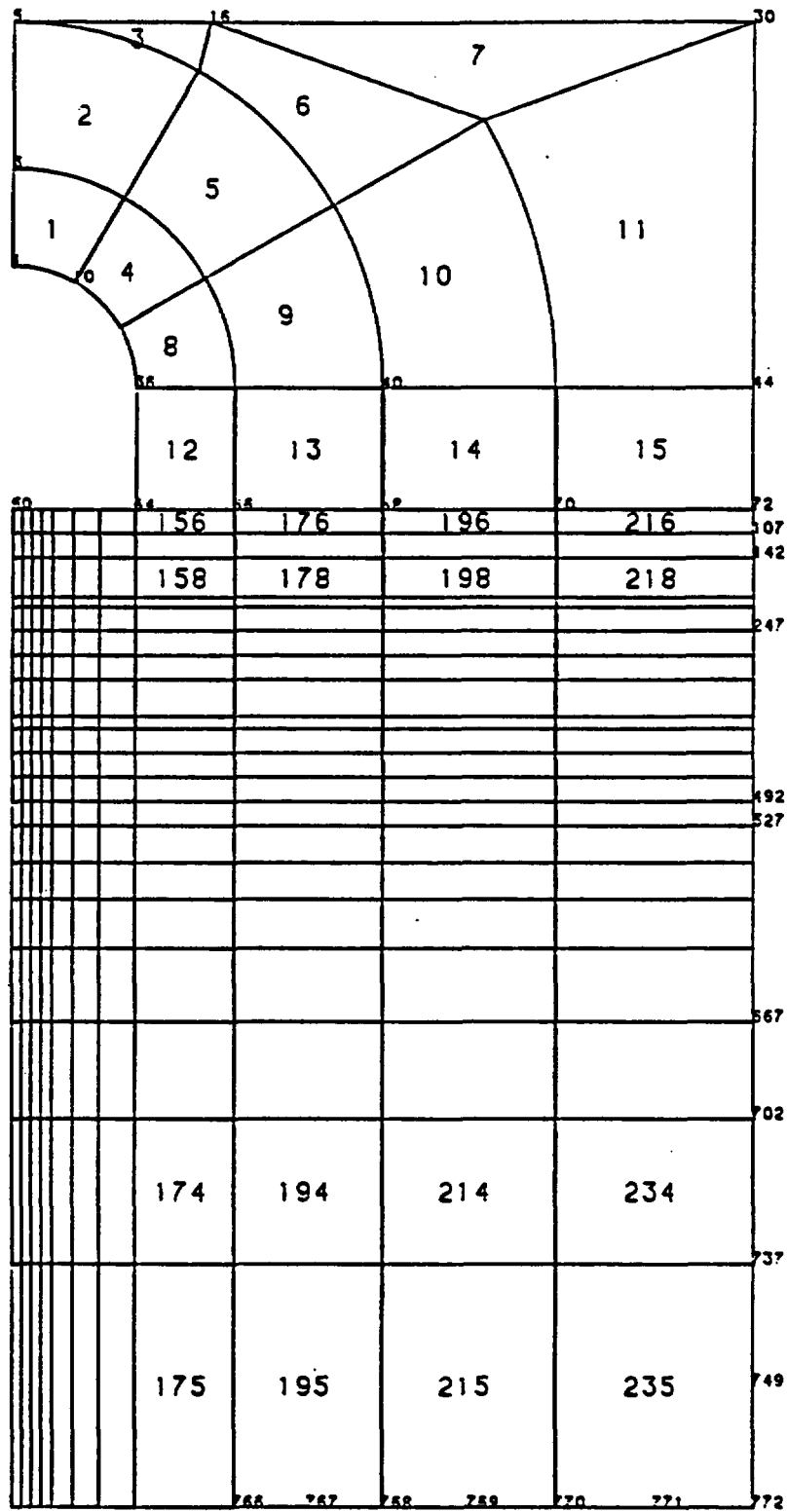
**Input Data** - The finite element mesh used for VISCOT was the same axisymmetric, 8-noded finite element mesh defined for DOT, and is shown in Figure 8.8-1. As discussed in Section 6.6, the axisymmetric model is not truly valid above the floor level. However, in the region where calculated displacements are to be compared to field measurements, the model is representative of actual conditions.

Problem 6.3 specifies bilinear elastic constants for the Pomona Basalt. VISCOT, however, is not capable of modeling bilinear properties, thus average elastic constants for the anticipated stress range were used. VISCOT used temperature data previously calculated by the thermal analysis code DOT. The material model selected for VISCOT in this problem used the Tresca yield criterion. A power-law creep function was selected, but since basalt is not a creep-sensitive material, all creep parameters were set to zero. Input data to VISCOT for Problem 6.3 were taken from the Benchmark Problems Report, and included:

- Material Properties of Basalt
  - Modulus of Elasticity  $E = 30,000 \text{ MPa}$
  - Poisson's Ratio  $\nu = 0.26$
  - Coefficient of Thermal Expansion  $\alpha = 5.82 \times 10^{-6} \text{ }^\circ\text{C}^{-1}$
- Tresca Yield Criterion Parameters
  - Initial Uniaxial Yield Stress  $K = 140$

**Run Problem** - As in all excavation models run with VISCOT, an initial geostatic analysis was made to determine the stress state due to the excavation. These initial stresses were used in the VISCOT thermo-mechanical analysis with the temperature data from a previous DOT run. The time step for the DOT analysis, and thus for the VISCOT analysis, was fifteen days. No code-related difficulties were encountered while running Problem 6.3 with VISCOT.

**Results** - Figures 8.8-2 and 8.8-3 compare the VISCOT results to field measured vertical displacements, offset 1.24 m and 1 m below (E02) and 1 m above (E04) the heater, respectively. The displacements calculated by VISCOT compare well with the field data in both of these figures. Horizontal displacements at a depth of 1.91 m, offset 1.77 m from the heater (E03), are compared in Figure 8.8-4. A poor agreement between field data and VISCOT values at this point may be due to several factors.



+-----+ 1.5 m in X  
 +-----+ 1.5 m in Y

Figure 8.8-1 VISCOT Problem 6.3  
Finite Element Mesh

# VISCOT — PROBLEM 6.3 BWIP

## VERTICAL DISPLACEMENT (E04)

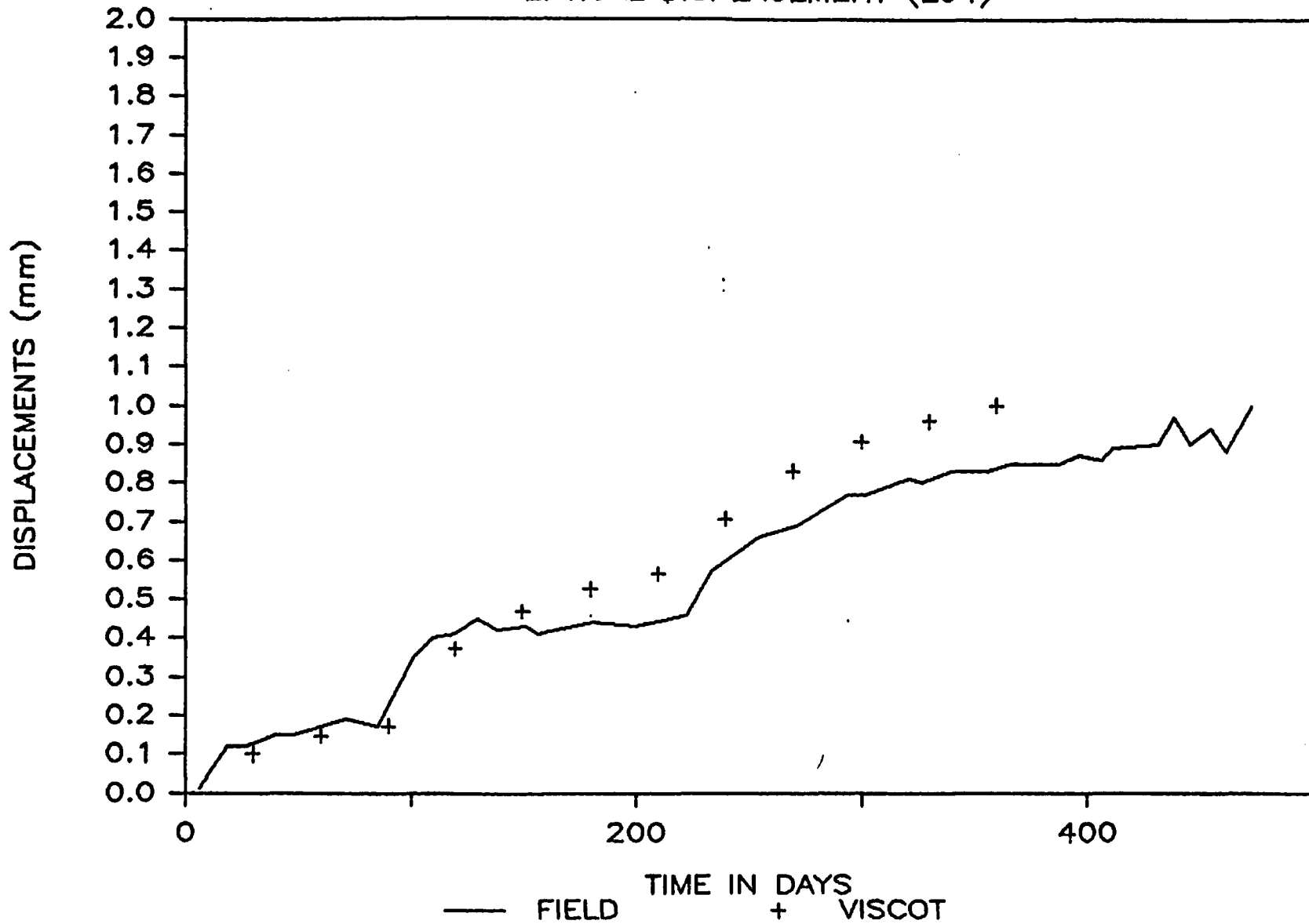


Figure 8.8-3 VISCOT Problem 6.3  
Vertical Displacement History  
for Point E04

## 9.0 BENCHMARKING OF SALT4

## 9.0 BENCHMARKING OF SALT4

### 9.1 Code Background and Capabilities

SALT4 is a two-dimensional thermal/thermomechanical code designed to analyze the effects of excavation and waste emplacement on the stress and displacement fields surrounding a radioactive waste repository in bedded salt. The current version of SALT4 is an enhancement of previous versions of the codes SALT and SALT3. The program and documentation<sup>(9)</sup> were obtained from the Office of Nuclear Waste Isolation (ONWI). SALT4 is one of the codes documented as part of the SCEPTER technology package is 420--05C-02.

In the SALT codes, repository openings are represented by thin horizontal seams. The temperature distribution and associated thermal stresses are approximated by analytic solutions for a line heat source in an elastic medium (Hart, 1981). The mechanical effects due to excavation of the repository openings are computed by the displacement-discontinuity method. These techniques are valid for homogeneous, elastic materials in a semi-infinite half space.

The horizontal seams along repository horizons are divided into a number of equal-length segments. Within each seam, individual segments are defined either as mined (excavated rooms) or unmined. The unmined segments may be comprised of either elastic or creeping material, and are defined as such automatically by the program. The current version of SALT4 allows the specification of 2 seams, each containing up to 200 segments.

Unlike other thermal and thermomechanical codes benchmarked in this study, SALT4 is designed specifically for far-field studies. The code may be used for near-field (repository code) analyses, but since the material above the room openings is assumed to be elastic and non-creeping, these studies will be limited in their accuracy. The major advantages of SALT4 are its computational efficiency, the small amount of required input data, and a creep law based upon and consistent with laboratory experimental data for salt. The code can be used for parameter sensitivity analyses of two-dimensional thermal and thermomechanical responses in bedded salt during excavation, operational, and post-closure phases. It is especially useful in evaluating alternative patterns and sequences of excavation and waste canister emplacement. SALT4 is well suited for large-scale analyses performed during the siting of a repository, and for verifying fully numerical codes. The major limitation of SALT4 is that some of the assumptions in its formulation, such as temperature independent material properties, render it unsuitable for canister scale analyses or analysis of lateral deformation of the pillars.

The solution method employed in SALT4 is based on the following basic displacement discontinuity equation:

$$\{\sigma\} = [A] \{D\}$$

## 9.2 Problem 5.2S - Hypothetical Near-Field Problem - Salt

Problem Statement - This problem consists of the two-dimensional transient thermomechanical simulation of a repository containing an infinite number of rooms. The rooms are ventilated (forced convection) for the initial 50 years of waste canister storage. After 50 years, the rooms are sealed, and natural convection and radiation occur within the repository openings. The SALT4 analysis of this problem used material properties for salt, thus creep effects were considered. A detailed presentation of this problem, and the accompanying very-near field and far-field problems, is included in Section 2.

Input Data - Analytically, this problem may be simplified by applying symmetry conditions along the room centerlines and within the pillars mid-way between the rooms. SALT4, however, cannot model symmetry conditions directly. To obtain symmetrical thermal and thermal-mechanical responses, it would be necessary to model a repository consisting of an infinite number of rooms. Since it is impossible to model an infinite number of rooms, several preliminary analyses were made to simulate symmetry conditions.

The first analysis consisted of one seam containing 40 rooms. The rooms were comprised of 3 elements each and, when combined with 6 segments for each pillar, a total of 360 segments were required. To accommodate this analysis, the SALT4 program was dimensioned to allow up to 400 segments per seam. A time step of 5 years was chosen and the analysis was to have run for the first 100 years. However, the program terminated after 2 iterations (5 years) when the time limit of 400 octal seconds was reached. Due to excessive computing costs required to run a full analysis for 10,000 years, the SALT4 code was redimensioned to 200 segments per seam, and a coarser model was selected.

The next analysis of this problem consisted of one seam of 60 rooms with one segment for each room, and two segments for each pillar. Thus, 180 segments were used. The time range and time step size were the same as the previous run, and the time limit was increased to 700 octal seconds. This time limit was reached and the program terminated after 13 time steps. Again, the computational effort necessary to accomplish a full analysis was considered excessive. A review of the output from this run revealed that the thermal responses of the interior 28 rooms were identical. Thus, symmetry conditions could be modeled in this problem by using 2 central rooms bounded by 16 rooms on both sides to act as buffers, or a total of 34 rooms.

To obtain temperature and stress contours comparable in detail to other codes, it was considered necessary to use at least 4 segments for each room and 8 segments for each pillar. The required 408 segments, however, would lead to extremely long computation times. Therefore, no further attempts to simulate symmetry conditions were made. Additional analyses, using 2 and 10 rooms, were run to obtain temperature and stress contours around a repository. These runs will be discussed below.

Run Problem - The first analysis from which results have been drawn consisted of two complete repository rooms, as shown in Figure 9.2-1. A time step of 5 years was used, and the program was run from 0 to 100 years. No difficulties were encountered while running this analysis. A second analysis, consisting of 10 rooms with 1 segment per room, was run to obtain results at greater distances from the seam. The time range considered was the first 1,000 years, using a time step of 100 years. After the first 600 years, the program terminated with the error message "Radial Stress Does not Converge with 40 Terms."

The third and final analysis made of this problem included a temporary modification to SALT4 that increased the number of iterations from 40 to 100 before convergence is declared and the program terminates. This analysis consisted of 5 rooms with 1 segment per room, 2 segments per pillar, and the same time range and time step size as the previous run. In this case, the program terminated after 1 time step due to the FORTRAN error "Bad Result Near Line HEAT Near Line 79." No further analyses of Benchmark Problem 5.2 were made with SALT4. The results which follow were drawn from existing output from the first and second analyses.

Results - Contours of the temperature, maximum principal stress, minimum principal stress, and displacements at 10, 30, and 100 years are presented in Figures 9.2-2 through 9.2-5. Visual comparisons of the temperature contours predicted by SALT4 (Figure 9.2-2), to temperature contours predicted by either DOT (Figure 6.4-4) or COYOTE (Figure 10.6-6), reveal that SALT4 predicts greater temperatures than these other codes. The inability of SALT4 to model symmetry conditions accurately would lead to temperatures lower than actual. However, this error is more than offset by the excessive temperatures predicted by SALT4 because this code cannot model radiation or forced or natural convection boundary conditions into the repository room. This fact is supported clearly by the relative magnitude of errors in the temperature contours for 3 times plotted. Both COYOTE and DOT modeled forced convection into the room for the first 50 years, thus the differences between the temperatures at 10 and 30 years for these codes and SALT4 are extreme. However, the error in the SALT4 temperatures at 100 years is much less, since the principal heat transfer mechanism at that time is conduction. Because the overestimation of temperatures will cause an overestimation of thermal stress, similar errors in the maximum principal stress, minimum principal stress, and displacement contours also exist. The inability to model symmetry or boundary heat transfer conditions render SALT4 unsuitable for the solution of Problem 5.2.

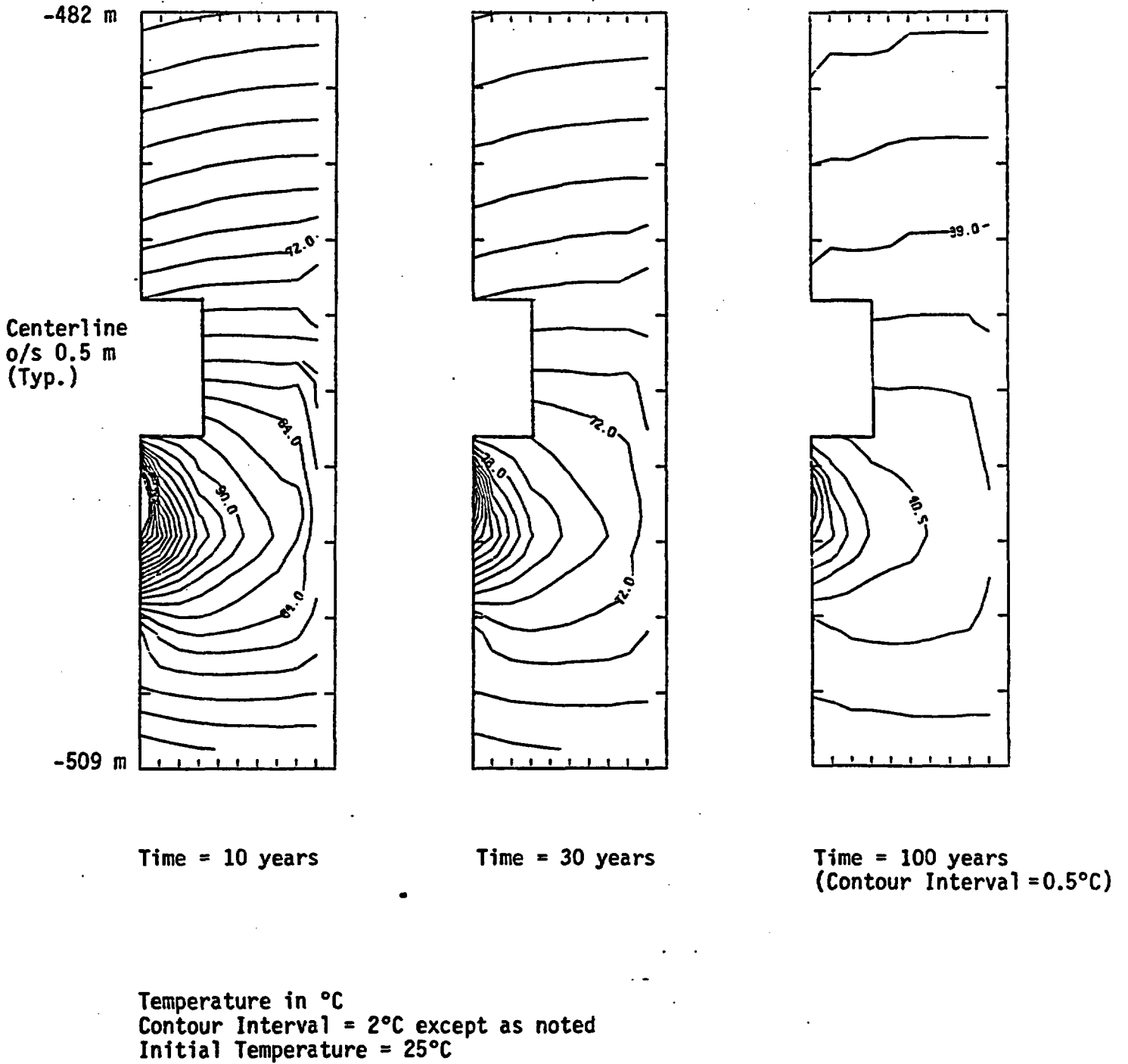
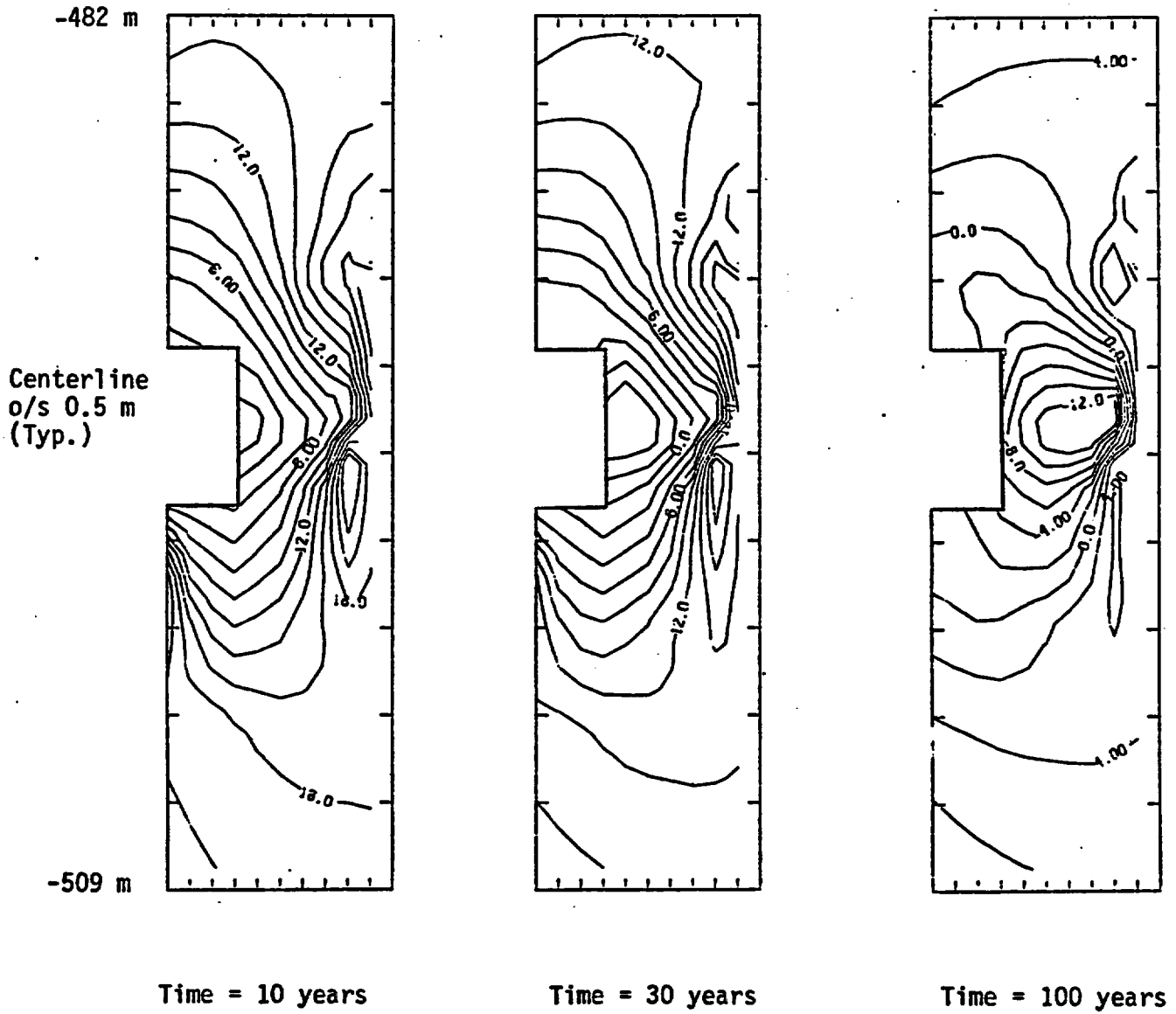


Figure 9.2-2 SALT4 Problem 5.2-Salt  
Temperature Contours



Stress in MPa  
Contour Interval = 2 MPa

Figure 9.2-4 SALT4 Problem 5.2-Salt  
Minimum Principal Stress Contours

## 10.0 BENCHMARKING OF COYOTE

## 10.0 BENCHMARKING OF COYOTE

### 10.1 Code Background and Capabilities

COYOTE<sup>(6)</sup> is a two-dimensional finite element conduction heat transfer computer program developed by David. K. Gartling at the Sandia National Laboratories (SNL) in Albuquerque, New Mexico. Two versions of COYOTE were obtained from SNL; COYOTECRAY and COYOTECDC. The first version obtained, COYOTECRAY (V 01.10C), is the most recent release of the code. It was developed to run on a CRAY computer. An initial attempt to use COYOTECRAY was unsuccessful due to numerous program format changes required to run this version on the Brookhaven National Laboratory's computer system. Subsequently, COYOTECDC (version V 01.007) was obtained, which is an earlier issue of COYOTE that had been run on a CDC system similar to the one at Brookhaven. Discussions with the author revealed that the only significant difference between COYOTECDC and COYOTECRAY is that the latter version can solve larger problems.

The COYOTE program can be used to solve steady and transient, linear and nonlinear, thermal conduction problems. The code incorporates anisotropic conductivity directly. Temperature and time-dependent thermal properties may be included by adding appropriate FORTRAN subroutines to the input data. These subroutines may be used to define the time and temperature relationship of the material conductivity, specific heat, density, and/or volumetric heat source generation. Boundary conditions for a conduction model may include:

- Constant and time-dependent temperature and heat flux functions;
- Convection to a constant environmental temperature from a material with a constant or temperature-dependent convection coefficient; and
- Radiation to or from an element surface from or to a constant source/sink temperature.

Elements in the present version of COYOTE are limited to one of each type of the radiation, convection, heat flux, or temperature boundary conditions. Elements exposed to two or more boundary conditions of the same type (i.e., convection on two sides of a corner element defined by separate functions) cannot be accommodated. This limitation is overcome by the subdivision of such rectangular elements into triangular elements. Other boundary condition types are not restricted.

Two basic integration procedures are provided in the current version of COYOTE. These include the generalized Crank-Nicolson family of methods and the modified Crank-Nicolson method. The generalized Crank-Nicolson family of methods, designated as TRANS2 in COYOTE, requires the specification of a weighting parameter,  $\lambda$ . The value of  $\lambda$ , which may range from 0 to 1, indicates where in the time step the heat transfer equation will be evaluated. The use of  $\lambda = 1.0$  produces a forward Euler integration (fully implicit) method, whereas  $\lambda = 0.0$  produces a

TABLE 10.1-1  
COYOTE CAPABILITIES TESTED OR UTILIZED

	Problem				
	<u>2.6</u>	<u>2.8</u>	<u>2.10</u>	<u>5.2S</u>	<u>6.3</u>
Problem Type					
- Planar	T	T		U	
- Axisymmetric					U
Equation Solution	T	T		U	U
Conductivity					
- Isotropic		T		U	
- Temperature and/or Time Dependent					U
- Anisotropic	T				
Material Volumetric Heat Source					
- Constant					
- Temperature and/or Time Dependent					U
Specific Heat					
- Constant	T	T		U	
- Temperature and/or Time Dependent					U
Density					
- Constant	T	T		U	U
- Temperature and/or Time Dependent					
Convection					
- Constant	T				U
- Temperature and/or Time Dependent					
Coefficient		T		U	
Heat Flux					
- Constant					
- Time Dependent				U	
Radiation					
- External Source/Sink					

T = Tested by comparison with Analytical Solution.

U = Utilized and results of analysis compared with other code results.

The COYOTE user manual is ambiguous regarding the application of multiple boundary conditions on more than one side of an element. To ascertain the limitations of the code, two independent analyses of Problem 2.6 were made. The first modeled element 15 as a rectangular element with convection boundary conditions on two element sides. In the second analysis, element 15 was replaced with two triangular elements, each with convection boundary conditions on one side. The results showed no difference in these two models. Thus, it was determined that more than one side of an element can have the same boundary condition applied. However, as previously stated, multiple functions of the same type of boundary conditions (i.e., convection) cannot be applied to an element. If the convection functions on the two sides of element 15 were different, it would have been necessary to use two triangular elements.

Results - As indicated above, this problem was run with COYOTE using several integration schemes. The temperatures along the x and y axes at 110 hours for these schemes are tabulated in Table 10.2-2. Generally, the run using TRANS2 with  $\lambda = 0.25$  resulted in the smallest error. The results from this run will be used to evaluate the performance of the COYOTE code for this problem.

The results of the analysis using TRANS2,  $\lambda = 0.25$  are shown graphically in Figures 10.2-2 through 10.2-4. In general, the COYOTE solutions exhibited lower temperatures than the analytical solution throughout the analysis. Since the problem calculated decreases in temperature with time, these comparisons demonstrate that COYOTE overestimates the rate of cooling.

Figure 10.2-2 compares the temperature history along the centerline of the bar from COYOTE with to the analytical solution. The maximum temperature difference between the COYOTE and predicted analytical solution is 24.5°K and occurs at time equals 800,000 seconds. Expressing this as a percentage of the difference between the initial bar temperature and the analytical solution at this time, yields an error of 28.3%.

Figures 10.2-3 and 10.2-4 show the temperature distribution along the x and y axes respectively, at time equals 110 hours (400,000 sec). At this time, temperatures computed by COYOTE are less than those predicted by the analytical solution, for all x and y values. The maximum x axis temperature difference between COYOTE and the analytical solution is 74.1°K while the maximum y axis difference is 24.4°K. These differences, when expressed as a percentage of the temperature difference between the analytical solution and the initial temperature, yield errors in the COYOTE solution of 89.5% and 96.9%, respectively, from desired results.

TABLE 10.2-2

COMPARISON OF COYOTE SOLUTIONS AT TIME = 110 HOURS  
PROBLEM 2.6

<u>y(m)</u>	Y - Axis Bar Centerline Temperatures (°K) by:			
	<u>Analytical</u>	<u>TRANS1</u>	<u>TRANS2, <math>\lambda = 0.25</math></u>	<u>TRANS2, <math>\lambda = 0.75</math></u>
0.00	547.8	523.4	525.4	524.1
0.20	543.2	520.5	521.9	521.0
0.40	529.0	510.8	510.6	510.8
0.60	504.6	492.2	490.4	491.6
0.80	469.7	462.6	459.3	461.4
0.90	448.5	443.1	439.9	442.0
1.00	425.1	421.0	419.9	419.9

<u>x(m)</u>	X - Axis Bar Centerline Temperatures (°K) by:			
	<u>Analytical</u>	<u>TRANS1</u>	<u>TRANS2, <math>\lambda = 0.25</math></u>	<u>TRANS2, <math>\lambda = 0.75</math></u>
0.00	547.8	523.4	525.4	524.1
0.225	547.1	521.1	522.5	521.6
0.45	544.9	513.7	514.0	513.9
0.675	540.7	501.4	501.1	501.2
0.90	534.0	483.9	485.0	483.6
1.125	523.8	462.5	462.1	462.6
1.35	509.4	439.1	439.2	439.8
1.575	490.2	416.1	419.6	417.1
1.80	465.9	395.9	397.3	396.5
2.00	440.2	379.8	383.4	380.2

# COYOTE PROBLEM 2.6

## CENTERLINE TEMPERATURE HISTORY

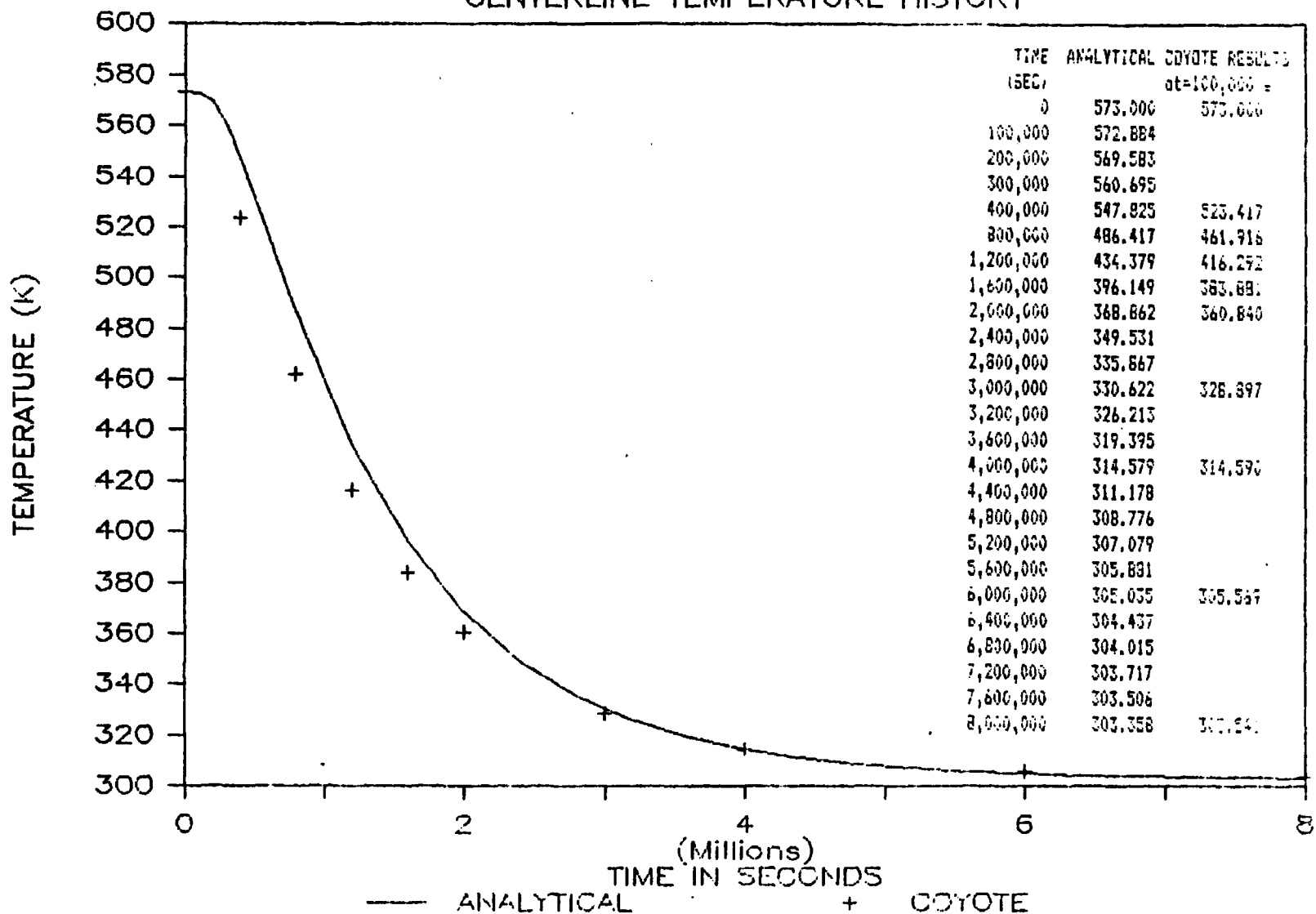


Figure 10.2-2 COYOTE Problem 2.6  
Centerline Temperature History

# COYOTE PROBLEM 2.6

Y-AXIS TEMPERATURES (t=400,000 s)

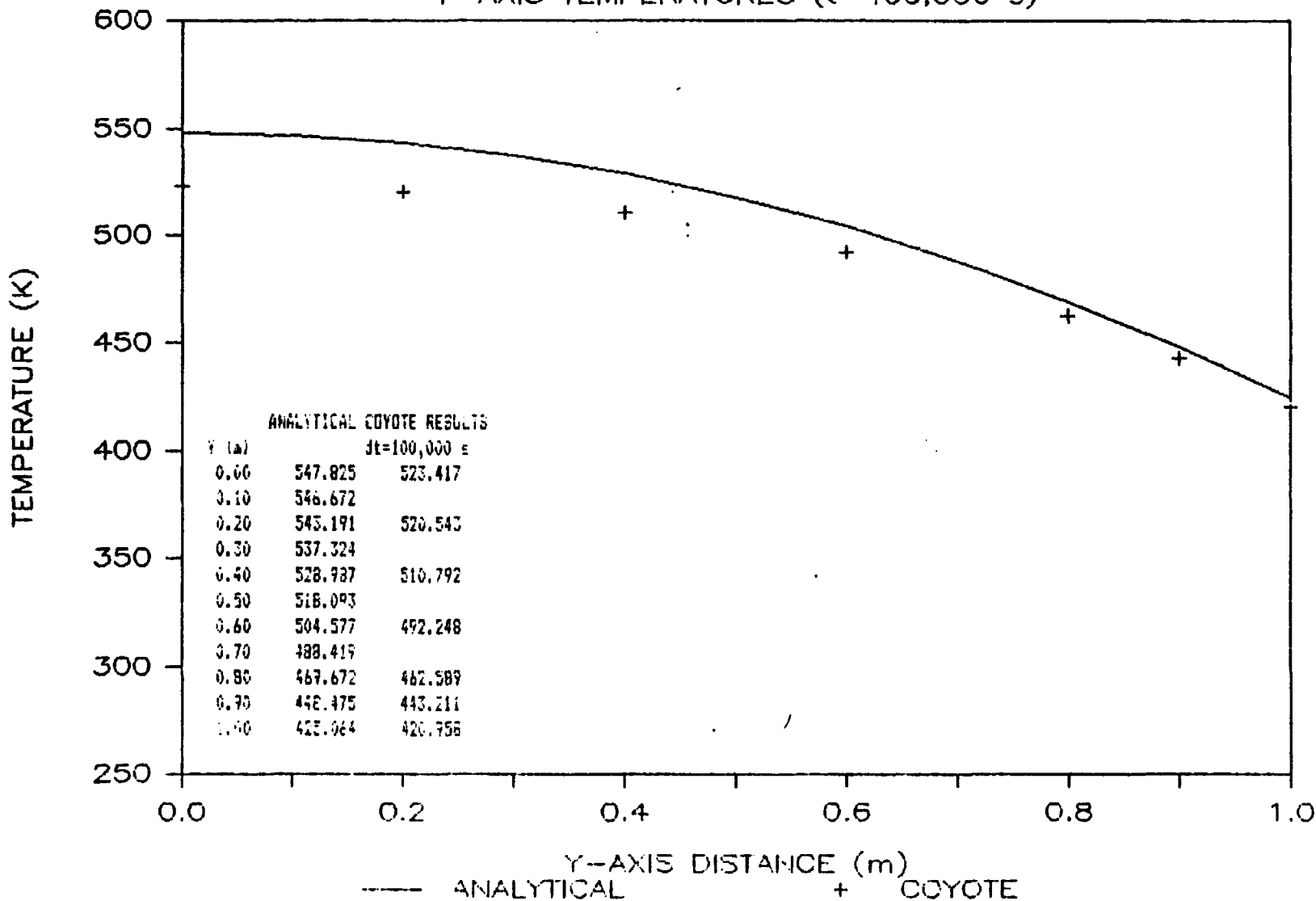
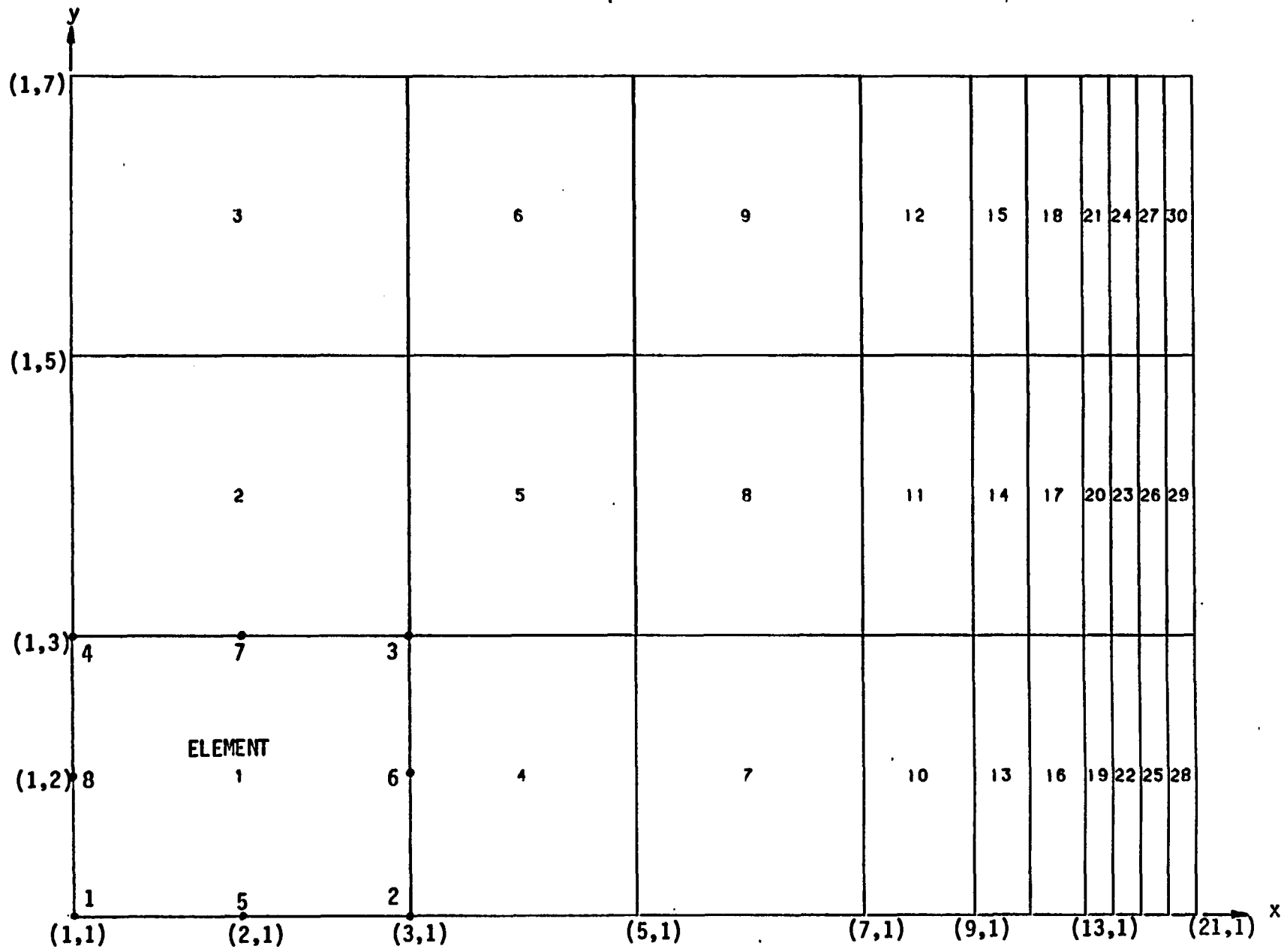


Figure 10.2-4 COYOTE Problem 2.6  
Y-Axis Temperature Distribution  
at Time = 400,000 sec.

Run Problem - A time step of 1,670 sec was used for this problem because it would provide output at times compatible with the given analytical solution. A procedure developed by Nicholl and Levi, and outlined by Gartling(6) in the COYOTE user manual, was used to confirm that this time step was suitable for the specified material properties and selected finite element mesh. No significant code-related difficulties were encountered in running Problem 2.8 with COYOTE.

Results - The analytical solution given for this problem included the temperature of the quenched surface at various times. These are compared to the results from COYOTE in Table 10.3-1. This table also includes the error present in the COYOTE solution. The error is defined as the difference between the analytical and COYOTE solutions divided by the analytical temperature drop. As with Problem 2.6, the temperatures calculated by COYOTE are lower than the analytical solution, thus the code overestimates the rate of cooling due to convection boundary conditions.



+-----+ 0.01 m in X  
 +-----+ 0.01 m in Y

Figure 10.3-1 COYOTE Problem 2.8  
Finite Element Mesh

## 10.4 Problem 2.9 - Transient Temperature Response of a Slab Exposed to a Uniform Radiative Environment

Problem Statement - This problem is concerned with the transient thermal analysis of an infinite slab, 0.25 m thick. The slab is initially at 546°K, one face is insulated, and the other is exposed to a radiative environmental temperature of 273°K at time zero. The temperature histories of both sides of the slab are to be determined.

Input Data - This problem was modeled using a single row of two-dimensional conduction elements as shown in Figure 10.4-1. The following input data, taken from the Benchmark Problems Report, were used to run this problem with COYOTE:

- Material Properties
  - thermal conductivity  $k = 1.15 \text{ W/(m}\cdot\text{°C)}$
  - density  $\rho = 2930 \text{ kg/m}^3$
  - specific heat  $c = 725 \text{ J/kg}\cdot\text{°C)}$
- Initial Conditions
  - radiative environmental temperature  $T_2 = 273^\circ\text{K}$
  - initial slab temperature  $T_0 = 546^\circ\text{K}$

Run Problem - The time step estimation procedure outlined in the COYOTE user manual indicated that the initial time step should be 3 sec. A review of the analytical solution indicated that a steep temperature gradient exists on the radiative face for the initial 10 hours. The use of a 3 sec. time step would require 1200 integrations during this period. Computational effort of this degree seemed extreme, thus the problem was run using the time steps listed in Table 10.4-1. The TRANS2 (Crank-Nicolson family of methods) integration option was used with a weighting factor ( $\lambda$ ) of 0.25. No code-related difficulties were encountered while running Problem 2.9 with COYOTE.

Results - Figures 10.4-2 and 10.4-3 compare the temperature histories calculated by COYOTE to the analytical solution at the radiative and insulated faces, respectively. The COYOTE results using the selected time steps compare favorably with the analytical solutions. Further refinement of the time steps may be made if desired, although it was not considered necessary for the purpose of benchmarking the COYOTE code.

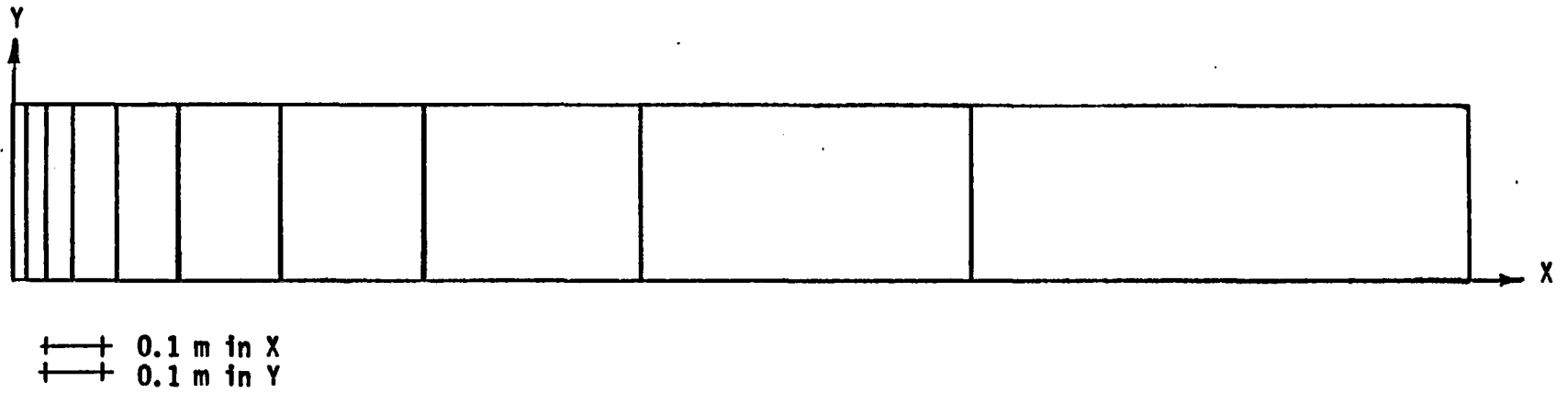


Figure 10.4-1 COYOTE Problem 2.9  
Finite Element Mesh

# PROBLEM 2.9 – COYOTE

TEMPERATURE HISTORY AT INSULATED FACE

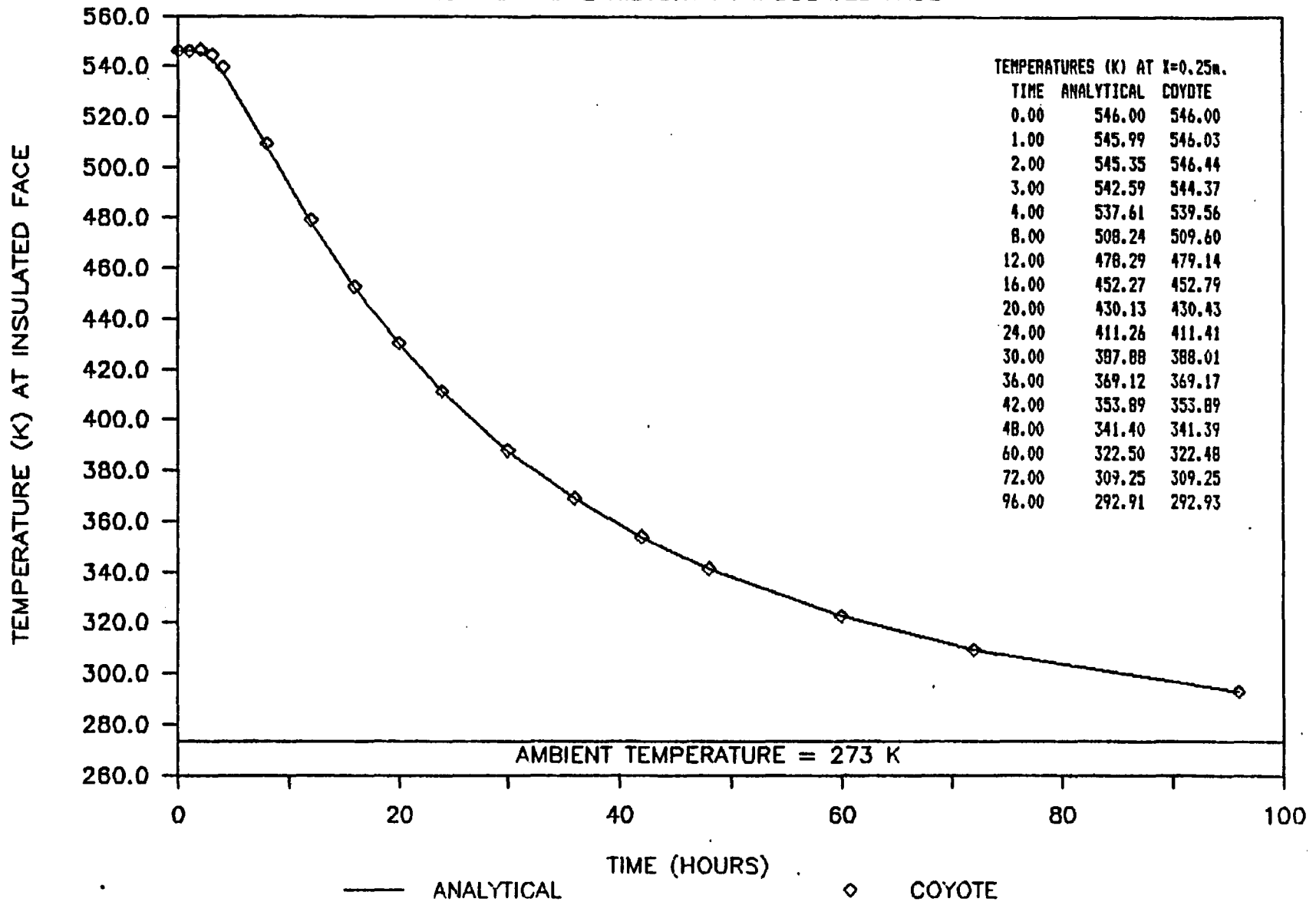


Figure 10.4-3 COYOTE Problem 2.9  
Temperature History at Insulated Face

## 10.6 Problem 5.2S - Hypothetical Near Field Problem - Salt

**Problem Statement** - This problem consists of a transient thermal simulation of the near field (single room region) of a hypothetical repository located in salt. In this analysis, waste canisters, which are emplaced vertically below the room at regular intervals along the room centerline, have been replaced by an equivalent heat generating trench. This problem exercises general transient heat transfer with mechanisms of conduction, heat storage, radiation, and free and forced (ventilation) convection. The room is ventilated for the first 50 years, after which the room is sealed, and natural convection and radiation occur. This problem, and the accompanying very-near field and far-field problems of the same repository, are summarized in greater detail in Section 3.3.

**Input Data** - A two-dimensional section of a single room in a repository with an infinite number of rooms was modeled using 3, 4, 6, and 8-noded isoparametric planar elements. The model extended from the ground surface to a depth of -3500 m, and contained 299 elements. Most of these elements are located between -479 m to -516 m, and are shown in Figure 10.6-1. The remainder of the model consists of "filler" elements with the vertical dimensions of each element limited to 1.5 to 2.0 times the vertical dimension of the previous element. While the aspect ratios of these "filler" elements may seem extreme, they numerically model the boundary conditions imposed upon the repository extremely well.

Input data used to mold this problem with COYOTE were taken from the Benchmark Problems Report and included:

- Material Properties of Salt

- Density  $\rho = 2150 \text{ kg/m}^3$
- Thermal conductivity  $= 4.5 \text{ W/(m}^\circ\text{C)}$
- Specific heat  $c = 830 \text{ J/(kg}^\circ\text{C)}$

- Initial Conditions/Boundary Conditions

- Initial temperatures
  - Between  $Z=-479 \text{ m}$  and  $Z=-516 \text{ m}$   $T = 24.7^\circ\text{C}$
  - All other depths  $T = [15-0.02(Z)]^\circ\text{C}$
- Environmental room temperature  $T_e = 15^\circ\text{C}$
- Convection coefficient
  - Initial 50 years  $h = 0.40 \text{ W/(m}^2\text{C)}$
  - After 50 years  $h = 0.00 \text{ W/(m}^2\text{C)}$
- Constant temperature at  $Z=0 \text{ m}$   $T_o = 15^\circ\text{C}$
- Constant temperature at  $Z=3,500 \text{ m}$   $T(-3500) = 85^\circ\text{C}$
- Externally supplied heat flux  $Q = Q_o \times e^{-k(t + t_o)}$

where:

- $Q_o =$  Initial heat flux  $26.546 \text{ W/m}^2$
- $k =$  Flux decay constant  $8.9724 \times 10^{-10} \text{ sec}^{-1}$
- $t_o =$  Time of canister emplacement  $3.156 \times 10^8 \text{ sec}$
- $t =$  Elapsed time since canister emplacement

TABLE 10.6-1

TIME STEP DATA USED BY COYOTE  
PROBLEM 5.2S

<u>Time Range</u> <u>(x 10<sup>9</sup> sec) [years]</u>		<u>Time Step Increment</u> <u>(x 10<sup>9</sup> sec) [years]</u>		<u>Number of</u> <u>Time Steps</u>
0 - 1.58	[0-50]	0.158	[5]	10
1.58 - 3.16	[50-100]	0.158	[5]	10
3.16 - 15.8	[100-500]	1.58	[50]	8
15.8 - 316.0	[500-10,000]	15.8	[500]	19

```

*IDENT SUBR
*D USER.17,19
  SUBROUTINE CURVE1 (NELEM,TSURF,TIME,VALUE)
C
C  SUBROUTINE TO EVALUATE A TIME DEPENDENT HEAT FLUX CONDITION
C  VALUE=VALUE OF HEAT FLUX (W/M**2)
C  TIME=CURRENT TIME (SEC)
C  FLUX0=INITIAL FLUX AT TIME=0 (W/M**2)
C  XK=FLUX DECAY CONSTANT (1/SEC)
C  VALUE=FLUX0*EXP(XK*(TIME+3.156E08))
C
  FLUX0=26.546
  XK=-8.9724E-10
  VALUE=FLUX0*EXP(XK*(TIME+3.156E08))
  RETURN
  END
*D USER.14,16
  SUBROUTINE HTCOEF (HT,TSURF,TREF,XSURF,YSURF,TIME,IVALUE,NELEM)
C
C  SUBROUTINE TO EVALUATE A TIME DEPENDENT HEAT TRANSFER COEFF.
C  TIME=CURRENT TIME (SEC)
C  HT=HEAT TRANSFER COEFFICIENT (W/M**2/K)
C
C  FOR FORCED CONVECTION TO BE ACTIVE FOR 50 YRS, THE CUT-OFF
C  STATEMENT SHOULD BE .LE. RATHER THAN .LT. . THIS MEANS THAT
C  K* (SEE PG.21 OF COYOTE USER MANUAL) AT 50 YRS WILL HAVE
C  CONVECTION BUT AT 55 YRS, CONVECTION WILL NOT OCCUR.
C
  HT=0.0
  IF (TIME.LE.1.58E09) HT=0.40
  RETURN
  END

```

Figure 10.6-2 COYOTE Problem 5.2S  
Program Subroutine Summary

# COYOTE PROBLEM 5.2 - SALT

## TEMPERATURE HISTORY

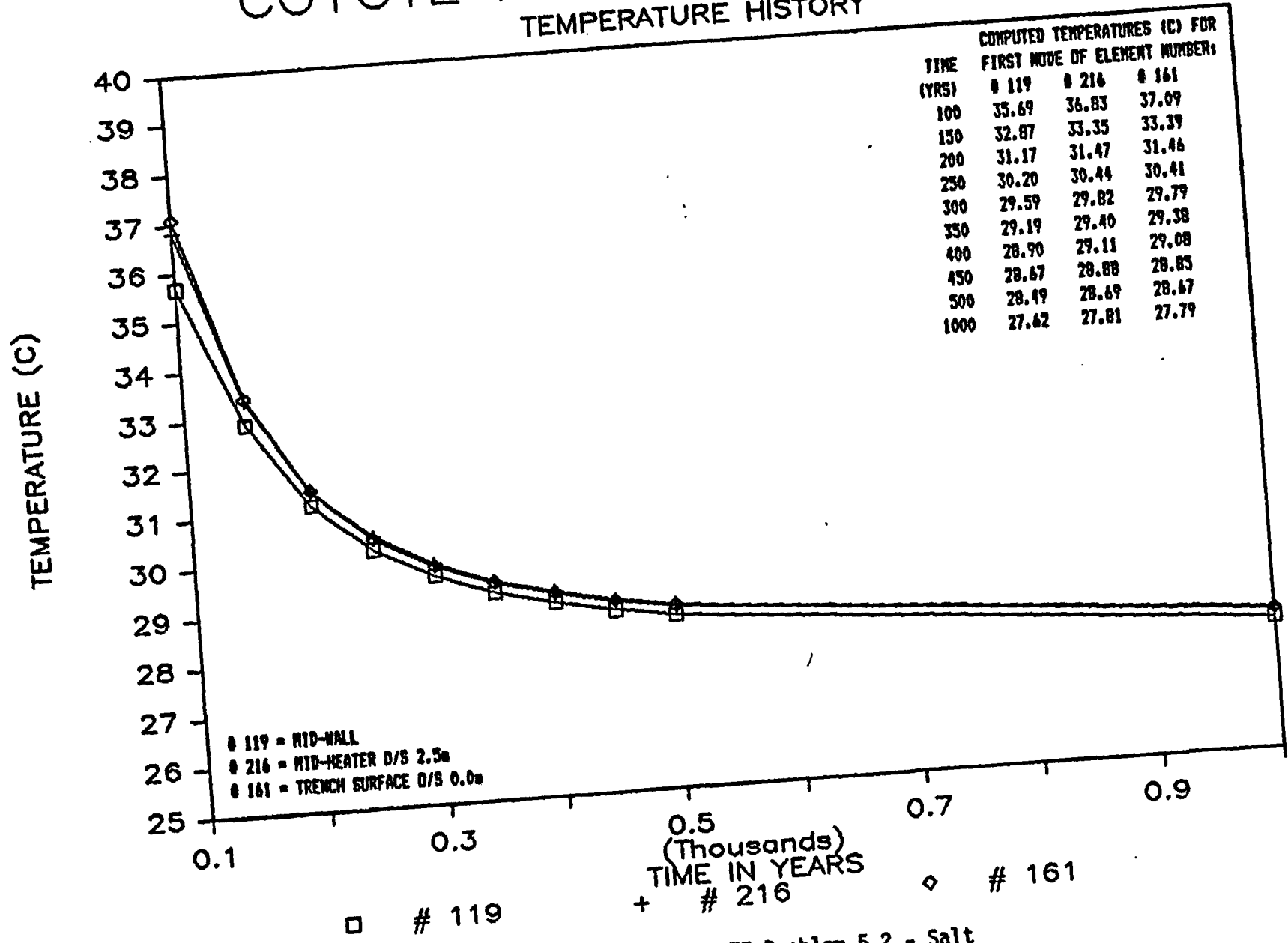
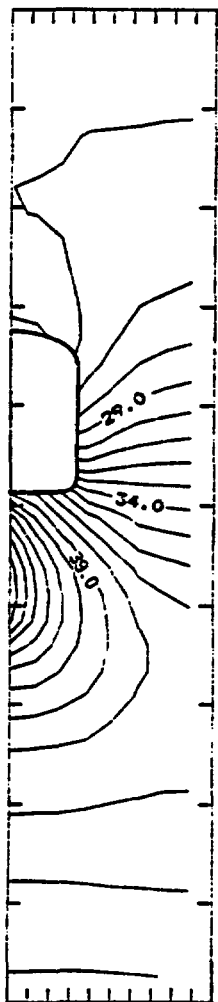
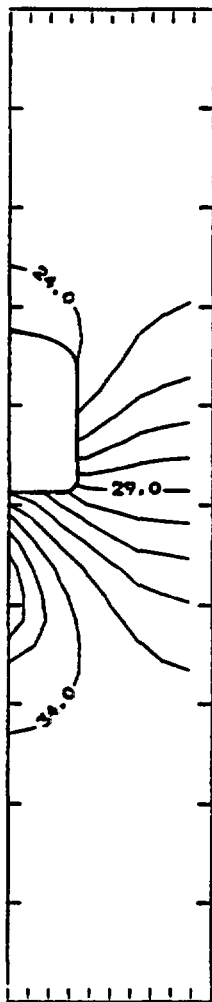


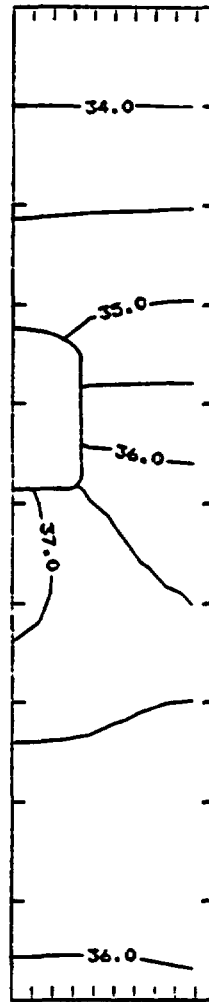
Figure 10.6-4 COYOTE Problem 5.2 - Salt Temperature History 100-1,000 years



Time = 10 years



Time = 30 years



Time = 100 years  
(Contour Interval = 0.5°C)

Temperature in °C

Contour Interval = 1°C except as noted

Initial Temperature = 25°C

Figure 10.6-6 COYOTE Problem 5.2-Salt  
Temperature Contours

## 10.7 Problem 6.3 - In-Situ Heater Test Basalt Waste Isolation Project

**Problem Statement** - This problem concerns the transient thermal simulation of basalt due to full-scale Heater Test #2, undertaken in 1980 at the Basalt Waste Isolation Project (BWIP), Hanford site near Richland, Washington. In this test, a single heater, vertically emplaced below the floor of a repository-type opening, was operated for 527 days. During this time, the power level was increased in a step-wise manner to a maximum of 5 kW as the thermal and mechanical response of the host rock was monitored. Laboratory-determined material properties for basalt accompany detailed description of this problem in the Benchmark Problems Report. This description has been summarized in Section 3.4.2.

**Input Data** - Problem 6.3 was modeled using a finite element mesh comprised of 3, 4, 6 and 8-noded axisymmetric elements. The heater was modeled as a heat generating solid material with the material properties of basalt. The geometry of the finite element mesh utilized is shown in Figure 10.7-1. The axisymmetric model, which models a single heater in a circular repository, is not truly valid above the floor level. However, in the region below the floor level, where the temperatures will be compared to field measurements, the model is representative of actual conditions. Inclusion of the room and rock above the floor level provides a better representation of boundary conditions than if they had been excluded. Model boundaries are set at a distance where, based on the field data, adiabatic boundary conditions can be assumed. The time history of BWIP Heater Test #2, as it pertains to the COYOTE solution of Problem 6.3, is shown in Table 10.7-1.

Input data to COYOTE for Problem 6.3 were obtained from the Benchmark Problems Report and included:

- Material Properties of Basalt

- Density  $\rho = 2850 \text{ kg/m}^3$
- Thermal conductivity  $k = (T - 273) \times 10^{-3} + 1.53 \text{ W/(m}^{\circ}\text{K)}$
- Specific heat  $c = 1280 - 0.108 T - 4.8 \times 10^7 \times T^{-2} \text{ J/(kg}^{\circ}\text{K)}$

where:

T = Temperature in Degrees Kelvin

The temperature dependent conductivity and specific heat were specified in COYOTE by user-supplied FORTRAN subroutines. These subroutines are included in Figure 10.7-2. Also shown in this figure are subroutines to define the time-dependent heat source, and generate nodes for the finite element mesh.

- Initial Conditions/Boundary Conditions

- Initial Rock Temperature  $T_o = 15.5^{\circ}\text{C}$
- Environmental Room Temperature  $T_e = 25^{\circ}\text{C}$
- Convection Coefficient  $h = 1.0 \text{ W/(m}^2\text{C)}$
- Internal Heat Generation Function Table 10.7-2
- Internal Heat Generation Multiplier (1/heater source volume)  $3.1831/\text{m}^3$

TABLE 10.7-1

TIME HISTORY OF BWIP HEATER TEST #2 FOR COYOTE  
PROBLEM 6.3

<u>Time (Days)</u>	<u>Event</u>
0	Heater turned on at 1 kW.
90	Heater boosted to 3 kW.
226	Heater boosted to 5 kW.
480	Last day of available field measurement data.
500	Last day of COYOTE analysis.
527	Heaters turned off.

TABLE 10.7-3

TIME STEP DATA USED FOR COYOTE  
PROBLEM 6.3

<u>Time Range</u> <u>(x 10<sup>6</sup> sec) [days]</u>	<u>Time Step Increment</u> <u>(x 10<sup>4</sup> sec) [days]</u>	<u>Number of</u> <u>Time Steps</u>
0 - 0.864 [0-10]	8.64 [1]	10
0.864 - 7.776 [10-90]	43.2 [5]	16
7.776 - 9.504 [90-110]	17.28 [2]	10
9.504 - 19.5264 [110-226]	125.28 [14.5]	8
19.5264 - 22.464 [226-260]	36.72 [4.25]	8
22.464 - 43.2 [260-500]	129.6 [15]	16

```

*IDENT SUBR
*D USER.2,5
  SUBROUTINE CAPACIT (RHOCP,T,X,Y,NNODES,MAT,NELEM,TIME)
  DIMENSION RHOCP(1),T(1),X(1),Y(1)
C
C  SUBROUTINE TO DETERMINE TEMPERATURE DEPENDENT HEAT CAPACITY
C  RHOCP=HEAT CAPACITY=RHO*CP
C  RHO=DENSITY=2850.0 (KG/M**3)
C  CP=SPECIFIC HEAT=1280.0-.108*TEMP-4.8E07/TEMP**2
C
  DO 10 I=1,NNODES
  RHO=2850.0
  CP=1280.0-0.108*T(I)-4.8E07/T(I)**2
  RHOCP(I)=RHO*CP
10  CONTINUE
  RETURN
  END
*D USER.6,9
  SUBROUTINE CONDUCT (COND1,COND2,T,X,Y,NNODES,MAT,NELEM,TIME)
  DIMENSION COND1(1),COND2(1),T(1),X(1),Y(1)
C
C  SUBROUTINE TO DETERMINE TEMPERATURE DEPENDENT HEAT CONDUCTIVITY
C  COND1=(TEMP-273.0)*1E-03+1.53
C
  DO 10 I=1,NNODES
  COND1(I)=(T(I)-273.0)*1E-03+1.53
  COND2(I)=COND1(I)
10  CONTINUE
  RETURN
  END
*D USER.10,13
  SUBROUTINE SOURCE (QVALUE,T,X,Y,NNODES,MAT,NELEM,TIME)
  DIMENSION QVALUE(1),T(1),X(1),Y(1)
C
C  SUBROUTINE TO DETERMINE TIME DEPENDENT VOLUMETRIC HEATING
C  QVALUE=HEAT(WATTS)PER M**3
C
  VOLUME=2.5*3.14159*0.2**2
  IF (TIME.GT.1.95264E07) GO TO 80
  IF (TIME.GT.7.776E06) GO TO 60
C
  DO 10 I=1,NNODES
  QVALUE(I)=1000./VOLUME
10  CONTINUE
  RETURN
  DO 60 I=1,NNODES
  QVALUE(I)=3000./VOLUME
60  CONTINUE
  RETURN
  DO 80 I=1,NNODES
  QVALUE(I)=5000./VOLUME
80  CONTINUE
  RETURN
  DO 90 I=1,NNODES
  QVALUE(I)=5000./VOLUME
90  CONTINUE
  RETURN
  END

```

Figure 10.7-2 COYOTE Problem 6.3  
Program Subroutine Summary

# COYOTE PROBLEM 6.3 – BWIP

## TEMPERATURE HISTORY

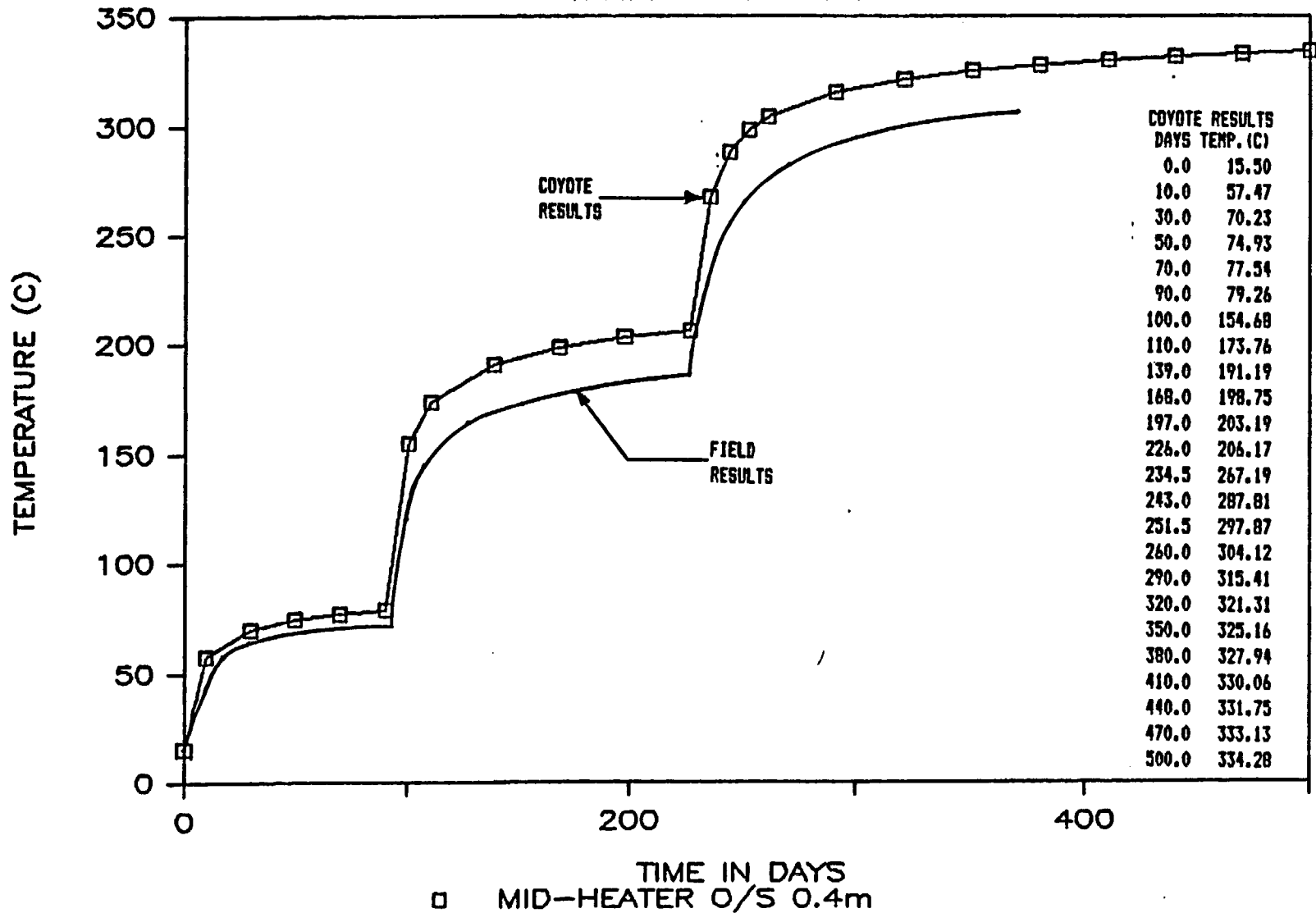


Figure 10.7-3 COYOTE Problem 6.3  
Temperature History

# COYOTE PROBLEM 6.3 — BWIP

VERTICAL TEMPERATURE PROFILES @ DAY 260

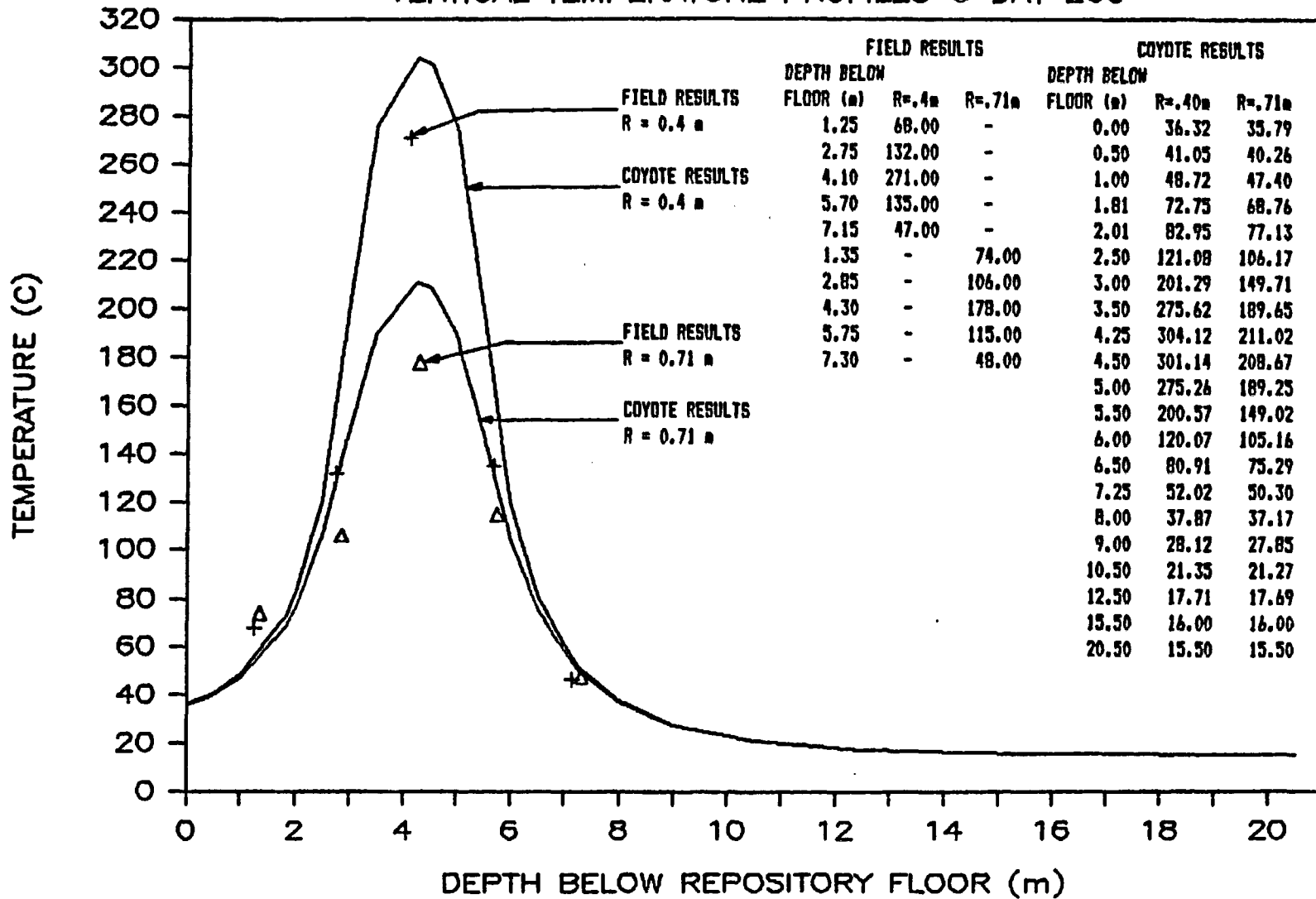


Figure 10.7-5 COYOTE Problem 6.3  
Vertical Temperature Profiles  
on Day 260

## REFERENCES

## REFERENCES

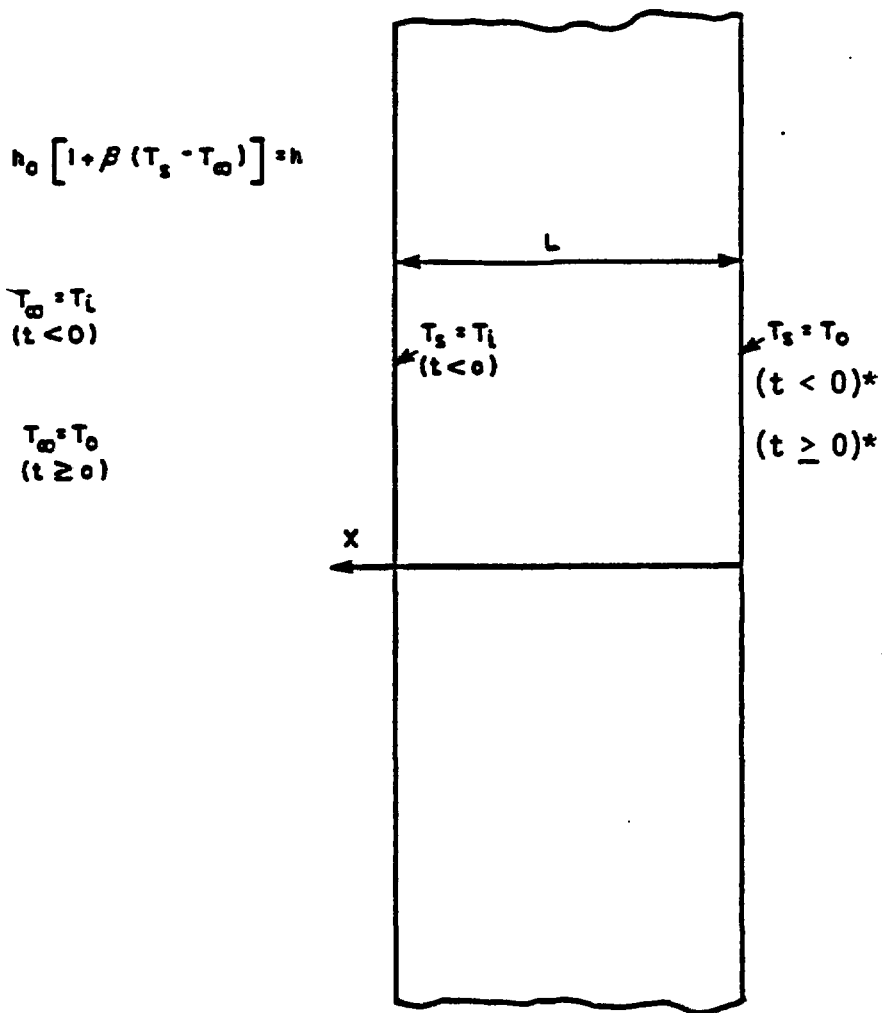
1. ADINA Engineering, Inc., "ADINA: A Finite Element Program for Automatic Dynamic Incremental Nonlinear Analysis," Report AE 81-1, September 1981.
2. ADINA Engineering, Inc., "ADINAT: A Finite Element Program for Automatic Dynamic Incremental Nonlinear Analysis of Temperatures," Report AE 81-2, September 1981.
3. Bradshaw, R.L. and W.C. McClain, "Project Salt Vault: A Demonstration of the Disposal of High-Activity Solidified Wastes in Underground Salt Mines," Prepared for U.S. Atomic Energy Commission by Oak Ridge National Laboratory, Report ORNL-4555, April 1971.
4. Curtis, R.H., R.J. Wart, and E.L. Skiba, "A Summary of Repository Design Models," prepared by Acres American Incorporated for the U.S. Nuclear Regulatory Commission, Report NUREG/CR-3450, October 1983.
5. Curtis, R.H. and R.J. Wart, "Parameters and Variables Appearing in Repository Design Models," prepared by Acres American Incorporated for the U.S. Nuclear Regulatory Commission, Report NUREG/CR-3586.
6. Gartling, D.K. "COYOTE - A Finite Element Computer Program for Nonlinear Heat Conduction Problems," Sandia National Laboratories, SAND 77-1332, October 1982.
7. INTERA Environmental Consultants, Inc. "DOT: A Nonlinear Heat-Transfer Code for Analysis of Two-Dimensional Planar and Axisymmetric Representations of Structures," ONWI-420 prepared for Battelle Memorial Institute, Office of Nuclear Waste Isolation, April 1983.
8. INTERA Environmental Consultants, Inc. "MATLOC: A Two-Dimensional and Axisymmetric Nonlinear Finite-Element Transient Thermal Stress Analysis Code for Rock Masses that Exhibit Bilinear Locking Behavior," ONWI-421, prepared for Battelle Memorial Institute, Office of Nuclear Waste Isolation, April 1983.
9. INTERA Environmental Consultants, Inc. "SALT4: A Two-Dimensional Displacement Discontinuity Code for Thermomechanical Analysis in Bedded Salt Deposits," ONWI-429, prepared for Battelle Memorial Institute, Office of Nuclear Waste Isolation, April 1983.
10. INTERA Environmental Consultants, Inc. "VISCOT: A Two-Dimensional and Axisymmetric Nonlinear Transient Thermoviscoelastic and Thermoviscoplastic Finite-Element Code for Modeling Time-Dependent Viscous Mechanical Behavior of a Rock Mass," ONWI-437, prepared for Battelle Memorial Institute, Office of Nuclear Waste Isolation, April 1983.

**APPENDIX**

## APPENDIX

The earlier report of this series, NUREG/CR-3636 entitled "Benchmark Problems for Repository Design Models", was issued in 1984. Minor errors were identified in that report during the modeling carried out for this report. The relevant pages have been corrected and are reproduced in this Appendix for reference purposes. The corrections to figures, text or mathematical equations are located by an asterisk in the margin. Reference should be made to the original document NUREG/CR-3636 to identify specific changes. The page numbers in NUREG/CR-3636 which have been corrected are:

- 30, 39, 59, 60, 65, 67, 81, 82, 83, 107, 109, 118, 119, 121, 125, 139, 164, 169, and 171.



\* Revised May 1986

Figure 2.8-1 Transient Response to the Quench of an Infinite Slab with a Temperature-Dependent Convection Coefficient

$$\sigma_r = \frac{1}{2} (S_x + S_y) \left( 1 - \frac{a^2}{r^2} \right) + \frac{1}{2} (S_x - S_y) \left( 1 + \frac{3a^4}{r^4} - \frac{4a^2}{r^2} \right) \cos 2\theta \quad (1) \quad *$$

$$\sigma_\theta = \frac{1}{2} (S_x + S_y) \left( 1 + \frac{a^2}{r^2} \right) - \frac{1}{2} (S_x - S_y) \left( 1 + \frac{3a^4}{r^4} \right) \cos 2\theta \quad (2)$$

$$\tau_{r\theta} = \frac{1}{2} (S_x - S_y) \left( 1 - \frac{3a^4}{r^4} + \frac{2a^2}{r^2} \right) \sin 2\theta \quad (3)$$

where:

- $r$  = radial coordinate, \*
- $\theta$  = angular coordinate measured counterclockwise from the x axis, \*
- $\sigma_r$  = radial stress,
- $\sigma_\theta$  = circumferential stress,
- $\tau_{r\theta}$  = shear stress,
- $S_x, S_y$  = in situ or initial stresses (tension positive), and
- $a$  = radius of circular hole or tunnel.

Displacements are given by:

$$u = \frac{1}{E'} \left[ \frac{S_x + S_y}{2} r + \frac{a^2}{r} + \frac{S_x - S_y}{2} r - \frac{a^4}{r^3} + \frac{4a^2}{r} \cos 2\theta \right] \quad (4)$$

$$- \frac{\nu'}{E'} \left[ \frac{S_x + S_y}{2} r - \frac{a^2}{r} - \frac{S_x - S_y}{2} r - \frac{a^4}{r^3} \cos 2\theta \right]$$

and

$$v = \frac{1}{E'} \left[ - \frac{S_x - S_y}{2} r + \frac{2a^2}{r} + \frac{a^4}{r^3} \sin 2\theta \right]$$

$$- \frac{\nu'}{E'} \left[ \frac{S_x - S_y}{2} r - \frac{2a^2}{r} + \frac{a^4}{r^3} \sin 2\theta \right] \quad (5) \quad *$$

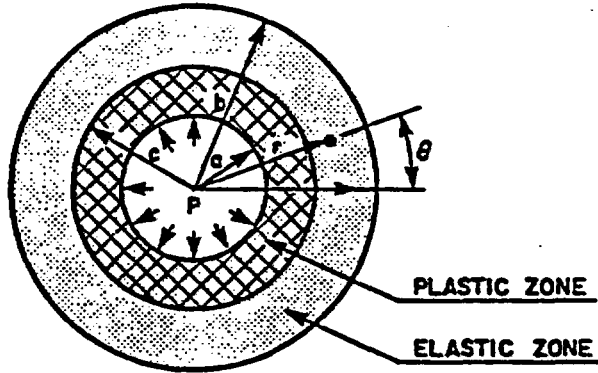
where:

$$E' = \frac{E}{(1 - \nu^2)} \quad \nu' = \frac{\nu}{(1 - \nu)} \quad *$$

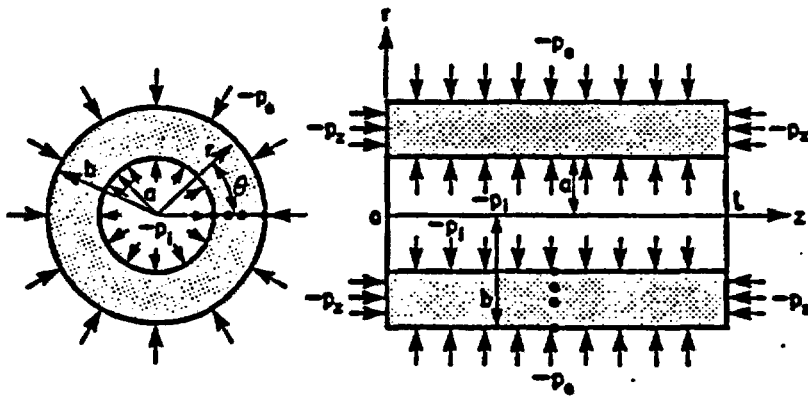
where:

- $u, v$  = displacements in radial and circumferential directions, respectively,
- $E$  = modulus of elasticity, and
- $\nu$  = Poisson's ratio.

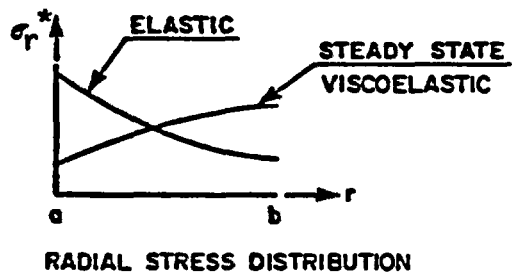
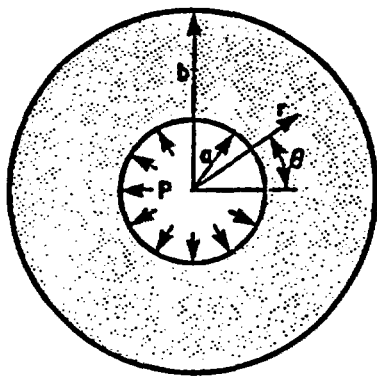
\*Revised May 1986



**(c) ELASTIC-PLASTIC ANALYSIS**



**(b) ELASTIC ANALYSIS**



**(c) VISCOELASTIC ANALYSIS**

\* Revised May 1986

Figure 3.3-1 Thick-walled Cylinder Subjected to Internal and/or External Pressure

where:

A = constant of integration defined above in terms of material properties, and  
 $\epsilon_2^E$  = elastic strain at initial yield.

With the assumption that the bulk modulus remains constant after yield,

$\epsilon_2^T$  can be computed from:

$$\epsilon_2^T = \frac{1}{3K} (-P + \sigma_3) - \epsilon_1^T \quad (6)$$

where:

K = E/3(1-2ν) = bulk modulus,  
 $\epsilon_2^T$  = total lateral strain, and  
 $\epsilon_1^T$  = total strain in the direction of loading.

The analytical solution for the problem using the Drucker-Prager yield criterion is based on stress-strain relationships given by Reyes and Deere (1966). The Drucker-Prager yield function is:

$$F = \alpha I_1 + \sqrt{J_2} - k_{DP} \quad \begin{cases} < 0 & \text{before yield, and} \\ = 0 & \text{at initial yield and} \\ & \text{during plastic flow.} \end{cases} \quad (7)$$

where:

α, k<sub>DP</sub> = material constants defining yield,  
I<sub>1</sub> = first stress invariant, and  
J<sub>2</sub> = second deviatoric stress invariant.

When expressed for the boundary and load conditions of this problem, the yield condition is as follows and can be used to solve for σ<sub>3</sub> directly at any time after yield:

$$F = \alpha (-P + \sigma_3) - k_{DP} + \sqrt{(P^2 + P\sigma_3 + \sigma_3^2)/3} = 0 \quad (8)$$

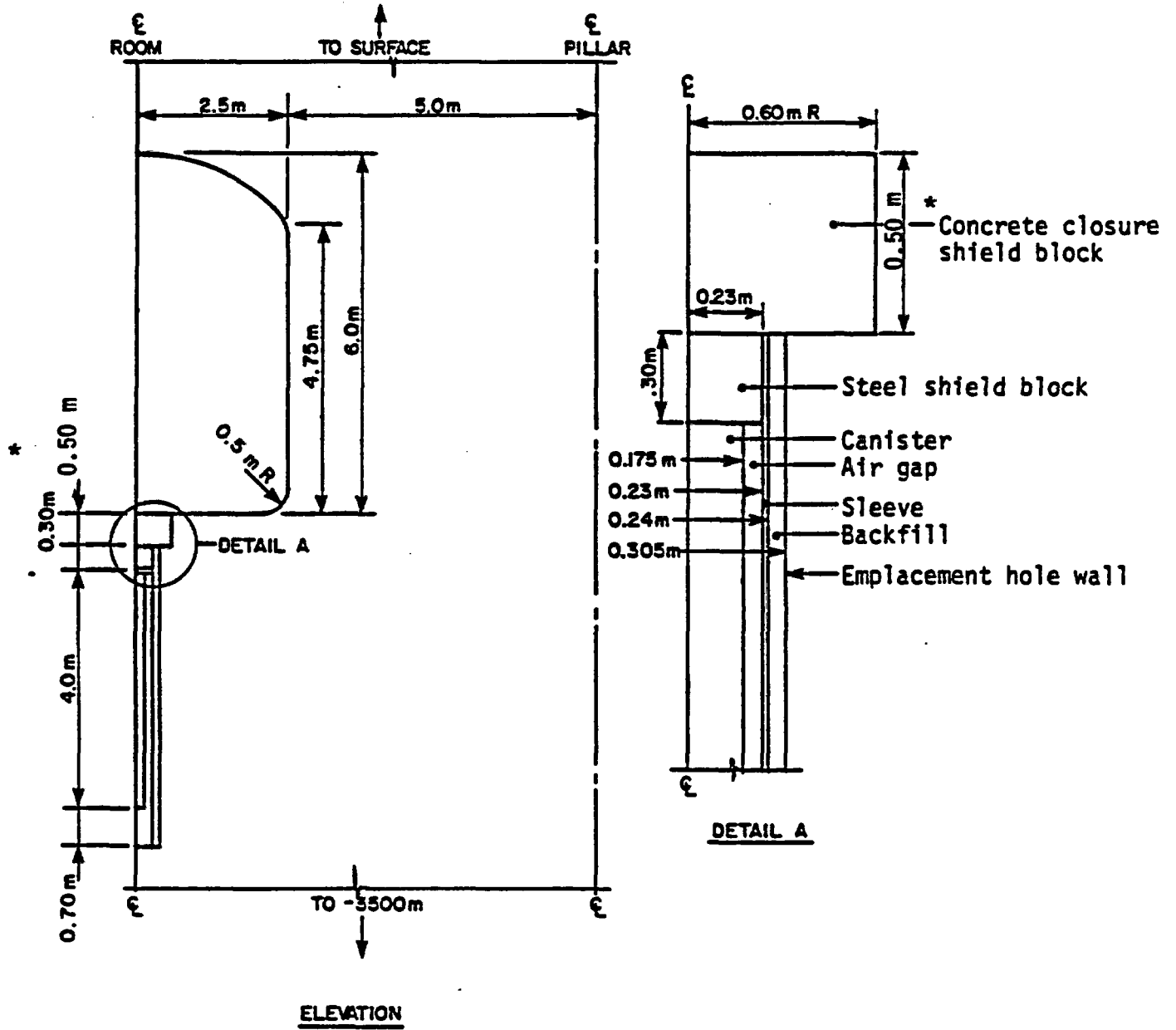
At initial yield, σ<sub>3</sub> = -νP, which leads to the following:

$$P = k_{DP} \left[ -\alpha(1+\nu) + \sqrt{(1-\nu+\nu^2)/3} \right] \quad (9)$$

The elastic-plastic stress-strain relationship can be expressed as:

$$\dot{\sigma}_1 = D_{11} \dot{\epsilon}_1^T + D_{12} \dot{\epsilon}_2^T \quad (10) \quad *$$

$$\dot{\sigma}_2 = D_{21} \dot{\epsilon}_1^T + D_{22} \dot{\epsilon}_2^T \quad (11) \quad *$$



\* Revised May 1986

Figure 5.1-1 Very Near Field (Canister) Model

## 5.2 - Hypothetical Near Field Problem

Problem Statement - This problem consists of transient thermal simulation of the near field (single-room region) of a hypothetical repository, followed by static stress analysis at two specified times. This and the accompanying very near field (canister region) and far field (repository region) problems form a set of problems at different scales of modeling for the same hypothetical repository configuration.

Objectives - The objectives of this hypothetical problem can be related to general, thermal, and stress issues.

Generally, the problem tests two-dimensional plane thermal and plane strain geometry and symmetry conditions as applied in the models.

The results of this room scale problem can be compared to the accompanying canister and repository scale problems. This comparison will indicate differences in numerical results due to scale of modeling and also qualitative differences in response. Compromises between local detail and generality (average response in a region) will become evident and the adequacy of typical modeling approaches and scales can be evaluated.

Thermally, this problem exercises general transient heat transfer, with mechanisms of conduction, heat storage, radiation, and free (natural) and forced (ventilation) convection. The analysis is applied to the emplacement hole (in which the canister and other hole contents are modeled with the inter-canister rock as an emplacement trench in two dimensions), the rest of the rock, and the room above. The room is ventilated for the initial 50 years after emplacement. After room sealing at 50 years, the ventilation is replaced by natural convection and radiation heat transfer between room surfaces.

In the stress analysis, the simulations will test elastic, elastoplastic, and viscoelastic behavior of the rock around the room. The phenomena under consideration will depend on the medium assumed. Non-rock materials are not to be modeled in stress. The emplacement trench is considered filled with rock in the stress analyses.

Physical Description - The single level repository, of unspecified extent, is located at a depth of 500 m (canister mid-height) in the host rock. A geothermal heat flux is present, specified by a temperature rise of 20°C per kilometer of depth below the surface, which is at a temperature of 15°C. The in situ stress is isotropic ( $K_0 = 1.0$ ) and is given by the overburden pressure.

The waste is ten-year old PWR spent fuel canisters containing one intact spent fuel assembly stored in vertical emplacement holes in the floors of an array of parallel rooms. The rooms are spaced on 15 m centers and the canister spacing in the rooms is 3 m on center. Room and emplacement configurations are shown in Figure 5.2-1. The power level at the time of emplacement is 600 w/canister which gives power density on emplacement 20.0 W/m<sup>2</sup>. The decay heat is shown in Figure 5.1-2. \*

\*Revised May 1986

Input Specifications - Thermal, mechanical (deformation), strength, failure parameters, and creep parameters are presented in Tables 5.1-1 through 5.1-5 for the materials under consideration for this hypothetical repository problem.

Thermal properties for air, free and forced convection parameters, and radiation parameters are given in Table 5.1-6. The ventilation flowrate is 0.6 m<sup>3</sup>/s per canister, or, in a room of 50 canisters (150 m long) and the given cross-section, the ventilation flow speed is 1.0 m/s. \*  
Ventilation air temperature is 15°C.

Output Specifications - The desired outputs are:

- (a) Temperature history at the trench surface, at the trench mid-height offset 2.5 m, for 0-10,000 years; \*
- (b) Temperature contours over the modeled region at 10, 30, 100, 300, and 1,000 years; \*
- (c) Radiation and convection coefficient values as a function of time;
- (d) Contours of maximum and minimum principal stresses at 10, 30, 100, 300, and 1,000 years; \*
- (e) Room vertical and horizontal closures at 10, 30, 100, 300, and 1,000 years; and \*
- (f) Plots and dimensions of any failed zones that may be present around the room at 10, 30, 100, 300, and 1,000 years. \*

Special Comments - This problem has not been simulated. When simulations begin, some adjustment of input parameters may be required to produce the desired behavior (i.e., failure) in the physical system in this problem. Should such adjustment be required, it should be coordinated between this room scale problem and the accompanying canister and repository scale problems.

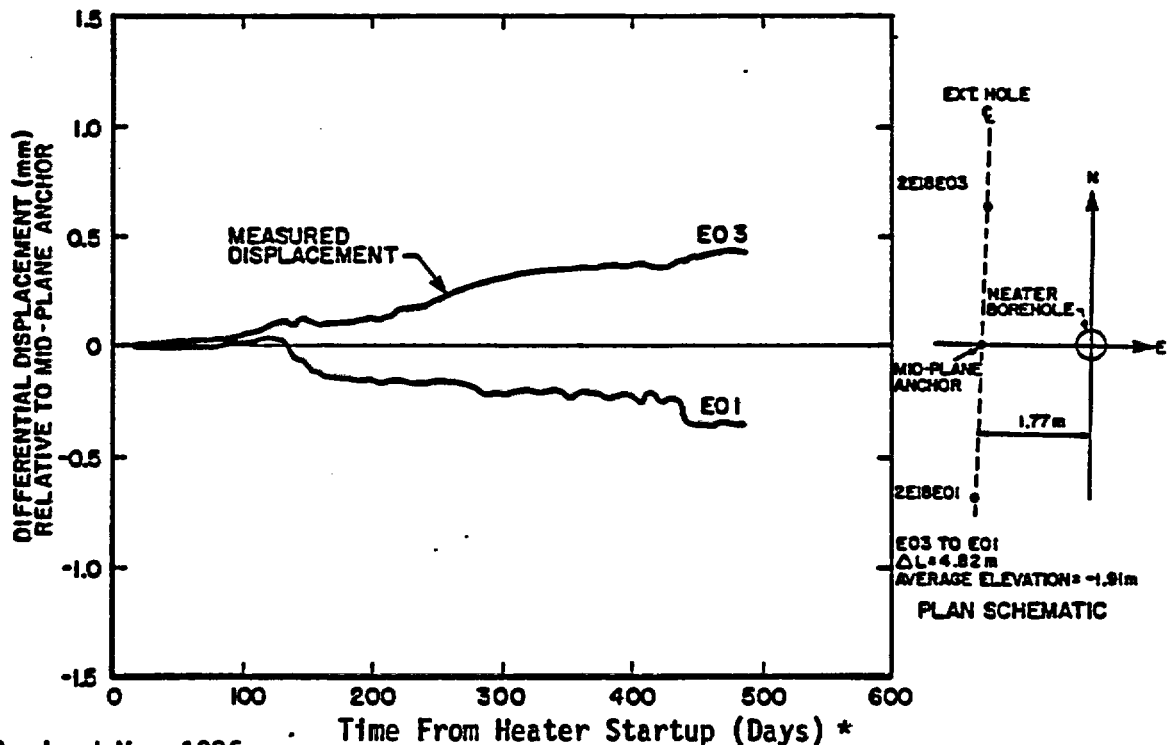
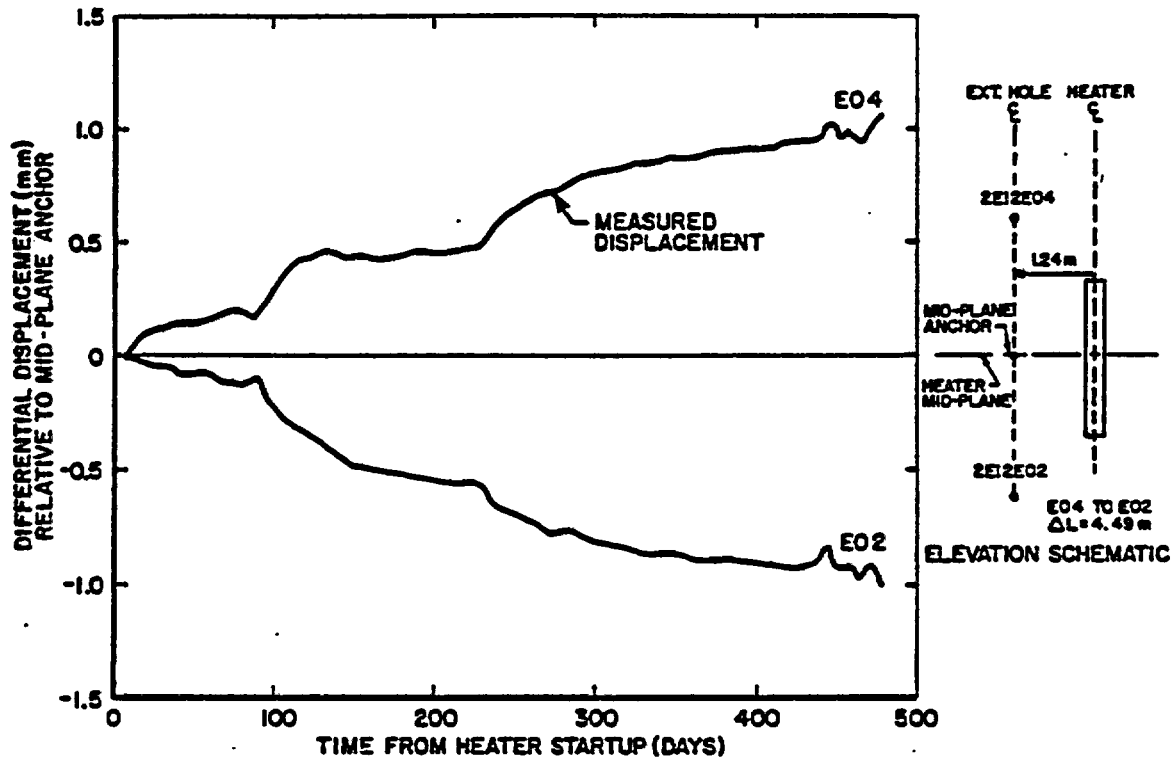
\*Revised May 1986

Table 6.1-1 Time History of Project Salt Vault  
(Bradshaw and McClain, 1971)

Standard Day <sup>+</sup>	Date	Event	*
366	9/2/64	Initiation of experimental area excavation	
571	3/25/65	Completion of experimental area excavation	
806	11/15/65	Start of experiment; array power activated at power level of 1.53 kW per heater	
1170	11/14/66	Pillar heaters activated at power level of 1.5 kW per heater	
1240	01/23/67	Array power increased to 2.14 kW per heater	
1382	06/14/67	Array power terminated	
1499	10/09/67	Pillar heater power terminated	

+ Standard Day 1 was September 1, 1963.

\*Revised May 1986



\* Revised May 1986

Figure 6.3-8 Relative Displacement Histories for BWIP Heater Test 2 (Baxter, et al.)